Investigating the use of *Bacillus subtilis* spores as a mucosal vaccine adjuvant

Laura Sibley

PhD Thesis

Royal Holloway University of London

Abstract

Mucosal vaccines are attracting increasing amounts of attention because of their ability to stimulate immune responses mucosally at the site of pathogen entry as well as systemically. *Bacillus subtilis* produces spores that are ~1 µM in size and can be modified to carry antigens on the surface, either by binding directly or by genetic modification, and have previously been tested as a vaccine adjuvant. The aim of this thesis was to further investigate the suitability of *B. subtilis* spores as a mucosal vaccine adjuvant. As an adjuvant carrying *Mycobacterium tuberculosis* (MTB) antigens (MPT64 and Ag85B-Acr), *B. subtilis* spores were able to demonstrate immunogenicity by stimulating Th1 cytokine production and provided some degree of protection against MTB challenge in the mouse model. The adjuvant behaviour of spores and initial interactions with host immune cells were investigated. Autoclaved spores were found to interact with different cells to live spores, which was hypothesised to be due to damage to the spore surface proteins prohibiting interactions with cell pattern recognition receptors. The cells that spores interacted with appeared to be dependent on tissue and dosing route and may highlight the differing roles of the lungs, gut and NALT in processing foreign material. The innate immune responses that were examined after nasal dosing demonstrated that spores could activate innate immune responses in the lungs and lymphoid tissue, and suggested that they were able to stimulate dendritic cells that could act as antigen presenting cells to activate adaptive immunity. In conclusion, the data generated provided further evidence on the utility of spores as a mucosal vaccine adjuvant and provided an insight into how they are able to stimulate immune responses.

Declaration of Authorship

I, Laura Sibley, hereby declare that this thesis and the work presented in it is entirely my own. Where I have consulted the work of others, this is always clearly stated.

Signed:

Acknowledgements

I would like to thank my supervisor, Professor Simon Cutting for providing me with this opportunity to carry out a PhD in his lab and to Dr Hong Huynh for her help throughout. I would also like to thank my advisor, Dr Chris Rider for his input on my transfer and second year reports.

I acknowledge Dr Rajko Reljic for the CL3 TB study work in Chapter 3 and Chapter 5 of this thesis, to Dr Illaria Pepponi for supplying the Ag85B-Acr protein, and to Gil Reynolds Diogo for the TB challenge work in Chapter 5, all of whom are from St Georges Medical School, University of London. I would also like to acknowledge Dr Andreas Hoppe, from Kingston University for the confocal microscopy work in Chapter 4. I also acknowledge my funding bodies; BBSRC and Boehringer Ingleheim.

I am grateful to everyone who has worked in the Royal Holloway lab over the years for either teaching me techniques or just providing companionship; Reena Khaneja, Patima ‘Anna’ Permpoonpattana, Jutarop ‘Peach’ Phetcharaburanin, Elisabeth Tolls, Claire Colenutt, Michelle Cashin-Cox, Jen-Min Huang, Lluis Semper-Bordes, Saba Anwar, Karen Smith, Niccolò Monaco, Irene Bianconi, Krisztina Hitri, Sara Aziz, Célia Rodrigues, Anil Chandrashekran, Jacob Goonesena and Stephanie Willing.

Finally, I am grateful to my family, friends and especially to Tom for their love and support.

Contents

Table of Figures

Table of Tables

Abbreviations

A	Area
Ad	Adenovirus
ACDP	Advisory Committee on Dangerous Pathogens
AFRC	Agricultural and Food Research Council
Ag	Antigen
AIDS	Acquired Immunodeficiency Syndrome
ALP	Alkaline Phosphatase
Alum	Aluminium hydroxide
AM	Alveolar Macrophages
amy	Amylase gene
APC	Antigen presenting cell
APC	Allophycocyanin
BAL	Bronchoalveolar Lavage
BALB/c	Laboratory strain of mouse
BCG	Bacillus Calmette-Guérin
BCIP/NBT	5-bromo-4-chloro-3-indolyl-phosphate/ nitro blue tetrazolium
BD	Becton Dickinson
BSA	Bovine serum albumin
^{o}C	Celsius
C	Complement protein
C57BL/6	Laboratory strain of mouse
CBA	Cytokine Bead Array
CD	Cluster of differentiation
CD3+	T-lymphocytes
CD4+	T-lymphocytes involved in Th1/Th2 helper functions

CD8+	T-lymphocytes involved in cytotoxicity
CD11c	Dendritic cell marker
CFP	Culture Filtrate Protein
CFU	Colony forming units
CL	Containment level
CT	Computerised Tomography
CT	Cholera Toxin
CTL	Cytotoxic lymphocyte
CTL	Cellular Technology Limited
CO_2	Carbon dioxide
Cot	*Bacillus* spore coat protein
CXC	Chemokine
Cy	Cyanine
DAPI	4',6-diamidino-2-phenylindole
DC	Dendritic cell
dH_20	Deionised water
DMEM	Dulbecco's Modified Eagle Medium
DMSO	Dimethyl sulphoxide
DNA	Deoxyribonucleic acid
DSM	Difco sporulation media
dsRNA	Double-stranded RNA
ssRNA	Single-stranded RNA
DTT	Dithiothreitol
DX5	NK cell marker
ECL	Electro Chemiluminescence
ELISA	Enzyme linked immunosorbent assay

ELISPOT	Enzyme linking immunosorbent spot
ESAT	Early Secretory Antigenic Target
et al	'*et al*ii' (and others)
F4/80	Macrophage marker
F_{ab}	Light chain region of an Immunoglobulin
F_c	Heavy chain region of an Immunoglobulin
FCAP	Flow Cytometry Data Analysis and Processing Software
FCS	Foetal calf serum
FL	Fluorescence
FITC	Fluorescein isothiocyanate
FSC	Forward Scatter
g	Gravitational force
g	gram
GALT	Gut associated lymphoid tissue
G-CSF	Granulocyte-colony stimulating factor
GE	General Electric
GFP	Green Fluorescent Protein
GI tract	Gastrointestinal tract
GM	Genetically modified
GP	Glycoprotein
h	Hour
H	Haemagglutanin
H	Height
H_2SO_4	Sulphuric Acid
HBsAg	Hepatitis B surface antigen
H&E	Hematoxylin and eosin stain

HIV	Human Immunodeficiency Virus
HPA	Health Protection Agency
HPV	Human Papillomavirus
HRP	Horse Radish Peroxidase
IFN	Interferon
Ig	Immunoglobulin
IGRA	Interferon-gamma Release Assay
IL	Interleukin
IP	Intraperitoneal
IPTG	Isopropyl β—D-thiogalactopyanoside
KCl	Potassium Chloride
kDa	Kilodaltons
L	Litre
L	Ligand
LB	Luria Bertani
LF	Lethal Factor
LN	Lymph node
LPS	Lipopolysaccharide
Ly6G	Neutrophil marker
LT	*E. coli* Labile Toxin
M	Macrophage
M cell	Microfold cell
MAC	Membrane Attack Complex
MALT	Mucosal associated lymphoid tissue
MAPK	Mitogen-activated protein kinase
MCP	Monocyte Chemoattractant Protein

MDG	Millennium Development Goals
MDR	Multi-Drug Resistant
mg	Milligram
ml	Millilitre
MHC	Major Histocompatibility Complex
MLN	Mesenteric lymph node
MTB	*Mycobacterium tuberculosis*
MVA	Modified Vaccinia Ankara
Mwt	Molecular weight
MyD88	Myeloid differentiation primary response gene
N	Neuraminidase
NaCl	Sodium Chloride
NADPH	Nicotinamide adenine dinucleotide phosphate
NALT	Nasal associated lymphoid tissue
NBF	Neutral Buffered Formalin
NHP	Non-Human Primate
NHS	National Health Service
NIAID	The National Institute of Allergy and Infectious Diseases
NK	Natural Killer
OD	Optical density
OVA	Ovalbumin
p	Probability
PAMP	Pathogen Associated Molecular Pattern
PBS	Phosphate buffered saline
PE	Phycoerythrin
PerCP	Peridinin chlorophyll

pET	Plasmid Expression vector, T7 promoter
PDGF	Platelet-derived growth factor
pg	Picogram
pg	Page
PGE	Prostaglandin
PI	Propidium Iodide
PLGA	Poly(lactic-co-glycolic acid)
PMA	Phorbol 12-myristate 13-acetate
PPD	Purified Protein Derivative
PRR	Pattern Recognition Receptor
psi	Pound per square inch
PVDF	Polyvinylidene fluoride
r	Recombinant
r	Regression
R	Receptor
RAW264.7	Murine macrophage cell line
RD	Region of Difference
RER	Rough Endoplasmic Reticulum
RHUL	Royal Holloway University of London
RNA	Ribonucelic Acid
ROS	Reactive Oxygen Species
rpm	Rotations per minute
RT	Room temperature
RT-PCR	Reverse Transcription Polymerase Chain Reaction
Rv	Tuberculosis genes identified and classified in strain H37Rv
SD	Standard deviation

SDS-PAGE	Sodium dodecyl sulphate polyacrylamide gel electrophoresis
SFU	Spot forming units
SGUL	St. Georges Medical School, University of London
sIgA	Secretory IgA
SPICE	Simplified Presentation of Incredibly Complex Evaluations
SSC	Side Scatter
SWAN	South-West Alliance Network
TAP	Transporter Associated with Antigen Processing
TB	Tuberculosis
TBS	Tris buffered saline
Tc	T cytotoxic lymphocyte
TCR	T-cell Receptor
Tfh	T follicular helper lymphocyte
TGFβ1	Transforming growth factor beta1
Th	T helper lymphocyte
TLR	Toll-like receptor
TNF	Tumour necrosis factor
TO	Thiazole Orange
Tregs	Regulatory T-cells
TRITC	Tetramethyl rhodamine iso-thiocyanate
TSLP	Thymic stromal lymphopoietin
TST	Tuberculin Skin Test
TTFC	Tetanus toxin fragment C
UK	United Kingdom
USA	United States of America
UV	Ultraviolet

v/v	Volume per volume
VLP	Virus Like Particles
vs	Versus
WHO	World Health Organisation
w/v	Weight per volume
γδ	Gamma-delta: A subset of T-cells
µg	Microgram
µl	Microlitre
%	Percent

Chapter 1: Introduction

1.1. Tuberculosis

A third of the world's population is estimated to be infected with Tuberculosis (WHO 2014c) and the WHO reported almost nine million cases and two million deaths from TB worldwide in 2011 (WHO 2011). *M. tuberculosis* (MTB) is the primary cause of TB disease in humans, although other species such as *M. bovis* can cause disease occasionally. MTB is an aerobic bacillus, characterised by a waxy lipid rich outer coat and a very slow replication rate (16-20 hours) (Todar 2012).

1.1.1. Diagnosing disease

The traditional diagnostic methods for TB include X-ray and computerised tomography (CT) scanning of the lungs for tissue damage, and the sputum smear test where a sputum sample is stained with a Ziehl-Neelson acid fast stain and examined under the microscope (Todar 2012). Because of the lipid rich wall of MTB, the Gram stain used for basic bacterial strain identification is unable to stain MTB. The Tuberculin Skin Test (TST) uses a range of TB proteins injected subcutaneously to determine if the immune system is primed for TB, by looking for inflammation (Gideon & Flynn 2011). However, it does not distinguish between individuals infected with TB and those vaccinated with BCG but currently the tuberculin skin test is used to determine whether an individual requires a BCG vaccination. IFNγ release assays (IGRA) can also be used for diagnosis as they take advantage of the region of difference (RD1) between MTB and BCG using proteins ESAT-6 and CFP-10, which are not present in BCG to diagnose infection with MTB (Gideon & Flynn 2011). No assay is available yet that can differentiate between active and latent disease.

1.1.2. Disease

There are three main outcomes of TB disease, which depend on the balance between host immune response and MTB replication; primary disease, latency and reactivation. Primary disease generally occurs within two years of encountering MTB but is relatively rare. Here, MTB multiplies and spreads through the lung causing tissue damage leading to the symptoms of weight loss and haemoptysis. During primary disease, induction of an inflammatory response and actively replicating MTB, mean that an individual is positive in the sputum smear test and IFNγ release assay (Gideon & Flynn 2011).

Latent disease occurs when the primary immune response is unable to clear MTB resulting in encapsulation in a granuloma (also known as a tubercule) so as to isolate the bacteria. The granuloma consists of macrophages, T-cells, B-cells, neutrophils and fibroblasts that wall off MTB and form a stratified structure to prevent disease spread (Gideon & Flynn 2011). However, there are several types of granuloma, including caseous, mineralised and non-necrotising, which are characteristic of either latent or active disease and are indicative of how well the immune system is coping to contain the infection. For example, the mineralised granuloma is associated with latent disease, whilst caseous is more characteristic of active TB (Lin *et al*. 2009). MTB is thought to enter a slow or non-replicating persistent phase of growth inside the granuloma (Hampshire *et al*. 2004). However, this is debated because Isoniazid, a drug that targets cell wall synthesis, is effective in reducing reactivation in latent cases, which suggests that some bacteria are actively replicating (Schechter *et al*. 2006). Live MTB has also been reportedly isolated from granulomas of autopsies of individuals that died from other causes (Loring *et al*. 1955). Individuals with latent disease have no symptoms and no bacteria are isolated from sputum

smears due to the bacteria being trapped in the granuloma, but they test positive in the TST or IGRA immunoassay as they have mounted a cellular immune response (Gideon & Flynn 2011).

Reactivation, leading to post primary disease can occur many years after infection, and may be due to the individual subsequently becoming immunocompromised. Evidence for this comes from observations that individuals undergoing arthritis treatment using anti-TNFα antibodies and those with human immunodeficiency virus (HIV) are more likely to have reactivation of MTB disease (Keane 2004; Selwyn *et al*. 1989), which suggests that a sustained immune response is required to control MTB pathogenesis. After reactivation, the granulomas break down and cause cavitation and tissue damage that can then spread the bacteria to other organs and cause further injury (Nasser Eddine *et al*. 2006).

Although disease can be characterised, the groupings are very heterogeneous and can be viewed as a dynamic spectrum of disease. Markers for distinguishing between active and latent disease have not been discovered, which makes monitoring persons at risk of developing disease and spreading MTB difficult (Gideon & Flynn 2011).

1.1.3. Immune responses to Tuberculosis

1.1.3.1. Primary infection and the innate immune response

The innate immune response is non-specific and can be activated quickly to prevent infections. The innate immune system includes barriers such as the skin and mucous membranes, as well as phagocytes, antimicrobial proteins and inflammation.

MTB is spread by the aerosol route, in droplets exhaled from infected individuals (Todar 2012). Once MTB enters the lungs, the surface proteins interact with pattern recognition receptors (PRRs) such as toll-like receptors (TLRs). There are several types of TLRs that exist on host cells that have specificities for different ligands, for example TLR2 binds to peptidoglycan found in Gram positive bacteria. Once activated, transcriptional regulators that control cytokine production are upregulated and phagocytosis can be instigated. TLR2, TLR4 and TLR9 have been implicated in MTB infection, because knock-out mice were shown to be more susceptible to MTB infection (Korbel *et al*. 2008). Other PRRs include scavenger receptors, Fc receptors and mannose binding receptors (Aderem & Underhill 1999).

Complement proteins are also part of the innate immune response and are constantly in circulation. Once activated, the complement cascade is activated that causes a series of hydrolysis reactions of other complement proteins, which can lead to the generation of a membrane attack complex (MAC) that forms a pore in the bacterial membrane causing lysis. Complement protein C3 can also bind bacteria and act as an opsonin to activate phagocytosis. Complement has been demonstrated to bind to MTB, which can initiate phagocytosis by macrophages (Ferguson *et al*. 2004). However, in C3 knock out mice, disease burden was the same as in control mice and it was hypothesised that alternative receptors would still be able to activate phagocytosis of MTB (Hu *et al*. 2000).

Once the bacterium is inside the macrophage, the phagosome fuses with a lysosome to form the phagolysosome, where upon degradative enzymes can attack the bacteria. Macrophages also produce reactive oxygen species (ROS) that can cause damage to bacteria (Aderem 2003). However, MTB is able to avoid degradation and will actively proliferate inside macrophages (Ehrt &

Schnappinger 2009). MTB are able to resist successful phagocytosis through a number of mechanisms; i) MTB produces enzymes including superoxide dismutases, catalases and antioxidants that detoxify the reactive oxygen species within the macrophage phagolysosome, ii) MTB has DNA repair enzymes that fix any damage resulting from ROS (Ehrt & Schnappinger 2009), iii) MTB is able to arrest phagosome maturation and reduce acidity, therefore delaying killing. The host immune response is important here because IFNγ produced by T-cells can influence the phagosome to become acidic, iv) the thick waxy coat of MTB adds to its resistance against acidic conditions by preventing entry of protons into the cell (Ehrt & Schnappinger 2009), v) MTB can also inhibit antigen presentation and promote release of anti-inflammatory mediators to aid its escape (Andersen & Woodworth 2014).

DCs are also activated by TLR interactions with MTB. They also phagocytose the bacteria, but the phagosome is less destructive than macrophages because the main role of DCs is as an antigen presenting cell (APC) (Savina & Amigorena 2007). The peptides from the bacteria are exposed on the surface of the cell via an MHCII complex, which can interact with T-cells after migrating to the lymph nodes and provides the bridge between the innate and adaptive immune systems(Andersen & Woodworth 2014). It takes between eight to ten days for delivery of MTB to the lymph nodes after aerosol infection (Blomgran & Ernst 2011).

There is an influx of neutrophils to the lungs after MTB infection and these neutrophils will phagocytose MTB. The neutrophils will then be taken up by macrophages, which enhances the macrophages killing ability by utilising the neutrophil granules that contain degradative enzymes (Tan *et al*. 2006). Neutrophils can also enhance DC maturation because apoptotic neutrophils are

phagocytosed by DCs which can cross-present the antigens to stimulate the T-cell response (Alemán *et al*. 2007). MTB can prevent cross presentation of antigens by DCs so as to delay the T-cell response, allowing MTB time to replicate and establish infection. This is achieved by inhibiting prostaglandin 2 (PGE2) in the neutrophil, which is involved in mitochondrial membrane integrity and leads to necrosis of the infected neutrophil, preventing apoptosis, therefore decreasing uptake of apoptotic bodies containing MTB by DCs (Chen *et al*. 2008).

NK cells are another set of cells involved in the innate immune response, which act by directly killing infected cells by using perforin to make holes in the membranes and granzymes that cause lysis or apoptosis. NK cells recognise diseased cells by forming synapses with cells and can recognise changes in inhibitory ligands and MHCI expression. DCs at the site of infection produce IL-12 and IL-18, which stimulate NK cells to release IFNγ that can activate macrophage phagocytic activity and improve killing of the bacteria (Andersen & Woodworth 2014). However, studies by Junqueira-Kipnis *et al* showed that although NK cells were recruited to the lungs after MTB infection in mice, but when NK cells were depleted there was no effect on disease progression (Junqueira-kipnis *et al*. 2003).

1.1.3.2. Adaptive immunity

The adaptive immune response is a specific immune response and takes longer to develop than the innate response. The adaptive response is important because memory can develop which means that a faster response can be mounted against a repeat exposure from the pathogen. The adaptive immune system is comprised of the cellular and humoral arms; T-cells are part of the cellular response and there are many different subtypes that have a variety of

different roles, including producing cytokines to activate other cell types. B-cells are part of the humoral immune response and responsible for the production of antibodies, that can recognise pathogens after a repeat exposure.

1.1.3.2.1. T-cells

It is widely recognised that a T-cell response is important in controlling MTB infection, especially T-helper cells (Th), although Tc, Th17 and Tregs have been implied to have a role. Th cells are characterised by the CD4+ ligand and circulate as naïve cells until activated, by interaction with antigen presented by an MHCII ligand on an APC. The two main Th subsets are Th1 and Th2 cells. Th1 cells are characterised by producing pro-inflammatory cytokines including IFNγ, TNFα and IL-2, whereas Th2 cells are anti-inflammatory and produce cytokines IL-4, IL-5 and IL-10 (Kidd 2003).

Evidence for the importance of T-helper CD4+ cells comes in part from HIV infected individuals, who have a decreased number of CD4+ cells and are far more susceptible to TB. TB is the biggest killer among those with HIV (Kalsdorf *et al*. 2009) and it is reported that approximately 20% of individuals infected with MTB are co-infected with HIV, ranging from 6.2% in Europe to 40% in Africa (WHO 2014a). After retroviral therapy for HIV, CD4+ counts increase and susceptibility to TB decreases, which further supports the essential role of CD4+ T-cells in controlling TB infection (Gideon & Flynn 2011). Th1 cytokines such as IFNγ have been shown to be essential in controlling MTB disease progression, and IFNγ knock-out mice are very susceptible to TB (Di Pietrantonio & Schurr 2005). This is because IFNγ classically activates macrophages and influences formation of the granuloma structure to control the MTB infection (Ehrt & Schnappinger 2009). However, IFNγ production alone does not correlate with protection and may actually correlate better with

bacterial load (Abebe *et al*. 2006). Evidence for this comes from studies that showed that mycobacterial inhibition by BCG vaccinated individuals did not correlate with IFNγ production and that mice with depleted IFNγ could control TB by CD4+ cells using other mechanisms including reactive nitrogen species (Abebe 2012). Other Th1 cytokines that are considered to have a part in MTB control are IL-2 and TNFα. IL-2 is thought to enhance memory cell development (Malek & Castro 2010) and TNFα is a proinflammatory cytokine and those with arthritis taking treatment to inhibit TNFα production are more susceptible to TB (Lin *et al*. 2010). Polyfunctional T-cells, producing more than one cytokine (IFNγ, TNFα, IL-2) are supposedly better effector cells and are more long lived (Kaveh *et al*. 2011).

Cytotoxic T-cells (Tc) are characterised by the CD8+ ligand, and interact with MHCI presented peptides. MHCI has the potential to be present on all cells, and when a cell is infected, pathogens peptides are presented by MHCI to the CD8+ T-cell. The Tc can then produce perforin and granzyme B, which enter the cell and activate apoptosis (Harty *et al*. 2000). Tc cells can also activate apoptosis by binding to the Fas receptor and stimulating apoptosis pathways (Harty *et al*. 2000). Tc cells can produce Th1 cytokines that can activate macrophages and neutrophils. including IFNγ, IL-2 and TNFα (Lepone *et al*. 2010). The importance of Tc cells in MTB control had been suggested by Chen *et al* that demonstrated that primates with depleted CD8+ cells had more severe disease than naïve animals (Chen *et al*. 2009). In adoptive transfer studies in mice, it was also demonstrated that when Tc was given to $Rag1^{-/-}$ mice (deficient in B-cell and T-cells), they had lower bacterial burdens in the spleen when challenged with BCG, which suggested that they had a role in preventing dissemination of disease (Feng & Britton 2000).

Th17 cells are thought to be important in TB infection as it has been shown that their presence will accelerate the initial response because IL-17 recruits other leukocytes, such as neutrophils to the site of infection and can enhance Th1 responses (Khader & Cooper 2008; Wareham *et al*. 2014).

Tregs regulate inflammation and control the balance of the immune response by producing IL-10 and influences Th1 and Th2 cells (Sojka *et al*. 2008). In non-human primates (NHP) it has been shown that Tregs are recruited to the airways soon after TB infection. It was also found that those NHPs that developed latent TB had higher numbers of Tregs before challenge compared to those that developed active TB (Gideon & Flynn 2011). This could indicate that a controlled, rather than solely proinflammatory response is important in modulating disease.

γδ T-cells are a small T-cell subset that have a γδ T-cell receptor (TCR) rather than a conventional αβ TCR. The TCR is involved in antigen recognition when presented by the MHC complex. γδ T-cells are unrestricted and do not interact with the MHC complex, but instead are activated by microbial phosphoantigens. γδ T-cells have been implicated in TB because they increase after infection and produce IFNγ, but in knock-out mice studies, the disease progression has been similar. γδ T-cells are thought to have an immunoregulatory role and an involvement in granuloma formation (Boom 1999).

1.1.3.2.2. Humoral response

B-cells produce antibodies that are specific for particular pathogens. B-cells are activated in the lymph nodes, in what is known as the germinal centre reaction. Once an antigen is brought there by an APC, naïve B-cells proliferate and undergo somatic hypermutation to produce antibodies that are high affinity to

the antigen. The cells then differentiate into B-cells and plasma cells which circulate until activated by pathogen recognition. Antibodies are important for immune responses to extracellular pathogens because they recognise and bind the pathogen, which then can either activate the complement cascade or phagocytosis by opsonising the pathogen and interacting with Fc receptors.

Since MTB is an intracellular pathogen the humoral response is not considered to have a significant role in TB protection and disease progression (Abebe & Bjune 2009). Although B-cells have been overlooked, there is some evidence to suggest that B-cells are important because B-cell knock out mice were shown to have higher bacterial burden than control mice in a study by Vordermeier *et al*. The IFNγ responses were unaffected, and when administered BCG, the infection was reduced, implying that the cellular immune response was not affected but that B-cells were required for control of infection (Vordermeier *et al*. 1996). Passive immunisation using immune sera has also been shown to help SCID mice control infection when used as an immunotherapy (Guirado *et al*. 2006).

To summarise, the immune response towards MTB is complex and not completely understood. Studies analysing biomarkers of active disease have provided clues to what components characterise immune responses to TB (Joosten *et al*. 2013), but what a protective immune response comprises of has not been defined, which makes vaccine development difficult.

1.1.4. TB vaccines

1.1.4.1 BCG

BCG is an attenuated form of *M. bovis*, which was developed in the early 20th century by Calmette and Guérin at the Pasteur Institute in Paris (Behr & Small 1999). It is the only licensed vaccine for TB and has been in use since the 1920's. The use of BCG is promoted by the WHO and 157 countries worldwide vaccinate with BCG at birth (Zwerling *et al*. 2011). There are several different strains of BCG in use across the world because they have diverged over time from the original stock (Behr & Small 1999).

BCG appears to be effective in preventing serious disease in children, including tubercular meningitis and miliary TB, but whilst BCG can be an effective vaccine and is able to induce Th1 responses, the immunity is not sterilising, and only helps to control disease (Andersen & Woodworth 2014). Protective ability is reduced in adults and appears to decrease over 10-15 years. This is thought to be because BCG preferentially stimulates production of terminally differentiated effector T-cells rather than memory T-cells (McShane *et al*. 2012). BCG efficacy also varies according to geographical location; in the UK the effectiveness is reported to be 80%, whereas in Malawi it is as low as 0% (Black *et al*. 2002). The reasons for this are unclear, but could be due to increased exposure to environmental *Mycobacteria* species in some areas (McShane *et al*. 2012). Other factors that could contribute to this difference geographical efficacy are the variation in BCG strain used, and at what age vaccination is given. One other reason why BCG shows poor efficacy could be because it is attenuated and missing a large number of MTB antigens, which could be important in stimulating a relevant immune response (Andersen & Woodworth 2014).

BCG is a live vaccine and is generally safe, but for immunocompromised persons it can cause disease (Hawkridge & Mahomed 2011). This is particularly a problem in areas where AIDS is prevalent and HIV co-infection with TB is an issue.

1.1.4.2. TB Vaccine formulations

The WHO initiated the 'Stop TB' Strategy, which aims to eradicate TB by 2050, and one of the goals is to develop novel TB vaccines (WHO 2010). As a result, there are many new vaccines under clinical evaluation **(Table 1-1)**, many of which are either based on BCG or use BCG in a prime-boost regimen because BCG does show some efficacy and is widely used. BCG is able to generate cells that are responsive to mycobacterial antigens, but its ability to limit MTB growth in the lungs is poor (Cooper 2009). The immune responses to BCG are not well understood, so it is unclear how a protective immune response is generated, which makes vaccine development in this area difficult (McShane *et al*. 2012).

BCG has been in use for a long period of time so it is likely that BCG will be involved in a new TB vaccination strategy, either as a recombinant form, or used in a prime-boost regimen **(Figure 1-2)**. Any completely novel vaccine would have to be proven to be more efficacious than and as safe as BCG therefore replacing BCG would be challenging. It is estimated that 85% of the world are vaccinated with BCG (McShane *et al*. 2012) and it would be difficult to assess what effect a new vaccine would have without the interaction with BCG.

Many vaccines focus on using a particular MTB antigen to stimulate a specific response. The choice of MTB antigen is challenging, and can be based on immunogenicity, functional role of the antigen or expression stage during MTB infection (Andersen & Woodworth 2014). However, these characteristics do not

Table 1-1. Vaccines in clinical trials as reported by the 'Stop TB' Partnership (2011).

Phase I	Phase II	Phase IIb	Phase III
AdAg85A McMaster University	M72-A501 GSK, Aeras	MVA85A/AERAS-485 OETC, Aeras	Mw (M. indicus pranii (MIP) Dept of Biotechnology (India), M/s. Cadila
Hybrid I+CAF01 SSI, TBVI	VPM 1002 Max Plank, Vakzine, Projekt Mgmt, TBVI	AERAS-402/Crucell Ad35 Crucell, Aeras	
Hyvac 4/AERAS-404+IC31 SSI, Sanofi Pasteur, Aeras, Intercell	Hybrid-1+IC31 SSI, TBVI, EDCTP, Intercell		
AERAS-422 Aeras	RUTI Archivel Farma, SL		

TB Vaccines and the companies that are producing and testing them. Phase I trials involve small numbers of healthy volunteers to test the safety, Phase II is larger and measures positive outcomes in the target group, whereas Phase III are large scale trials and compare the drug or vaccine to a placebo and best available treatment (NHS 2014b).

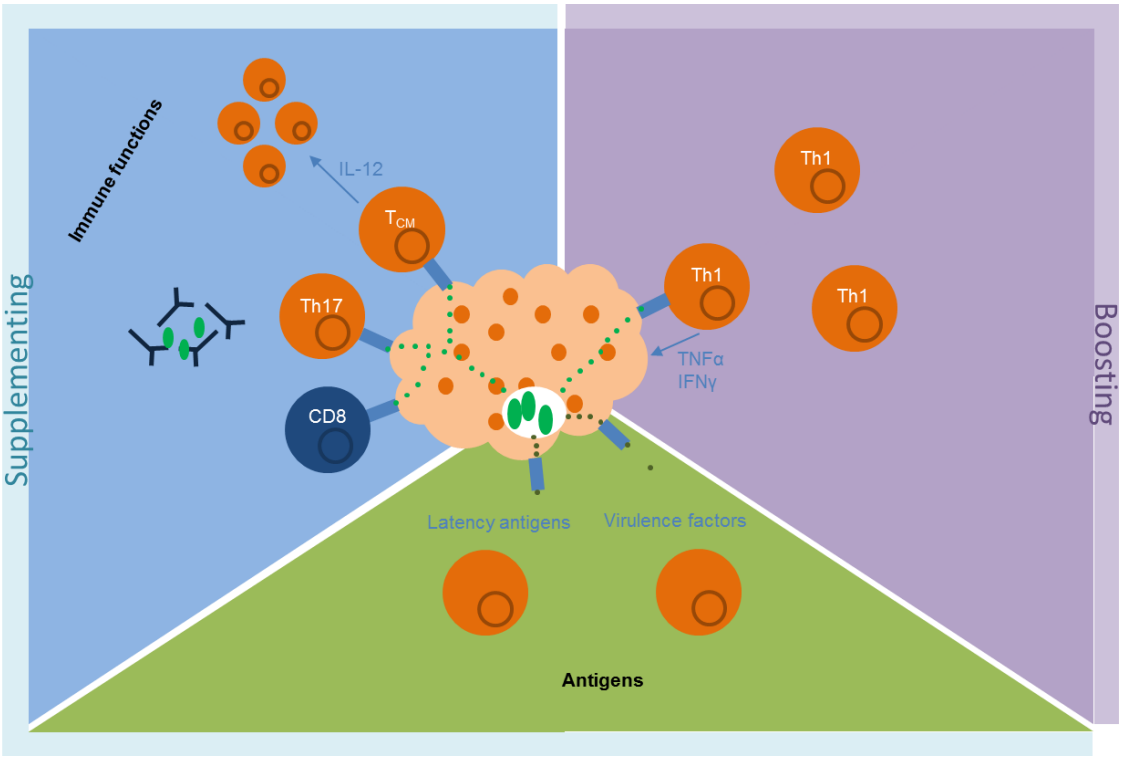

Figure 1-1. Strategies under investigation to improve BCG immunity. The main strategy is to boost Th1 responses (purple). BCG could also be supplemented with other antigens that are missing from BCG that would improve the ability of T-cells to recognise MTB (green). Supplementation of the T-cell response by enhancing T central memory cells (T_{CM}), Th17 or CD8+ cells or improving antibody production could improve the early immune response and long-term memory (blue). Adapted from (Andersen & Woodworth 2014)

always correlate with the generation of a successful protective immune response and it is difficult to find a single antigen, which provides consistent and comparable protection to BCG. There are several formats for subunit vaccines delivering antigens including DNA vaccines, protein vaccines and viral vectors (e.g. adenovirus and MVA) (Checkley & McShane 2011). Other strategies for novel TB vaccines are investigating the delivery route of TB antigens and the use of mucosal vaccination because TB is a pathogen that primarily affects the lungs and stimulating specific immune responses here could be key (White *et al*. 2013; Stylianou *et al*. 2013).

One of the major difficulties in TB vaccine discovery is that there is no biomarker of protection, which means that TB vaccines require clinical trials to assess efficacy in the field because there is no other way of testing protection (Hawkridge & Mahomed 2011). However, considerable investigation is being undertaken into the immune response to TB, as discussed above and to discovering what characterises a defensive memory response. The MVA85A boost vaccine, which was developed at Oxford University, has been shown to stimulate the production of polyfunctional T-cells, which are considered to be important for disease control (Odutola *et al*. 2012). This vaccine has reached Phase IIb clinical trials, but the current study showed no significant benefit in the vaccine (Tameris *et al*. 2013). This illustrates the difficulties of working with TB, even after animal studies (Sharpe *et al*. 2010; White *et al*. 2013) and clinical trials, the vaccine still may not provide significant protection. Clinical studies are also long because it can take years for disease to develop and therefore are also costly.

1.2. *Bacillus subtilis*

B. subtilis is a spore forming Gram-positive bacterium from the *Bacillus* genus. The *Bacillus* genus comprises around 69 species, which can be clustered into three or four groups. *B. subtilis*, *B. lichenformis, B. coagulans, B. cereus, B. thuringiensis* and *B. anthracis* are all part of one group, and are similar to one another according to 16S ribosomal typing (Oggioni *et al*. 2003). *B. subtilis* is a well characterised *Bacillus* species and is used as a model prokaryote to understand gene regulation of other spore forming bacteria (Nicholson & Setlow 1990).

B. subtilis is not a pathogen and is used as a probiotic in animal feed. Probiotics are defined as "live microbial feed supplement which beneficially affects the animal host by improving its intestinal microbial balance" (AFRC 1989). The beneficial outcome of *B. subtilis* as a probiotic has prompted investigation into its positive effects on the immune system and use as a vaccine adjuvant.

1.2.1. *B. subtilis* life cycle and spore formation

B. subtilis exists is a vegetative form when conditions are favourable and appears as a rod shaped organism, which can exist in various niches including soil, and the mammalian and insect gut (Nicholson 2002; Huynh A. Hong *et al*. 2009). During vegetative growth, *B. subtilis* replicates by binary fission **(Figure 1-3)** whereby the chromosomes replicate and the cell grows and divides in the middle (Angert 2005).

Sporulation of *B. subtilis* is initiated under nutrient limited conditions. The spores enter into a dormant phase of the life cycle and develop a proteinaceous coat that makes them resistant to heat and chemical assault. In brief, the steps that the bacteria undergo to form spores are as follows **(Figure 1-3)**; two copies of

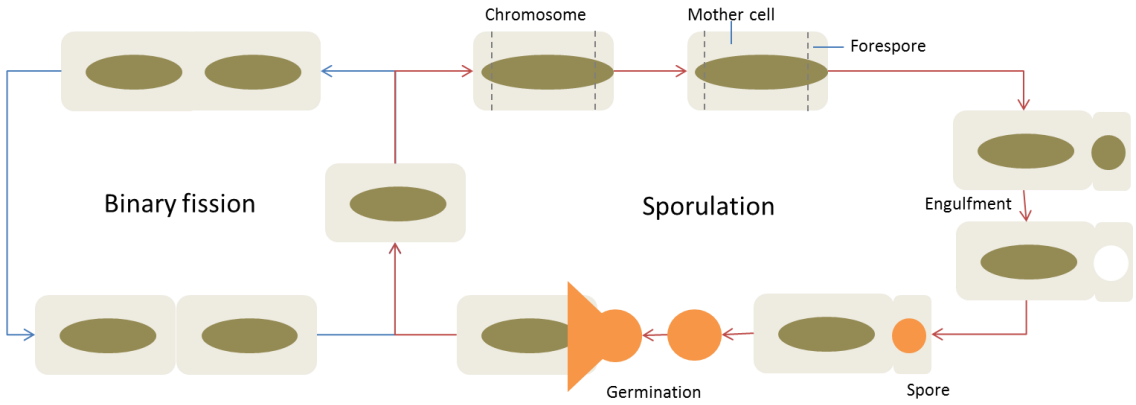

Figure 1-2.Schematic of the life cycle of *B. subtilis* Binary fission of the vegetative cell by replication of the chromosome and division. Sporulation in nutrient limited conditions. The chromosomes stretching between poles, creation of forespore and mother cells and engulfment of forespore. Creation of spore and lysis of mother cell to release spore. Germination of spore in favourable conditions. Based on (Angert 2005).

the chromosome stretch between the poles of the bacteria but cell division occurs only at one end of the cell. Part of one chromosome is trapped by the division septum, and is packaged into a smaller cell called the forespore. This is then engulfed by the larger mother cell, which nurtures and prepares the forespore for dormancy. This requires the DNA to be protected, the cell cytoplasm to be mineralised and the protective coat to be produced (Angert 2005). The spore coat itself is created by the forespore and the mother cell. The inner coat produced by the forespore has two layers consisting of a germ cell wall and the cortex, which is responsible for the dehydrated state of the spore. The mother cell creates the outer coat, which also has two layers. Once the spore coat has been created, the mother cell lyses to release the spore. The creation and assembly of the spore coat is under the regulation of sigma factors, which control the timing of the creation and release of the spore. Sporulation takes approximately eight hours to complete (Driks 1999). When spores return to favourable conditions, they germinate and become vegetative cells again (Angert 2005).

1.2.2. Immune responses to spores and their use as a vaccine adjuvant

B. subtilis spores have been shown to have adjuvant properties both as killed microparticles and as live delivery vehicles (L. H. Duc *et al*. 2003; Song *et al*. 2012). The use of spores as a vaccine was first demonstrated with heat attenuated *B. anthracis* spores to protect against anthrax infection in animals, in the 1880's. *B. anthracis* spores were found to be protective, but formulations gave variable protection and so were discontinued and replaced with an acellular vaccine (Turnbull 1991).

Other particles such as liposomes and nanoparticles have also been investigated as vaccine and drug delivery vehicles and adjuvants. The

advantage of using microparticles is that they are of a similar size to pathogens so they are readily processed by the immune system using the same mechanisms. Spores have an advantage over nanoparticles because they are bioparticles and their safety is well characterised because of their use as a probiotic (Hong *et al*. 2005; Cutting *et al*. 2009), whereas nanoparticles are not natural and their deposition and pharmacokinetics is not fully understood (Cho *et al*. 2009; Moghimi *et al*. 2012). Spores would also be an attractive vaccine adjuvant because they are heat stable, and therefore would be convenient to transport and store (L. H. Duc *et al*. 2003; Amuguni & Tzipori 2012).

Spores can be used as a non-recombinant or recombinant antigen delivery microparticle. As a non-recombinant vaccine, hydrophobic and electrostatic interactions between the *B. subtilis* spore and antigen of choice provide a stable delivery vehicle. Both live and dead spores can be used for this purpose, with little difference to the stability or effect (Huang, Hong, *et al*. 2010; Song *et al*. 2012; de Souza *et al*. 2014). Spores carrying H5N1 Influenza particles have been tested in mice and have been found to confer full protection to challenge with H5N1 (Song *et al*. 2012).

Spores can also be genetically modified to carry heterologous antigens (Duc *et al*. 2004). Antigens can be fused to coat proteins (CotB and CotC are commonly used) so that they are surface expressed (Mauriello *et al*. 2004). Tetanus Toxin Fragment C (TTFC) has been successfully expressed and tested in the mouse model and found to provide protection against challenge with tetanus toxin (Le H. Duc *et al*. 2003).

Although *B. subtilis* is a model organism and is well characterised genetically, the immune responses to *B. subtilis* are not well known because it is non-

pathogenic, therefore there has been little interest in its interactions with the mammalian immune system. However, *B. anthracis* is the causative agent of anthrax infection, which can be highly pathogenic, so there has been much investigation into how *B. anthracis* causes disease. Because *B. anthracis* is related to *B. subtilis*, the mechanisms may be similar and information about *B. anthracis* could be used as a guide for *B. subtilis* interactions. *B. anthracis* spores are taken up by alveolar macrophages (AM) that produce proinflammatory cytokines but later in infection, lethal factor (LF) toxin production causes immunosuppression and IL-10 is produced by the host which then downregulates TNFα and IL-1β (Shetron-Rama *et al* 2010). The macrophages lyse and the bacteria are released into the bloodstream (Guidi-Rontani *et al*. 1999), where they cause bacteraemia, leading to oedema, haemorrhage and death. DCs containing *B. anthracis* move to the lymph nodes (LN) within five to twelve hours of infection, and this migration is dependent upon DCs since DC knockout mice had no bacteria in the lymph nodes (Shetron-Rama, *et al* 2010). Although information about infection with *B. anthracis* can provide some useful guidance as to potential interfaces of *B. subtilis* with the host, they are quite different organisms, as *B. anthracis* produces toxins and has an exosporium, which are thought to be important in their adherence and persistence, which could mean that there are differences in host interactions between *B. anthracis* and *B. subtilis*.

B. subtilis has been shown to interact with macrophages *in vitro* (Huang, Ragione, *et al*. 2008; Duc *et al*. 2004; Ceragioli *et al*. 2009). *B. subtilis* spores have also been shown *in vitro* and *in vivo* to cause maturation of DCs, which may also affect the DCs antigen presenting capacity (Song, H. A. Hong, *et al*. 2012, de Souza *et al*., 2014). When delivered orally, Rhee *et al* (Rhee *et al*.

2004) reported that *B. subtilis* spores in the appendix of rabbits were taken up by M cells, so they could then be presented to underlying tissues and leukocytes.

Several studies using *B. subtilis* spores as vaccines in the murine model have indicated that spores induce a Th1 response. IFNγ, a classic Th1 cytokine has been shown to be increased after vaccination along with other proinflammatory cytokines (Song *et al*. 2012; Huang, La Ragione, *et al*. 2008; Duc *et al*. 2004). However, other papers have shown that spores are able to illicit a balanced Th1/Th2 response (Andrew G. C. Barnes, Vuk Cerovic & Peter 2007).

Antigen-specific antibody production has been demonstrated in numerous studies **(Table 1-2)**. The increases in IgG1 and IgG2a, which are subclasses of IgG that indicate Th2 or Th1 responses in mice, respectively, also add to evidence that the spores elicit a balanced immune response (Song *et al*. 2012; Huang, Hong, *et al*. 2010; L. H. Duc *et al*. 2003). Protection against infection has also been demonstrated in several studies in different animal models with different delivery routes **(Table 1-2)**.

If the vaccine is for a mucosal pathogen such as MTB, a successful vaccine should elicit production of mucosal associated IgA. Secretory IgA has been demonstrated to be increased when mice were dosed with spores in several studies (L. H. Duc *et al*. 2003; Uyen *et al*. 2007; Huang, Hong, *et al*. 2010; Permpoonpattana *et al*. 2011; Isticato, Sirec, Treppiccione, *et al*. 2013; Amuguni *et al*. 2011).

The innate immune response was implicated in protection against influenza challenge when spores with no associated influenza antigen were dosed to mice and there was 100% protection after challenge (Song *et al*. 2012). In the

Table 1-2. Examples of some of the studies that have demonstrated antigen-specific increases in antibody production and/or protection after immunisation with *B. subtilis*.

Pathogen	Vaccine delivery route	Model organism	Antibody detected	% Protection	Publication
C. difficile	Oral	Hamster	Yes	75	(Permpoonpattana *et al*., 2011)
Influenza	Nasal	Mouse	Yes	100	(Song *et al*. 2012)
Tetanus	Sublingual	Mouse	Yes	100	(Amuguni *et al*. 2011)
	Oral	Mouse	Yes	100	(L. H. Duc *et al*. 2003)
	Oral	Mouse	Yes	-	(Ciabattini *et al*. 2004)
	Nasal	Mouse	Yes	-	(Uyen *et al*. 2007)
	Oral and Nasal	Mouse	Yes	- 90	(Huang, Hong, *et al*. 2010)
	Oral	Mouse	Yes	-	(Mauriello *et al*. 2004)
B. anthracis	Injection	Mouse	Yes	100	(Duc *et al*. 2007)
White spot syndrome virus	Oral	Shrimp	N/A	65	(Nguyen *et al*. 2014)
	Oral	Crayfish	N/A	50	(Ning *et al*. 2011)
C. sinensis	Oral	Rat	Yes	45	(Zhou *et al*. 2008)
	Oral	Mouse	Yes	-	(Qu *et al*. 2014)
***E. coli* LT**	Nasal	Mouse	Yes	-	(Isticato, Sirec, Treppiccione, *et al*. 2013)
Helicobacter acinonychis	Oral	Mouse	Yes	-	(Hinc *et al*. 2014)
HIV	Injection	Mouse	Yes	-	(de Souza *et al*. 2014)

same study, the innate immune mechanisms were examined further. It was found that there was an infiltration of NK cells to the lungs 24h after immunisation and that spores increased DC maturation *in vitro* (Song *et al*. 2012). Interestingly, TLR expression was upregulated *in vitro* (Song *et al*. 2012). An earlier study also supported that TLR2 and TLR4 were up regulated *in vitro* by live spores in macrophages following 6h cell culture as measured using RT-PCR (Huang, La Ragione, Nunez, & Cutting, 2008).

Work by de Souza *et al* has investigated the adjuvant properties of *B. subtilis* spores when delivered subcutaneously (de Souza *et al*. 2014). They tested live vs heat inactivated spores, to identify whether this had an effect on the immune responses stimulated. de Souza *et al* used a HIV antigen; gag p24 either adsorbed to the spore surface or in recombinant form and found that recombinant and adsorbed were both able to generate antibody responses, and that there was little difference between live and dead spores. However, live spores were better at enhancing DC maturation, which could affect cellular responses. de Souza *et al* found that TLR2 was important for the generation of antibody responses by spores using knockout mice. This adds evidence that spores are an immune-potentiator class of adjuvant. The work by de Souza *et al* is also important because it characterised responses using two strains of mouse: BALB/c and C57BL/6, which are said to have a Th2 and Th1 bias respectively, and showed that the spores generated similar immune responses in both strains and were unaffected by the genetic background of the host (de Souza *et al*. 2014).

1.3. Aims

The central objective of this project was to further investigate the potential use of *B. subtilis* spores as a mucosal vaccine adjuvant. The first project aim was to investigate how *B. subtilis* spores carrying antigens Ag85B-Acr and MPT64 could protect against infection with MTB in mice. Two different strategies were tested. One scheme used heat killed spores carrying Ag85B-Acr or MPT64, or both proteins bound to the surface of the spores. The second approach was to use recombinant spores expressing MPT64 that were inactivated using formaldehyde.

The second project aim was to examine how spores, when delivered mucosally were initially taken up by the host. A comparison of sublingual, oral and nasal administration routes were used, and the lungs, NALT and gut tissues were investigated as the prime target sites. The cells that were monitored were M cells, DCs, macrophages and neutrophils. The final project aim was to profile the innate immune response to spores after intranasal dosing. The cells chosen for analysis were macrophages, DC, neutrophils and NK cells and TLR2 and TL4 expression was investigated. Cytokine production and complement killing was also monitored.

1.4. Hypotheses

1. Can *B. subtilis* spores carrying TB antigens protect against challenge with MTB in the murine model?
2. Will the quantity of spores that are able to enter the lung, gut and NALT vary between nasal, sublingual and oral dosing?
3. Will the types of cells that initially interact with spores vary depending on location and dosing route?
4. Will the interactions be different between live and autoclaved spores?
5. After nasal dosing, will certain cells and innate immune characteristics be activated in the mucosal and systemic immune system compartments?

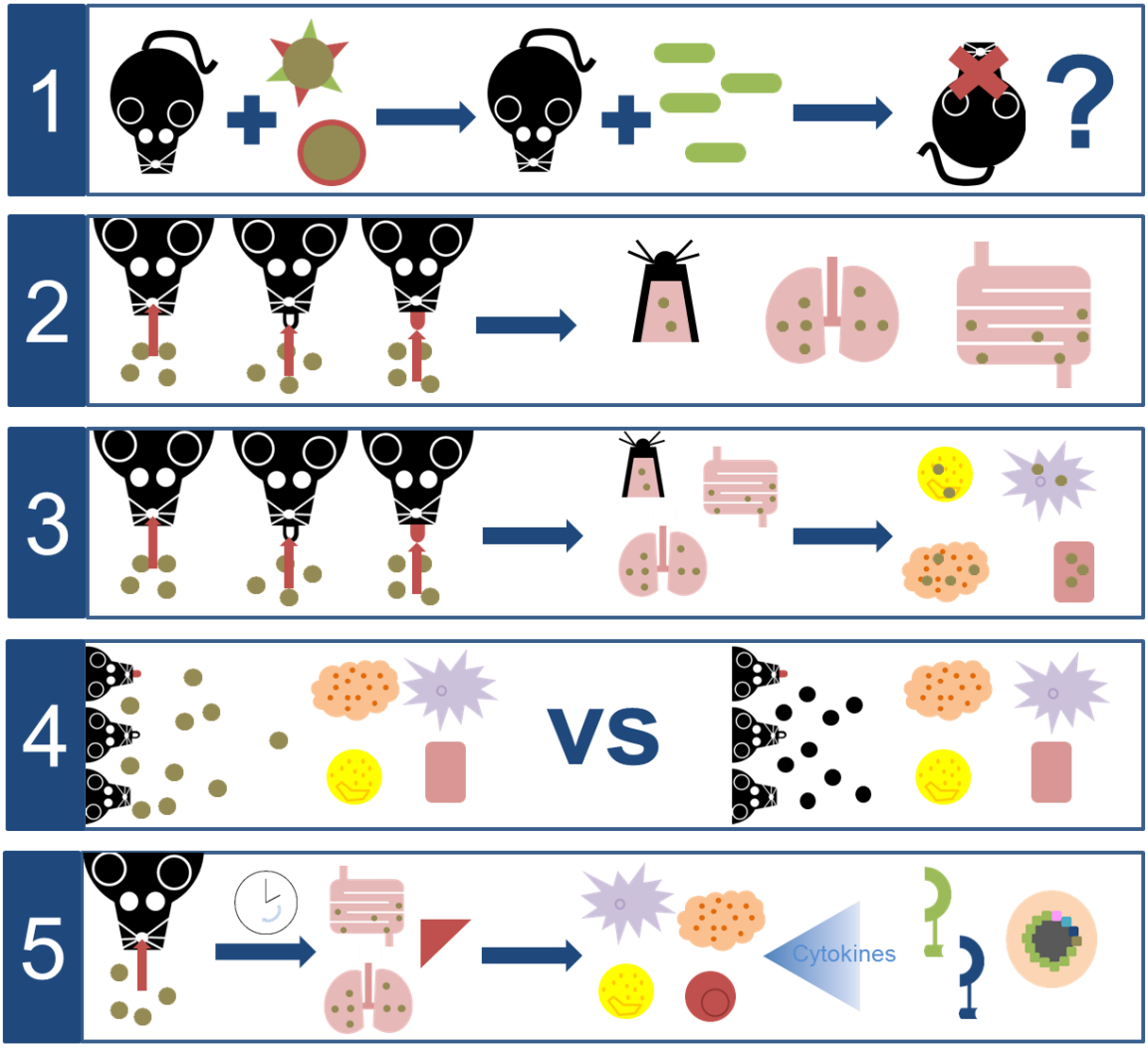

Figure 1-3. Diagram to illustrate the hypotheses. 1) Mice were dosed nasally with non-recombinant (with spikes) or recombinant (red outline) spores and challenged with MTB (green) to see whether the spores provided protection, 2) Mice were dosed nasally, orally and sublingually and distribution of spores in the NALT, lungs and gut examined to determine differences, 3) Mice dosed nasally, orally and sublingually and determined differences in cell interactions in the NALT, lungs and gut, 4) Mice dosed nasally, orally or sublingually with either live or autoclaved spores to determine difference in cell interactions, 5) Mice dosed nasally and followed for seven days to assess the effect on the cell populations, cytokine production, TLR expression and complement killing ability assessed in different tissues (gut, lungs, spleen).

Chapter 2: Materials and Methods

2.1. Bacillus subtilis strains

HU58 is a non-domesticated strain of *B. subtilis* isolated from the human GI-tract (Huynh A Hong *et al*. 2009) and to which proteins were adsorbed to the spore surface. PY79 is a laboratory strain that is isogenic to the 168 strain (Zeigler *et al*. 2008). HU58 (*cotB-MPT64*) (rHU58(MPT64)) is a genetically modified strain of HU58 expressing the protein MPT64 on the spore surface via chimeric fusion to the coat protein CotB and was created at Cobra Biologics Ltd (Keele, UK) by Dr David Radford. This strain has resistance to erythromycin and lincomycin. DS127 (*cotC-GFP*) is the strain described by Isticato (Isticato *et al*. 2007) and expresses GFP on the spore surface by fusion with CotC. This strain has chloramphenicol resistance and is derived from PY79.

2.2. Culturing and purification of Bacillus subtilis spores

For spore production of all strains, strains were grown overnight on plates containing relevant antibiotics. A single colony was then used to inoculate Difco sporulation media (DSM) and incubated at 37 °C for 5-6 h. DSM agar was then inoculated with the culture and incubated at 30 °C for two days. Spores were then harvested, washed, and treated with lysozyme (Sigma-Aldrich, UK), followed by sequential washes with NaCl and KCl and then heat treatment (68 °C, 30 min) (Nicholson & Setlow 1990). The salt washes help clean the spores of residual membrane integuments while heat treatment kills any residual vegetative cells ensuring a preparation of pure spores. Aliquots were stored at -20 °C until use. For preparation of 'killed' spores, HU58 was autoclaved (121 ^{o}C, 15 psi, 30 min) before use.

2.3. MPT64 protein production and purification (Chapter 3)

MPT64 (26 kDa) expressed in *E.coli* BL21 carrying a pET28b expression vector (Novagen, USA) where MPT64 was fused to an N-terminal polyhistine (Yu & Cutting 2009). Cultures were grown in LB media and protein expression induced by Isopropyl β-D-1-thiogalactopyranoside (IPTG) and the cell free lysate passed through a nickel affinity binding column to bind poly-His-tagged recombinant MPT64 using the ÄKTA Prime system (GE Healthcare, UK). Purity was checked using SDS-PAGE electrophoresis and fractions were dialysed using PBS. Protein concentration was determined using the Bradford assay. Protein was concentrated further using VivaSpin20 columns (Sartorius, Germany) by centrifugation at 4500 *g* for 30 min – 3 h at 4 °C.

2.4. Ethics statement

Mice were housed and used in studies according to the Animals (Scientific Procedures) Act 1986, issued from the Home Office, UK. Studies at Royal Holloway University of London (RHUL) were carried out under licence number 70/7025 and those that were performed at St. George's Medical School (SGUL) using licences 70/6625 and 70/7490.

2.5. Production of antisera (Chapter 3)

C57BL/6 mice from Charles River (UK) were immunised by intraperitoneal injection three times with 2 µg protein over a period of six weeks. After a further two to eight weeks, mice were culled and terminally bled. Serum was separated from the blood by centrifugation at 10,000 *g* for 20 min. Antisera was purified using Protein G Spin Trap columns (GE Healthcare, UK).

2.6. Adsorption of protein onto spore surface (Chapter 3)

$2x10^9$ HU58 spores were aliquoted into eppendorfs and washed using PBS of the appropriate pH. 10 µg of protein was added and mixed gently. The mixture was incubated at room temperature (RT) for 30 min. The sample was then washed three times using the pH7 PBS. Detection of protein bound to the spores was detected using Western immunoblotting and immunofluorescence.

2.7. Spore coat extraction (Chapter 3)

$2x10^9$ spores were pelleted at 16,000 *g* for 2 min and spore coat extraction buffer added. Samples were incubated at 68 °C for 80 min. Spores were centrifuged for 10 min at 12,000 *g* and the supernatant collected.

2.8. Western blot of spore coat extracts (Chapter 3)

Spore coat was extracted for use in Western blot to detect bound protein and run on an SDS-PAGE gel at 200 V for 60 min. The fractionated samples were transferred to nitrocellulose membranes and probed with appropriate mouse anti-sera (anti-MPT64 or anti-Ag85B-Acr) diluted in 5 % milk in TBS buffer and incubated for 1 h at RT. Mouse anti-IgG-HRP conjugate was added diluted in 5 % milk in TBS buffer and incubated for 1 h at RT. Membrane developed using ECL membrane developing reagents (GE Healthcare, UK) and captured onto Amersham Hyperfilm ECL (GE Healthcare, UK).

2.9. Whole spore ELISA (Chapter 3)

Spores were diluted to $1x10^6$ spores/ml in PBS with 4% formaldehyde and used to coat a high binding ELISA plate for 2h at RT. The plate was washed with PBS and blocked with 4% BSA for 1h at 37°C. 1% BSA with 0.05% Tween20 and 4% FCS was added to the plate. MPT64 antisera at a 1/50 concentration was added to the top row and serially diluted 1:2 down the plate. Incubated for 1

h at 37 °C. Washed with PBS + 0.05 % Tween20. Anti-mouse IgG-HRP diluted 1:200 in 1 % BSA with 0.05 % Tween20 and 4 % FCS. Incubated for 1 h at 37 °C. Washed with PBS with 0.05 % Tween20 and colour developed for 5-15 min using 3,3',5,5'-tetramethylbenzidine (TMB) and reaction stopped using 2 M H_2SO_4 (both Sigma-Aldrich, UK).

2.10. Immunofluorescence of purified spores (Chapter 3)

Spores were washed with PBS and 20 µl aliquoted onto coverslips coated with 0.01 M poly-l-lysine (Sigma-Aldrich, UK) and incubated for 5 min. Excess liquid was removed and spores were left to dry. Spores were washed with PBS, then blocked with 2 % BSA (Sigma-Aldrich, UK) for 15 min and washed nine times with PBS. Primary antibody (antisera MPT64 or Ag85B-Acr) was added (1:500) and incubated at room temperature for 45 min. Slips were washed three times with PBS, then anti-mouse IgG-TRITC (1:200) (Sigma-Aldrich, UK) was added and incubated at room temperature for 45 min. Cover slips were washed three times with PBS and mounted onto slides and read with the Nikon Eclipse fluorescent microscope (Nikon, Japan) using the Cy3 laser (530-560 excitation) with 100 millisecond exposure.

2.11. Inactivation of spores with formaldehyde (Chapter 3)

Formaldehyde was supplied in a 37 % w/v solution (Sigma-Aldrich, UK) and was diluted to 4 % formaldehyde using sterile water. Spores were aliquoted into tubes, centrifuged (12,000 *g*, 2 min), supernatant discarded and resuspended in a formaldehyde solution. Samples were then incubated in a roller at either 37 °C for 24 h. Before dosing, spores were washed with PBS to remove formaldehyde.

2.12. Measurement of formaldehyde content using the HACH test (Chapter 3)

The supernatant from spores that had been inactivated with formaldehyde were tested for their formaldehyde content after washing with PBS. To wash, the spores were centrifuged at 12,000 *g* for two min, supernatant removed and replaced with new PBS and this was repeated twice. Formaldehyde concentrations were measured using the HACH formaldehyde detection kit (HACH, USA) according to the manufacturer's instructions. The 'formaldehyde 1 reagent powder pillow' was added to 1 ml of the sample diluted in dH_2O and swirled for 20 seconds. Two drops of thymolphthalein was added and mixed and the solution turned blue if formaldehyde was present. To assess the concentration of formaldehyde present 1.9 N sulphuric acid was added using a dropper and the drops counted until the solution turned clear. Each drop accounted for 0.5 % formaldehyde. For solutions from 0-1 %, 10 ml of solution was used and each drop of sulphuric acid accounted for 0.05 % formaldehyde.

2.13. Experimental design of TB Study (Chapter 3)

C57BL/6 mice (Charles River, UK) were used to test the efficacy and immunogenicity of MPT64 and Ag85B-Acr. At week zero, mice receiving BCG (groups B, G and I) were vaccinated with $5x10^5$ CFU of BCG Pasteur (from Rajko Reljic at SGUL). At week three, the groups that had not received BCG, were administered their first dose of protein/spores intranasally. All mice were anaesthetised using isoflurane for dosing. The amount of protein in the doses was 10 µg. The number of spores per dose was $2x10^9$. At week six, all groups received a second dose and at week nine, all groups received their third immunisation. Two mice from each group were culled by CO_2 for immunogenicity experiments. Eight mice from each group were transferred to

SGUL to be challenged intranasally with $5x10^5$ CFU H37Rv MTB. After four weeks, all mice were culled and lungs and spleen homogenised and plated onto 7H11 agar (Difco, BD, UK) and grown at 37 °C for 28 days to estimate the bacterial burden in the organs.

2.14. IFNγ ELISPOT (Chapter 3)

IFNγ ELISPOT was carried out using a kit and used according to the manufacturers recommendations (Mabtech, Sweden). Polyvinylidene fluoride (PVDF) 96-well plates were coated with coating antibody in PBS and incubated at 4 °C overnight. $5x10^5$ splenocytes were added to wells along with antigens MPT64 (10 µg/ml), Ag85B-Acr (10 µg/ml), PPD (purified protein derivative) (20 µg/ml) (Statens Serum Institute, Denmark) or positive control mitogens PMA (phorbol 12-myristate 13-acetate (Sigma-Aldrich, UK)) (10 µg) and Ionomycin (1 µg) (Sigma-Aldrich, UK) in 100 µl DMEM media supplemented with 20 % FCS, penicillin, streptomycin, 2-mercaptoethanol and L-glutamine (all Sigma-Aldrich, UK). Plates were incubated at 37 °C in a CO_2 incubator overnight. Plates were washed and primary antibody added (1:1000) and incubated at RT for 2 h, washed and Streptavidin-ALP (1:1000) added and incubated for 1h at RT. Plates were washed and developed using BCIP/NBT (5-bromo-4-chloro-3-indolyl-phosphate/nitro blue tetrazolium) for 25 minutes until spots developed. Plates were counted using CTL reader (CTL, Germany). Media only wells were subtracted from antigen stimulated wells and Spot Forming Units (SFU) were calculated per 10^6 cells using Microsoft Excel (Microsoft, USA).

2.15. DS127 spores detection of fluorescence (Chapter 4)

Approximately $1x10^8$ DS127 spores were added to a cover slip coated with 0.01 % poly-l-lysine, incubated at RT for 45 minutes and washed seven times with PBS. The coverslip was mounted onto a microscope slide and observed using the FITC band pass filter (475 – 490 excitation) on a Nikon Eclipse Ti fluorescent microscope.

2.16. Experimental design – DS127 spores intranasal dosing (Chapter 4)

Studies were performed using six to eight week old C57BL/6 mice (Charles River, UK). Mice were sedated using isoflurane and immunisations were given by the intranasal route. DS127 spores were given at a concentration of $2x10^9$ spores/dose. Mice were euthanized using CO_2 and lungs were fixed in 10% neutral buffered formalin (NBF) and sent to TUPI Ltd for histological processing and half were stained with haematoxylin and eosin (H&E) stain. The stained samples were examined using a Nikon microscope at 100 x magnification to look for spores in the tissue. The unstained samples were read using a confocal microscope at SGUL, by Dr Andreas Hoppe (from Kingston University, London).

2.17. Infection of RAW267.4 macrophages with DS127 spores (Chapter 4)

RAW267.4 macrophages were grown for two days on coverslips coated with 0.01 % poly-l-lysine until confluent. Wells were then infected with approximately $1x10^6$ DS127 freeze dried spores and incubated at 37 °C for 30 min. Supernatant was then removed, cells washed with PBS and fixed with 4 % formaldehyde. 4',6-diamidino-2-phenylindole (DAPI) (Sigma-Aldrich, UK) was used to stain the macrophage nuclei. Slips were mounted onto slides and read using the EVOS fluorescent microscope (Life Technologies, UK) using the blue and green laser blocks.

2.18. Experimental design of localisation of spores after different routes of dosing with spores (Chapter 4)

Studies were performed using six to eight week old Balb/c mice (Charles River, UK). Mice were sedated with isoflurane before dosing. All mice were given $2x10^9$ HU58 spores, but the volumes varied for the dosing routes. Nasal immunisation spores were in 30 µl, sublingual dosing in 9 µl and oral dosing using 100 µl. 6 h and 24 h after dosing, six mice were culled using CO_2 and the lungs, gut and NALT removed from each mouse. The set of lungs and gut from one mouse per group were incubated with 10 % (v/v) NBF at room temperature for 48 h. The other tissues were used for flow cytometric analysis.

2.19. Isolation of single cells from the mouse spleen and lymph nodes

Spleen was removed from mice culled by CO_2 and placed in DMEM supplemented with 10 % FCS, penicillin/streptomycin and L-glutamine. The spleen was pushed through a 70 µm cell sieve and the cells collected and centrifuged at 400 *g* for 10 min. Spleen cells were resuspended in red blood cell lysis solution (Sigma-Aldrich, UK) and incubated at room temperature for 5 min. Cells were washed with media and then resuspended for counting. Cells were diluted 1/10 in media for counting with the Millipore Sceptre cell counter (Millipore, Germany).

2.20. Isolation of single cells from the mouse lungs and gut

The lungs and gut were removed from mice culled by CO_2 and placed in DMEM supplemented with 10 % FCS, penicillin/streptomycin and L-glutamine. Tissues were homogenised using the GentleMACS (Miltenyi Biotec, Germany). Collagenase and DNAse (both Sigma-Aldrich, UK) were added and tissues were incubated for 37 ºC in the gyrorotarory shaker for 30 min. The tissues

were homogenised again with the GentleMACS and then the cells were put through a 70 µm cell sieve and the cells collected and centrifuged at 400 *g* for 10 min. Lung cells were resuspended in red blood cell lysis solution (Sigma-Aldrich, UK) and incubated at room temperature for 5 min. Cells were washed with media and then resuspended for counting. Cells were diluted 1/10 in media for counting with the Millipore Sceptre cell counter.

2.21. Experimental design of innate immunity study (Chapter 5)

Studies were performed using six to eight week old Balb/c mice (Charles River, UK). Mice were sedated with isoflurane before dosing. All mice were given $2x10^9$ HU58 spores suspended in 30 µl water for dosing. The experiment was carried out twice. The first time, at days one, two, three, four and seven after immunisation, three mice were culled, plus one naïve mouse using CO_2 asphyxiation and the lungs, gut and spleen were removed and placed in DMEM 10 % FCS ready for processing. In the second experiment, six mice were culled on days one, two, three, four, and seven and the lungs, gut, spleen, peripheral lymph nodes (axillary, inguinal, thymus) and the NALT tissue was removed. The NALT tissue was washed in DMEM 10 % FCS media and then each NALT was put into a well of a 24-well plate in 250 µl media and incubated at 37 °C 5 % CO_2 for 48 h before collecting the supernatant for detecting cytokines. The other tissues were homogenised and single cells isolated as described elsewhere in the methods (2.20, 2.21) and used for flow cytometry staining. $5x10^5$ splenocytes from each mouse were also used to seed a 96-well plate and incubated at 37 °C 5 % CO_2 for 48h to collect supernatants for detecting cytokines.

2.22. Flow cytometric analysis of samples from experiment of localisation of spores after different routes of mucosal immunisation (Chapter 4)

After isolation of single cells from the lungs, gut and NALT, $1x10^6$ cells were used for staining. Cells were centrifuged at 200 *g* for 10 min and washed in 10 % FCS. Cells were resuspended in 10 % FCS and antibodies added according to titration results. Two panels were used i) Macrophage F4/80-PerCP (clone BM8, Biolegend, UK) and Dendritic cells CD11c-APC (clone N418, Miltenyi, Germany) and ii) Neutrophils Ly6G-APC (clone 1A8, Miltenyi, Germany) and M cell (clone NKM 16-2-4-PE, Miltenyi, Germany). The cells were then incubated with Cytofix (BD Biosciences, UK), washed and then incubated with PermWash (BD Biosciences, UK). All further wash steps used PermWash solution. The spores were detected using anti-spore rabbit antibody (generated at RHUL) followed by a secondary antibody, anti-rabbit IgG-FITC (Sigma-Aldrich, UK). Samples were then analysed using the BD Accuri C6 flow cytometer (BD Biosciences, UK). The populations of lymphocytes and monocytes were gated using FSC-A vs SSC-A and single cells gated using FSC-A vs FSC-H. DCs were gated as cells that were CD11c+, Macrophages were F4/80+, Neuutrophils were Ly6G+ and M cells were NKM 16-2-4+. All cell populations were plotted against anti-spore+ events. Double positive samples that included FITC showed populations that contained spores. Free spores were identified by using FSC-A vs SSC-A to gate on the spore population. Using information from the optimisation experiment anti-spore antibody and anti-IgG-FITC was used to positively identify spores. The results were analysed using Microsoft Excel. The percentage of total population was used for calculation and the unstained samples were subtracted from the stained samples.

2.23. Flow cytometric analysis of samples from the innate immunity study (Chapter 5)

After isolation of single cells from the lungs, gut and NALT, $1x10^6$ cells were used for staining. Cells were centrifuged at 200 *g* for 10 min and washed in 10 % FCS. Cells were resuspended in 10 % FCS and antibodies added according to the titration results. Three panels were used i) Macrophage F4/80-PerCP (clone BM8, Biolegend, UK) and Dendritic cells CD11c-APC (clone N418, Miltenyi, Germany), ii) Neutrophils Ly6G-APC (clone 1A8, Miltenyi, Germany) and NK cell CD49b-PE (clone DX5, Miltenyi, Germany) and iii) TLR2 CD282-PE (clone REA109, Miltenyi, Germany) and TLR4 CD284-APC (clone MTS510, Miltenyi, Germany). After incubation, cells were washed with 10 % FCS and samples analysed using the BD Accuri C6 flow cytometer (BD Biosciences, UK). The data was analysed using the BD Accuri C6 software by gating on the lymphocytes, monocytes and granulocyte populations and gating on single cells. To determine DCs, M1 and M2 macrophages, the cells were analysed using CD11c-APC vs F4/80-PerCP. Those cells that were CD11c+ F4/80- were classified as DCs, CD11c+ F4/80+ were M1 macrophages and CD11c- F4/80+ were M2 macrophages, as described in other works (Li *et al*. 2010; Fujisaka *et al*. 2009). NK cells were CD49b+, neutrophils were Ly6G+, TLR2 were CD282+ and TLR4 were CD284+.

2.24. Embedding of tissues for histology and immunofluorescence (Chapter 4 and 5)

Tissues taken from mice were incubated at RT for 24 – 48 h in 10 % NBF. Tissues were then put into individual cassettes and immersed in 70 % ethanol, followed by 90 % ethanol and 100 % ethanol with four changes of solution. The ethanol was displaced by immersing the tissue in three changes of xylene

(Sigma-Aldrich, UK). The tissue was then submerged in molten paraffin wax (Leica, Germany) for three changes. The tissue was then embedded in wax in a mould and the wax allowed to solidify. The tissues were processed using a Bright 3500 Microtome (Bright, UK) to a thickness of either 5 µM or 10 µM and heat fixed onto microscope slides (65 ºC, 20 min). To rehydrate the sections for staining, the slides were incubated with three changes of xylene, followed by two changes of 100 % ethanol and two changes of 95 % ethanol. Slides were washed twice with dH_20 and once with PBS before incubating in 5 % BSA for 1 h at RT. Primary antibody was then added in 1 % BSA (1:500 anti-spore (rabbit) (RHUL) 1:100 anti-M cell (Miltenyi, Germany) or 1:100 MHCII (Miltenyi, Germany and 1:500 CD3 (Biolegend, UK)) and incubated overnight at 4ºC. Slides were washed with PBS three times and then incubated with secondary antibody diluted in 1% BSA (anti-rabbit-IgG-FITC and anti-mouse-IgG-TRITC both 1:500 and incubated for 1h at RT). Slides were washed with PBS three times, mounting media added and coverslip added. Slides were read using an EVOS fl digital microscope (Life Technologies, UK).

2.25. Cytokine bead array (Chapter 5)

Mouse splenocytes were isolated and $5x10^5$ cells were aliquoted into a 96-well plate in duplicate, with a positive control incubated with PMA and Ionomycin and incubated in DMEM media containing L-glutamine, penicillin, streptomycin, Hepes Buffer and 10 % FCS for 48 h at 37°C. The supernatants were then collected and stored at – 20 °C until used in the assay. The BD cytokine bead array mouse inflammation kit was used (BD Biosciences, UK), which measures the cytokines IL-6, IL-12, TNF, IL-10, IFNγ and MCP-1. This kit was chosen because a lot of these cytokines are implicated in the innate immune response. The method was followed according to the manufacturer's instructions. The

lyophilised standards were reconstituted in 2 ml assay diluent for 15 min at room temperature and then diluted 1:2 in assay diluent with a final dilution of 1:256 achieved. The capture beads were vortexed and for the master capture bead mix 10 µl of each cytokine capture bead x (number of standards and samples) was added to a tube (e.g. 10 µl of IL-6 cytokine bead x 50 samples = 500 µl x 6 cytokines = 3000 µl total). 50 µl of the master capture bead mix was added to each sample tube. 50 µl of either a dilution of standard or unknown sample was added to each tube followed by addition of 50 µl of the PE detection reagent. Samples were incubated in the dark for 2 h and then 1 ml of wash buffer was added to each tube and centrifuged at 200 *g* for 5 min. The supernatant was discarded and the pellet was resuspended in 300 µl of wash buffer and read on the BD Accuri C6 using a CBA template from the BD website (BD Biosciences 2014). Each cytokine capture bead fluoresces differently in the FL4 channel and the quantity of cytokine is measured using the FL2 channel. The results, once obtained, were analysed using the BD FCAP Array v3 software, which calculates the standard curves for all the cytokines and then calculates the pg/ml of cytokine per sample.

2.26. Complement killing assay (Chapter 5)

The method for the assay was developed by Virta *et al* (Virta *et al*. 1998). $1x10^6$ HU58 spores in dH_20 were incubated with 20 µl of sera from immunised mice and incubated at 37 °C for 90 min, not shaking. The samples were then put on ice for 10 min to stop the reaction. After treatment, the spores were serially diluted 1:10 and plated out on DSM agar and incubated at 37 °C overnight. The total number of spores was calculated and percentage of dead spores calculated against the no sera control.

2.27. Infection of mice with MDR-TB after therapy with spores or IL-4D2 (Chapter 5)

Ten C57BL/6 mice per group were used. One group was given PBS as a control. One group was dosed with $2x10^9$ autoclaved HU58 spores, one with IL4-D2 and other with both autoclaved HU58 spores and IL4-D2. All groups were given doses by the intranasal route three days prior to infection with MDR-TB (Peru strain) and treated with doses every other day for three doses **(Figure 2-1)**. The strain of MTB was isolated from a Peruvian patient who was enrolled on a clinical trial (strain number: 10094G), which was resistant to Rifampicin and Isoniazid. Four weeks after treatment, the mice were culled and the lungs homogenised and plated out onto 7H11 media and incubated for 28 days at 37 ºC to examine bacterial burden in the lungs. Work carried out by Dr Rajko Reljic and Gil Reynolds Diogo at SGUL.

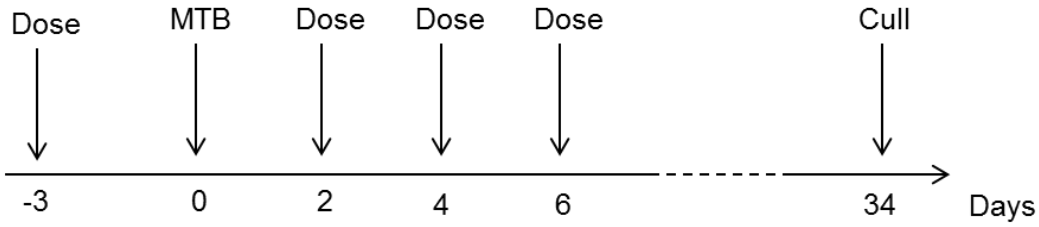

Figure 2-1. Study design of stimulating the innate immune response to protect against MTB. N=10 Balb/c mice were dosed intranasally with either HU58 spores, IL4D2, or HU58 + IL4D2. Three days later they were challenged with MTB (Peru strain) and three further doses were administered. 28 days later, the mice were culled and the lungs were plated out to examine bacterial burden.

Chapter 3: Spores as a Vaccine Adjuvant for Tuberculosis

3.1. Introduction

The current TB vaccine, BCG, is widely used and is able to prevent serious disease in children (Trunz *et al*. 2006). However, efficacy is variable, and the use of live vaccines is problematic because they are considered to be unsuitable for immunocompromised individuals (Hawkridge & Mahomed 2011). This is a particular problem for TB, where there are large numbers of people co-infected with HIV (43% of TB cases are co-infected with HIV in Africa in 2012 (WHO 2014a)). The 'STOP TB' campaign, organised by the WHO aims to eradicate TB by 2050 (WHO 2001) and one of the approaches is to develop novel vaccines. Some of the strategies being tested for novel TB vaccines is to use an adjuvant carrying a TB antigen, for example MVA85A (Ibanga *et al*. 2006) is a virus (modified vaccinia Ankara (MVA)) expressing Ag85A, and is used as a booster vaccine after priming with BCG. The benefits of using the prime-boost strategy are that many people are already vaccinated with BCG (it has been estimated that four billion doses of BCG have been given in total (Kaufmann & Gengenbacher 2012)) and that a booster would build on the protection that BCG confers. Boosting BCG with BCG is carried out in some countries and administered to teenagers (Zwerling *et al*. 2011) but it does not appear to significantly improve protection (Orme 1999). Other novel TB vaccine strategies include modifying BCG to include extra antigens, for example, Aeras-422, is based on BCG but overexpresses antigens Ag85A, Ag85B and Rv3407 (Kaufmann & Gengenbacher 2012).

Vaccine development for TB is difficult because of the lack of biomarkers and correlates of protection. IFNγ, a Th1 cytokine, and initiation of the Th1 immune response is important, because individuals with HIV, who have a reduction in CD4+ T-cells, are far more susceptible to MTB infection (Kalsdorf *et al*. 2009). Therefore, a new TB vaccine should activate Th1 immune responses. BCG does not completely eradicate MTB, but is able to help control the infection, so it is possible to still be latently infected with MTB after BCG vaccination. Any TB vaccine needs to reduce bacterial burden and enhance control of disease to the same degree or better than BCG.

B. subtilis spores have been tested as vaccine adjuvants for diseases including anthrax (Duc 2007) and influenza (Song 2012). Work investigating their use as a vaccine adjuvant using TB antigens was initiated at RHUL. Three immunogenic antigens from MTB were tested; Ag85B (Rv1886c) (30kDa); a secretory mycolyl transferease protein involved in cell wall synthesis that is common in novel TB vaccines (Eddine 2006), Acr (Rv2031c, HspX) (16kDa); a stress protein important in latency and rMPT64 (Rv1980c) (26kDa); another secretory protein found in actively dividing MTB cells and used in diagnostics (Galliard 2011).

All three antigens have been previously tested in various vaccine formats. MPT64 has been tested at RHUL by Huang *et al* in a *Salmonella* vector, which showed MPT64 to be immunogenic and stimulating an IFNγ response, but the reduction in MTB CFU in the lungs was not comparable to BCG (Huang, Sali, *et al*. 2010). Ag85B has been tested in DNA vaccines (Kamath *et al*. 1999), with nanoparticles (Stylianou *et al*. 2013) and in recombinant BCG (Kaufmann &

Gengenbacher 2012). Acr has been tested as an immune complex (Pepponi *et al*. 2013) and DNA vaccine (Khera *et al*. 2005) formats.

In an experiment carried out by Jen Min Huang at RHUL using spores that carried either rMPT64 or rAg85B-Acr, and recombinant spores expressing rMPT64, protective efficacy was measured by CFU isolated from the lungs and spleen (unpublished). MTB found in the spleen is evidence of dissemination of MTB. The results to date show a reduction in CFU in the lungs comparable to BCG in groups given spores with rMPT64 or rAg85B-Acr **(Figure 3-1)**. Reduction was better with spores rather than protein only, with and without BCG. Recombinant spores expressing rMPT64 after a BCG prime also showed a reduction in CFU in the lungs. Reduction in CFU in the spleen was seen in groups that had BCG followed by a booster vaccination with spores and antigens.

Immunogenicity of the vaccines was tested by IFNγ release and IgG subclass ELISA. IFNγ release from cells was observed in groups given spores with MTB antigens, which meant the immunisations were able to stimulate an antigen-specific Th1 response. Total IgG, IgG1 and IgG2a were also measured. Total IgG increased after administration of spores alone and also BCG with boosts of spores and antigens (Huang, unpublished).

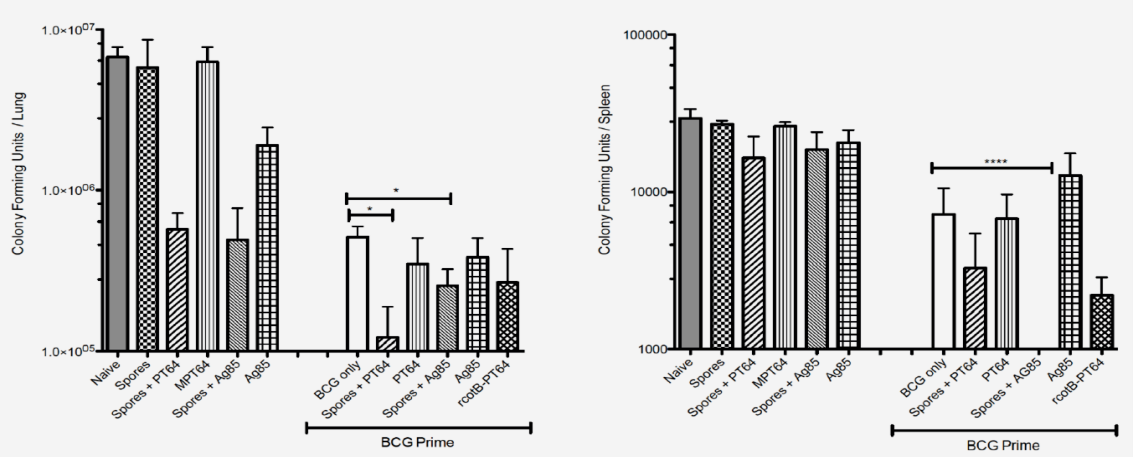

Figure 3-1. Log reduction in CFU counts of MTB in lung and spleen samples from mice challenged with MTB after immunisations. Mice were immunised with HU58 spores, spores with rMPT64 adsorbed to the surface, rMPT64 protein alone, spores with rAg85B-Acr and rAg85B-Acr protein alone. The different vaccine preparations were also tested after a BCG prime. The BCG primed groups showed the greatest reduction in CFU in comparison to the naïve group. Spores with either rMPT64 or rAg85B-Acr had a lower bacterial burden in the lungs in comparison to protein alone, demonstrating spores can enhance the immunogenicity of the antigens. JM Huang, R Reljic, S Cutting unpublished data.

3.1.1. Aims

The aim of this chapter was to continue to test the efficacy and immunogenicity of rMPT64 and rAg85B-Acr using *B. subtilis* spores as an adjuvant. HU58 spores with rMPT64 or rAg85B-Acr were tested to confirm previous results and further characterise immune responses. rMPT64 and rAg85B-Acr were also combined, and were named 'SWAN' (after 'South West Alliance Network' who funded the study) to assess whether; a) more than one antigen could be adsorbed to the surface of the spores and b) whether the antigens could have a synergistic effect on inducing an immune response. SWAN was tested as protein alone, as well as adsorbed to spores and in a prime-boost regimen with BCG.

The recombinant spores expressing MPT64 (rHU58(MPT64)) were further characterised. They were used alone, and in a prime-boost regimen with BCG. These spores were inactivated with formaldehyde before dosing because they were genetically modified and by inactivating them they pose less risk to the environment since they carry antibiotic resistance genes that could be transferred to other bacteria.

C57BL/6 mice were challenged intranasally with MTB to assess how well protected they were following immunisation by examining the bacterial burden in the lungs and spleen. The immune responses were assessed after immunisations by IFNγ ELISPOT and IgG subclass ELISAs.

3.2. Results

3.2.1. Protein

rAg85B-Acr (1–2mg/ml) was supplied by Dr Illaria Pepponi and Dr Rajko Reljic (SGUL). Ag85B (30 kDa) was co-expressed with Acr (16 kDa) in *E. coli* DH5α. rMPT64 (26 kDa) was expressed in *E. coli* BL21 and expression induced using IPTG and the clone was created by Jen Min Huang (RHUL) as described by Huang *et al* (Huang, Sali, *et al*. 2010). The protein was purified using the ÄKTA purification system and checked for purity using SDS-PAGE electrophoresis, as described in the methods **(Figure 3-2)**. The concentration of protein was measured using the Bradford assay and the concentration ranged from 0.6–1.3mg/ml. Figure 3-3 illustrates the expression and purity of rMPT64 obtained. The rMPT64 and rAg85B-Acr proteins were mixed together when used for dosing, or adsorbed to the surface of autoclaved HU58 spores.

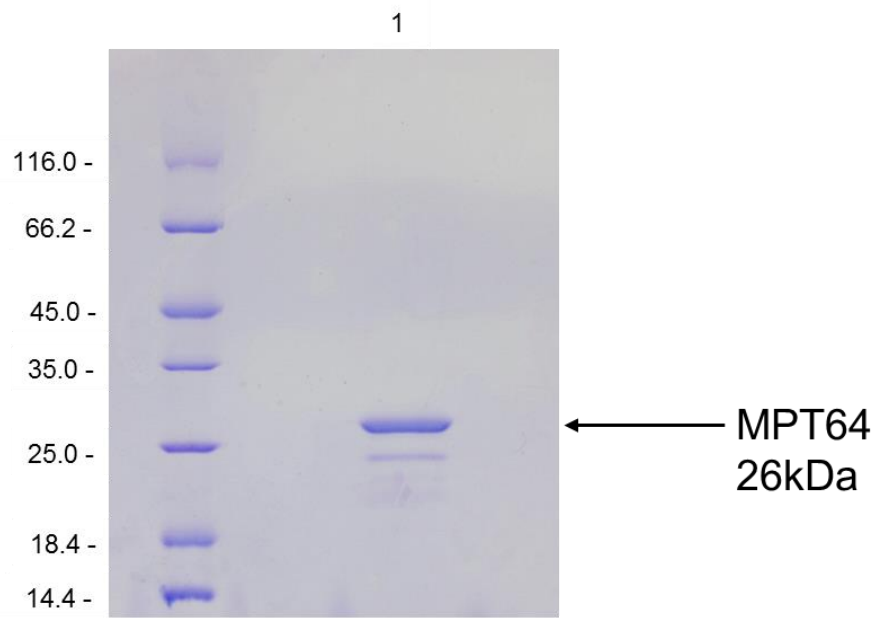

Figure 3-2. Coomassie blue stained SDS-PAGE electrophoresis gel of purified rMPT64 protein (26kDa). Lane 1. His-tagged rMPT64 expressed in *E. coli* LH22 grown to OD 0.5-0.7 and protein expression induced by IPTG. Bacteria were sonicated, filtered and run on the AKTA His-tag purification programme. Suitable fractions were dialysed and concentrated. Ladder indicates kDa of protein.

3.2.2. Adsorption of spores with proteins rMPT64 and Ag85b-Acr

To deliver the antigenic proteins, they need to be bound to the surface of the spore. The adsorption of proteins onto the spore surface is dependent on pH, which is affected by the isoelectric point (pI) of each protein. The optimum binding conditions for rAg85B-Acr and rMPT64 were tested. PBS was prepared at pH4, pH7 and pH10 and used for the various wash steps involved in binding protein to spores. Spore coats were extracted and fractionated by SDS-PAGE followed by Western electroblotting to detect the bound protein. rMPT64 and rAg85B-Acr bound to autoclaved HU58 at pH4 and pH7 but not at pH10 **(Figure 3-3, Figure 3-4)**. Both proteins were able bind to spores together and neither was affected by the presence of the other as demonstrated by the ability to detect both proteins on the Western blot.

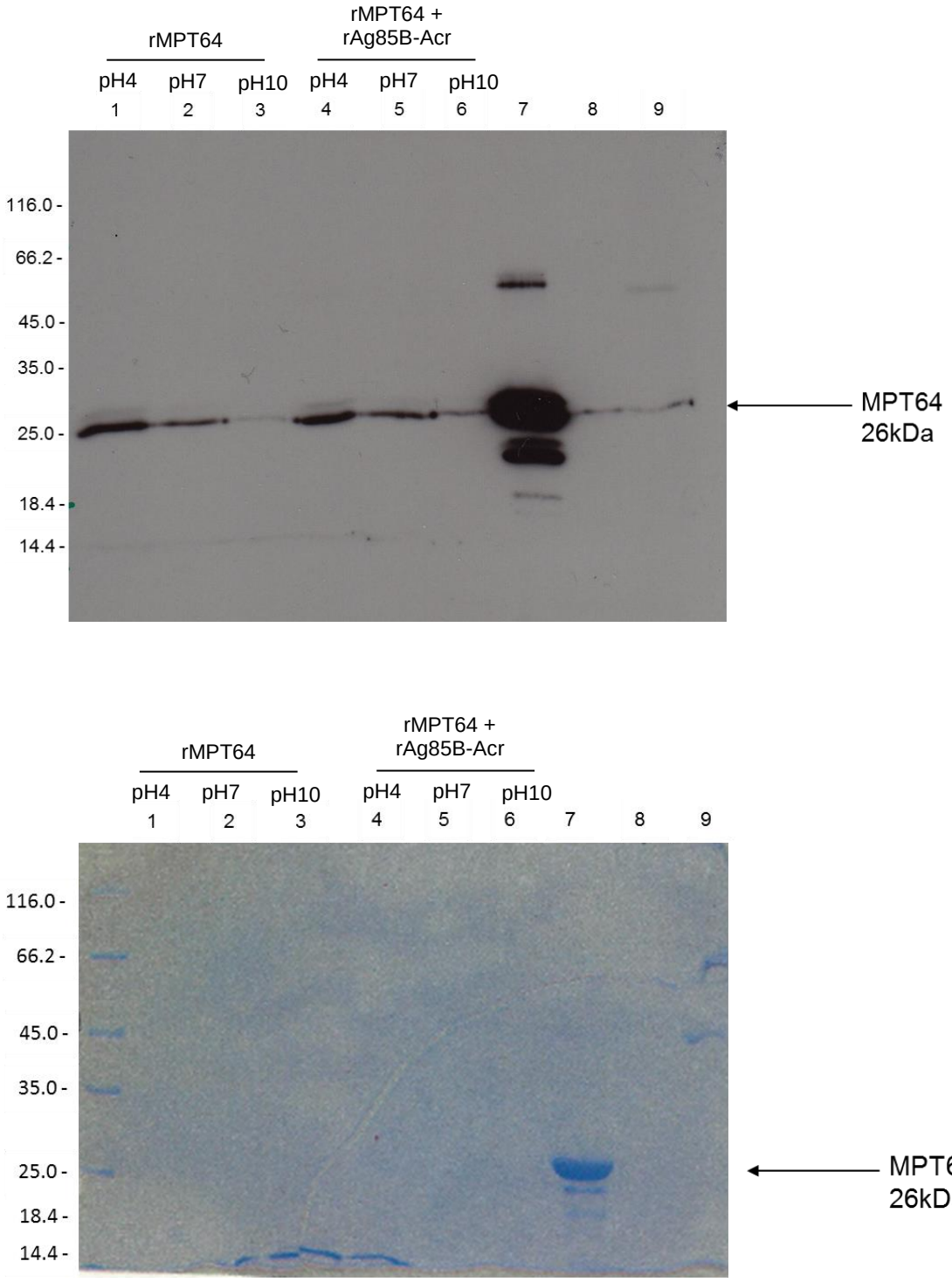

Figure 3-3. Western blot transfer and 12% SDS-PAGE gel showing binding of rMPT64 (26kDa) to autoclaved HU58 spores at different pH's. Western blot protein detected with anti-rMPT64 antibody. rMPT64 (2µg) or in conjunction with rAg85B-Acr (2µg) and $2x10^9$ HU58 spores combined for 30 minutes using PBS at different pH's. Lanes 1-3 HU58 with rMPT64; Lane 1; pH4 PBS, Lane 2; pH7, Lane 3; pH10, Lanes 4-6 HU58 with rAg85B-Acr and rMPT64; Lane 4; pH4, Lane 5; pH7, Lane 6; pH10, Lane 7; rMPT64 protein alone, Lane 8; rAg85B-Acr with HU58 at pH7, Lane 9; rAg85B-Acr protein. Ladder indicates kDa of protein.

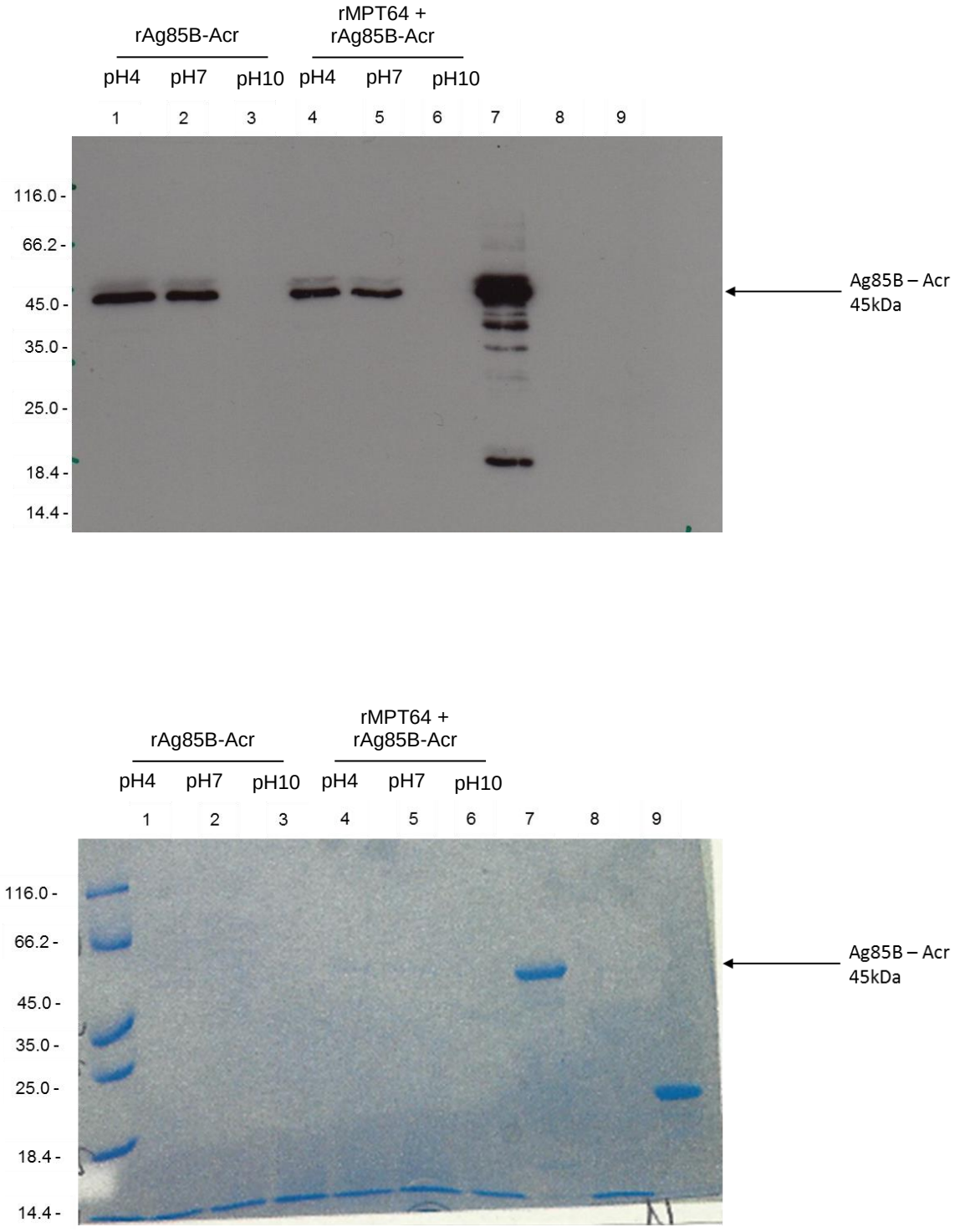

Figure 3-4, Western blot transfer and 12% SDS-PAGE gel of the binding of rAg85B-Acr (45kDa) to autoclaved HU58 spores at different pH's. Western blot detected with anti-rAg85B-Acr antibody. rAg85B-Acr (2µg) or in conjunction with rMPT64 (2µg) and $2x10^9$ HU58 spores were combined for 30 minutes using PBS at different pH's. Lanes 1-3 HU58 with rAg85B-Acr Lane 1; pH4 PBS, Lane 2; pH7 PBS, Lane 3; pH10, Lanes 4-6 HU58 with rAg85B-Acr and rMPT64; Lane 4; pH4, Lane 5; pH7, Lane 6; pH10, Lane 7; rAg85B-Acr protein alone, Lane 8; rMPT64 with HU58 at pH7, Lane 9; rMPT64 protein. Ladder indicates kDa protein.

3.2.3. Kinetics of protein binding to spores

The interactions between the protein and autoclaved HU58 spores was characterised by how readily the protein bound to HU58 over time. Protein was incubated with spores for 5, 10, 20 and 30 minutes. Binding was seen at 5 minutes for rMPT64 and 20 minutes rAg85B-Acr **(Figure 3-5, Figure 3-6)**.

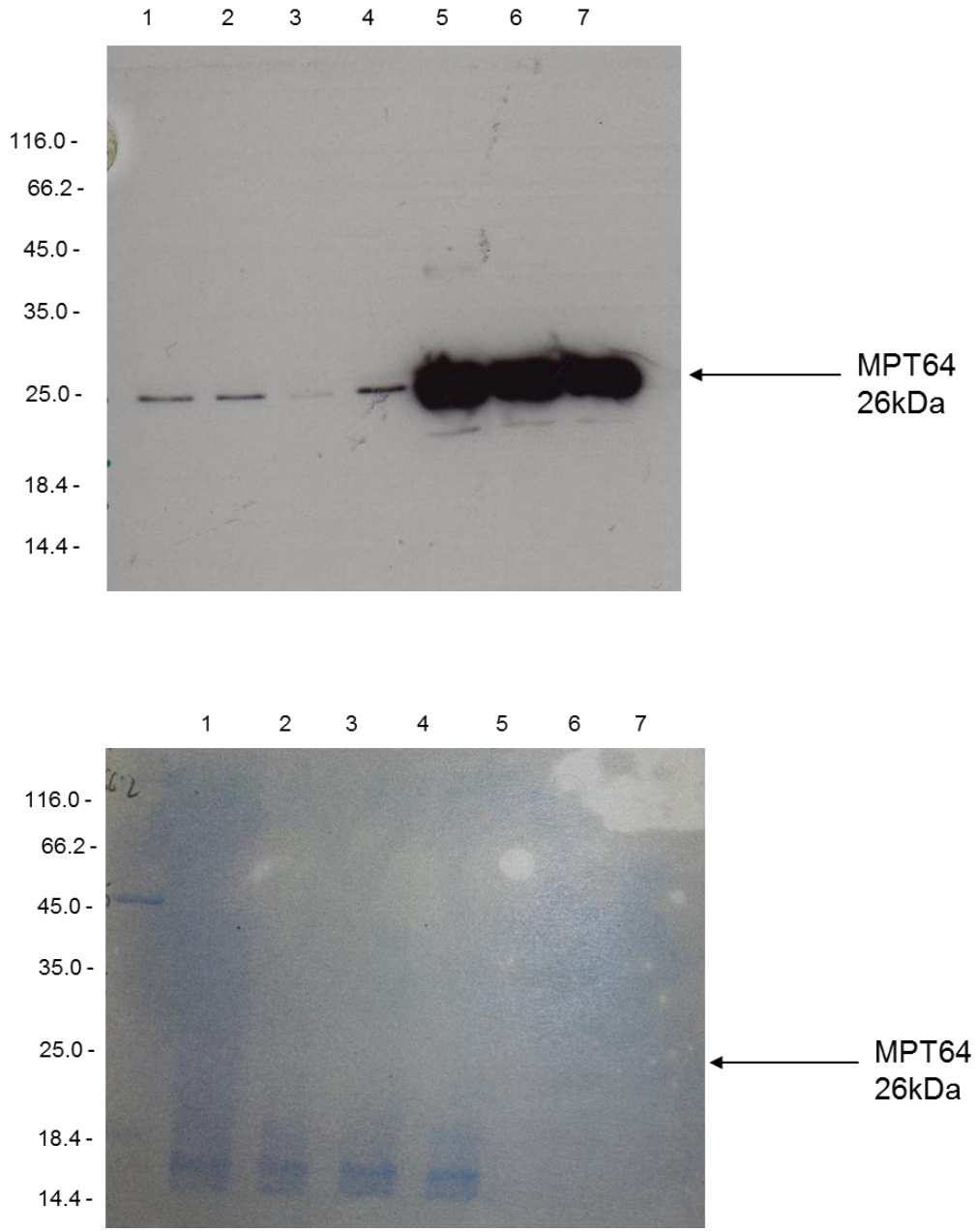

Figure 3-5, Western blot transfer and 12% SDS-PAGE gel showing binding of rMPT64 to autoclaved HU58 over time detected using anti-rMPT64 antibody. Lane 1; 5 min, Lane 2; 10 min, Lane 3; 20 min, Lane 4; 30 min, Lane 5; 0.25 µg rMPT64, Lane 6; 0.125 µg rMPT64, Lane 7; 0.065 µg rMPT64, Lane 8; 0.03 µg rMPT64, Lane 9; rAg85B-Acr + HU58, Lane 10; rAg85B-Acr. Ladder indicates kDa protein.

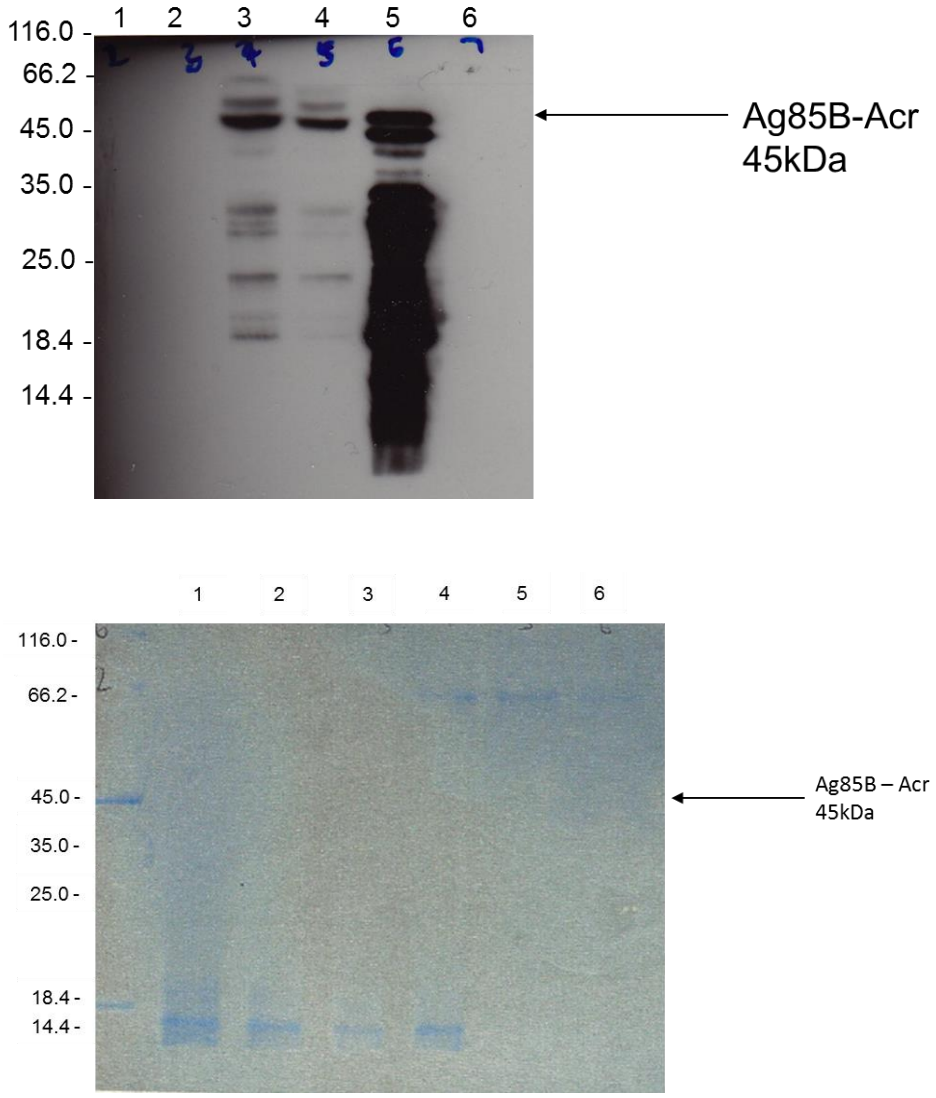

Figure 3-6, Western blot transfer from 12% SDS-PAGE gel showing binding of rAg85B-Acr to autoclaved HU58 over time detected using anti-rAg85B-Acr antibody. Lane 1; 5 min, Lane 2; 10 min, Lane 3; 20 min, Lane 4; 30 min, Lane 5; rAg85B-Acr, Lane 6; rMPT64. Ladder indicates kDa protein.

3.2.4. Stability of protein bound to spores

Spores with protein bound to the surface were stored at different temperatures for 24h, to assess whether the protein would dissociate from the spores over time, an attribute which would have implications for storage if they were used as vaccines. At 4°C and -20°C, there seemed to be less protein bound than in the original preparation. However, in both storage conditions protein was still bound which showed that spores can be stored, but the dose may be affected **(Figure 3-7)**.

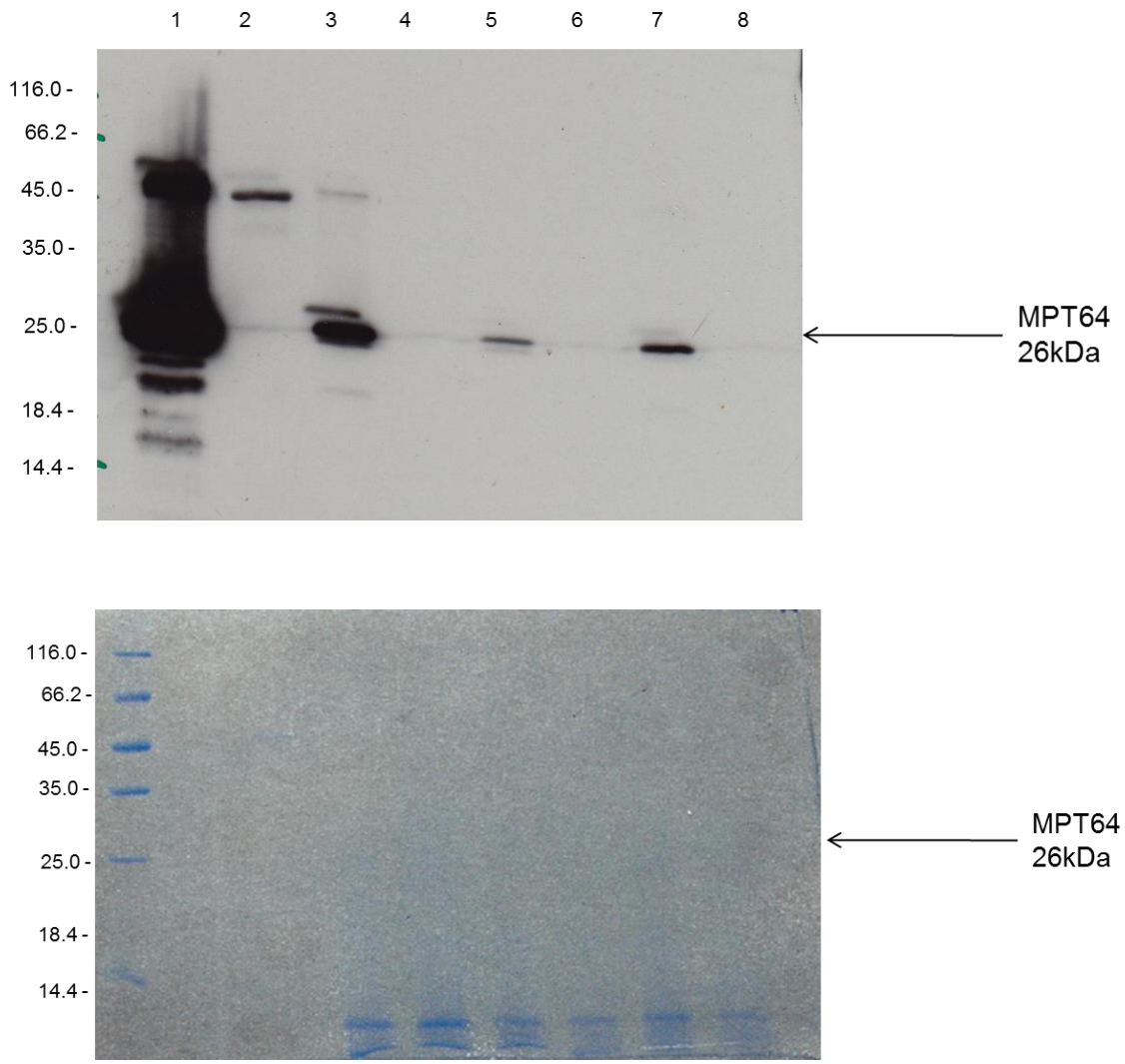

Figure 3-7. Spores with MTP64 bound to the surface stored at different temperature.
1; rAg85B-Acr protein, 2; rMPT64 protein, 3; rAg85B-Acr and spores incubated 30 min RT, 4; rMPT64 and spores incubated 30 min RT, 5; rAg85B-Acr and HU58 stored at 4°C overnight, 6; rMPT64 and HU58 stored at 4°C overnight, 7; rAg85B-Acr and HU58 stored at -20°C overnight, 8; rMPT64 and HU58 stored at -20°C overnight.

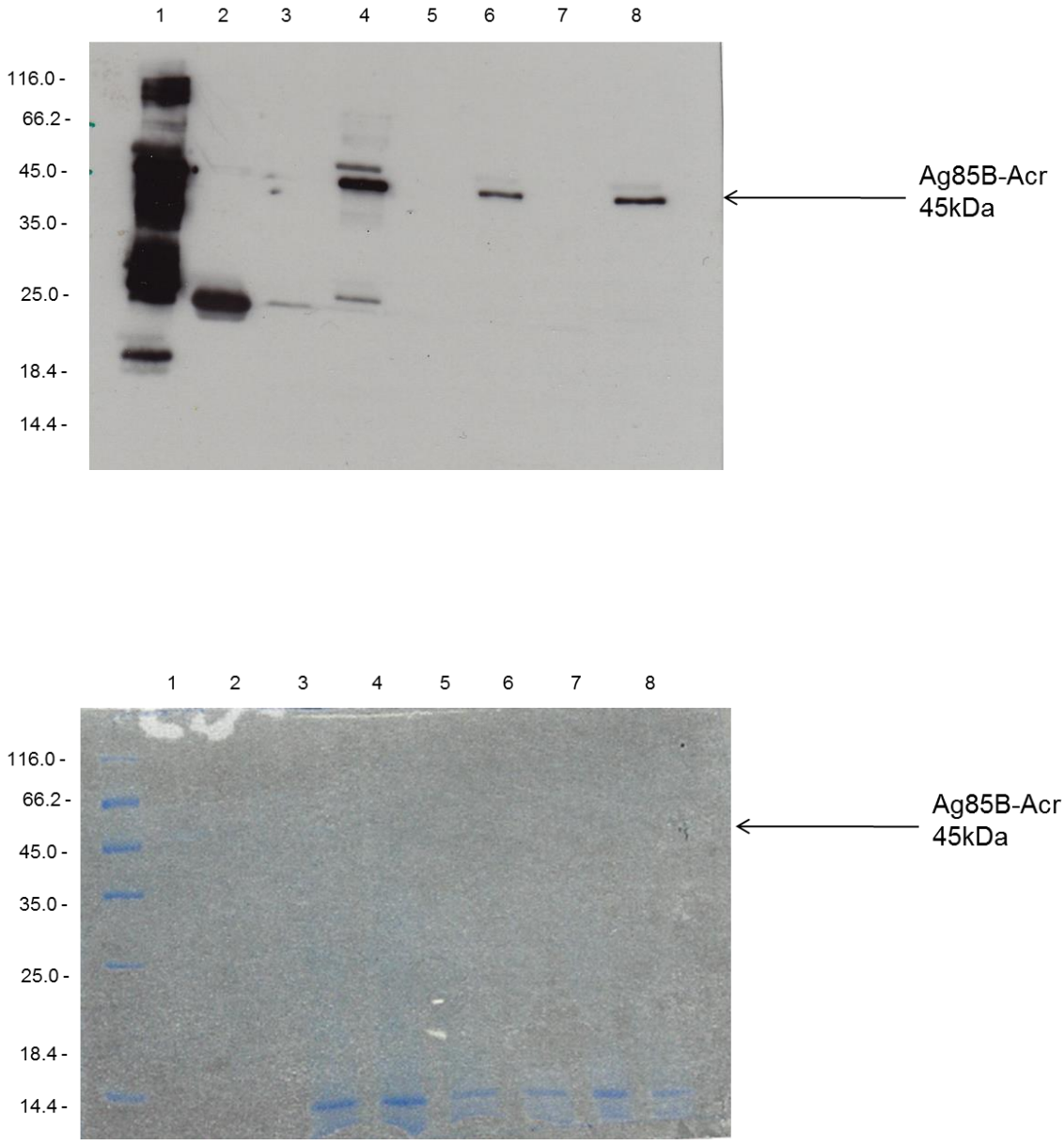

Figure 3-8. Spores with Ag85B-Acr bound to the surface stored at different temperature. 1; rMPT64 protein, 2; rAg85B-Acr protein, 3; rMPT64 and spores incubated 30 min RT, 4; rAg85B-Acr and spores incubated 30 min RT, 5; rMPT64 and HU58 stored at 4°C overnight, 6; rAg85B-Acr and HU58 stored at 4°C overnight, 7; rMPT64 and HU58 stored at -20°C overnight, 8; rAg85B-Acr and HU58 stored at -20°C overnight. Ladder indicates kDa protein.

3.2.5. Immunofluorescence of proteins adsorbed to spores

To provide additional confirmation that protein had been bound to the spores, and to validate the fluorescence microscope method, immunofluorescence of rAg85B-Acr and rMPT64 bound to the spores was evaluated. Fluorescence was brighter on the spores with protein bound compared to HU58 samples **(Figure 3-9)**.

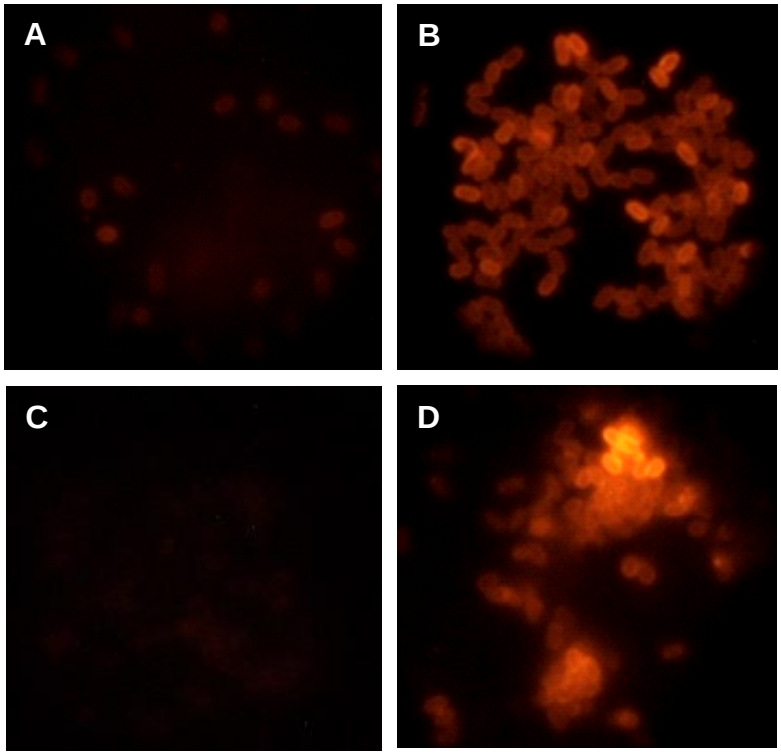

Figure 3-9. Immunofluorescence of autoclaved HU58 spores with protein adsorbed to the surface. A) HU58 no protein adsorbed, detected using anti-rAg85B-Acr primary antibody and TRITC conjugated anti-mouse IgG secondary antibody B) HU58 with rAg85B-Acr adsorbed to the surface, detected using anti-rAg85B-Acr primary antibody and TRITC conjugated anti-mouse IgG secondary antibody, C) HU58 no protein adsorbed, detected using anti-rMPT64 primary antibody and TRITC conjugated anti-mouse IgG secondary antibody D) HU58 with rMPT64 adsorbed to the surface. Detected using anti-rMPT64 primary antibody and TRITC conjugated anti-mouse IgG secondary antibody. 1s exposure.

3.2.6. rHU58(MPT64) expression of rMPT64

The rHU58(MPT64) strain was created by COBRA Bio-manufacturing Plc (UK) and expressed the rMPT64 protein in the spore coat of the HU58 spores because it was fused to a spore coat protein (CotB) (unpublished). rMPT64 expression was confirmed by extracting the spore coat proteins and using Western blotting to detect rMPT64 using anti-rMPT64 antibody. Bands were seen at around 60 kDa which indicated that rMPT64 (26 kDa) was expressed fused to CotB (42 kDa) **(Figure 3-10)**. Another measure of rMPT64 expression was to use ELISA to detect MPT64 on the intact spores and in the extracted spore coat proteins **(Figure 3-11)**. ELISA plates were coated with either spores of HU58 or rHU58(MPT64), spore coat extract or spores after spore coat extraction and then detected using anti-rMPT64 antibody. These results showed that rMPT64 could be detected in the spore coat extract, but only a small amount was present on the surface of spores and no rMPT64 could be detected on spores after extraction. Therefore the results suggested that rMPT64 was expressed in the spore coat, but may not be surface exposed.

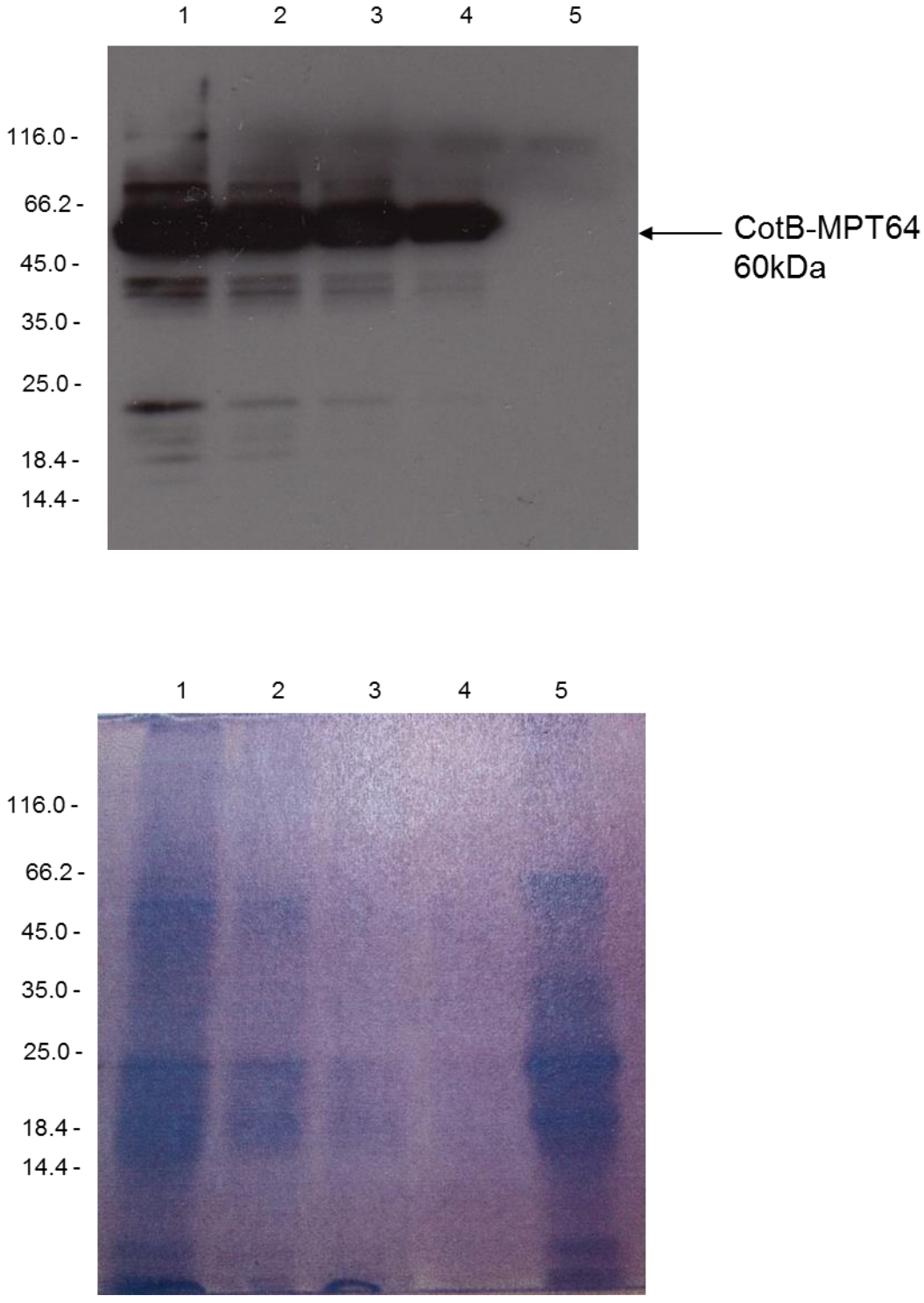

Figure 3-10. Western blot from and 12% SDS-PAGE of recombinant HU58 (cotB-rMPT64) spores probed with anti-rMPT64 antisera and anti-mouse IgG-HRP secondary antibody. Lane 1; rHU58(MPT64) spore coat extract 2; rHU58(MPT64) spore coat extract 1:2 dilution, 3; rHU58(MPT64) spore coat extract 1:4 dilution, 4; rHU58(MPT64) spore coat extract 1:8 dilution, 5; HU58 spore coat extract. Protein measured in kDa according to ladder.

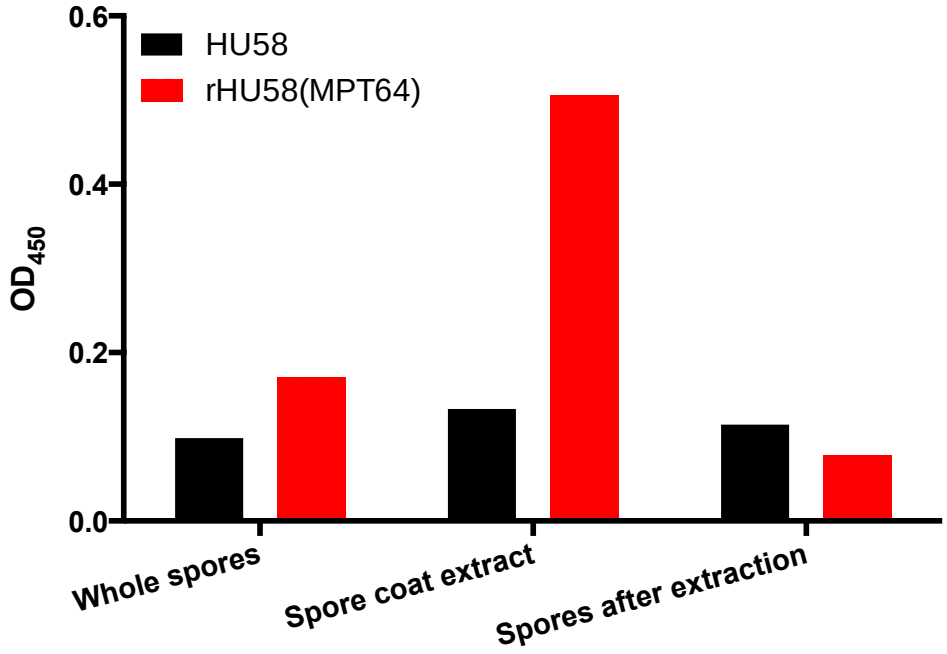

Figure 3-11. ELISA results showing rMPT64 detection. HU58 and rHU58(MPT64) spores ($1x10^6$), spore coat extracts and spores after the coat was extracted were used to coat the plate, and anti-rMPT64 antibody followed by anti-mouse IgG-HRP secondary antibody used to detect rMPT64 expression.

3.2.7. Inactivation of rHU58(MPT64) with formaldehyde

rHU58(MPT64) is a genetically modified (GM) organism, and as such there are potential safety concerns about using it as a live vaccine. Inactivation with formaldehyde would inactivate the spores thus alleviating any potential danger because they would be unable to replicate and spread in the environment. Vaccines including polio vaccine are inactivated using formaldehyde (Martin 2003). According to the literature, formaldehyde activity is affected by time and temperature (Salk & Salk 1984), therefore rHU58(MPT64) spores were subjected to different concentrations of formaldehyde for different lengths of time at a variety of temperatures. Aliquots were plated onto DSM media and colony counts recorded as an indication of survival. Spores were washed after treatment with PBS to minimise the percentage of formaldehyde left in the sample, which could be toxic in the preparation. The residual formaldehyde was measured in the supernatants after washing using a formaldehyde testing kit. The greatest reduction in CFU was seen at 4% formaldehyde after incubation at 37°C for 24h **(Figure 3-12)**.

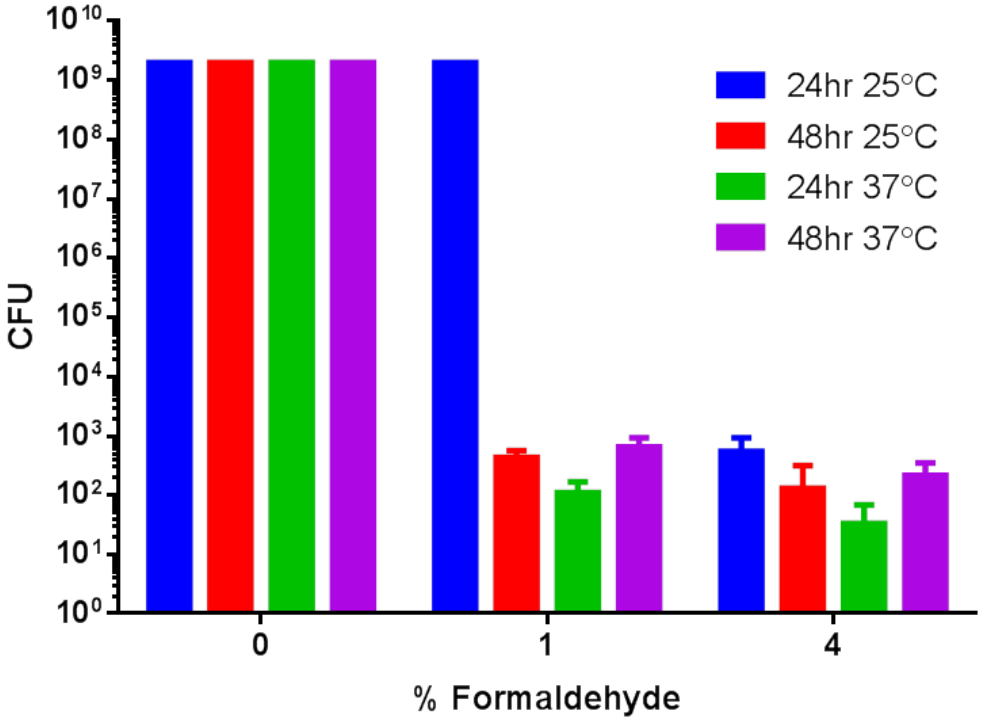

Figure 3-12. rHU58(MPT64) CFU after exposure with concentrations of 0%, 1% or 4% formaldehyde, and PBS washes after incubations at various times and temperatures. After treatment, spores were washed by centrifugation and PBS and plated out onto DSM media and incubated at 37°C overnight to measure recovery. The largest decrease in CFU was after 24h at 37°C and 4% formaldehyde.

3.2.8. Detection of formaldehyde in samples

Formaldehyde is toxic and classed as a probable carcinogen and so the levels of formaldehyde in the vaccine preparation had to be reduced before administration to mice. The guidelines state that the maximum amount of formaldehyde permitted in a vaccine preparation is 0.2g/L (Pharmacopeia 2014). Reducing the formaldehyde content was achieved by washing the inactivated spore preparation with PBS. The percentage of formaldehyde decreased over time and after two washes with PBS, the level of formaldehyde in the preparation was reduced to <0.05 % as detected using a formaldehyde test kit (HACH, USA) **(Figure 3-13).**

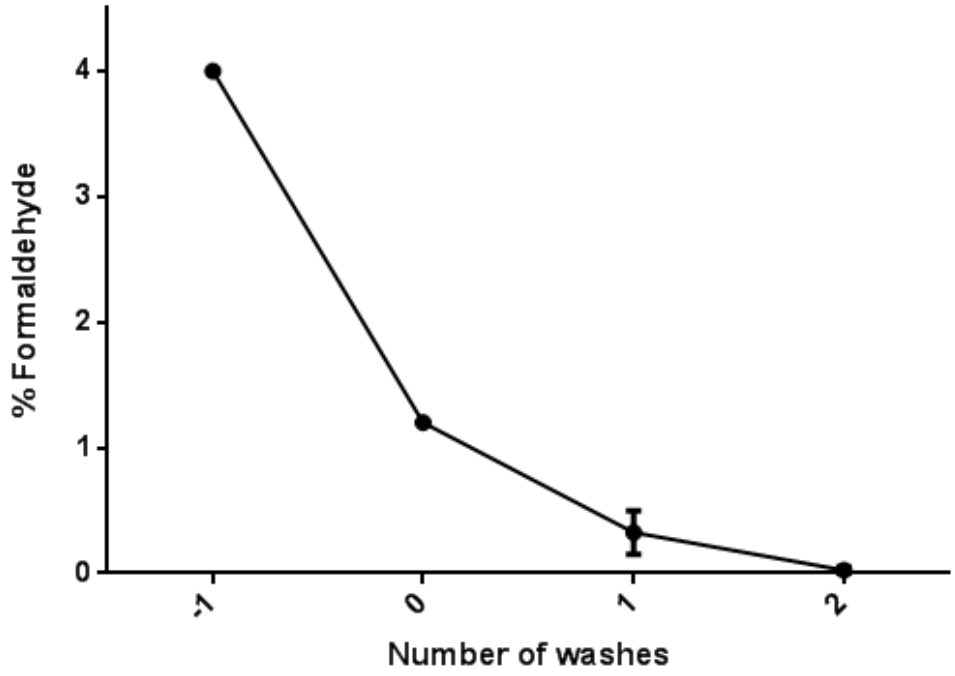

Figure 3-13. Graph depicting % formaldehyde present in inactivated rHU58(MPT64) samples after PBS washes using centrifugation. -1 indicated starting concentration of formaldehyde, 0 indicates % formaldehyde after 24h at 37°C prior to washing, 1 and 2 indicate the number of PBS washes and % formaldehyde detected. % formaldehyde was reduced to <0.05% after 2 washes.

3.2.9. TB Study

After determining the conditions for binding the MTB antigens to the spores and inactivating the recombinant spores, the spores were assessed *in vivo* and mice were dosed as described in **(Figure 3-14)**. Groups included: naïve (Group A), BCG (Group B), HU58 + rMPT64 (Group C), HU58 + rAg85B-Acr (Group D), SWAN proteins (Group E), HU58 + SWAN (Group F), BGG with a booster vaccine of HU58 + SWAN (Group G), rHU58(MPT64) (Group H) and BCG with a booster of rHU58(MPT64) (Group I). The aim of the study was to i) asses the safety of the regimens, ii) measure the immunogenicity of the different regimens using ELISA and ELISPOT and iii) efficacy by measuring bacterial burden in the lungs and spleen as a marker of protection.

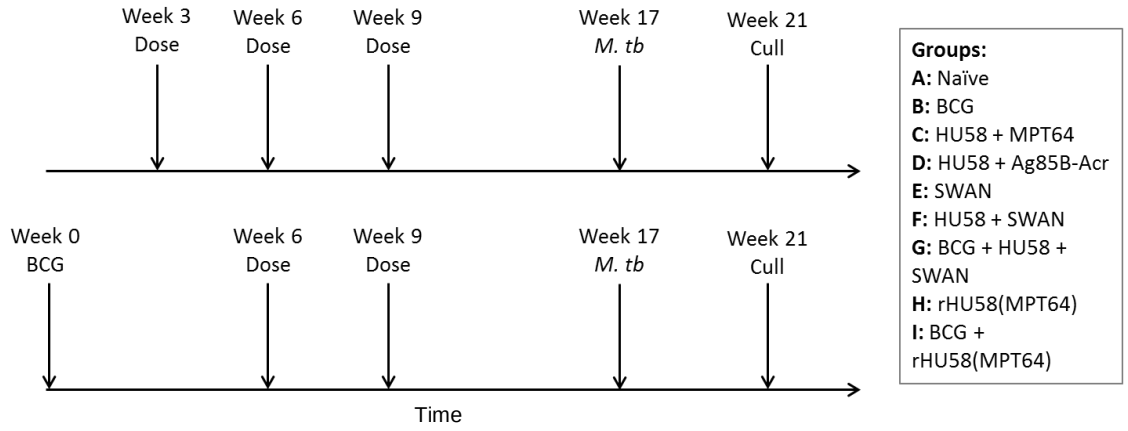

Figure 3-14. Study plan for immunisations and challenge. Mice (n=10) in groups C, D, E, F and H were immunised intranasally at weeks 3, 6 and 9. Mice (n=10) in groups G and I were dosed with BCG subcutaneously, followed by intransal dosing with spores at weeks 6 and 9. Group A received PBS at dosing time points. Group B had a single dose of BCG delivered subcutaneously. n=8 from each group were challenged with MTB at week 17, and four weeks later were culled and the lungs and spleens used to examine bacterial burden.

3.2.10. TB Study – Weight changes

After the mice were administered with the relevant doses, the weights were monitored throughout the study as a marker of animal health and assess the safety of the dosing regimens **(Figure 3-15)**. The mice all put on weight, which would indicate no adverse effect due to the immunisations.

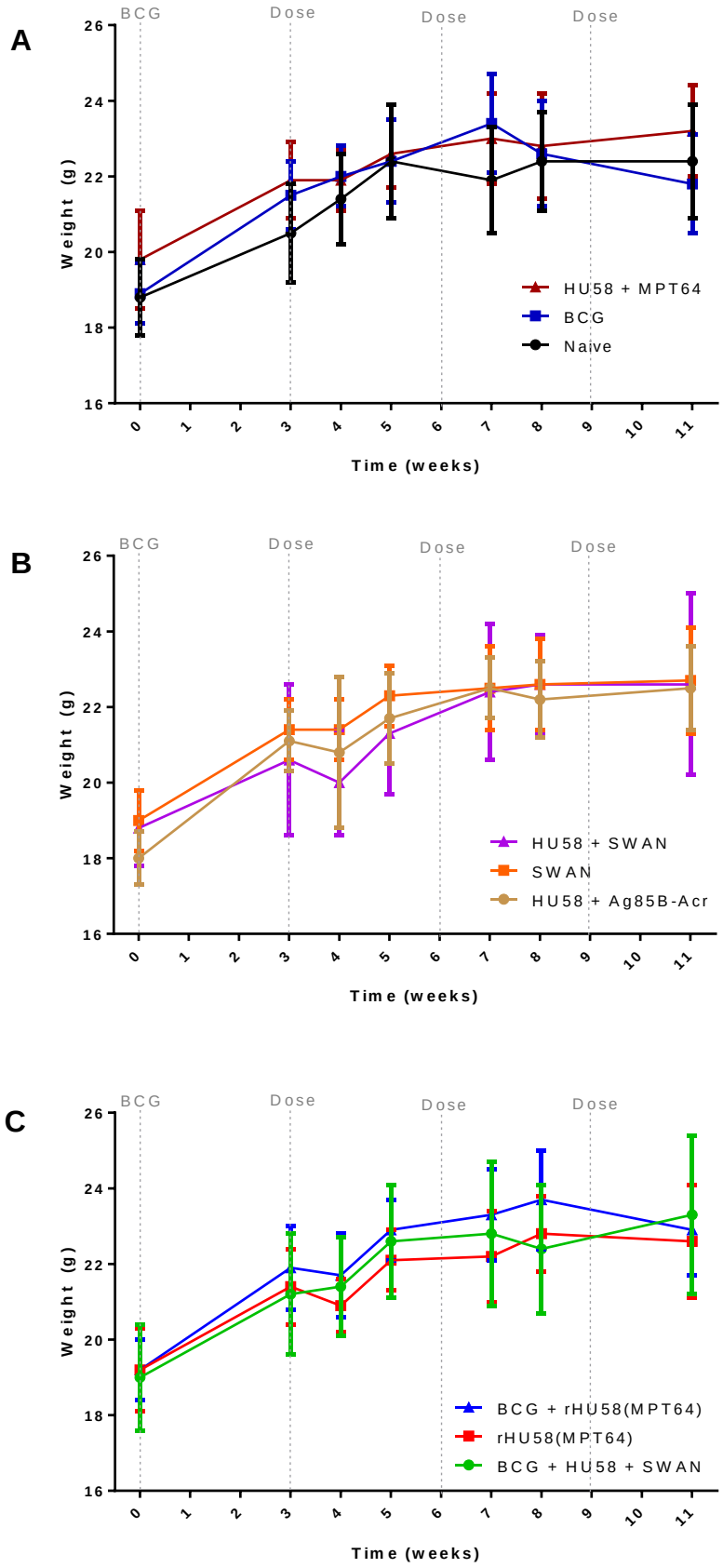

Figure 3-15. Median weights of groups of mice recorded throughout the study. Weight increased until week 7, and then plateaued. Timing of doses indicated by dotted lines. BCG was given by subcutaneous injection. Spores and protein vaccinations were given intranasally. A; groups naïve (Group A), BCG only (Group B), HU58 + rMPT64 (Group C), B; groups HU58 + rAg85B-Acr (Group D), SWAN (Group E) and HU58 + SWAN (Group F), BCG + HU58 + SWAN (Group G), rHU58(MPT64) (Group H) and BCG + rHU58(MPT64) (Group I)

3.2.11. TB Study dose verification

Western blot analysis was carried out on the leftover doses (as an excess was originally made) for the groups after the doses were administered to verify that they had received the antigens. rMPT64 was identified in the HU58 + rMPT64 dose, SWAN protein dose and HU58 + SWAN dose. rAg85B-Acr was identified in the HU58 + rAg85B-Acr dose, SWAN protein dose and HU58 + SWAN dose **(Figure 3-16)**.

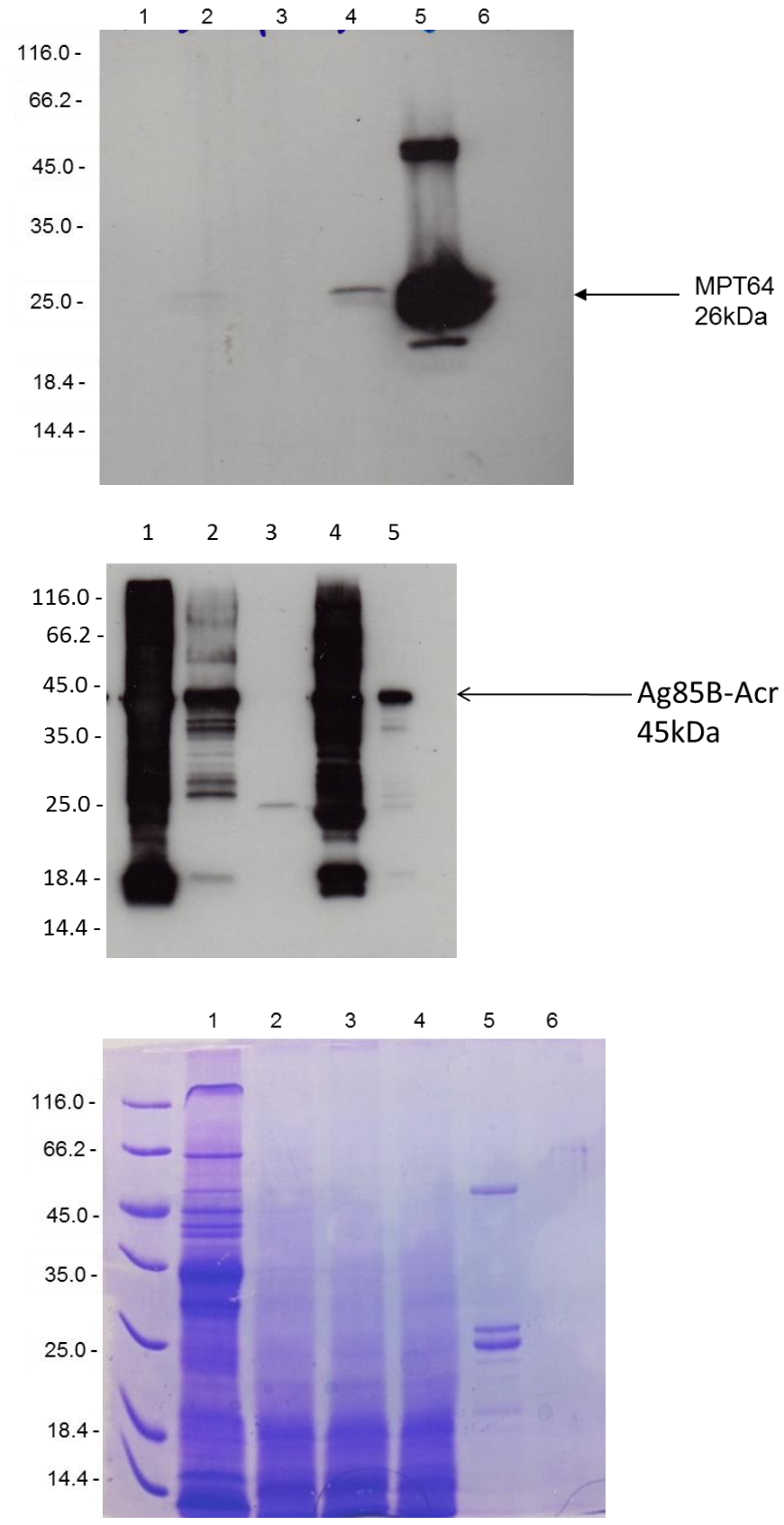

Figure 3-16, Western blot transfer and 12% SDS-PAGE electrophoresis using anti-rAg85B-Acr and anti-rMPT64 antisera of the doses for TB Study. After dosing the mice, 10µl of what remained of the doses was used for Western blot analysis to confirm that the mice had received correct doses (i.e. protein had bound to spores). Lane 1; rAg85B-Acr protein , Lane 2; HU58 + rAg85B-Acr (10 µg), Lane 3; HU58 + rMPT64 (10 µg), Lane 4; SWAN (10 µg each), Lane 5; HU58 + SWAN (10 µg each).

3.2.12. Antibody subclass ELISA

To assess the immunogenicity of the vaccination regimens, serum was taken from tail bleeds before the study began and from terminal heart bleeds from two representative mice per group at the end of the immunisations (week 16) **(Figure 3-14)**. The sera was used to measure rMPT64 and rAg85B-Acr specific total IgG, IgG1 and IgG2a **(Figure 3-17, Figure 3-18)**. IgG1 is indicative of a Th2 response and IgG2a of a Th1-biased response.

The antibody levels appear highest in the SWAN protein only group (Group E) across the MPT64 IgG subtypes. In the MPT64 coated plates, only HU58 + SWAN (Group F) has a higher than baseline response on the IgG1 plate, and HU58 + MPT64 (Group D) and HU58 + SWAN (Group F) in the IgG2a ELISA. The total IgG levels have a high background level on the MPT64 coated plates, which may mask the total IgG levels in the samples. This could be an assay problem and the antibodies may not be specific enough to MPT64.

The Ag85B-Acr coated plates are more variable, with only one mouse in certain groups making a response, suggesting that the induction of systemic immune responses by the nasal route is variable.

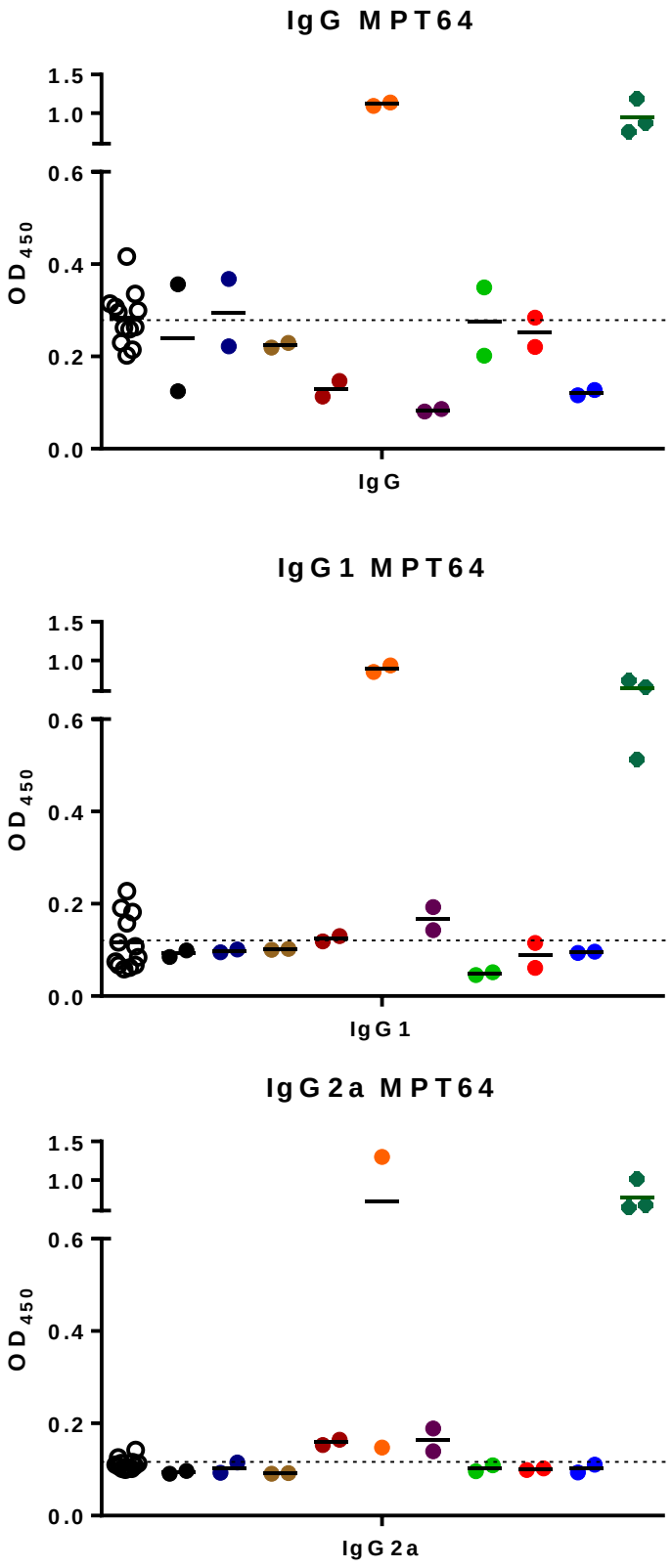

Figure 3-17. IgG subclass ELISA of serum samples on plates coated with rMPT64 (5µg/ml). Serum samples taken after immunisations (week 17) **(Figure 3-2)**. Serum was diluted 1:50 and then serially diluted down the plate. Anti-mouse IgG, IgG1 and IgG2a secondary antibodies were all HRP conjugates. The OD at 450 wavelength shown. Each dot represents and individual sample and the line shows the mean. White – pre immune, black – naïve, navy – BCG, brown – HU58 + Ag85B-Acr, dark red – HU58 + MPT64, orange – SWAN protein, purple – HU58 + SWAN, green – BCG + HU58 + SWAN, red – rHU58(MPT64), blue – BCG + rHU58(MPT64), dark green – MPT64 protein as a positive control.

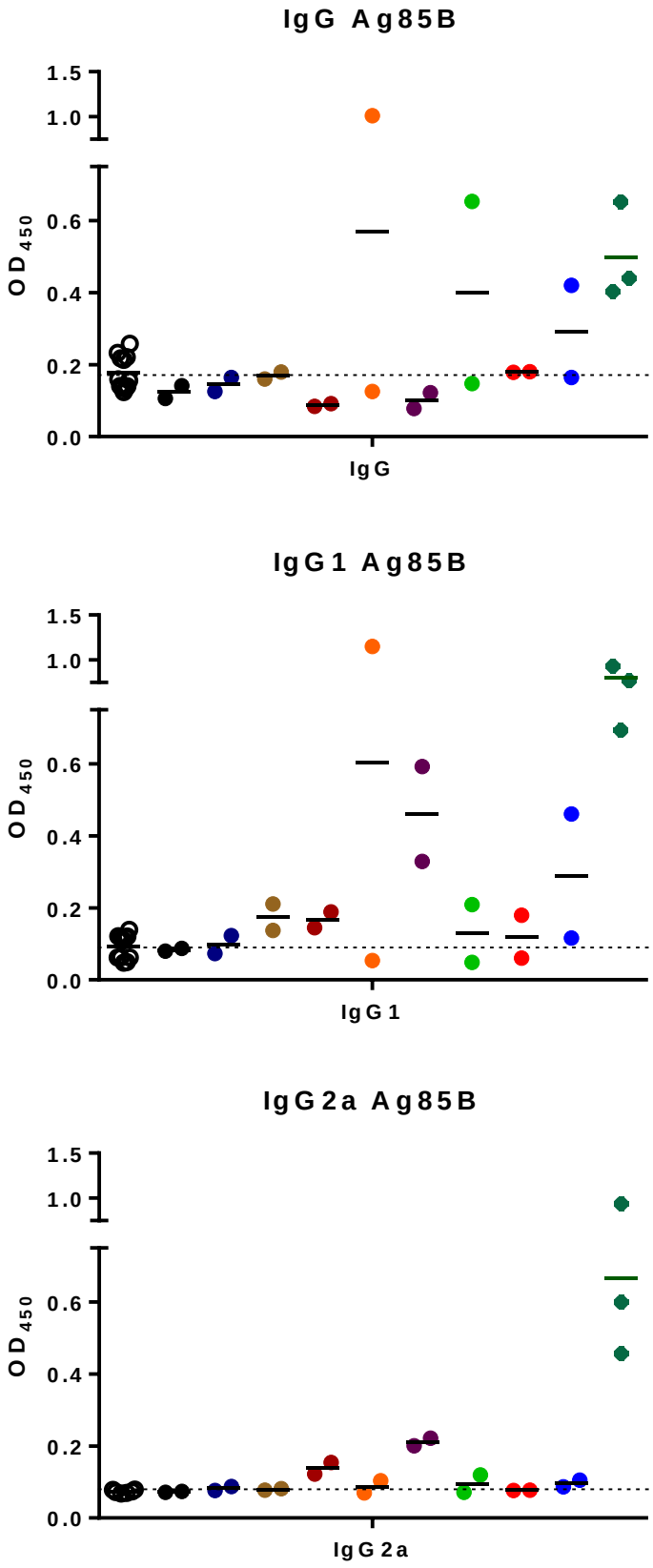

Figure 3-18. IgG subclass ELISA of serum samples on plates coated with rAg85B-Acr (5µg/ml). Serum samples taken after immunisations (week 17) **(Figure 3-2)**. Serum was diluted 1:50 and then serially diluted down the plate. Anti-mouse IgG, IgG1 and IgG2a secondary antibodies were all HRP conjugates. Each dot represents an individual sample and the line represents the mean. White – pre immune, black – naïve, navy – BCG, brown – HU58 + Ag85B-Acr, dark red – HU58 + MPT64, orange – SWAN protein, purple – HU58 + SWAN, green – BCG + HU58 + SWAN, red – rHU58(MPT64), blue – BCG + rHU58(MPT64), dark green – Ag85B-Acr protein as a positive control.

3.2.13. IFNγ ELISPOT

Splenocytes were isolated from two mice from each immunisation group as a representative sample of the cellular immunogenicity induced by the immunisations. Splenocytes were stimulated overnight with rMPT64, rAg85B-Acr and PPD MTB antigens and then IFNγ production calculated per 10^6 cells **(Figure 3-20)**.

There does appear to be some MPT64 specific IFNγ production in splenocytes from the HU58 + MPT64 group (Group D), HU58 + SWAN (Group F) and BCG + rHU58(MPT64) (Group I). Mice in the following groups show some Ag85B-Acr specific immune responses; BCG (Group B), HU58 + Ag85B-Acr (Group C), HU58 + SWAN (Group F) and BCG + HU58 + SWAN (Group G). PPD is used as a general stimulation for MTB specific cells but only animals in the BCG boosted groups show any responses to PPD (Group G and Group I). Only two mice were used in the ELISPOT assay, therefore there was a significant amount of variation and the induction of an IFNγ immune response seems to be inconsistent. If the study was repeated with more mice, it would give a clearer picture as to the reliability of the vaccines to induce a Th1 response.

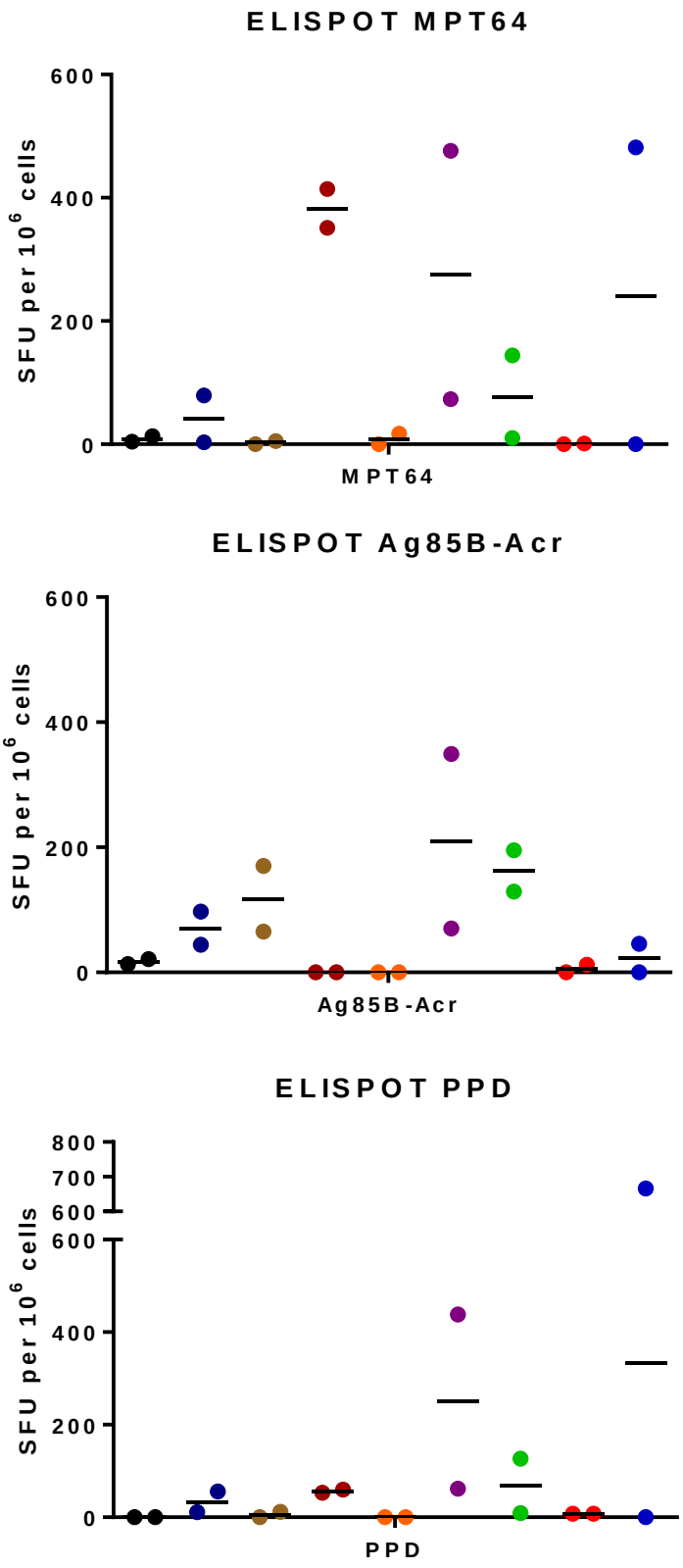

Figure 3-19. Graph of IFNγ ELISPOT results of SFU/10^6 splenocytes from two representative mice from each group. Spleens were taken from representative mice at week 16 after immunisations **(Figure 3-2)**. Cells were isolated from the spleen and $5x10^5$ cells were stimulated overnight with either rMPT64 (10µg), rAg85B-Acr (10µg) or PPD (20µg) at 37°C on an ELISPOT plate coated with anti-IFNγ capture antibody. The ELISPOT was developed according to manufacturer instructions and spot forming units (SFU) were measured using a CTL ELISPOT reader. Media only wells were subtracted from antigen stimulated wells and results were calculated to SFU/10^6 cells. Dots show individual samples and lines represent the mean. White – pre immune, black – naïve, navy – BCG, brown – HU58 + Ag85B-Acr, dark red – HU58 + MPT64, orange – SWAN protein, purple – HU58 + SWAN, green – BCG + HU58 + SWAN, red – rHU58(MPT64), blue – BCG + rHU58(MPT64).

3.2.14. Protection data

Following the immunisation regimens, eight of the ten mice were challenged intranasally with MTB at week 17 and followed for four weeks by Dr Rajko Rejlic (SGUL) **(Figure 3-14)**. At the end of the four weeks, the mice were culled and the lungs and spleens were plated out and colony counts used to estimate bacterial load **(Figure 3-20, Figure 3-21)**. Mice with no recoverable MTB were excluded from calculations because it could indicate that they were not successfully challenged with MTB. However, this means that strong conclusions cannot be made from the resulting data because the reliability of the challenge method cannot be verified. Bacteria in the lungs would indicate active disease, and bacteria in the spleens were a characteristic associated with dissemination.

BCG (Group B) was used to compare the vaccine preparations against, as this is the current vaccine so any future vaccine would need to perform at least as well or better than BCG. Spores with rAg85B-Acr (Group C) showed the greatest reduction in comparison to PBS (Group A). In the lungs, the spores with rMPT64 (Group D) in general showed a reduction in bacterial burden, but two mice returned higher MTB counts than PBS, so protection seems to be inconsistent. SWAN protein alone (Group E) did not reduce the bacterial burden greatly. It was improved with spores (Group F), but the median reduction was not better than rAg85B-Acr (Group C), so there appears to be no additive effect of using all proteins (Ag85B-Acr and MPT64 in the SWAN preparation). The responses to rHU58(MPT64) (Group H) were mixed as there were clear groups that were protected and not protected. rHU58(MPT64) with BCG (Group I) showed a lower bacterial burden in comparison to the recombinant spores alone. The greatest reduction in bacterial burden in the lungs were in the BCG

(Group B), spores with rMPT64 (Group D), BCG with HU58 + SWAN (Group G) and rHU58(MPT64) spores booster (Group I).

Overall, it would seem that both proteins separately in conjunction with spores (Groups C and D) were able to reduce bacterial burden after challenge with MTB, and were much better than protein alone (Group E). However, when both proteins were used together with the spores (Group F), there appeared to be no further decrease in CFU. The recombinant spores rHU58 (MPT64) (Group H) were not as successful as the protein adsorbed to spores, but when used with BCG (Group I), they did reduce the bacterial burden in the lungs and spleen to lower levels than BCG alone (Group B).

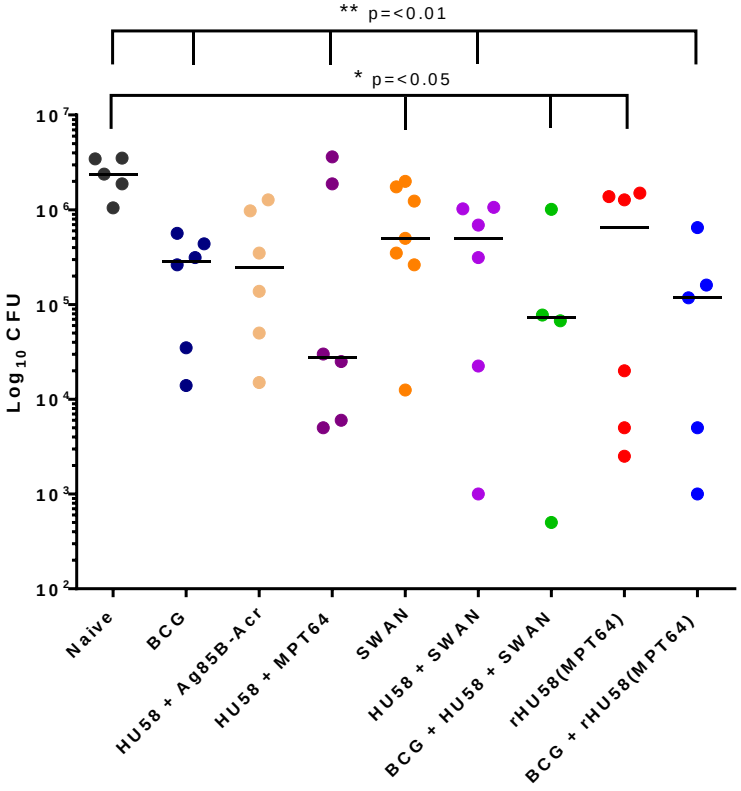

Figure 3-20. Lung CFU data. Four weeks after MTB challenge of mice that had been immunised according to the schedule with spores/protein **(Figure 3-2)** the lungs were homogenised and plated out on 7H11 agar and incubated for four weeks to measure MTB CFU. Median data shown and Mann-Whitney test performed (p=0.05).

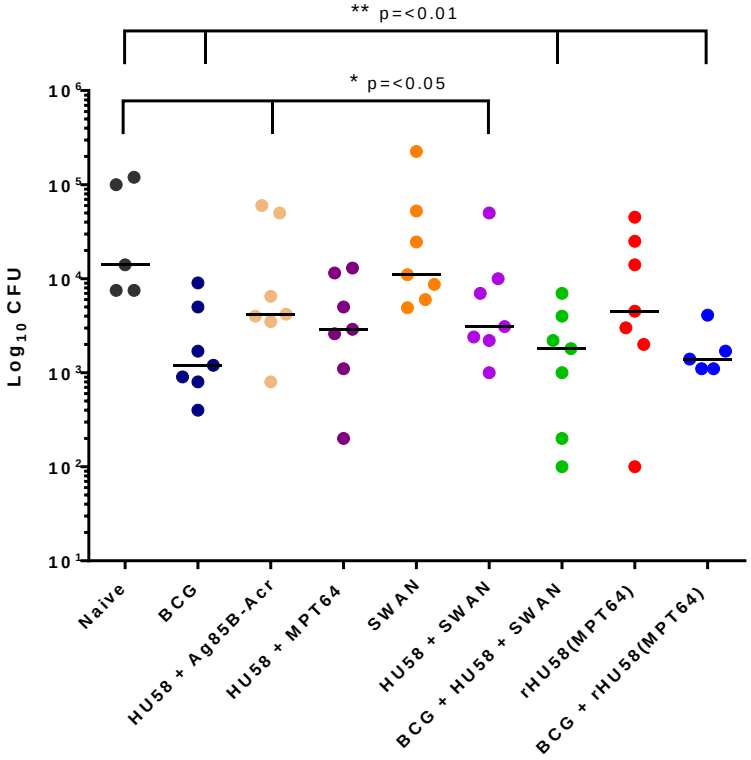

Figure 3-21. Spleen CFU data. Four weeks after MTB challenge of mice that had been immunised according to the schedule with spores/protein **(Figure 3-2)** the spleen was homogenised and plated out on 7H11 agar and incubated for four weeks to measure MTB CFU. Median data shown and Mann-Whitney carried performed (p=0.05).

3.3. Discussion

3.3.1. Vaccine formulations

3.3.1.1. Protein bound to the surface of the spores

B. subtilis spores have been used as a vaccine adjuvant carrying protein previously, including one experiment where whole virus was adsorbed to the spore surface (Song *et al*. 2012). In general, spores have been used to carry one protein only but in this work, it has been demonstrated that the spores were able to bind two proteins at the same time, and that one protein did not affect the binding of the other. This could be useful in the future for spore vaccines because more antigens may improve the diversity of the immune response since the immune system would be able to recognise more than one antigen. In the TB field, vaccines are being produced that carry more than one antigen to improve the range of the immune response (Khera *et al*. 2005). For example, vaccine H56, which carried early antigens Ag85B and ESAT6, as well as latency antigen Rv2660c showed an enhanced level of protection in comparison to BCG against TB challenge in mice, and protection was longer-lasting (Aagaard *et al*. 2011). The optimum pH of binding of rAg85B-Acr and rMPT64 in this case was similar, but this would need to be taken into account when adding more or different proteins to the vaccine. In terms of practical use as a vaccine, it was demonstrated that the protein remained bound to the spores after storage at 4°C and -20°C, but that the concentration of protein was reduced. A method for stabilising the protein on the surface to guarantee dose would need to be optimised, or the reduction taken into account when dosing.

3.3.1.2. Recombinant spores

Recombinant spores have been used previously against *C. difficile* (Permpoonpattana *et al*. 2011) and anthrax (Duc *et al*. 2007). One of the advantages of using recombinant spores is that the expression of antigen is more uniform than protein bound to the surface. We demonstrated here that the spores could express rMPT64 in the spore coat and were weakly expressed on the surface. Other spore vaccine preparations have used CotB as a fusion protein because it is abundant in the spore coat, and have detected the antigen using confocal microscopy (Permpoonpattana *et al*. 2011; Duc *et al*. 2007). In this experiment, the fusion of MPT64 to CotB could not be detected on the surface strongly using ELISA, immunofluorescence or flow cytometry (data not shown) but this could be because these techniques depend on the antigen being surface exposed whereas confocal microscopy can examine interior structures. The results here are supported by data from Hinc *et al* that showed that when UreA was expressed fused to CotB, CotC and CotG, the fluorescence was weakly detected with CotB when using immunofluorescence (Hinc *et al*. 2010). Isticato *et al* also demonstrated that CotB could be detected using flow cytometry, but when CotB-TTFC was expressed, the antigen-specific fluorescence was very weak (Isticato *et al*. 2001a). Isticato *et al* hypothesised that the low surface expression was due to the full-length CotB also being present (Isticato *et al*. 2001a). Imamura *et al* have examined the localisation of different spore proteins using immunofluorescence and have found that whilst CotB is in the outer spore coat, it is not on the outside of the spore, and therefore it could be that the antigen is covered by the spore crust (Imamura *et al*. 2011). Other researchers have investigated using spore crust proteins; CotZ and CgeE as fusion proteins for surface display of enzymes or antigens instead

(Mascher *et al*. 2012; Negri *et al*. 2013).Despite the antigen possibly not being surface expressed, the MPT64 antigen was confirmed to be expressed in the spore coat using Western blotting and the spores expressing CotB-MPT64 still provided some protection against TB challenge. This could be because the spores are phagocytosed and degraded and therefore the digested spore coat proteins and antigens can still be presented by APCs to provoke the production of antigen-specific antibodies.

There are several vaccines that use formaldehyde to inactivate active components before delivering the vaccine. Examples include; Polio (Salk & Salk 1984) and Hepatitis A (Pellegrini *et al*. 1993) vaccines. Recombinant *Bacillus* spores need to be inactive because they carry antibiotic resistance genes that could be potentially transferred to other bacteria. The levels of formaldehyde have to be reduced to a safe level before administration, as formaldehyde is a likely carcinogen and relatively toxic. In this experiment, recombinant spores were able to be significantly inactivated by formaldehyde. The formaldehyde was removed effectively with washing so that it did not affect the health of the animals. The main problem with this method of inactivation was that not all of the spores were inactivated, so there is a chance some of them could proliferate in the host. However, the method is being further optimised by other lab members as part of the CDVAX project, which is developing the spore based vaccine described by Permpoonpattana *et al* for use in a human clinical trial (Permpoonpattana *et al.* 2011, www.CDVAX.org). An alternative method for using recombinant spores is also being investigated in the Cutting lab is to clone antigens into *B. subtilis* without using antibiotics, therefore removing the risk of antibiotic resistance transmission (unpublished).

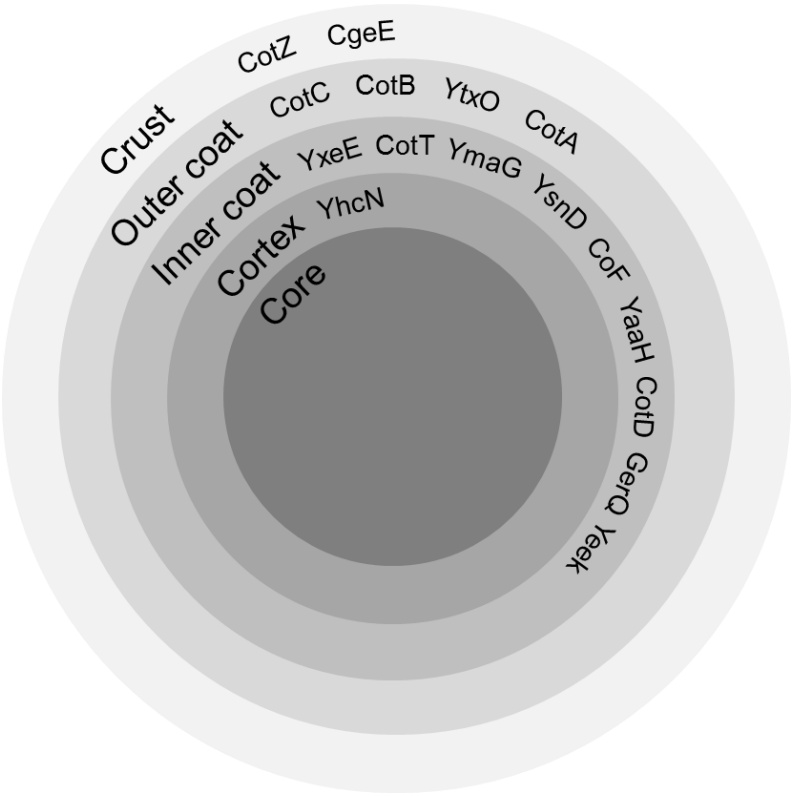

Figure 3-22. Schematic of the organisation of the spore coat proteins. Adapted from (Imamura *et al*. 2011)

3.3.2. Immune responses and protection

3.3.2.1. Antibody ELISA

The antibody titres after vaccination were very low, apart from the SWAN protein alone samples. The SWAN protein was delivered intranasally using Alum, which is an adjuvant that is known to stimulate Th2 biased immune responses (Marrack *et al*. 2009), which could account for why the antibody titres were higher. The dosing route may also have affected the systemic immune responses. White *et al* has shown in NHPs that the antibody titres were much lower when aerosol BCG was compared to BCG delivered subcutaneously (White *et al*. 2013).

In previous studies carried out at Royal Holloway by Huang *et al*, three doses of spores were given, the last dose on day 43 and the serum taken for ELISA on day 63 (Huang, Hong, *et al*. 2010). In this study there was an eight week gap (approximately 56 days) between the last dose and taking the samples for immunogenicity experiments because we wanted to see what the state of the immune system was around the time of MTB challenge. However, this could mean that the antibody titre could have waned by this point. The study should be repeated and serum taken earlier after vaccination to detect antibody responses and more animals should be used.

3.3.2.2. IFNγ ELISPOT

There appeared to be some antigen specificity in the IFNγ ELISPOT immune responses, and together with the IgG ELISA data, the spores appear to promote cellular immune responses over antibody responses. However, the ELISPOT responses are low overall in comparison to some studies (Kamath *et al*. 1999) but are comparable to those reported by Esparza-Gonzalez *et al*, who also used

B. subtilis spores to deliver MTB antigens ESAT-6 subcutaneously (Esparza-Gonzalez *et al*. 2014) and Kaveh *et al* also showed ELISPOT results of between 100-500 SFU/million cells in splenocytes after BCG vaccination (Kaveh *et al*. 2011). Picking an earlier time point after vaccination may have shown stronger responses. Santosuosso *et al* has shown that there was a high level of IFNγ production two weeks after vaccination intramuscularly with AdAg85A, which had declined by week eight (Santosuosso *et al*. 2006). Therefore, due to the immunological analysing being undertaken 17 weeks after BCG and 8 weeks after the other vaccination regimens, the peak IFNγ ELISPOT response may have been missed.

The route of immunisation is also important as although in some studies, mucosal dosing has shown comparable systemic immune responses to injection routes (Cuburu *et al*. 2007), other studies have shown that there are poor systemic antigen specific T-cell responses after intranasal dosing in comparison to injectable delivery of vaccine, although the responses in the lungs and BAL were higher (Santosuosso *et al*. 2006; White *et al*. 2013).

The study could be improved by using more animals, changing the time that immune responses were monitored to be earlier after vaccination and analysing responses in mucosal tissues as well as splenocytes.

3.3.2.3. Protection

The data suggested that the spores that carried MPT64 and Ag85B-Acr proteins did cause a reduction in bacterial burden below that of PBS. However, because some animals did not appear to be infected with MTB, as demonstrated by the lack of CFU from some of the tissues, strong conclusions cannot be drawn from the data. Either the animals were able to fight off the TB infection completely or

the nasal dosing of MTB was not consistently able to cause disease, which means that the dose of MTB could be variable for all animals. The study needs to be repeated to get more consistent infection.

3.4. Conclusions

Although there was a lack of strong immune responses seen in the test animals, there does appear to be some reduction in bacterial burden after nasal dosing with spores. In the literature, it has been shown that Adenovirus carrying Ag85A delivered nasally had poor systemic immune responses in mice, but provided better protection than when delivered intramuscularly (Santosuosso *et al*. 2006) so a lack of peripheral immune response may not necessarily mean that no protective immune responses have been mounted. It would be important in the future to use lung samples and BAL washes to assess mucosal immune responses, as done by others in the field (Redford *et al*. 2010; Algood & Flynn 2004; White *et al*. 2013).

Vaccine development for TB is difficult because of the lack of correlates of protection. IFNγ is known to be important because IFNγ knock-out mice are much more susceptible to TB (Cooper *et al*. 1993). IFNγ activates macrophages, which are important in the initial infection by MTB (Ehrt & Schnappinger 2009). The problem with IFNγ is that it is required for protection, but high levels do not guarantee protection. This was also observed by Sharpe *et al* in a non-human primate (NHP) study, where primates who had high post-vaccination levels of IFNγ succumbed to infection quickly after challenge (Sharpe *et al*. 2010).

In this study, a reduction in bacterial burden in the lungs and spleen in mice in test groups compared to PBS was observed. The mouse model is useful

because there is the capacity to measure the immune response. However, disease progression in mice is very different to human disease as they do not form granulomas in the lungs and control the disease differently. The mouse model also does not develop latent disease, but has chronic disease instead, and host-to-host transmission has not been successfully mimicked (Korbel *et al*. 2008). The other rodent model that is utilised for TB research is the guinea pig because it is sensitive to TB and forms granulomas (Williams *et al*. 2009). However, there are not many immunological reagents developed for the guinea pig so it is useful for looking at survival, but not at immune responses. The non-human primate (NHP) model is the best animal model for TB because disease is much closer to the human disease, there are reagents available to monitor the immune response and multiple and relatively large blood samples can be taken at intervals to monitor the immune response over time (Sharpe *et al*. 2010). However, the NHP model is expensive and specialist facilities are required to house NHPs at containment level 3 (CL3) because MTB is an ACDP3 organism. Other general problems with animal models are that the immune system does differ to humans; for example in mice, the antibody subclasses are different, and therefore it can be difficult to relate the results back to humans. This was important in the TGN1412 clinical trial. The TGN1412 treatment was for autoimmune diseases and was safe in primate studies, but caused severe life-threatening illness in primary clinical trials. The cause of this was that there was a difference in the structure of the CD28 receptor the antibody recognised between primates and humans, which explained why they saw no adverse effects in primates (Attarwala 2010).

The lack of correlates of protection makes research into novel vaccines difficult and relies on big clinical trials with large cohorts of patients to see any

protective effects. Clinical trials are expensive and time consuming, as TB is a slow infection and it can take years for active TB disease to develop so long follow up times with patients are required. Research is underway to investigate *in vitro* tests that can be used to validate biomarkers and vaccines. For example, continuous culture of MTB has been used to mimic conditions of oxygen limitation and latency, which has provided gene expression data that could yield useful targets for vaccine development (Bacon & Marsh 2007). Another approach is to find early correlates of protection after vaccination to reduce the length of time of clinical trials. A mycobacterial inhibition assay is showing some promise and can show that BCG vaccinated individuals inhibit MTB growth better than unvaccinated persons (Marsay *et al*. 2013; Fletcher *et al*. 2013).

Chapter 4: Localisation of Spores after Dosing by Different Mucosal Routes

4.1. Introduction

There is considerable interest in mucosal vaccines as an alternative to injectable vaccines for many reasons including ease of use and needle-free administration which reduces the risk of transmission of blood-borne diseases. A major advantage of mucosal vaccines is that the mucosa is the major portal of entry for many pathogens and therefore immune cells active at mucosal sites as more relevant (Neutra & Kozlowski 2006) and in some cases are able to stimulate systemic immune responses as well. For example, Kowolski *et al* demonstrated that after nasal, rectal and vaginal immunisation with cholera toxin, IgG in the sera could be detected (Kozlowski 2002). There is evidence that suggests that injectable vaccines are less able to elicit mucosal immune responses, as demonstrated by Santusuosso *et al* that after intramuscular vaccination with AdAg85A there were fewer CD4+ and CD8+ cells in the BAL and lungs in comparison to intranasal vaccination in mice (Santosuosso *et al*. 2006). However, Kaveh *et al* showed IFNγ ELISPOT responses in the lung after intradermal BCG vaccination in mice (Kaveh *et al*. 2011).

There are three main routes for mucosal vaccination; nasal, oral and sublingual (Holmgren & Czerkinsky 2005; Czerkinsky *et al*. 2011). The MALT tissues are linked and immunisation via each route should be able to stimulate specific immune responses at other mucosal locations (Holmgren & Czerkinsky 2005). One of the challenges of using oral dosing is that the gut is specialised to

tolerate foreign entities such as food and commensal bacteria, which means that it can be difficult to induce an immune response and for the gut to not develop tolerance to the antigens. The immunosuppressant environment of the gut is regulated by Tregs and Th3 cells producing IL-10 and TGFβ. DCs in the gut default to Th2/Th3 cell stimulation in comparison to Th1 biased spleen DCs, and so produce anti-inflammatory cytokines including IL-4, IL-5, IL-10 and TGFβ that reduce potential immune stimulation (Iwasaki & Kelsall 1999). Despite the problems associated with oral dosing, there are licenced oral vaccines against polio, cholera and typhoid (Holmgren & Czerkinsky 2005).

Nasal dosing can directly access the lungs and so would be suitable for respiratory pathogens, such as TB. There is a nasal vaccine licensed for influenza (Van Kampen *et al*. 2005) and aerosol vaccines are also under investigation for TB (White *et al*. 2013). Safety concerns exist for nasal vaccination, most notable of which is that it could cause Bell's palsy, which is a form of facial paralysis (Czerkinsky *et al*. 2011), as has been the case after nasal administration of cholera toxin and *E.coli* labile toxin as adjuvants in the flu vaccine 'Nasalflu' (Rath *et al*. 2007). After investigation, it was found that the toxicity was due to the toxins binding to neuronal cells. 'Flumist', a nasal flu vaccine that does not contain any toxins, has had no cases of Bell's palsy associated with it (Rath *et al*. 2007). Therefore, the risk of Bell's palsy after nasal administration is small, and is dependent on the adjuvant used.

Sublingual dosing is administered under the tongue, and for example, glyceryl trinitrate medication for angina is administered by this route (NHS 2014a) since the drug can access the bloodstream faster because the sublingual mucosa is highly vascular. The other advantages are that sublingual dosing avoids

destruction by the acid in the stomach and avoids metabolism in the liver that could affect the vaccine formulation and potency. Sublingual dosing is attracting more attention as a vaccine delivery route because they have been used for allergy treatments with no adverse effects and show good humoral and cellular immune responses (Shim *et al*. 2013). The sublingual mucosa is packed with DCs, which are mobilised on immunisation, so that large proteins can be disseminated to lymphoid tissue (Amuguni *et al*. 2012). A comparison of the different routes of mucosal vaccination by Czerkinsky *et al* indicated that systemic antibody responses were highest after sublingual and nasal vaccination with ovalbumin and cholera toxin adjuvant. Secretory IgA (sIgA) was detected in the respiratory tract, stomach, small intestine, genital tract and blood after sublingual dosing, respiratory tract and blood after nasal dosing and in the stomach, small intestine, colon, rectum and blood after oral dosing (Czerkinsky *et al*. 2011).

B. subtilis spores have been shown to be efficacious in oral (Permpoonpattana *et al*. 2011), sublingual (Amuguni *et al*. 2011) and nasal (Song *et al*. 2012) dosing regimens, but the mechanism of how the spores cross mucosal barriers to be able to generate responses is not well defined. M cells, the specialised epithelial cells that are able to transport antigens across the epithelium to immune cells are a target in the development of mucosal vaccines because if uptake by M cells can be increased, then the presentation of the antigen to the immune cells would also be improved. The uptake of spores by M cells has been shown in the appendix of rabbits (Rhee *et al*. 2004), but in this chapter, lung and NALT M cells have also been investigated as M cells are present in all epithelium. MTB has been demonstrated to be able to enter lung tissue via M cells (Teitelbaum *et al*. 1999) and Group A *Streptococci* can translocate M cells

of the NALT (Park *et al*. 2003), therefore providing some evidence that certain bacteria translocate into tissues via M cells in these locations.

Macrophages have been shown to phagocytose spores *in vitro* (Huang, La Ragione, *et al*. 2008; Duc *et al*. 2004), but how much of a role they play *in vivo* is less well understood. DC maturation, which is an indication that DCs are presenting antigen and are capable of migration, was demonstrated with spores *in vitro* by Song *et al* (Song *et al*. 2012) and *in vivo* by de Souza *et al* (de Souza *et al*. 2014). DCs may be important in activation of the immune system after delivery of spores because of their ability to sample the lumen outside of the epithelial layer. Macrophages and DCs, as APCs are important immune cells for vaccine research because of their ability to prime T-cells and develop the memory response. Neutrophils were also examined because they are usually the first phagocyte to reach the site of infection and are responsible for bacterial clearance. Identifying the phagocytes responsible for clearance of spores could be advantageous because it would provide evidence that the spores were cleared and would not induce inappropriate immune responses.

The epithelium in the mucosa is an important barrier to keep pathogens from entering tissues and causing infections, but this also means it is a barrier to mucosal vaccines. It is important for the spores to be able to cross the epithelium so that they can elicit immune responses. In this chapter, the distribution of spores, ability to enter the lung tissue and the clearance of spores in the lungs after nasal dosing was examined to provide some preliminary information about how well the spores could enter the lungs and the length of time before they were cleared. The information from this study informed the following experiment, where the nasal route was compared to the oral and

sublingual routes to investigate the distribution of spores to the lungs, gut and NALT tissue. The distribution of spores after dosing by each route is also important as it may dictate where the strongest immune responses will be.

Spores were also characterised by flow cytometry. Flow cytometry uses light scattering to determine relative size and granularity of cells and is commonly used in haematological analysis to determine granulocytes, monocytes and lymphocyte populations. Flow cytometry is not as frequently used in microbiology as in the immunology field, but there are applications for it to be used; i) in identifying bacteria (Holm *et al*. 2004), ii) analysing cell cycles, iii) sporulation, iv) taxonomy (Cronin & Wilkinson 2010) and v) biofilm formation (Garcia-Betancur *et al*. 2012) in bacteria. Some previous publications have described evaluating spores on the flow cytometer to detect antigen expression (Isticato *et al*. 2001b; Kim *et al*. 2005), GFP expression when fused to CotG (Kim *et al*. 2007) or live/dead populations (Virta *et al*. 1998) however this has not been done using the BD Accuri C6 nor were the populations of spores and vegetative cells described. Analysis of the FSC-SSC profile of *Paenibacillus polymyxa,* (a spore former) was able to identify vegetative cells and two types of spores, which was confirmed using electron microscopy (Comas-Riu & Vives-Rego 2002) and demonstrated that flow cytometry is a useful and sensitive tool for characterising spore forming bacteria.

The method for intracellular staining of spores inside mammalian cells was optimised prior to the *in vivo* experiments. Examining uptake of particles using the flow cytometer has been described by Byersdorfer and Chaplin (Byersdorfer & Chaplin 2001) using stained beads and tracking their temporal movement to from the lungs to the lymph nodes. Trouillet *et al* described a method for

staining *Staphylococcus aureus* inside cells *in vitro* after invasion and detecting these on the flow cytometer using saponin to permeabilise the cells so as to allow entry of the antibody into the cell interior to label the bacteria (Trouillet *et al*. 2011). The method is not dissimilar to intracellular cytokine staining used in Chapter 3 and described by Beveridge *et al* (Beveridge *et al*. 2007).

Live and autoclaved spores were used for the experiments because both states could potentially be used in vaccine preparations. The advantage of using autoclaved spores is that they will not germinate and therefore will present the antigen for longer because the antigen is on the surface of the spore. Autoclaved spores have been shown to be able to carry antigens and elicit antibody responses (Song *et al*. 2012; Huang, Hong, *et al*. 2010), but there is evidence to suggest that they are less immunogenic, as de Souza demonstrated that heat-killed spores induced lesser amounts of IL-4, IFNγ, TNFα, IL-12, IL-1β and there was lower expression of MHC I and MHC II on DCs in comparison to live spores (de Souza *et al*. 2014). Therefore, the initial interactions of live and autoclaved spores with host cells were examined to see whether it could be responsible for the differences in adaptive immune responses later on.

4.1.1. Aims

The overall aim of this chapter was to compare oral, nasal and sublingual routes of immunisation and their ability to deliver spores to different tissues. The capability of spores to cross the mucosal barrier is important as it might affect dosing and could imply where the strongest immune responses could be generated. The cells that phagocytose the spores are also important and will have downstream implications for the adaptive immune responses. Live and

autoclaved spores were compared to see whether there was a difference in uptake dependent on the physiological state of the spore.

4.2. Results

4.2.1. Detection of fluorescent spores, DS127

A strain of *B. subtilis*, DS127 (*amyE::cotC-GFP*), that expresses Green Fluorescence protein (GFP) on the spore surface was used and has been described elsewhere (Isticato *et al*. 2001b). GFP is fused in frame to the carboxy-terminus of the outer spore coat protein CotC. Spores of DS127 were purified and GFP expression confirmed by fluorescence microscopy using a FITC laser and green fluorescent spores were observed. PY79 spores, which are isogenic to DS127 and do not express GFP were used as the negative control in parallel and PY79 spores were found to exhibit little background fluorescence **(Figure 4-1)**. Background fluorescence is caused by the natural autofluoresence of biological material and can be due to certain proteins and molecules. In the case of spores autofluorescence is hypothesised to be due to the dityrosine proteins that crosslink coat proteins and pigments present (Magge *et al*. 2009). The poles of DS127 exhibited greater fluorescence, which corresponds with data from Isticato *et al* that demonstrated that CotC was localised here (Isticato, Sirec, Giglio, *et al*. 2013).

4.2.2. Analysis of infection of RAW267.4 macrophages with DS127 spores

Macrophages have previously been shown to phagocytose spores *in vitro* (Duc *et al*. 2004), and was confirmed here to determine whether DS127 spores could be identified in cell culture. RAW267.4 macrophages were infected with DS127 spores. After thirty minutes co-infection with spores, the cells were fixed and the nuclei stained with DAPI. Slides were examined using an EVOS microscope at 100x magnification. Large clumps of spores were evident in the cytoplasm of some of the macrophages **(Figure 4-2)**. This demonstrates that macrophages

are indeed capable of engulfing spores and that DS127 can be detected inside RAW267.4 cells in culture.

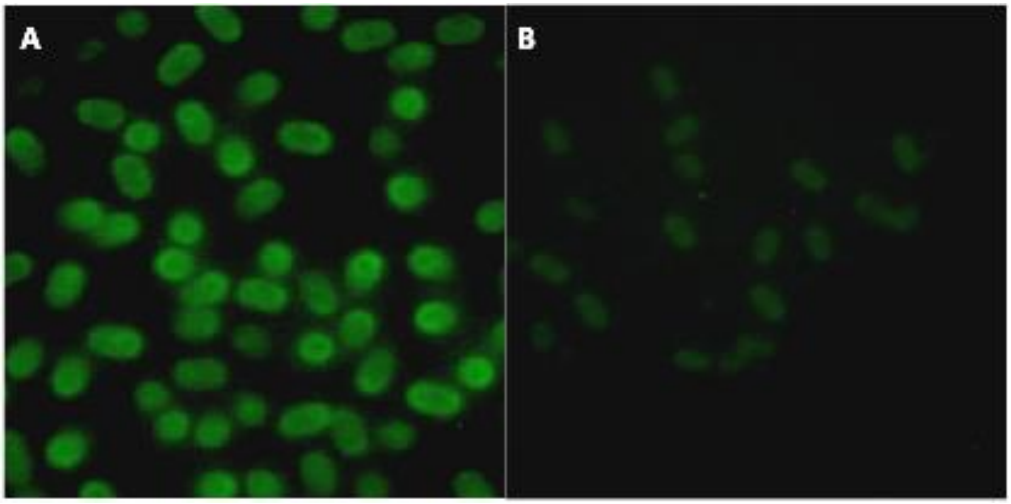

Figure 4-1. Fluorescence microscope images showing DS127 spores expressing GFP. Spores were grown and purified as outlined in the methods (Chapter 2) and ~1x10^8 aliquoted and dried onto coverslips. Slides were examined using a Nikon fluorescent microscope with a FITC laser. Panel A, DS127 spores expressing GFP; panel B, PY79 spores.

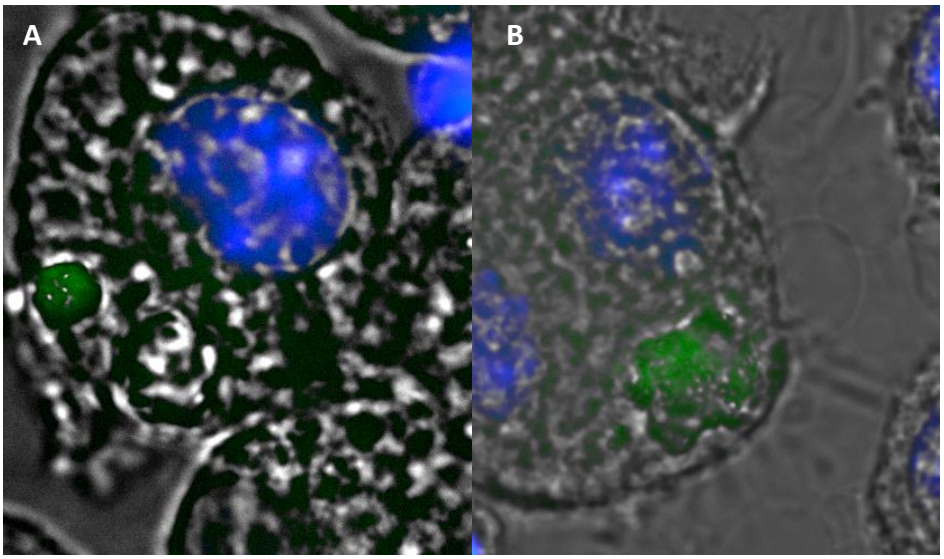

Figure 4-2. Immunofluorescence images of DS127 spores inside the cytoplasm of RAW267.4 macrophages. Macrophages were grown as a monolayer for 48h and then incubated with 1x10^8 spores for 30 min at 37°C. Green (spores). Macrophage nuclei were stained for 5 min at RT with DAPI (blue). Examined at 100x magnification using an EVOS fl microscope.

4.2.3. Analysis of lung tissue samples infected with DS127 spores

C57BL/6 Mice (n=4) were dosed intranasally with $2x10^9$ DS127 spores and culled at 2, 6, 24 or 48h post-immunisation. The lungs were removed and fixed in 10% (v/v) neutral buffered formalin (NBF). Embedding, tissue sectioning and staining was carried out at TUPI Ltd. Some lung section slides were left unstained and other tissue section slides were stained using haematoxylin and eosin stain (H&E) so that the lung tissue structure could be observed.

Although the spores were not stained, they were identified in the H&E sections by i) relative size in comparison to the cells and ii) being phase-bright, a characteristic of spores **(Figure 4-3)**. At 2h, spores were seen in the lungs, and were in general found to cluster in the bronchiolar regions and in the airways. This confirmed that spores administered intranasally could enter the lungs, but after 2h, did not penetrate the tissues to any great extent. After 6h, spores could still be identified in the bronchioles and had moved into the alveolar regions of the lung. There were changes in the tissue and there was an infiltration of cells and some phagocytosis could be observed. Spores were rarely identified in the 24h and 48h samples, but there was a change in the cell populations in the lung tissue. Cellular infiltration was identified and monocytes/macrophages were observed with many phagosomes in the cytoplasm. Confocal images were taken by Dr Andreas Hoppe (Kingston University, London). Spores could be identified in the airways, but the spores were not bright enough to be able to distinguish them from the natural autofluorescence of the lung tissue.

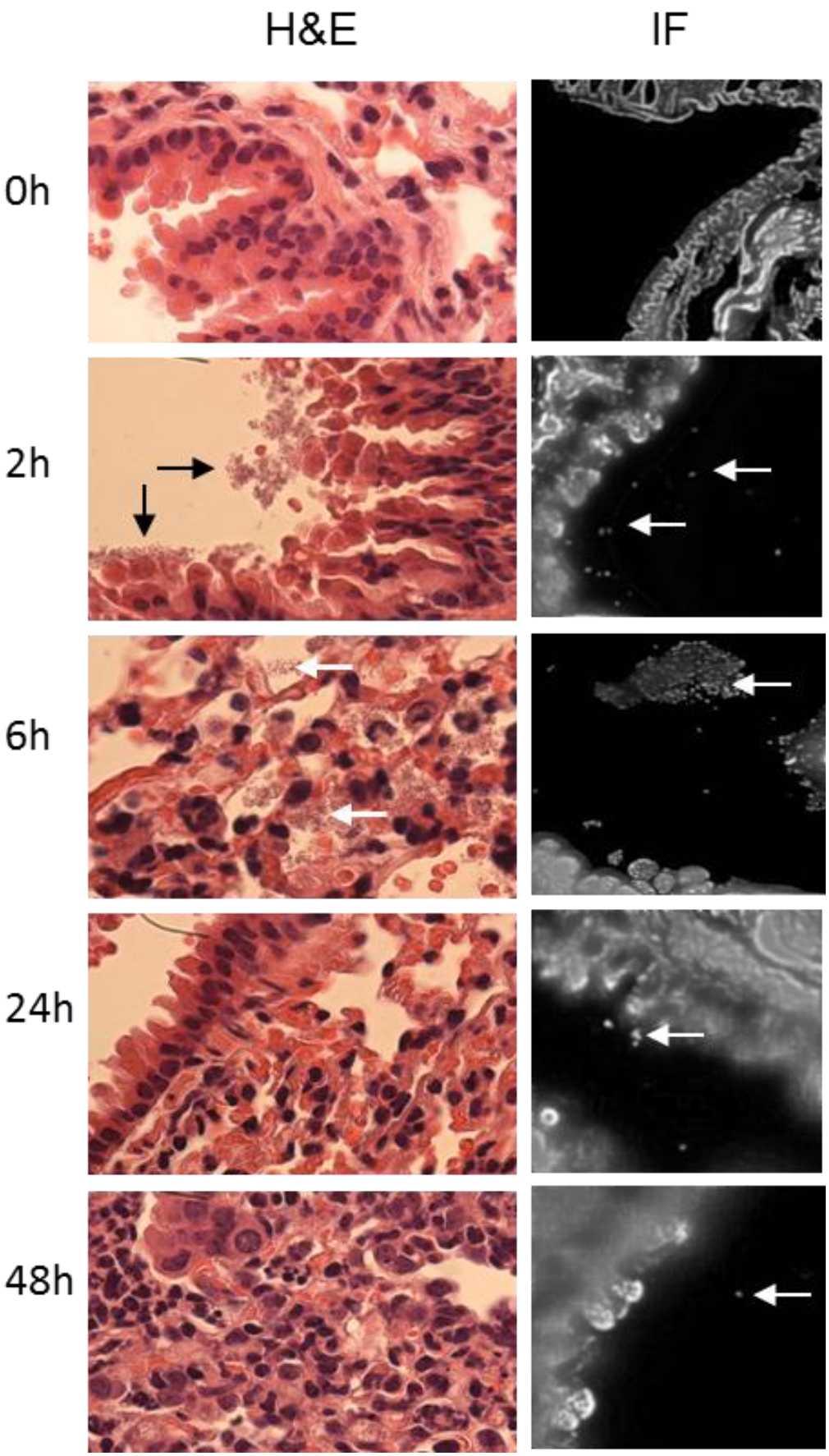

Figure 4-3. Representative images of H&E stained lung sections from mice that had been dosed intranasally with 2x10^9 DS127 spores and culled at time points after dosing. Samples from C57CL/6 mice at 0, 2, 6, 24 and 48h after intranasal dosing with 2x10^9 DS127spores. Arrows indicate spores.

4.2.4. Detecting spores using a flow cytometer

Before dosing the mice for the next study, DS127 spores were grown in liquid DSM at 37°C for 48h and samples were taken at intervals and compared to purified spores to i) characterise the populations of vegetative cells and spores in the medium, and ii) determine how these populations changed over time, so that they would be easier to identify in mouse tissue samples after dosing using the flow cytometer.

Forward Scatter (FSC) and Side Scatter (SSC) were used to characterise how the different cells appeared on the flow cytometry plot. There was a distinct difference in the FSC between actively growing vegetative cells and purified spores **(Figure 4-4)**. After 6h growth, only one population of cells could be detected and it was confirmed under the microscope that these were vegetative cells. After 24h, two distinct populations were apparent, one under 20,000 FSC units, and the other over 20,000 FSC units **(Figure 4-4)**. These populations became more distinct over time. After purification of spores, there was only one population which was above 20,000 FSC units and this was confirmed by microscopy as spores. Vegetative cells of *B. subtilis* are longer (1-2 µm) than spores (~1 µm) but are of smaller relative size as measured using FSC in the flow cytometer. This might be because FSC-A (forward scatter area) was used and the distance across the vegetative cell is smaller than that of a spore. These results were confirmed with spores of various other strains (HU58, PP108) and species such as *C. difficile* 630 by other lab members.

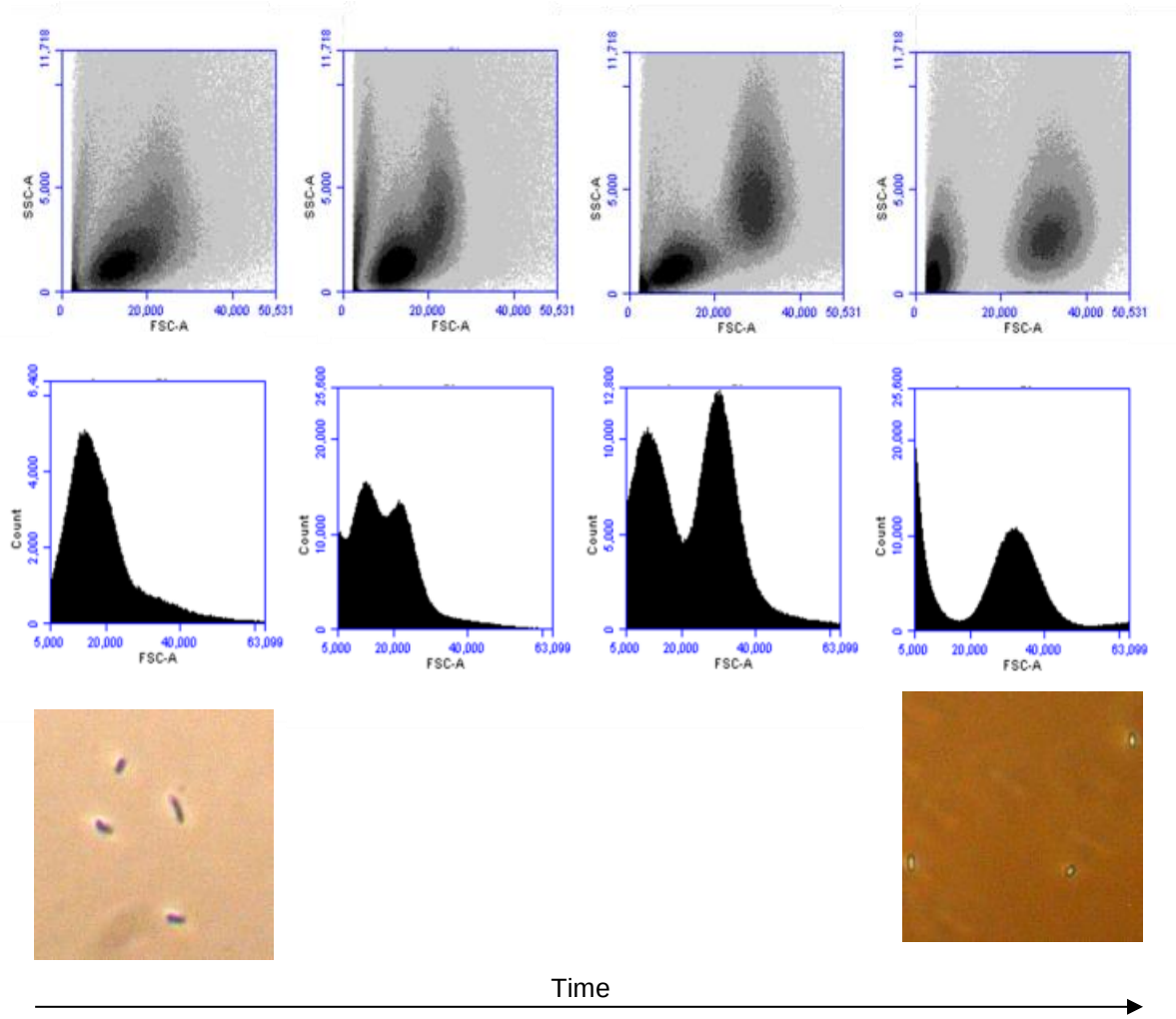

Figure 4-4. Spore development characterised on the flow cytometer. DS127 was grown in liquid DSM and 1ml samples taken at intervals and ~100µl run on the flow cytometer to determine how the populations of vegetative cells and spores appeared on the flow cytometer. Plots show two distinct populations separated by SSC and FSC on the density plot and by FSC on the histogram.

4.2.5. Detection of fluorescent spores

DS127 spores express GFP, but the fluorescence needed to be detectable on the flow cytometer to be able to identify them in the mouse dosing experiment. If the fluorescence could not distinguish between wild-type spores and DS127 then an antibody-based method would be required. Spores harvested at different days were also tested, but none of the DS127 batches expressing GFP had sufficient fluorescence to distinguish them from PY79 spores that did not express GFP. Anti-spore primary antibody was therefore used, followed by a secondary antibody conjugated to FITC, whereupon the spores were successfully shown to be fluorescent **(Figure 4-5)**.

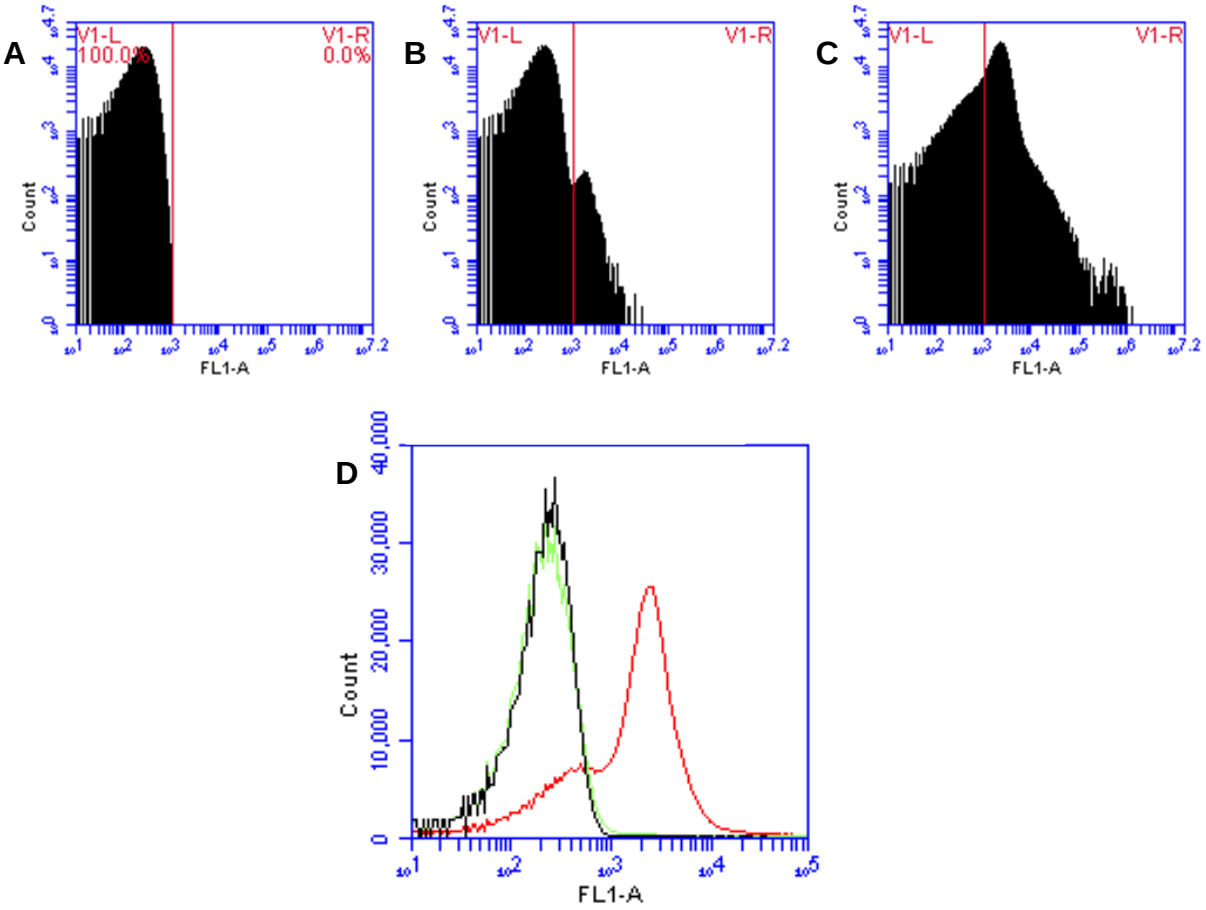

Figure 4-5. Detection of fluorescence using anti-spore and anti-FITC antibodies. Spores were blocked with BSA for 10 min and incubated with anti-spore primary antibody for 10 min, washing and using anti-rabbit IgG-FITC before washing with PBS and running on the BD Accuri C6. A; PY79 without antibodies, B; DS127 without antibodies, C; DS127 with antibodies, D, overlay of plots with and without antibodies; Black; PY79 wild-type spores with no antibodies, Green; DS127 with no antibodies. Red; DS127 with antibodies, showing a distinct shift in fluorescence.

4.2.6. Comparison of the morphology of live and autoclaved spores

Live and autoclaved spores were aliquoted onto a microscope slide to visually compare them and observe any obvious morphological differences that could account for potential differences observed in later experiments when used for dosing. The live HU58 spores were uniformly shaped, scattered and phase-bright **(Figure 4-6)**. In comparison, autoclaved spores were more clumped, less phase-bright and somewhat smaller. However, the spores did retain their shape. Therefore, even at the level of light microscopy, morphological differences can be observed between live and autoclaved spores.

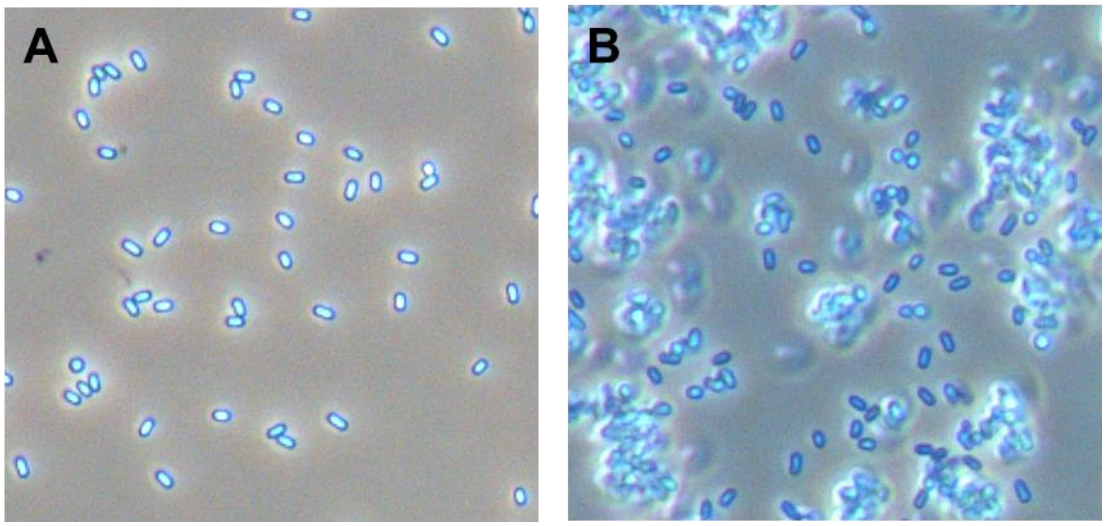

Figure 4-6. Phase contrast images of live HU58 and autoclaved HU58 spores. 1µl of each spore suspension added to slide with 5µl water and examined using oil immersion and phase-contrast microscope. Panel A; live HU58 spores, Panel b; autoclaved HU58 spores. Pictures taken at 100x magnification using Nikon Ti Eclipse microscope.

4.2.7. Spore coat extracts of live and autoclaved spores

To investigate the damage to the spore coat following autoclaving, the spore coats were extracted and run on an SDS-PAGE gel to look at whether the surface proteins were denatured after autoclaving. Anti-spore, anti-CotB and anti-CotC antibodies were used in a Western blot of the spore coat extracts to determine whether the antibodies could detect autoclaved spores and whether the coat proteins were damaged beyond antibody recognition. The results showed that no spore coat proteins could be seen in the SDS-PAGE gel and CotB and CotC spore coat proteins could not be detected by Western blot in autoclaved spores **(Figure 4-7)**. However, anti-spore antibody still was able to detect the autoclaved spores, so there must be some proteins that had remained intact for the antibody to bind to **(Figure 4-7)**.

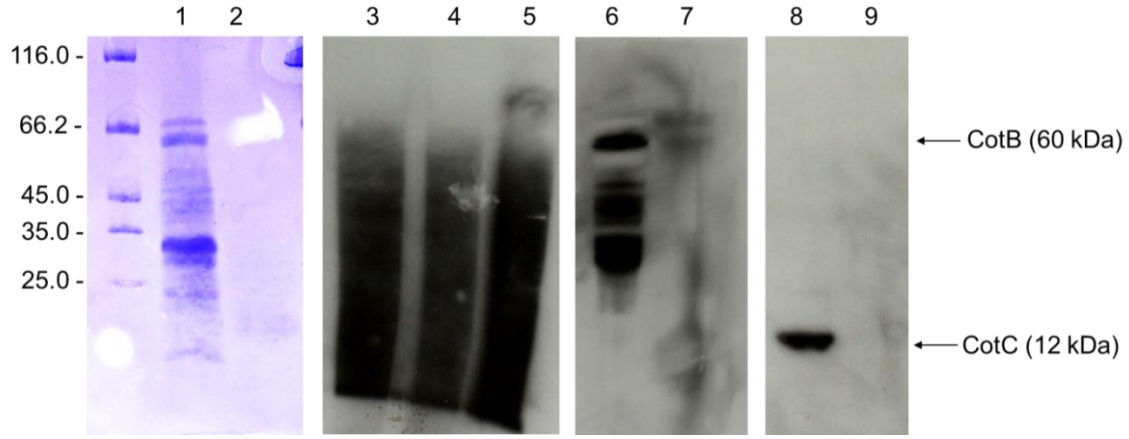

Figure 4-7. Spore coat extract analysis of live and autoclaved HU58 spores. Spore coats extracted from $2x10^9$ live and autoclaved HU58 spores were run on a 4-12% gradient SDS-PAGE gel and stained with coomassie blue and ladder shows kDa. Lane 1; live HU58, lane 2; autoclaved HU58. The gel was then transferred to a membrane and anti-spore, anti-CotB or anti-CotC antibodies (both 1:4000) used to detect spore coat proteins. Lane 3; live HU58, lane 4; live HU58 diluted 1:2, lane 5; autoclaved HU58 with anti-spore antibody, lane 6; live HU58, lane 7; autoclaved HU58 with anti-CotB antibody, lane 8; live HU58, lane 9; autoclaved HU58 with anti-CotC antibody. Anti-spore detected using anti-rabbit IgG-HRP, anti-CotB and anti-CotC detected with anti-mouse IgG-HRP.

4.2.8. Demonstration of fluorescent antibody binding to live and autoclaved spores

Anti-spore and anti-rabbit IgG-FITC antibodies were used to identify live and autoclaved spores using the flow cytometer. Autoclaved spores were able to bind the antibodies and showed a similar fluorescence intensity to live spores **(Figure 4-8)**.

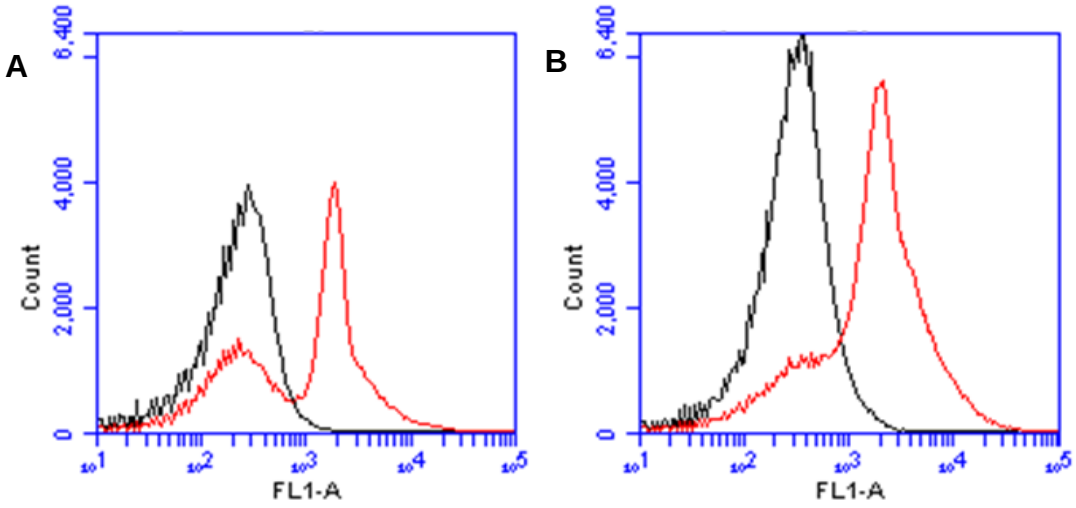

Figure 4-8. Detecting live and autoclaved spores using flow cytometry. ~1x10^8 **l**ive and autoclaved spores were incubated with anti-spore antibody for 10 min, followed by washing and anti-rabbit IgG-FITC antibody for 10 min. Samples washed and run on the flow cytometer. Black; HU58 without antibodies, Red; HU58 with antibodies. A; live HU58, B; autoclaved HU58.

4.2.9. Localisation of spores after intranasal, sublingual and oral dosing

Twelve BALB/c mice in each group were dosed with $2x10^9$ HU58 spores delivered intranasally, sublingually and orally. Mice (n=6) were culled at 6h and at 24h, since it was assumed that 6h would be representative of spores entering the cells (Section 4.2.2) and at 24h they should have been cleared. HU58 was used rather than DS127 spores because antibody was required to obtain adequate fluorescence (see Section 4.2.4) and HU58 was the strain that was used in the TB experiment presented in Chapter 3 and is more likely to be used as a vaccine adjuvant and is therefore more relevant.

Lung and gut samples from one mouse per group were used for flow cytometric analysis, and the other lung and gut samples were fixed in 10% (v/v) NBF for histological analysis. The NALT was removed from all mice, but was pooled into three groups of two defined NALT tissues for each group because the number of cells isolated from the NALT was considered quite low for flow cytometric analysis. The lung, gut and NALT samples were next labelled for M cells, macrophages, DCs, neutrophils and spores using fluorescent antibody, and analysed on a BD Accuri C6 flow cytometer.

4.2.10. Distribution of live spores

Using previous information about the size of spores as determined on the flow cytometer (Section 4.2.3) the correct forward and side scatter was identified on the flow cytometer and gated on. FITC positive events were then observed thus enabling the identification of free spores that had not associated with any murine cells.

In the lung, spores were seen after nasal and oral dosing with spore numbers being reduced after 24h post-nasal dosing and completely cleared after oral administration **(Figure 4-9)**. One explanation for spores being present following oral dosing is that the mice may have coughed after the gavage dosing and inadvertently inhaled spores into lungs via the nasopharyngeal route. In the NALT, again spores were seen after nasal and oral dosing, with a marked reduction observed after 24h. In the gut, spores were detectable following all dosing routes with concurrent decreases after 24h. The presence of spores after sublingual dosing suggests that the mice may have swallowed some of the administered dose, but that the spore numbers were very low.

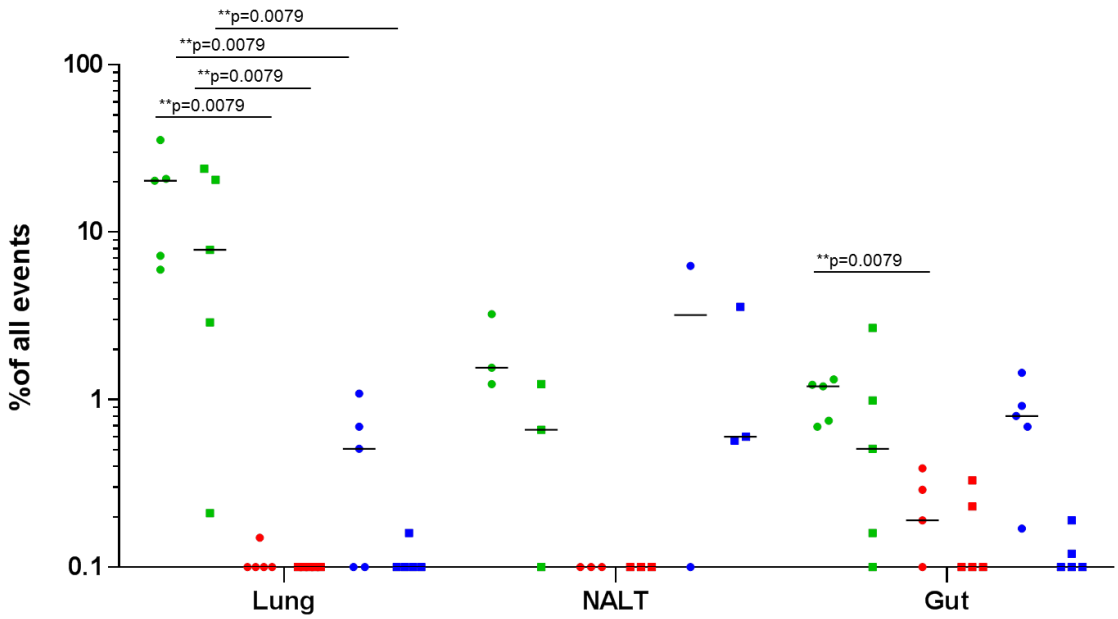

Figure 4-9. Flow cytometric analysis of spores identified inside different tissues. BALB/c mice (n=5) were dosed with $2x10^9$ HU58 spores either intranasally (green), sublingually (red) or orally (blue) and samples were taken 6h (circles) or 24h (squares) after dosing. Lungs, gut and NALT tissues were removed and homogenised as described in the methods (see Sections 2.20 and 2.21) and spores were labelled using anti-spore antibody and anti-rabbit IgG-FITC secondary antibody using intracellular staining. Spores were gated on using FSC and SSC (see Section 4.2.4) and FL1 (FITC fluorescence). Percentage of events from the whole population was used for calculations. Limit of detection = 0.1%. Dots indicate individual mice and median shown by the lines. Mann-Whitney was used to compare dosing routes at each time point.

4.2.11. Distribution of autoclaved spores

When groups of mice were dosed orally, sublingually or nasally, live spores could not be readily detected in the tissues tested after sublingual dosing **(Figure 4-9)**. In the experiment using autoclaved spores therefore, only oral and nasal dosing routes were examined. Autoclaved spores were tested since autoclaved spores were evaluated as a delivery system in Chapter 3. Inactive spores may be used as a vaccine in the future so investigating whether there are differences in the way spores are distributed and phagocytosed depending on whether they are live or autoclaved is important to examine. The experiment was a repeat of the experiment with live spores; BALB/c mice (n=10/group) were dosed with $2x10^9$ autoclaved HU58 spores either orally or nasally, and then n=5 culled after 6h and 24h. The lungs, gut and NALT from four mice were processed to isolate single cells. M cells, DC, macrophages and neutrophils with and without spores were measured using antibodies. The lung and gut tissue from one mouse from each group was used for histological analysis.

The results showed that the highest numbers of spores were delivered to the lungs after 6h but some were also delivered after oral dosing **(Figure 4-10)**. Nasal and oral dosing delivered autoclaved spores to the gut, but the highest numbers of spores were observed after oral dosing at 6h. Nasal dosing delivered the most spores to the NALT in comparison to oral and sublingual dosing. The results are quite similar to dosing with live spores so it appears that the initial distribution of spores after oral and nasal dosing is the same regardless of whether the spores are alive or dead. However, spores do seem to be cleared more quickly from the lungs when they are autoclaved.

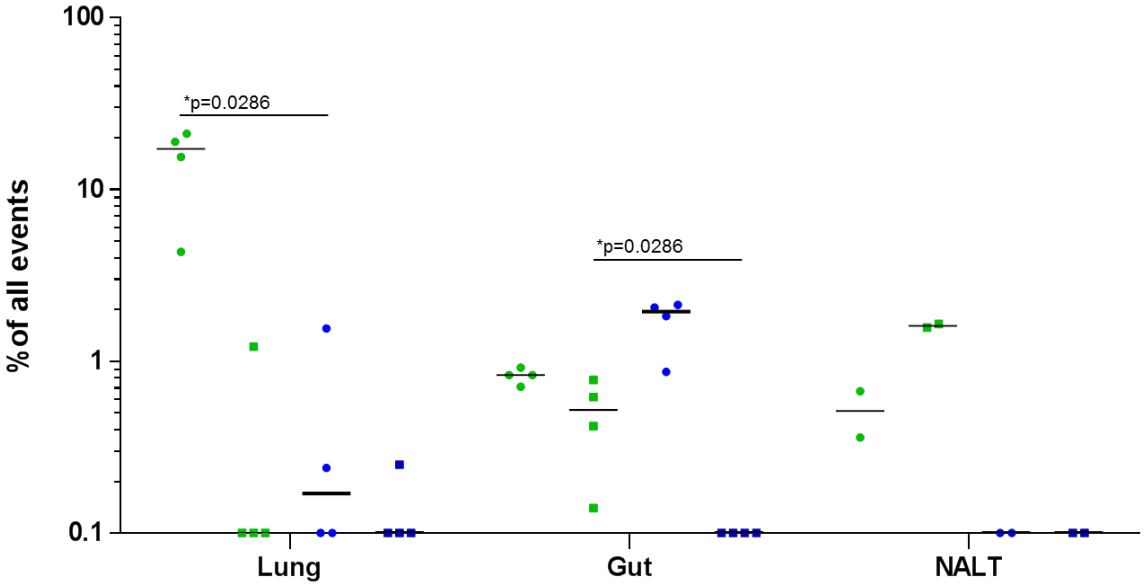

Figure 4-10. Distribution of autoclaved spores after nasal and oral dosing in the lungs, gut and NALT. BALB/c mice (n=4) were dosed with $2x10^9$ autoclaved spores either intranasally (green), sublingually (red) or orally (blue) and samples were taken 6h (circles) or 24h (squares) after dosing. Lungs, gut and NALT tissues were removed and homogenised as described in the methods (see Sections 2.20 and 2.21) and spores were labelled using anti-spore antibody and anti-rabbit IgG-FITC secondary antibody using intracellular staining. Spores were gated on using FSC and SSC (see Section 4.2.4) and FL1 (FITC fluorescence). Percentage of events from the whole population was used for calculations.The proportion of events that were positive for anti-spore and anti- FITC are in the whole populations. Limit of detection = 0.1%. Dots indicate individual mice and lines show the median. Mann-Whitney was used to compare dosing routes at each time point.

4.2.12. Immunofluorescence analysis of live spores in the lungs

The lungs and gut from one mouse per group were immersed in 10% NBF for 24h before embedding in paraffin wax and sectioning. Sections of lungs and gut from immunised mice were stained for spores, M cells and nuclei and examined using an EVOS microscope. After nasal dosing, there were a large number of spores seen in the lungs at the 6h time point. They were found clumped together around the airways, but individual spores could also be seen infiltrating the tissue **(Figure 4-12** and **Figure 4-13)**. At 24h, there was a reduction in the number of spores seen in the lungs, but there was still considerable clumping of spores. These results confirmed the integrity of flow cytometric analysis in that there were a large number of spores following nasal dosing in the lung tissue. The immunofluorescence adds useful information about the localisation of spores in tissue. Spores appear to be most concentrated around the airways, with single spores distributed through the lung tissue. There were also spores seen inside epithelial cells **(Figure 4-13)**.

After sublingual dosing, very few spores were identified at either time point in the lungs, and only single spores were observed rather than clumps **(Figure 4-12** and **Figure 4-14)**. After oral dosing, there were more spores observed than after sublingual dosing, but again they were generally seen as single spores rather than clumps **(Figure 4-12** and **Figure 4-14)**.

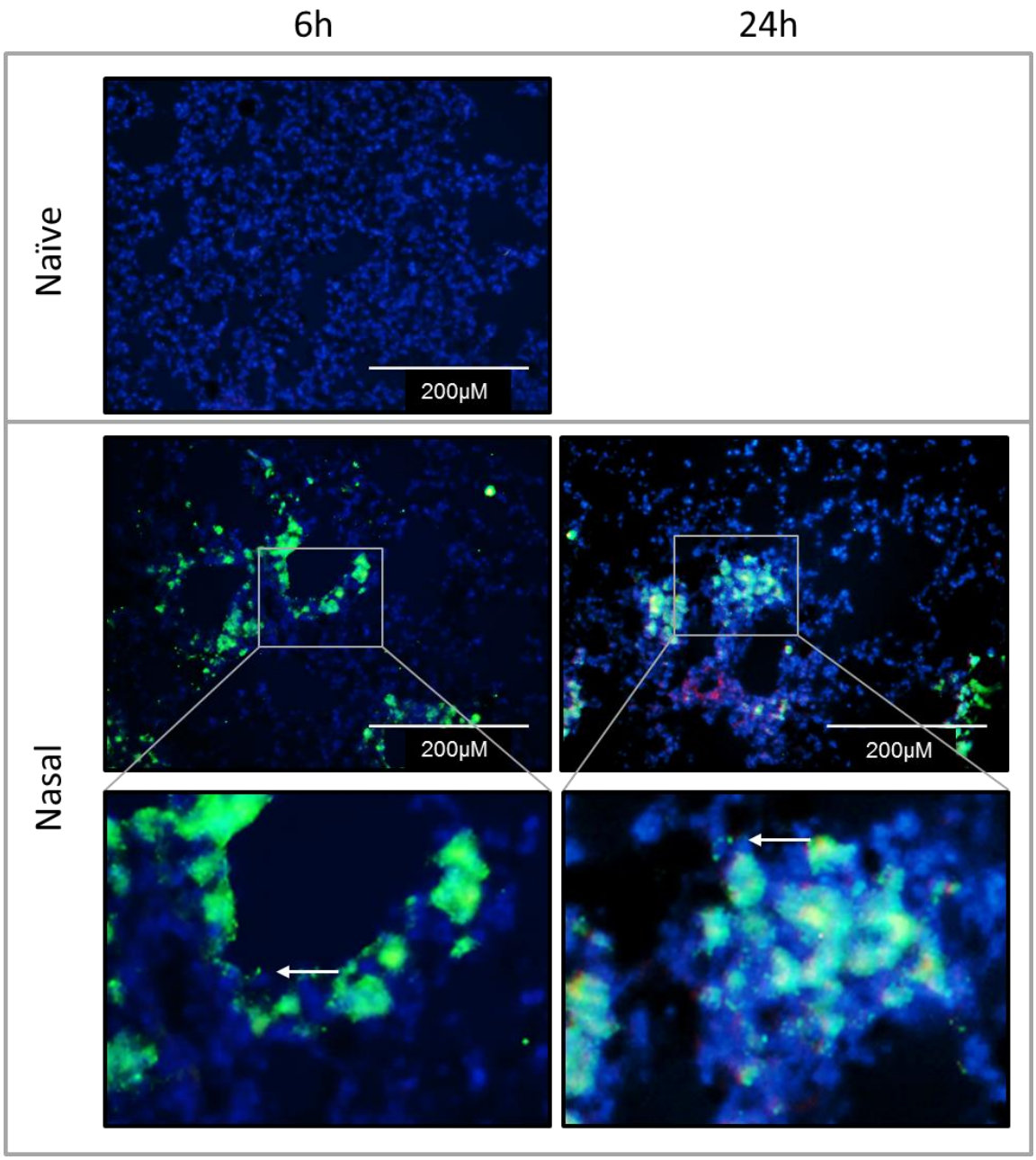

Figure 4-11. Immunofluorescence images of lung sections at 20x magnification taken from mice after different dosing regimens (naïve and nasal) after 6h and 24h. BALB/c mice were dosed with $2x10^9$ HU58 spores nasally and lungs were removed 6h and 24h after dosing. Tissues were immersed in 10% NBF and embedded in paraffin wax before sectioning and immunofluorescent staining. Stained for nuclei (DAPI (blue)), spores (anti-spore primary antibody followed by anti-rabbit IgG-FITC (green)) and M cells (anti M-cell (NKM 16-2-4) and anti-mouse IgG-TRITC (red)). Arrows indicate spores. Sections read at 20x magnification using the EVOS fl microscope.

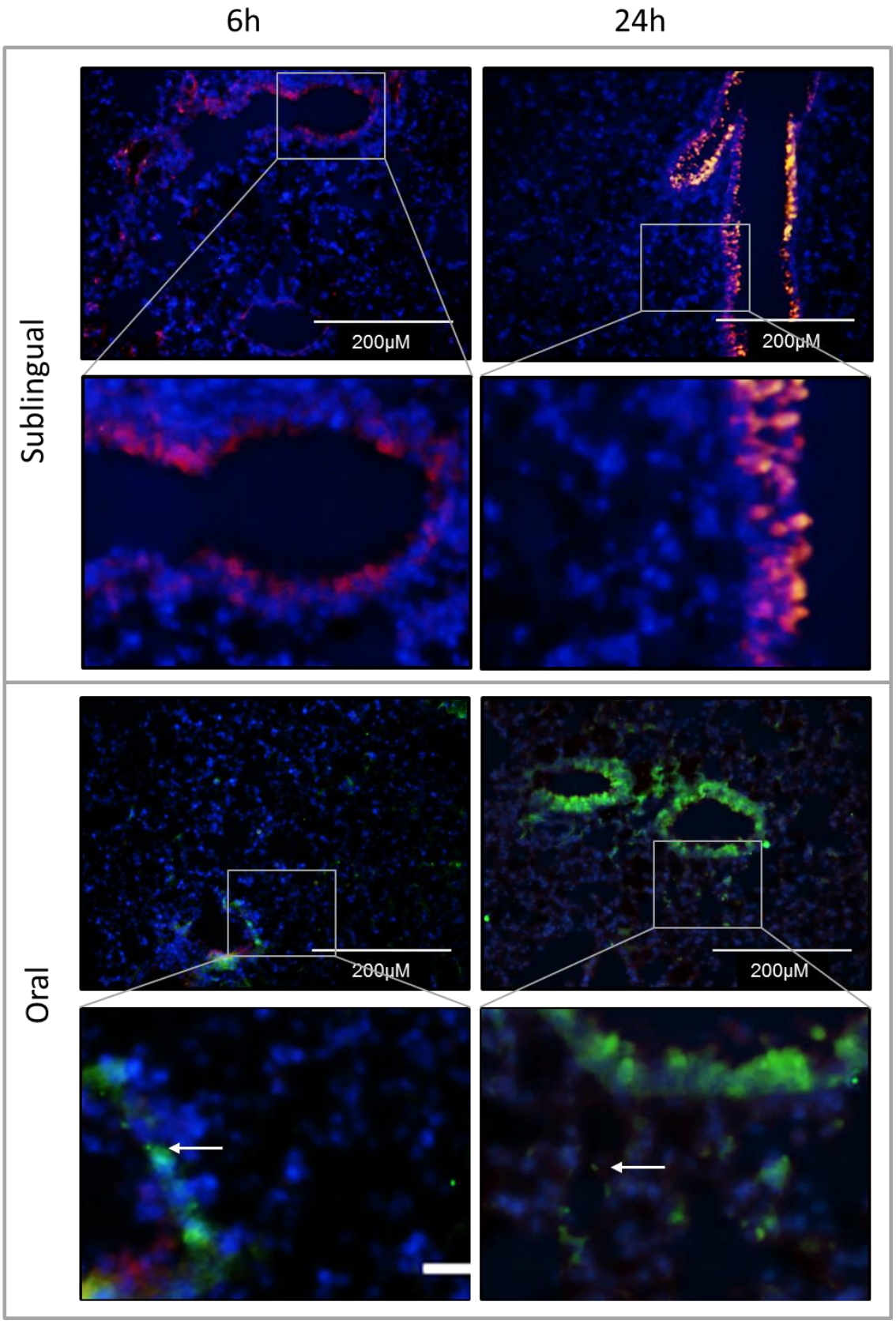

Figure 4-12. Immunofluorescence images of lung sections at 20x magnification taken from mice after different dosing regimens (sublingual and oral) after 6h and 24h. BALB/c mice were dosed with $2x10^9$ HU58 spores sublingually and orally and lungs were removed 6h and 24h after dosing. Tissues were immersed in 10% NBF and embedded in paraffin wax before sectioning and immunofluorescent staining. Stained for nuclei (DAPI (blue)), spores (anti-spore primary antibody followed by anti-rabbit IgG-FITC (green)) and M cells (anti M-cell (NKM 16-2-4) and anti-mouse IgG-TRITC (red)). Arrows indicate spores. Sections read at 20x magnification using the EVOS fl microscope.

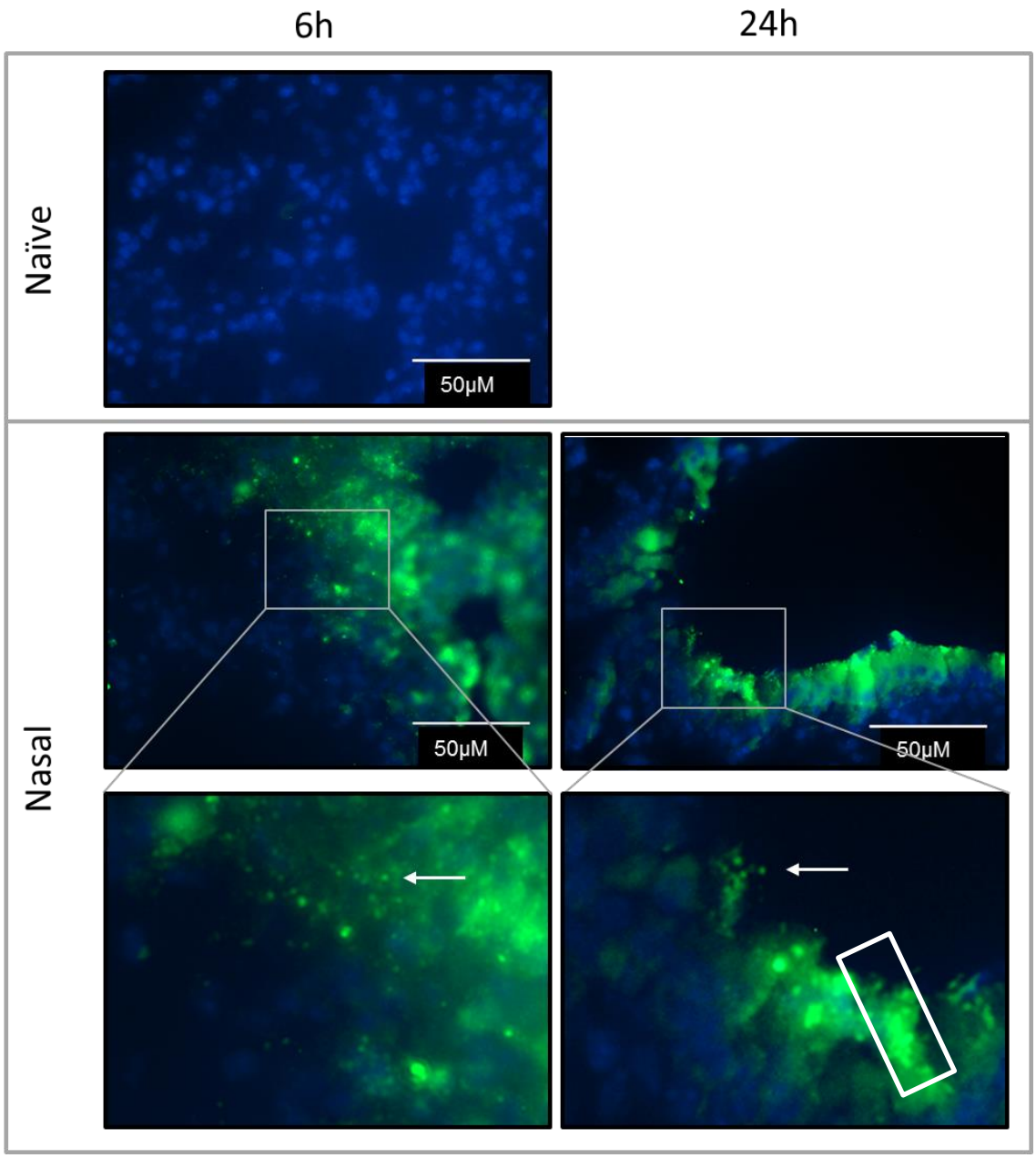

Figure 4-13. Immunofluorescence images of lung sections at 60x magnification taken from mice after different dosing regimens (naïve and nasal) after 6h and 24h. BALB/c mice were dosed with $2x10^9$ HU58 spores nasally and lungs were removed 6h and 24h after dosing. Tissues were immersed in 10% NBF and embedded in paraffin wax before sectioning and immunofluorescent staining. Stained for nuclei (DAPI (blue)), spores (anti-spore primary antibody followed by anti-rabbit IgG-FITC (green)) and M cells (anti M-cell (NKM 16-2-4) and anti-mouse IgG-TRITC (red)). Arrows indicate spores. Sections read at 60x magnification using the EVOS fl microscope.

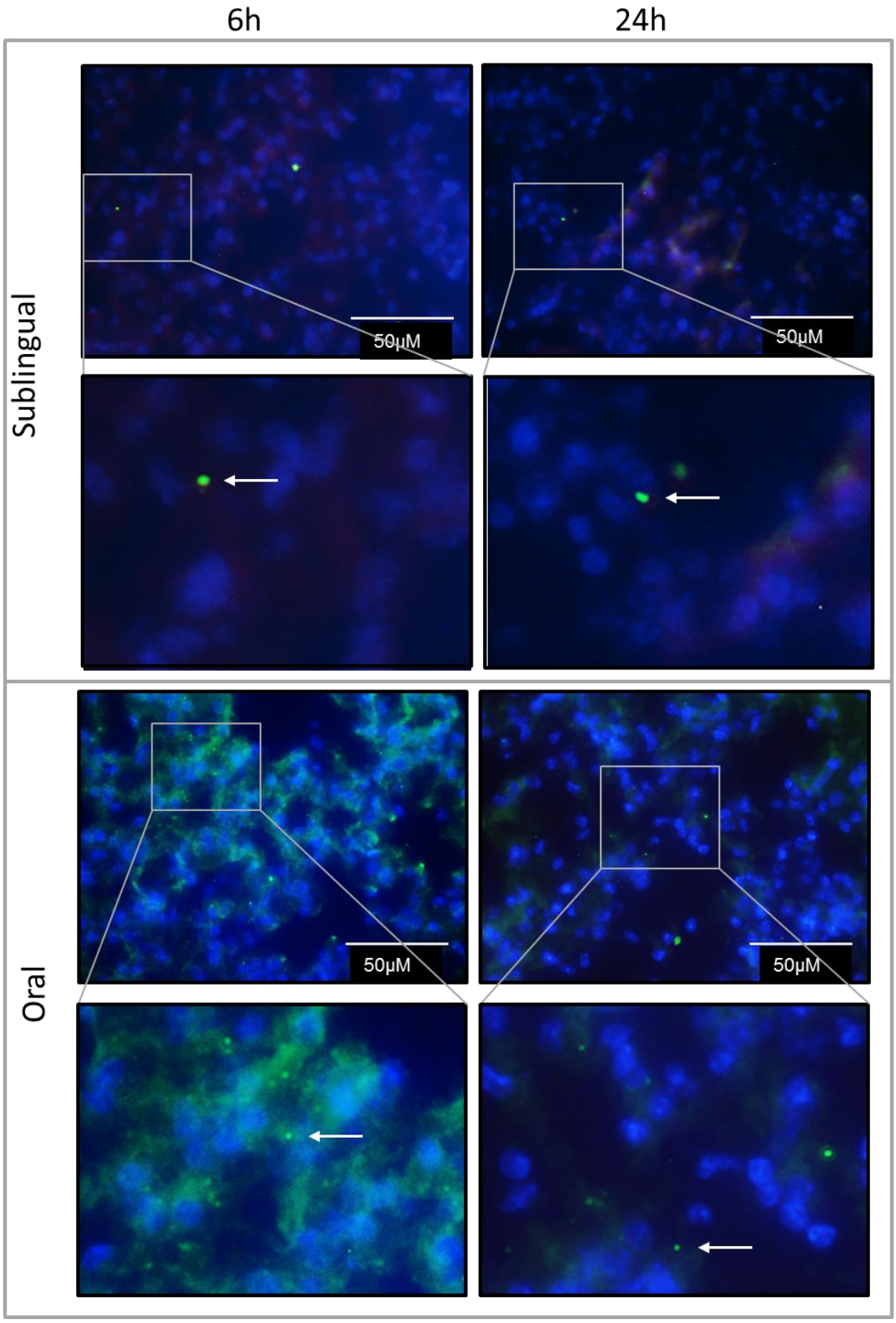

Figure 4-14. Immunofluorescence images of lung sections at 60x magnification taken from mice after different dosing regimens (sublingual and oral) after 6h and 24h. BALB/c mice were dosed with $2x10^9$ HU58 spores sublingually and orally and lungs were removed 6h and 24h after dosing. Tissues were immersed in 10% NBF and embedded in paraffin wax before sectioning and immunofluorescent staining. Stained for nuclei (DAPI (blue)), spores (anti-spore primary antibody followed by anti-rabbit IgG-FITC (green)) and M cells (anti M-cell (NKM 16-2-4) and anti-mouse IgG-TRITC (red)). Arrows indicate spores. Sections read at 60x magnification using the EVOS fl microscope.

4.2.13. Immunofluorescence analysis of autoclaved spores in the lungs

After nasal dosing, at 6h there are autoclaved spores distributed throughout the lung tissue, but there appear to be fewer than after immunisation with live spores **(Figure 4-15** and **Figure 4-17)**. The distribution of autoclaved spores in the lung tissue is quite different to live spores as instead of grouping around the airways, there are clusters of spores inside individual cells **(Figure 4-17)**. After 24h, the spores were still present, even though the flow cytometry indicated no spores, spores could be seen, but they were mostly inside cells whereas the flow cytometer was detecting free spores, which may account for the difference. The spores inside individual cells seem to be more densely packed at 24h. After oral dosing, there were fewer spores in the lung in comparison to nasal dosing and oral dosing of live spores but they were present. They also appear to be clustering inside certain cells **(Figure 4-16** and **Figure 4-18)**.

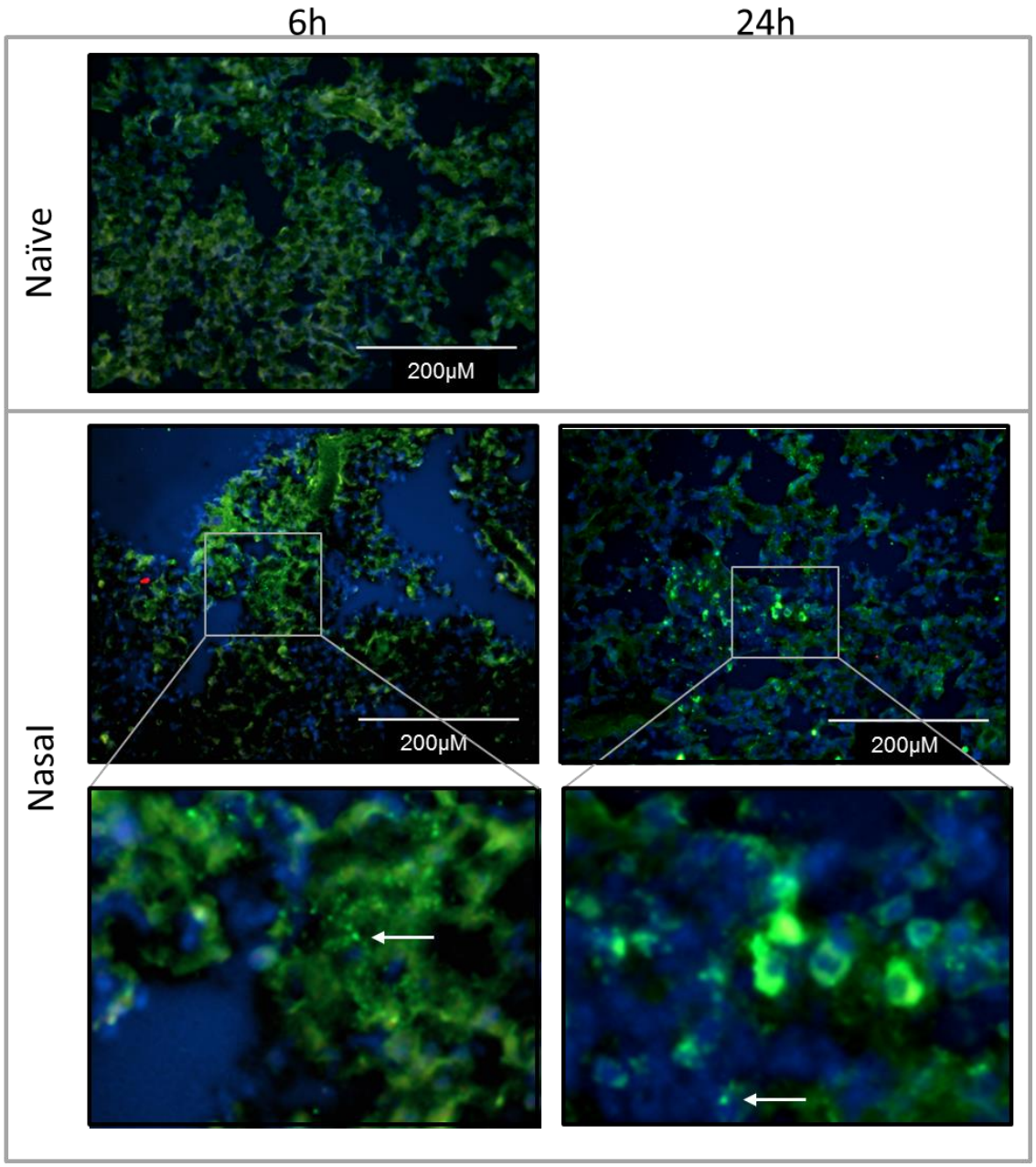

Figure 4-15. Immunofluorescence images of lung sections at 20x magnification taken from mice after different dosing regimens (naïve and nasal) after 6h and 24h. BALB/c mice were dosed with $2x10^9$ autoclaved HU58 spores nasally and lungs were removed 6h and 24h after dosing. Tissues were immersed in 10% NBF and embedded in paraffin wax before sectioning and immunofluorescent staining. Stained for nuclei (DAPI (blue)), spores (anti-spore primary antibody followed by anti-rabbit IgG-FITC (green)) and M cells (anti M-cell (NKM 16-2-4) and anti-mouse IgG-TRITC (red)). Arrows indicate spores. Sections read at 20x magnification using the EVOS fl microscope.

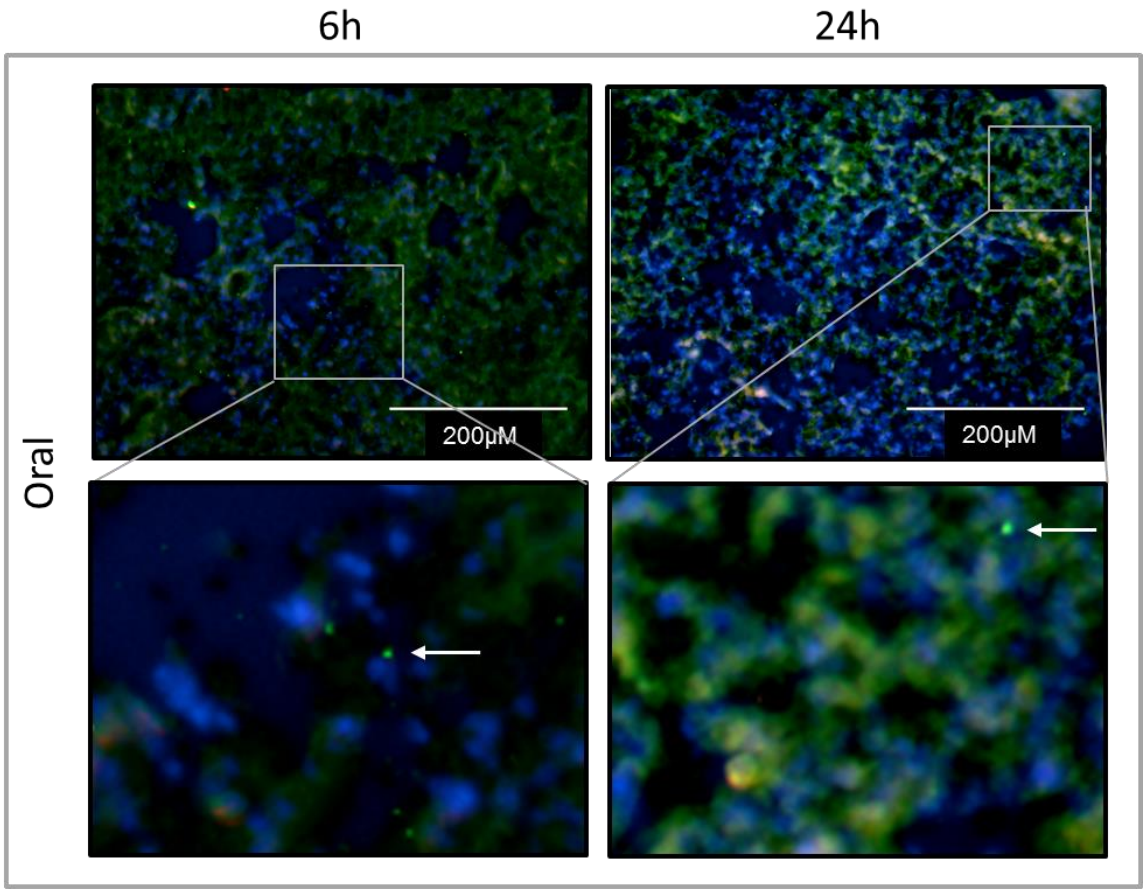

Figure 4-16. Immunofluorescence images of lung sections at 20x magnification taken from mice after oral dosing regimen after 6h and 24h. BALB/c mice were dosed with $2x10^9$ autoclaved HU58 spores orally and lungs were removed 6h and 24h after dosing. Tissues were immersed in 10% NBF and embedded in paraffin wax before sectioning and immunofluorescent staining. Stained for nuclei (DAPI (blue)), spores (anti-spore primary antibody followed by anti-rabbit IgG-FITC (green)) and M cells (anti M-cell (NKM 16-2-4) and anti-mouse IgG-TRITC (red)). Arrows indicate spores. Sections read at 20x magnification using the EVOS fl microscope.

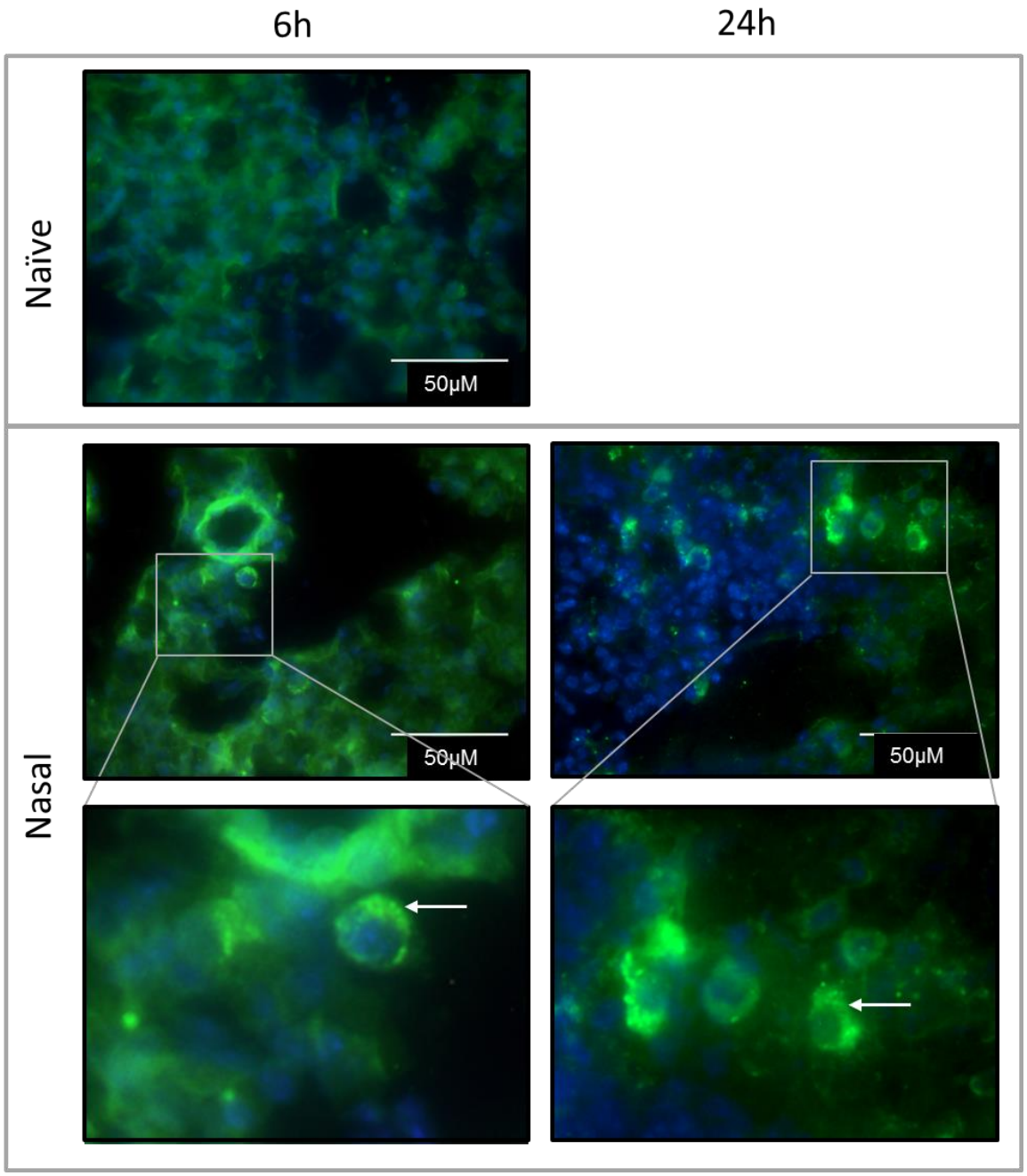

Figure 4-17. Immunofluorescence images of lung sections at 60x magnification taken from mice after different dosing regimens (naïve and nasal) after 6h and 24h. BALB/c mice were dosed with autoclaved $2x10^9$ HU58 spores nasally and lungs were removed 6h and 24h after dosing. Tissues were immersed in 10% NBF and embedded in paraffin wax before sectioning and immunofluorescent staining. Stained for nuclei (DAPI (blue)), spores (anti-spore primary antibody followed by anti-rabbit IgG-FITC (green)) and M cells (anti M-cell (NKM 16-2-4) and anti-mouse IgG-TRITC (red)). Arrows indicate spores. Sections read at 60x magnification using the EVOS fl microscope.

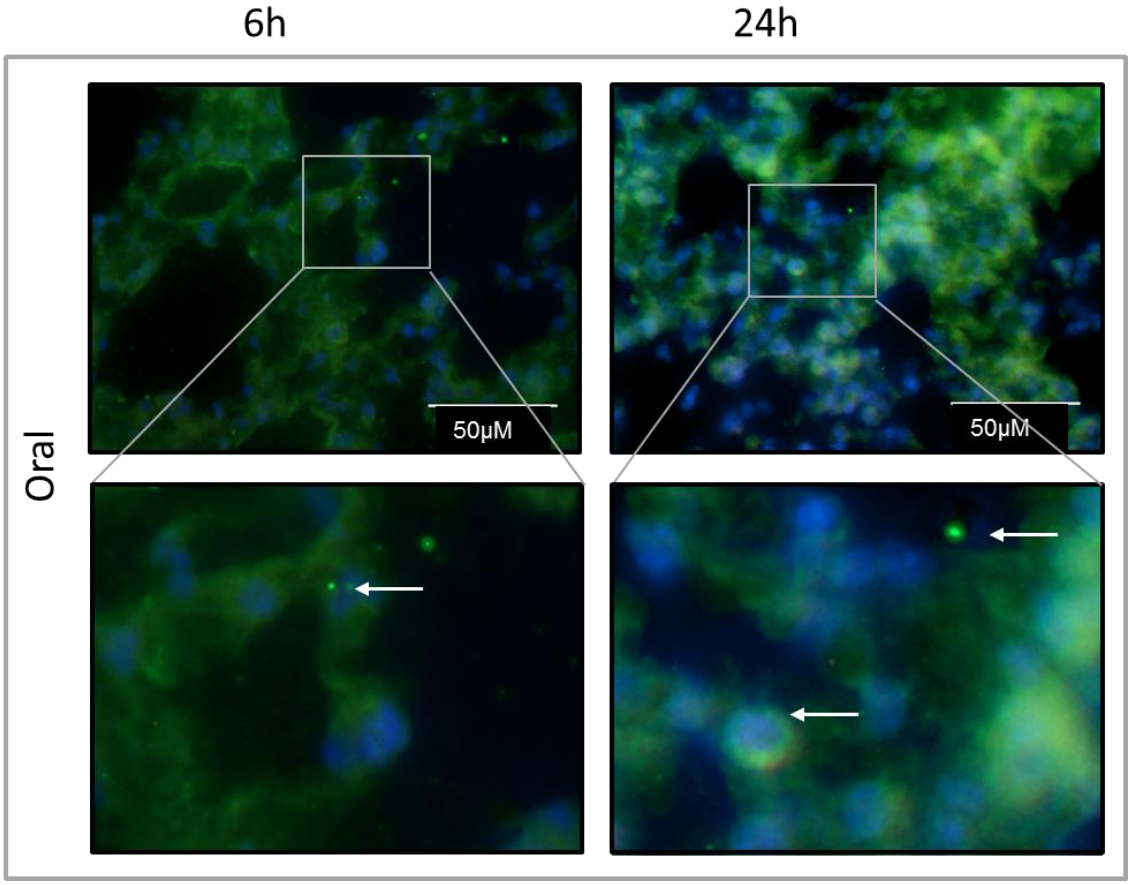

Figure 4-18. Immunofluorescence images of lung sections at 60x magnification taken from mice after oral dosing regimens after 6h and 24h. BALB/c mice were dosed with $2x10^9$ autoclaved HU58 spores orally and lungs were removed 6h and 24h after dosing. Tissues were immersed in 10% NBF and embedded in paraffin wax before sectioning and immunofluorescent staining. Stained for nuclei (DAPI (blue)), spores (anti-spore primary antibody followed by anti-rabbit IgG-FITC (green)) and M cells (anti M-cell (NKM 16-2-4) and anti-mouse IgG-TRITC (red)). Arrows indicate spores. Sections read at 60x magnification using the EVOS fl microscope.

4.2.14. Immunofluorescence analysis of live spores in the gut

The sections taken for immunofluorescence analysis were from the jejunum area, whereas the flow cytometric analysis corresponded to the duodenum, through to the cecum and so there could be a difference in the representation of spores between flow cytometry and immunofluorescence as the histology sample represented only a small section of the gut. In all of the gut samples, there appeared to be patches of M cell populations at the base of the villi **(Figure 4-19, Figure 4-20, Figure 4-21, Figure 4-22)**. Following intranasal dosing, spores could be identified at 6h and 24n inside the villi of the gut and near the basal membrane. After sublingual and oral dosing, spores were seen predominately nearer the M cells and closer to the basement membrane **(Figure 4-22)**.

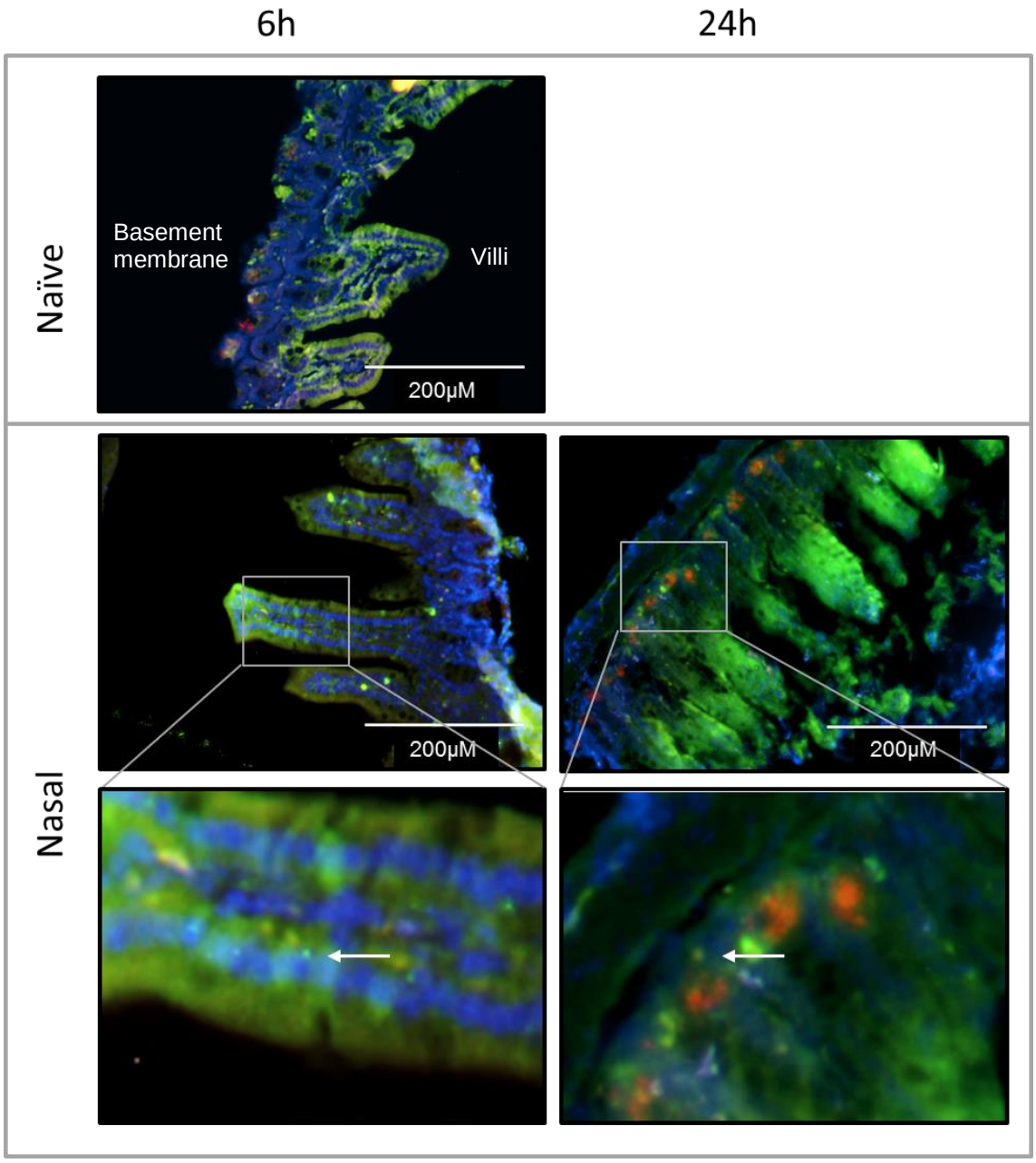

Figure 4-19. Immunofluorescence images of gut sections at 20x magnification taken from mice after different dosing regimens (naïve and nasal) after 6h and 24h. BALB/c mice were dosed with $2x10^9$ HU58 spores nasally and the gut was removed 6h and 24h after dosing. Tissues were immersed in 10% NBF and embedded in paraffin wax before sectioning and immunofluorescent staining. Stained for nuclei (DAPI (blue)), spores (anti-spore primary antibody followed by anti-rabbit IgG-FITC (green)) and M cells (anti M-cell (NKM 16-2-4) and anti-mouse IgG-TRITC (red)). Arrows indicate spores. Sections read at 20x magnification using the EVOS fl microscope. Villi and basement membrane labelled on naïve sample.

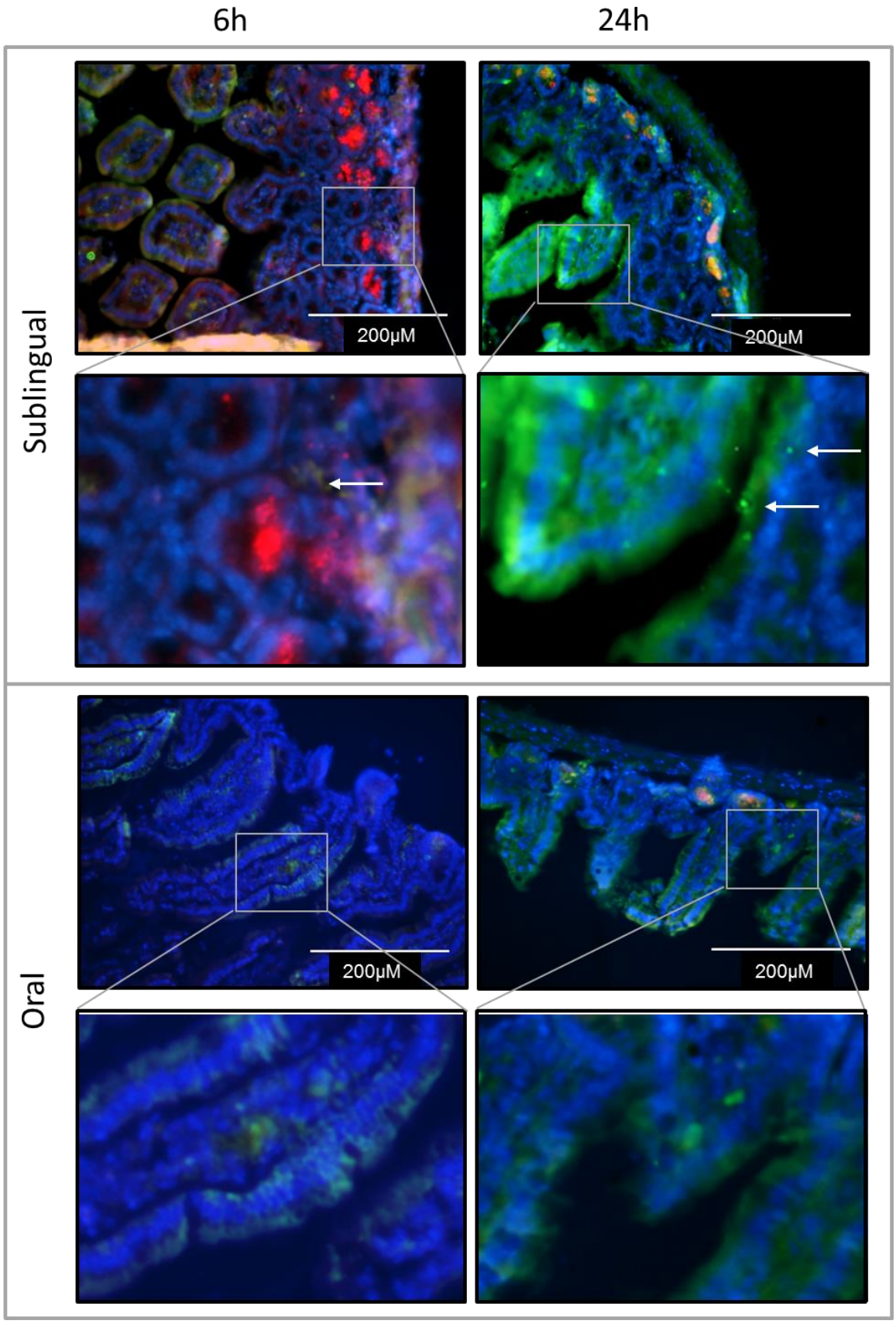

Figure 4-20. Immunofluorescence images of gut sections at 20x magnification taken from mice after different dosing regimens (sublingual and oral) after 6h and 24h. BALB/c mice were dosed with $2x10^9$ HU58 spores sublingually and orally and the gut was removed 6h and 24h after dosing. Tissues were immersed in 10% NBF and embedded in paraffin wax before sectioning and immunofluorescent staining. Stained for nuclei (DAPI (blue)), spores (anti-spore primary antibody followed by anti-rabbit IgG-FITC (green)) and M cells (anti M-cell (NKM 16-2-4) and anti-mouse IgG-TRITC (red)). Arrows indicate spores. Sections read at 20x magnification using the EVOS fl microscope.

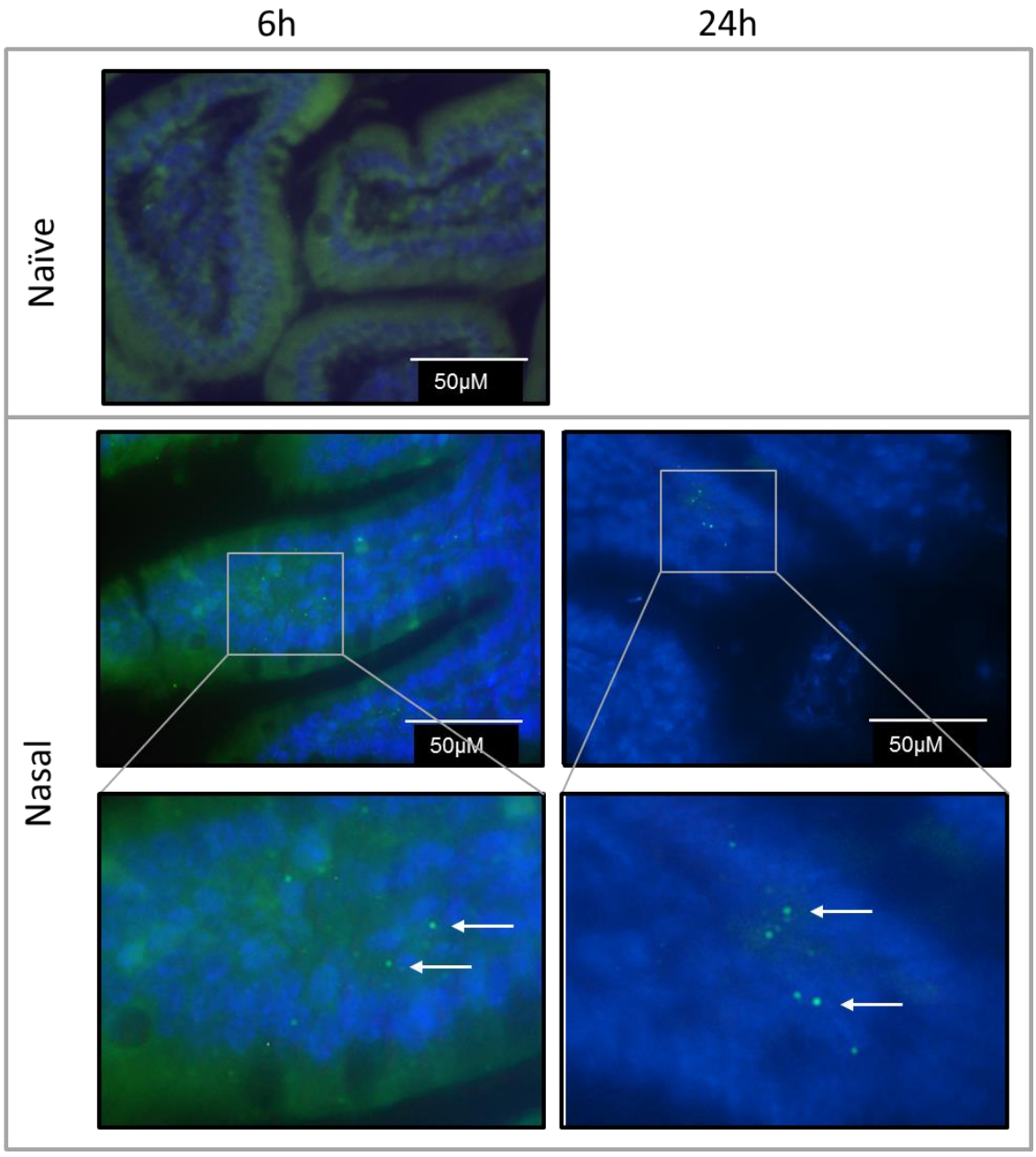

Figure 4-21. Immunofluorescence images of gut sections at 60x magnification taken from mice after different dosing regimens (naïve and nasal) after 6h and 24h. BALB/c mice were dosed with $2x10^9$ HU58 spores nasally and the gut was removed 6h and 24h after dosing. Tissues were immersed in 10% NBF and embedded in paraffin wax before sectioning and immunofluorescent staining. Stained for nuclei (DAPI (blue)), spores (anti-spore primary antibody followed by anti-rabbit IgG-FITC (green)) and M cells (anti M-cell (NKM 16-2-4) and anti-mouse IgG-TRITC (red)). Arrows indicate spores. Sections read at 60x magnification using the EVOS fl microscope.

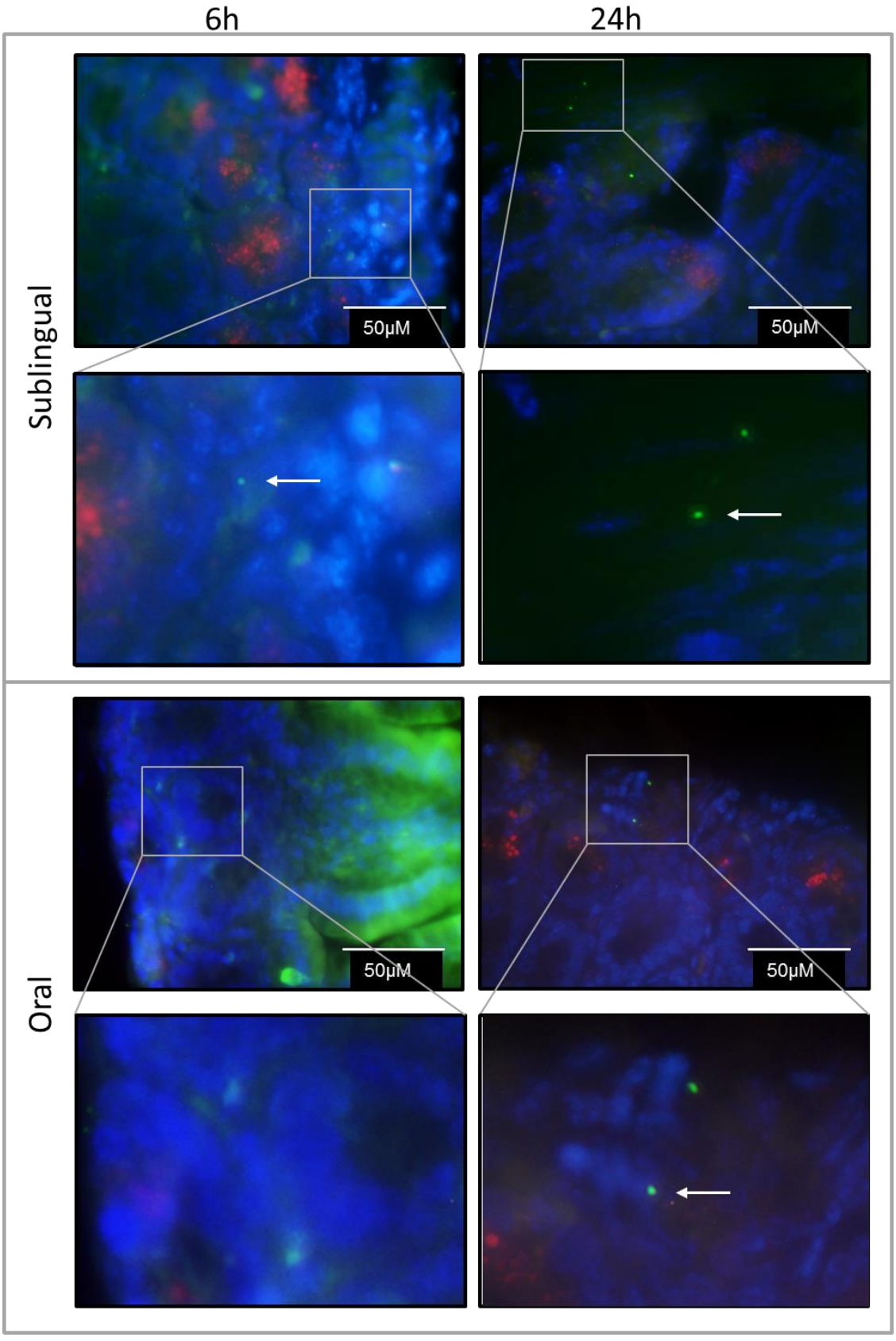

Figure 4-22. Immunofluorescence images of gut sections at 60x magnification taken from mice after different dosing regimens (sublingual and oral) after 6h and 24 h. BALB/c mice were dosed with $2x10^9$ HU58 spores sublingually and orally and the gut was removed 6h and 24h after dosing. Tissues were immersed in 10% NBF and embedded in paraffin wax before sectioning and immunofluorescent staining. Stained for nuclei (DAPI (blue)), spores (anti-spore primary antibody followed by anti-rabbit IgG-FITC (green)) and M cells (anti M-cell (NKM 16-2-4) and anti-mouse IgG-TRITC (red)). Arrows indicate spores. Sections read at 60x magnification using the EVOS fl microscope.

4.2.15. Immunofluorescence analysis of autoclaved spores in the gut

Autoclaved spores could be seen throughout the gut tissue after nasal dosing and were still present after 24h **(Figure 4-23** and **Figure 4-25)**. Following oral dosing of autoclaved spores, more spores could be seen in the gut in comparison to live spores **(Figure 4-24** and **Figure 4-26)**. Autoclaved spores appear to be mostly clustered at the basement membrane around the M cells **(Figure 4-26)**.

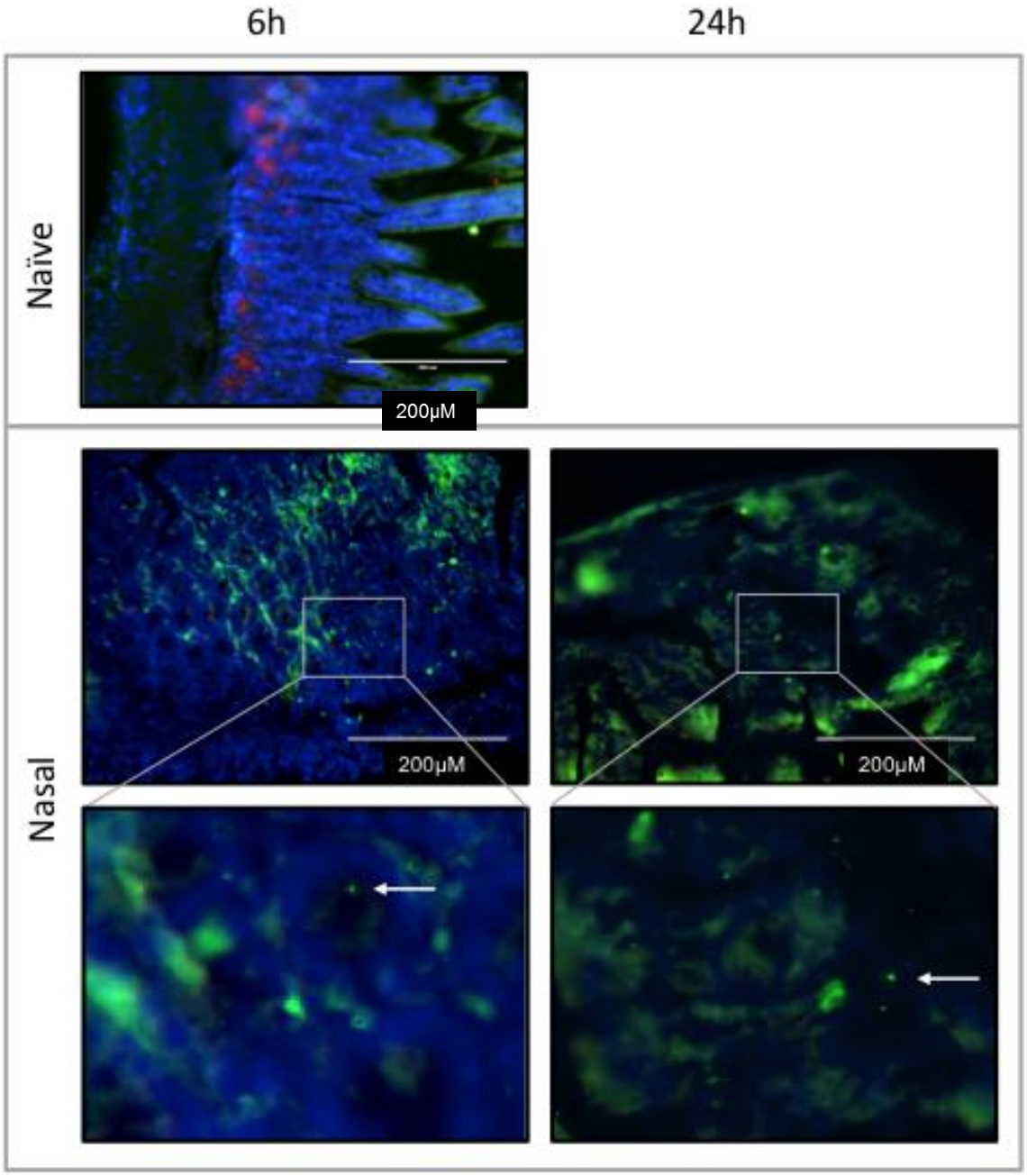

Figure 4-23. Immunofluorescence images of gut sections at 20x magnification taken from mice after different dosing regimens (naïve and nasal) after 6h and 24h. BALB/c mice were dosed with $2x10^9$ autoclaved HU58 nasally and the gut was removed 6h and 24h after dosing. Tissues were immersed in 10% NBF and embedded in paraffin wax before sectioning and immunofluorescent staining. Stained for nuclei (DAPI (blue)), spores (anti-spore primary antibody followed by anti-rabbit IgG-FITC (green)) and M cells (anti M-cell (NKM 16-2-4) and anti-mouse IgG-TRITC (red)). Arrows indicate spores. Sections read at 20x magnification using the EVOS fl microscope.

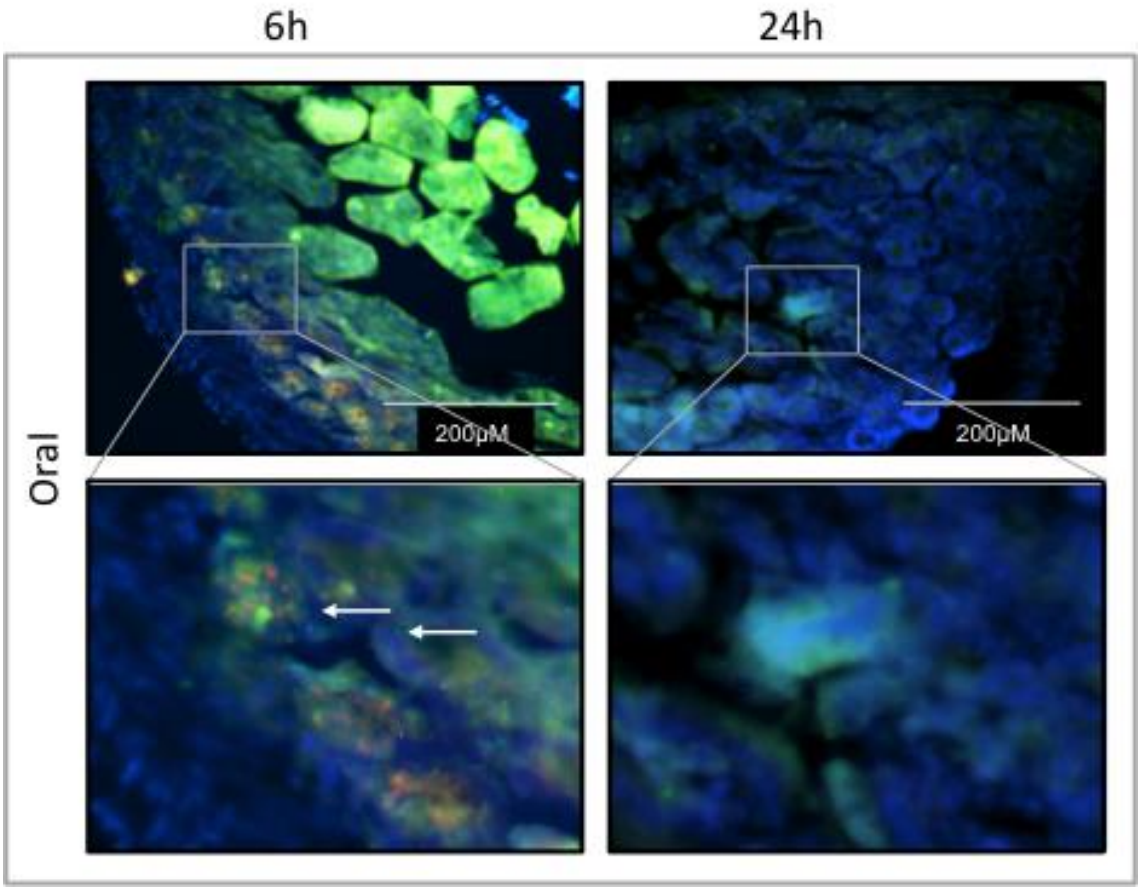

Figure 4-24. Immunofluorescence images of gut sections at 20x magnification taken from mice after different dosing regimens (oral) after 6h and 24h. BALB/c mice were dosed with $2x10^9$ autoclaved HU58 orally and the gut was removed 6h and 24h after dosing. Tissues were immersed in 10% NBF and embedded in paraffin wax before sectioning and immunofluorescent staining. Stained for nuclei (DAPI (blue)), spores (anti-spore primary antibody followed by anti-rabbit IgG-FITC (green)) and M cells (anti M-cell (NKM 16-2-4) and anti-mouse IgG-TRITC (red)). Arrows indicate spores. Sections read at 20x magnification using the EVOS fl microscope.

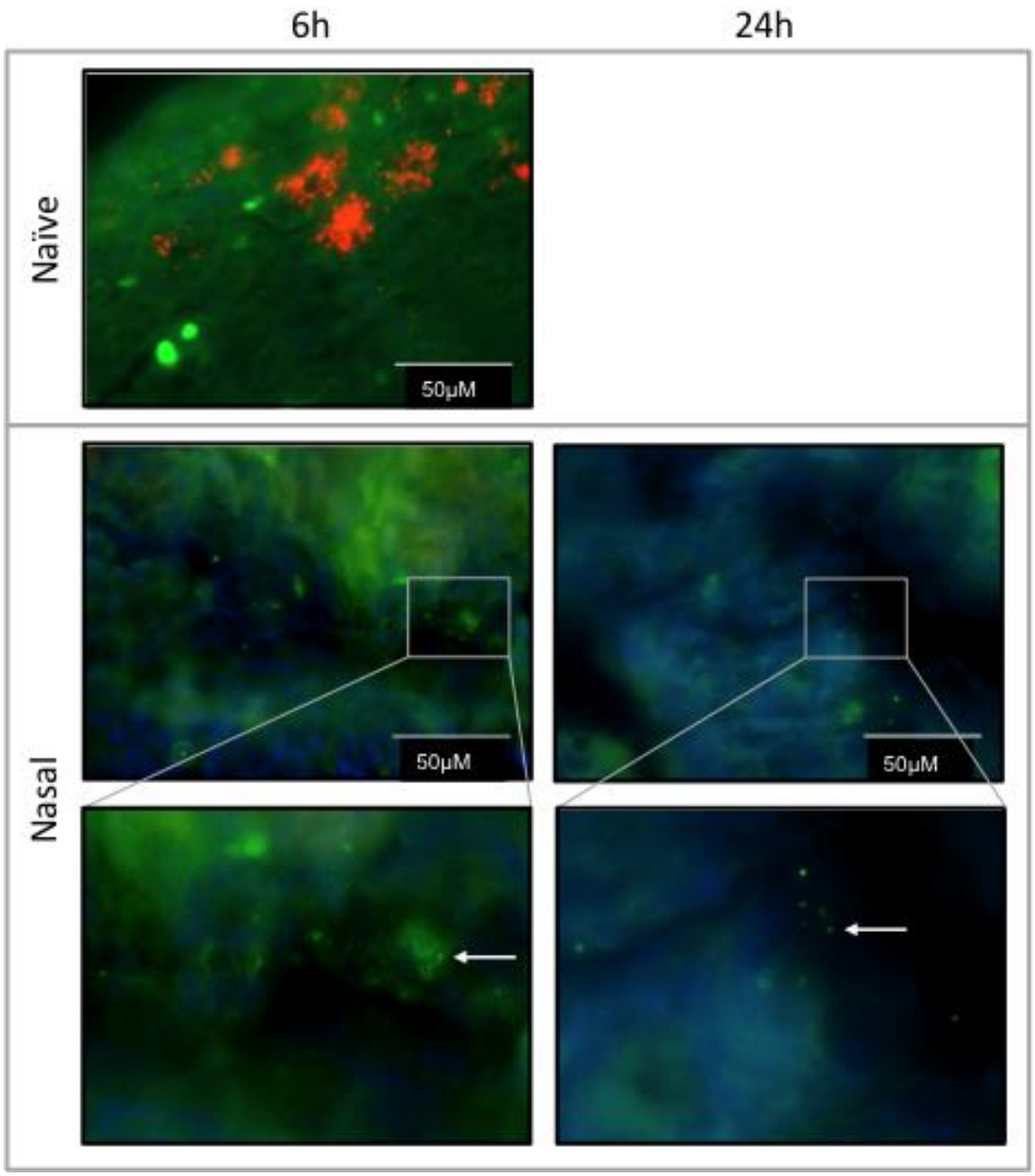

Figure 4-25. Immunofluorescence images of gut sections at 60x magnification taken from mice after different dosing regimens (naïve and nasal) after 6h and 24h. BALB/c mice were dosed with $2x10^9$ autoclaved HU58 nasally and the gut was removed 6h and 24h after dosing. Tissues were immersed in 10% NBF and embedded in paraffin wax before sectioning and immunofluorescent staining. Stained for nuclei (DAPI (blue)), spores (anti-spore primary antibody followed by anti-rabbit IgG-FITC (green)) and M cells (anti M-cell (NKM 16-2-4) and anti-mouse IgG-TRITC (red)). Arrows indicate spores. Sections read at 60x magnification using the EVOS fl microscope.

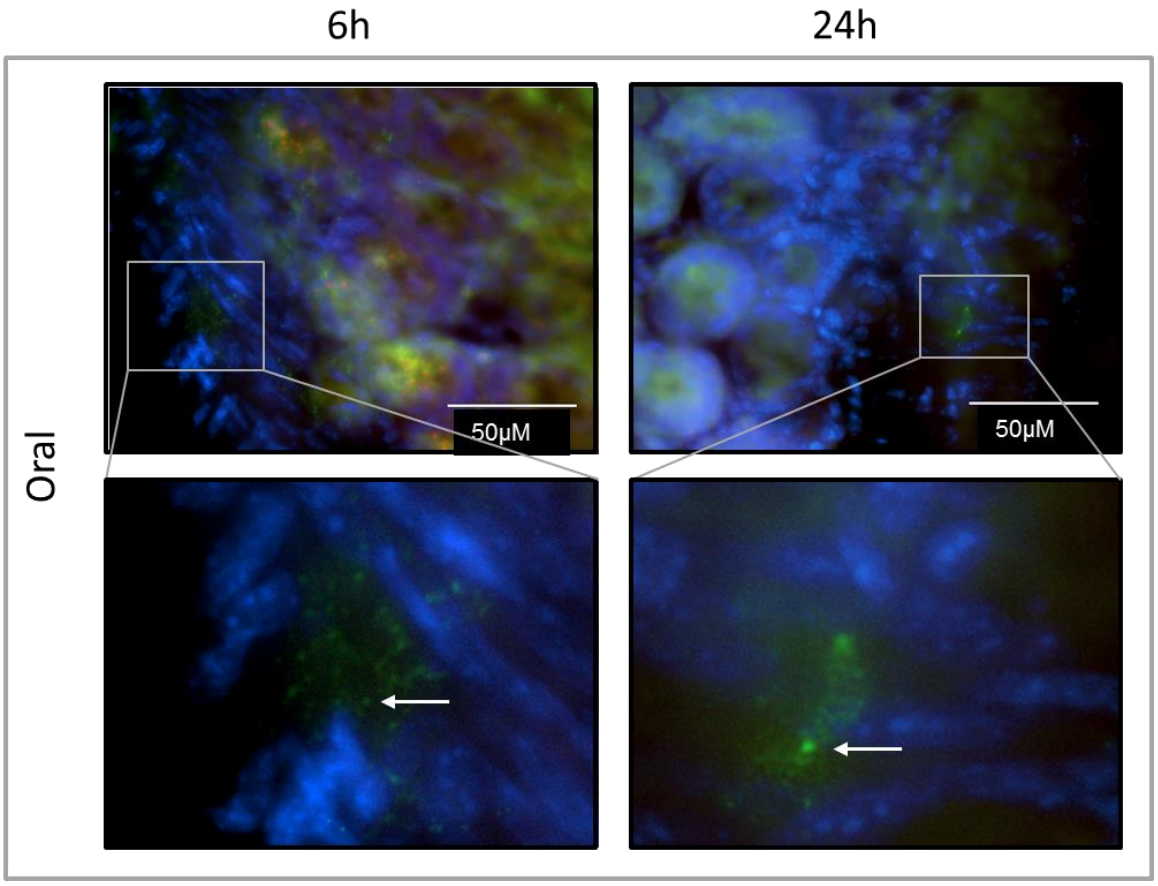

Figure 4-26. Immunofluorescence images of gut sections at 60x magnification taken from mice after different dosing regimens (oral) after 6h and 24h. BALB/c mice were dosed with $2x10^9$ autoclaved HU58 orally and the gut was removed 6h and 24h after dosing. Tissues were immersed in 10% NBF and embedded in paraffin wax before sectioning and immunofluorescent staining. Stained for nuclei (DAPI (blue)), spores (anti-spore primary antibody followed by anti-rabbit IgG-FITC (green)) and M cells (anti M-cell (NKM 16-2-4) and anti-mouse IgG-TRITC (red)). Arrows indicate spores. Sections read at 60x magnification using the EVOS fl microscope.

4.2.16. Live spores infiltrating the lungs

Spores inside cells were detected by first treating cells with saponin followed by the addition of anti-spore primary and anti-rabbit IgG-FITC secondary antibodies. Saponin perforates the cell membrane enabling intracellular access of antibodies. Populations that were positive for FITC labelled spores and either M cells, macrophages, neutrophils or dendritic cells were identified.

The population of spores in M cells did not vary significantly following any of the dosing routes used. Using the nasal dosing route most spores were found inside M cells at 6h, this reduced at 24h. After oral dosing, some spores were seen in the M cells at 6h **(Figure 4-27)**. The DC populations in the lung were also consistent after nasal dosing showing the highest numbers of intracellular spores inside DCs. Spores were also seen after sublingual dosing at 6h **(Figure 4-28)**. In the macrophage populations, only nasal dosing showed a significant number of spores within cells, and there was an increase in macrophage numbers following nasal and oral dosing **(Figure 4-29)**. The neutrophil population increased from 6h to 24h after nasal dosing, and the number of spores inside neutrophils also increased in line with this. Some spores were detected in neutrophils after sublingual and oral dosing at 6h **(Figure 4-30)**.

Based on these results, it appears that; i) nasal dosing delivered the highest number of spores to the lungs and ii) that all four cell types identified were involved in engulfment of spores by phagocytosis, iii) but DCs and neutrophils contained the highest numbers of spores. The neutrophils behaved differently to the other cells types as the population increased at 6h and again at 24h **(Figure 4-30)**. This may be a result of secretion of chemokines from other cells and/or

from damaged cells in the lung tissue, which recruited more neutrophils to the site later on.

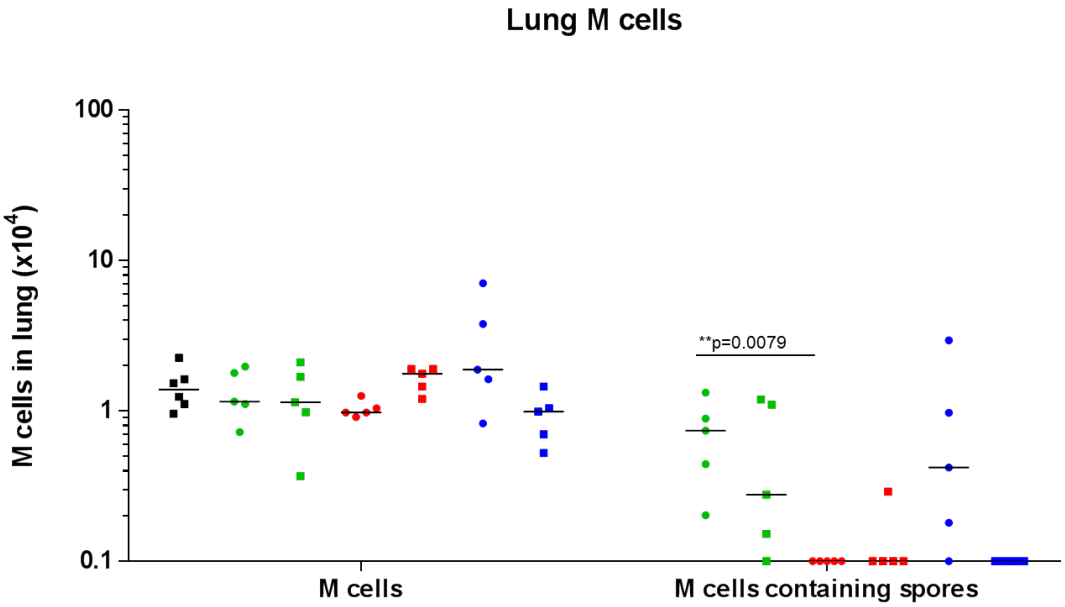

Figure 4-27. Flow cytometric analysis of M-cell populations in the lungs after dosing mice nasally, sublingually or orally with HU58 spores. BALB/c mice (n=5) were dosing with $2x10^9$ HU58 spores nasally, sublingually or orally and lungs taken at 6h or 24h after dosing. Lungs were homogenised as described in the methods (Section 2.21) and $1x10^6$ cells stained for spores (anti-spore primary with anti-rabbit IgG-FITC secondary) and M cells (NKM 16-2-4-PE). Black: naïve, green: nasal dosing, red: sublingual dosing, blue: oral dosing at 6h (circles) and 24h (squares). Limit of detection = $0.1x10^4$. Dots indicate individual mice and bars represent the median. Mann-Whitney were used to compare the dosing routes.

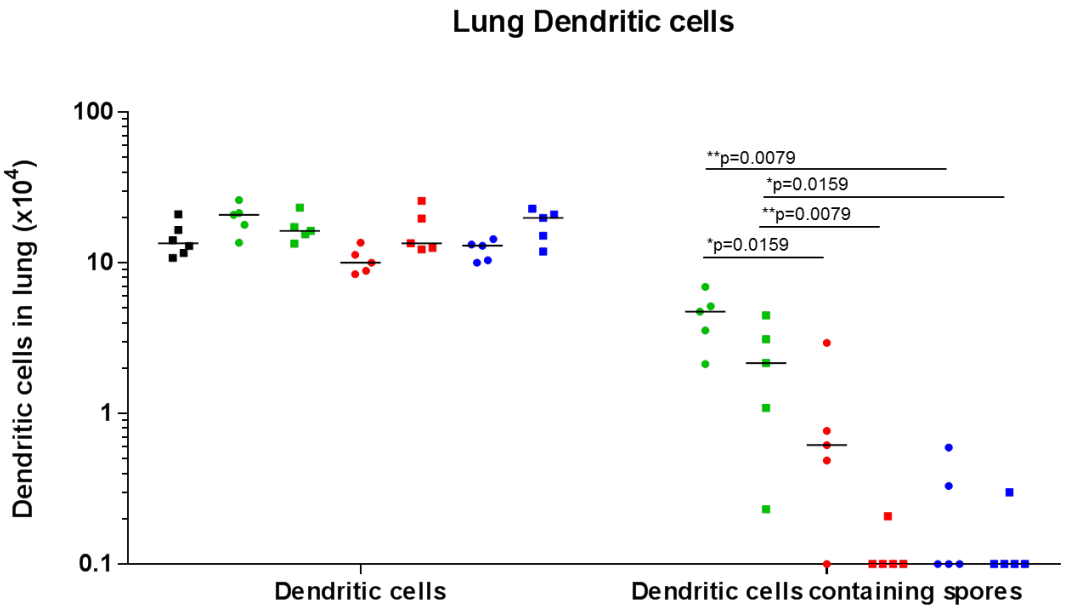

Figure 4-28. Flow cytometric analysis of DC populations in the lungs after dosing mice orally, nasally or sublingually with HU58 spores. BALB/c mice (n=5) were dosing with $2x10^9$ HU58 spores nasally, sublingually or orally and lungs taken at 6h or 24h after dosing. Lungs were homogenised as described in the methods (Section 2.21) and $1x10^6$ cells stained for spores (anti-spore primary with anti-rabbit IgG-FITC secondary) and DCs (CD11c-APC).Black: naïve, green: nasal dosing, red: sublingual dosing, blue: oral dosing at 6h (circles) and 24h (squares). Limit of detection = $0.1x10^4$. Dots indicate individual mice and bars represent the median. Mann-Whitney were used to compare the dosing routes.

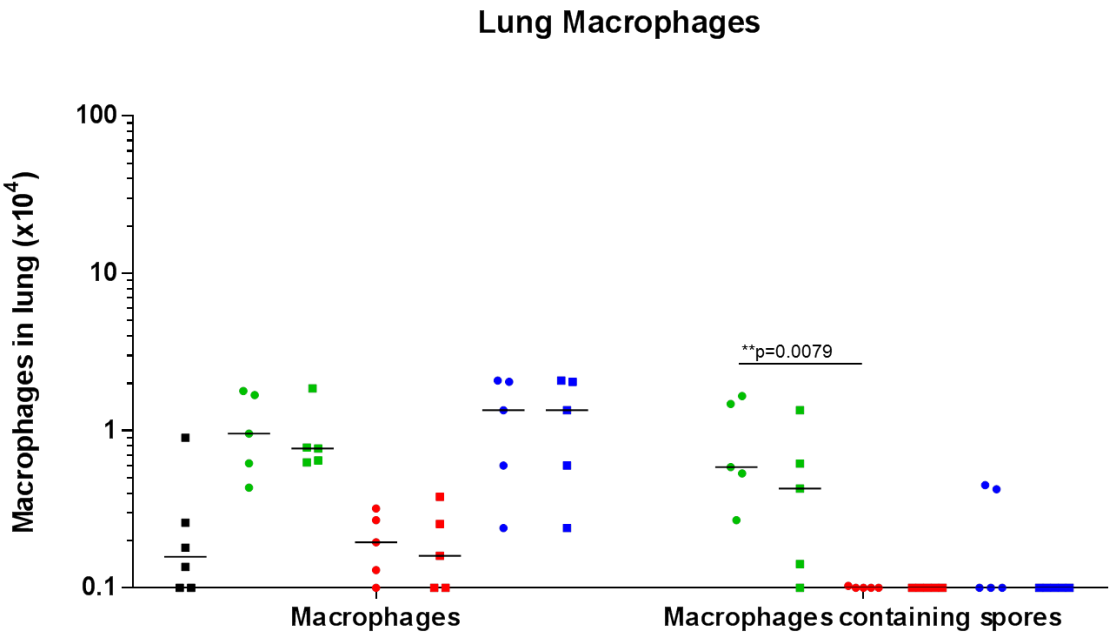

Figure 4-29. Flow cytometric analysis of macrophage populations in the lungs after dosing mice orally, nasally or sublingually with HU58 spores. BALB/c mice (n=5) were dosing with $2x10^9$ HU58 spores nasally, sublingually or orally and lungs taken at 6h or 24h after dosing. Lungs were homogenised as described in the methods (Section 2.21) and $1x10^6$ cells stained for spores (anti-spore primary with anti-rabbit IgG-FITC secondary) and macrophages (F4/80-PerCP).Black: naïve, green: nasal dosing, red: sublingual dosing, blue: oral dosing at 6h (circles) and 24h (squares). Limit of detection = $0.1x10^4$. Dots indicate individual mice and bars represent the median. Mann-Whitney were used to compare the dosing routes.

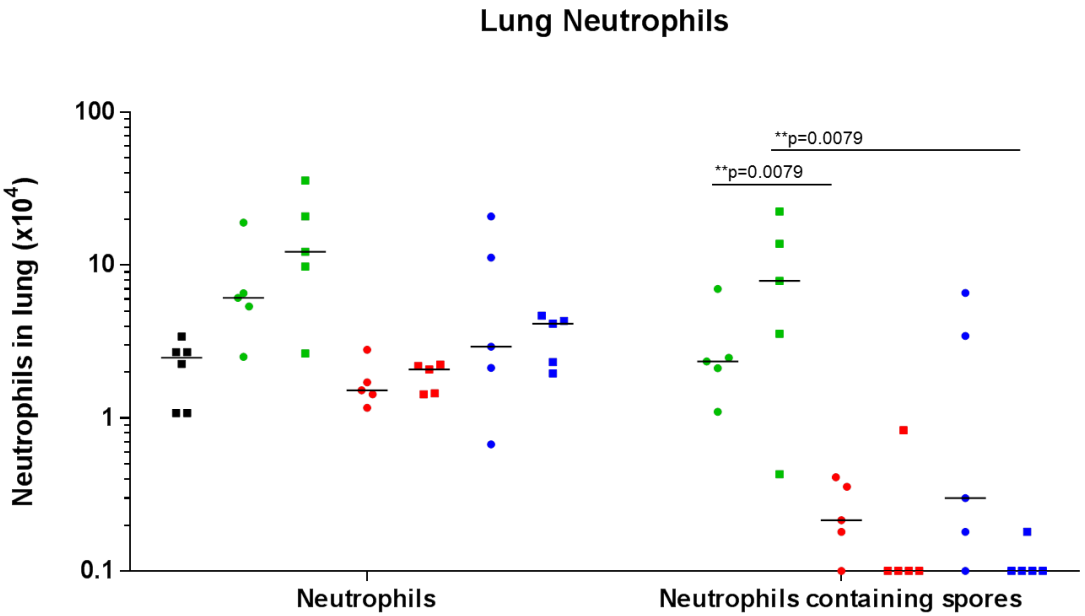

Figure 4-30. Flow cytometric analysis of neutrophil populations in the lungs after dosing mice orally, nasally or sublingually with HU58 spores. BALB/c mice (n=5) were dosing with $2x10^9$ HU58 spores nasally, sublingually or orally and lungs taken at 6h or 24h after dosing. Lungs were homogenised as described in the methods (Section 2.21) and $1x10^6$ cells stained for spores (anti-spore primary with anti-rabbit IgG-FITC secondary) and neutrophils (Ly6G-APC).Black: naïve, green: nasal dosing, red: sublingual dosing, blue: oral dosing at 6h (circles) and 24h (squares). Limit of detection = $0.1x10^4$. Dots indicate individual mice and bars represent the median. Mann-Whitney were used to compare the dosing routes.

4.2.17. Live spores infiltrating the gut

The gut data showed spores apparently infiltrating all four types of cells identified, but mainly the M cells and neutrophils **(Figure 4-31, Figure 4-32, Figure 4-33, Figure 4-34)**. Not all mice had detectable spores in the DCs and macrophages however. The nasal and oral dosing regimens exhibited the highest infiltration in M cells at 6 h and this reduced after 24h **(Figure 4-31)**. There were very few spores identified after sublingual dosing in any of the cell types examined. It would have been predicted that oral dosing would have resulted in the highest number of spores in the gut because oral dosing enters the digestive system directly, but the nasal dosing seems to have generated the highest numbers.

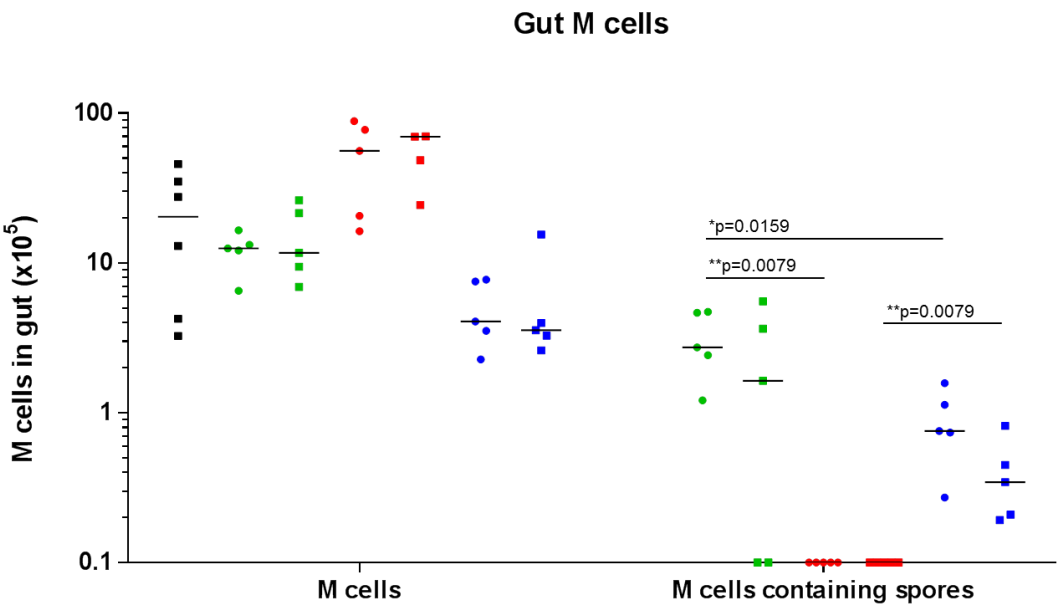

Figure 4-31. Flow cytometric analysis of M cell populations in the gut after dosing mice orally, nasally or sublingually with HU58 spores. BALB/c mice (n=5) were dosing with $2x10^9$ HU58 spores nasally, sublingually or orally and gut taken at 6h or 24h after dosing. The gut were homogenised as described in the methods (Section 2.21) and $1x10^6$ cells stained for spores (anti-spore primary with anti-rabbit IgG-FITC secondary) and M cells (NKM 16-2-4-PE). Black: naïve, green: nasal dosing, red: sublingual dosing, blue: oral dosing at 6h (circles) and 24h (squares). Limit of detection = $0.1x10^5$. Dots indicate individual mice and bars represent the median. Mann-Whitney were used to compare the dosing routes.

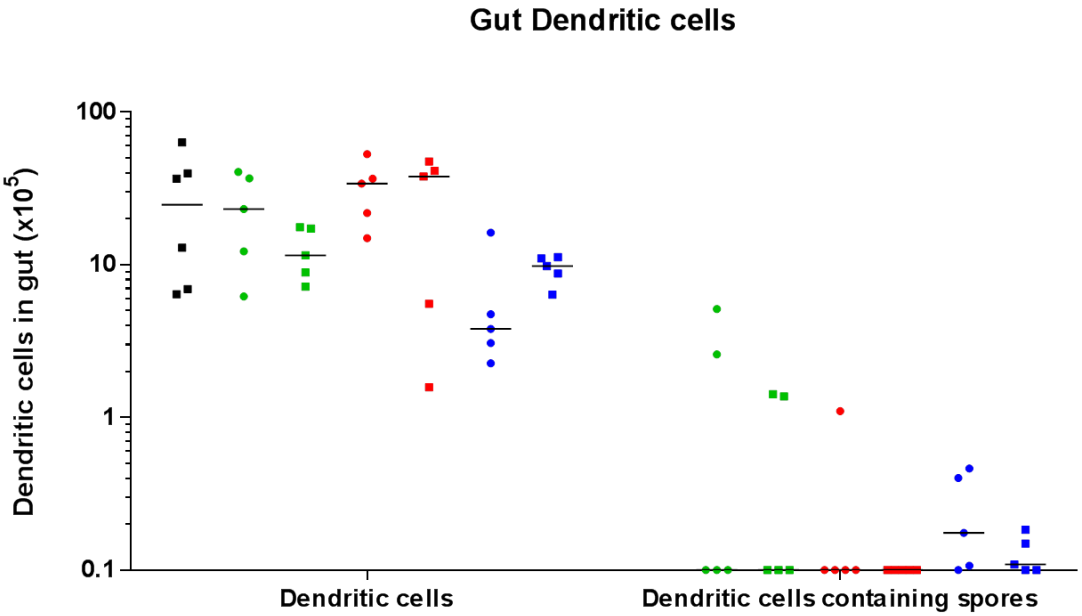

Figure 4-32. Flow cytometric analysis of DC populations in the gut after dosing mice orally, nasally or sublingually with HU58 spores. BALB/c mice (n=5) were dosing with $2x10^9$ HU58 spores nasally, sublingually or orally and gut taken at 6h or 24h after dosing. The gut were homogenised as described in the methods (Section 2.21) and $1x10^6$ cells stained for spores (anti-spore primary with anti-rabbit IgG-FITC secondary) and DCs (CD11c-APC). Black: naïve, green: nasal dosing, red: sublingual dosing, blue: oral dosing at 6h (circles) and 24h (squares). Limit of detection = $0.1x10^5$. Dots indicate individual mice and bars represent the median. Mann-Whitney were used to compare the dosing routes.

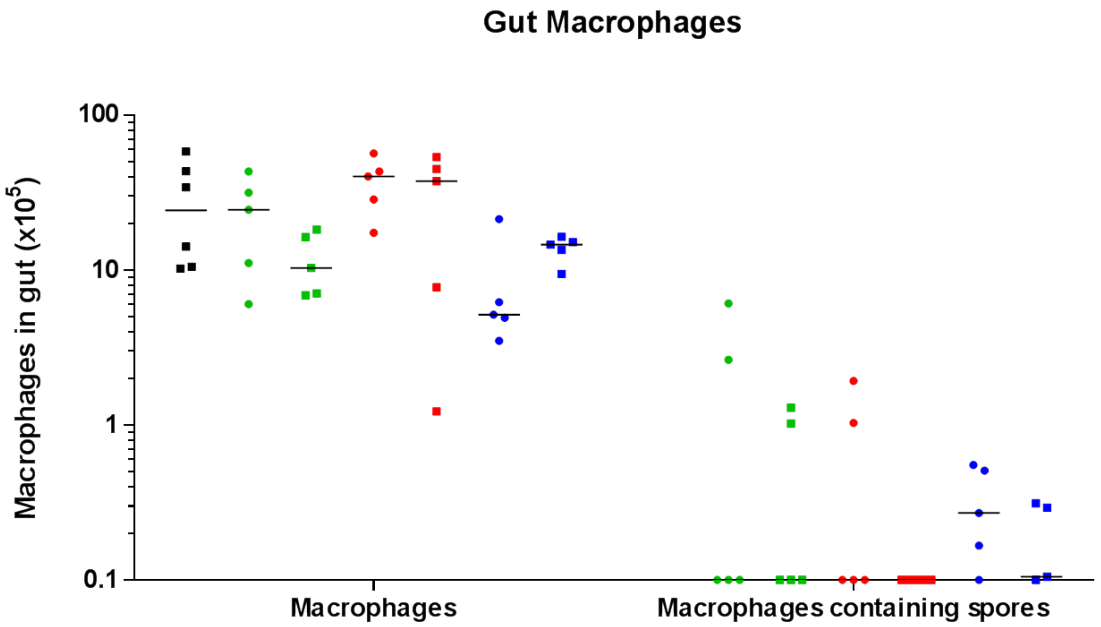

Figure 4-33. Flow cytometric analysis of macrophage populations in the gut after dosing mice orally, nasally or sublingually with HU58 spores. BALB/c mice (n=5) were dosing with $2x10^9$ HU58 spores nasally, sublingually or orally and gut taken at 6h or 24h after dosing. The gut were homogenised as described in the methods (Section 2.21) and $1x10^6$ cells stained for spores (anti-spore primary with anti-rabbit IgG-FITC secondary) and macrophages (F4/80-PerCP). Black: naïve, green: nasal dosing, red: sublingual dosing, blue: oral dosing at 6h (circles) and 24h (squares). Limit of detection = $0.1x10^5$. Dots indicate individual mice and bars represent the median. Mann-Whitney were used to compare the dosing routes.

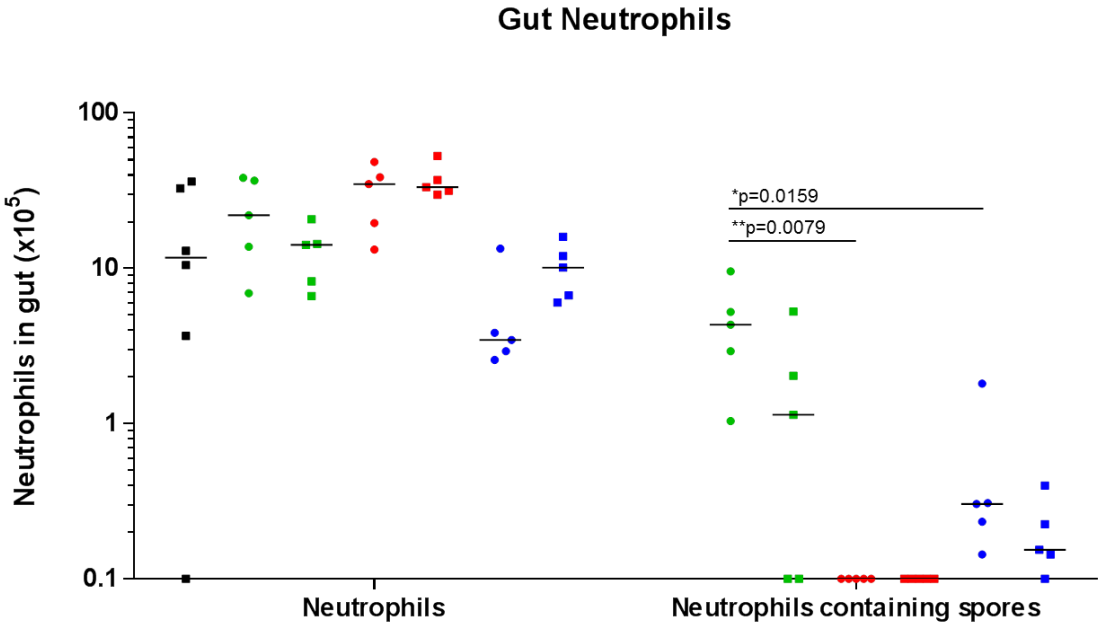

Figure 4-34. Flow cytometric analysis of neutrophil populations in the gut after dosing mice orally, nasally or sublingually with HU58 spores. BALB/c mice (n=5) were dosing with $2x10^9$ HU58 spores nasally, sublingually or orally and gut taken at 6h or 24h after dosing. The gut were homogenised as described in the methods (Section 2.21) and $1x10^6$ cells stained for spores (anti-spore primary with anti-rabbit IgG-FITC secondary) and neutrophils (Ly6G-APC). Black: naïve, green: nasal dosing, red: sublingual dosing, blue: oral dosing at 6h (circles) and 24h (squares). Limit of detection = $0.1x10^5$. Dots indicate individual mice and bars represent the median. Mann-Whitney were used to compare the dosing routes.

4.2.18. Live spores infiltrating the NALT

In the NALT following nasal dosing, M cells were shown to carry the most spores, which was expected as their role is to translocate particles across the epithelial barrier and the NALT has a large amount of epithelium **(Figure 4-35)**. There were a few spores seen in the DCs and macrophages after sublingual dosing, but at very low levels **(Figure 4-37, Figure 4-36)**. Although very few spores were seen in the other cell types, the numbers of macrophages and neutrophils increased at 6h **(Figure 4-37, Figure 4-38)**, which suggested that the dosing route has had an effect on the cell populations. It could be that an earlier time point would have provided more information about the NALT cell populations involved in spore uptake and by 6h spores were in the process of being cleared from the area.

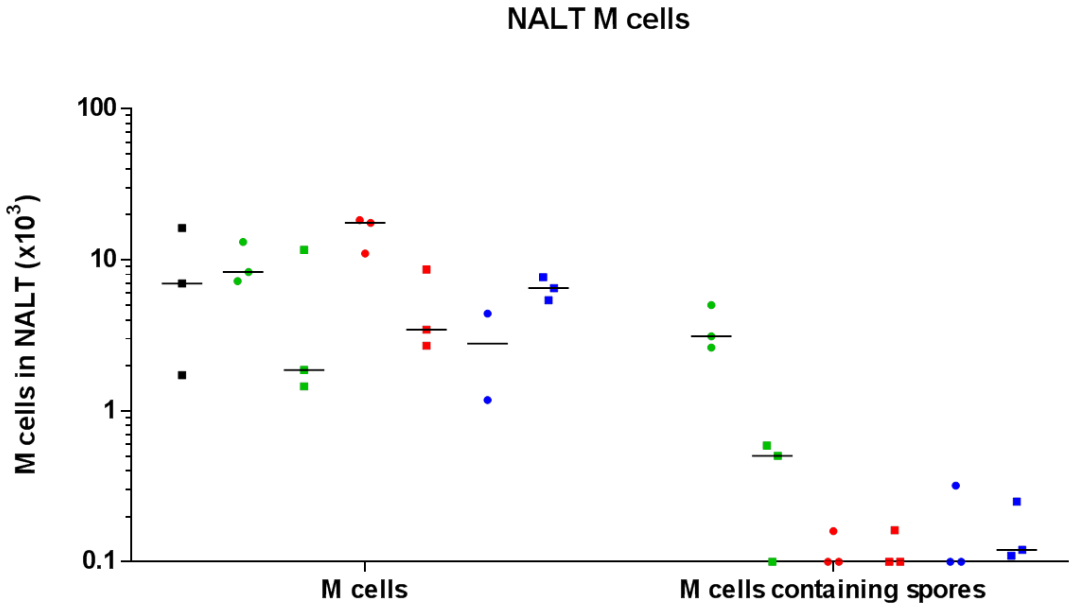

Figure 4-35. Flow cytometric analysis of M cell populations in the NALT after dosing mice orally, nasally or sublingually with HU58 spores. BALB/c mice (n=5) were dosing with 2x10^9 HU58 spores nasally, sublingually or orally and the NALT taken at 6h or 24h after dosing. The NALT were homogenised as described in the methods (Section 2.21) and 1x10^6 cells stained for spores (anti-spore primary with anti-rabbit IgG-FITC secondary) and M cells (NKM 16-2-4-PE). Black: naïve, green: nasal dosing, red: sublingual dosing, blue: oral dosing at 6h (circles) and 24h (squares). Limit of detection = 0.1x10^3. Dots indicate individual mice and lines represent the median. Mann-Whitney were used to compare the dosing routes.

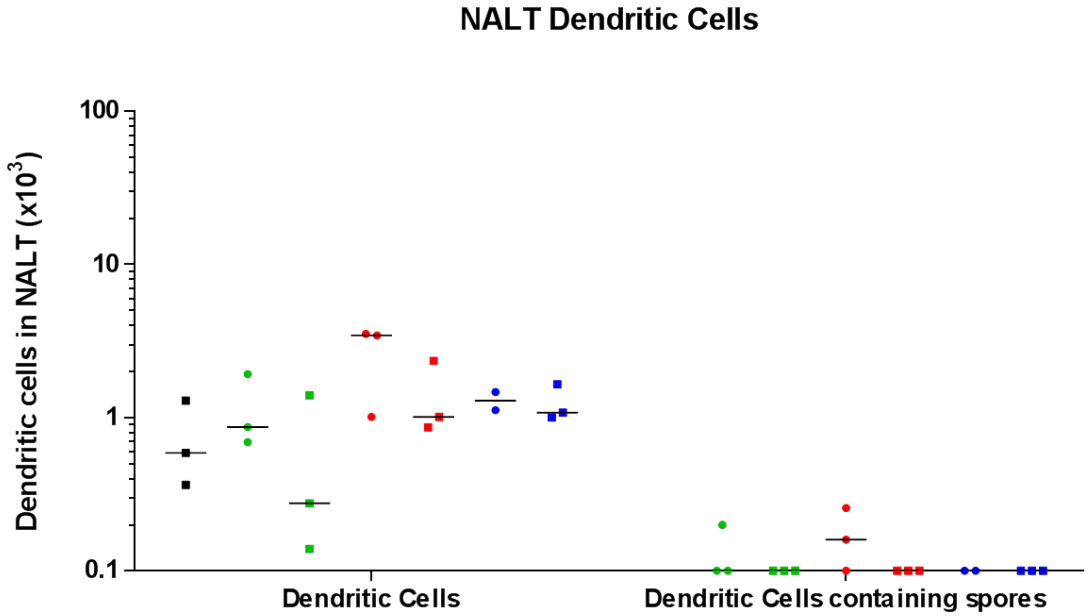

Figure 4-36. Flow cytometric analysis of DC populations in the NALT after dosing mice orally, nasally or sublingually with HU58 spores. BALB/c mice (n=5) were dosing with 2x10^9 HU58 spores nasally, sublingually or orally and the NALT taken at 6h or 24h after dosing. The NALT were homogenised as described in the methods (Section 2.21) and 1x10^6 cells stained for spores (anti-spore primary with anti-rabbit IgG-FITC secondary) and DCs (CD11c-APC). Black: naïve, green: nasal dosing, red: sublingual dosing, blue: oral dosing at 6h (circles) and 24h (squares). Limit of detection = 0.1x10^3. Dots indicate individual mice and bars represent the median. Mann-Whitney were used to compare the dosing routes.

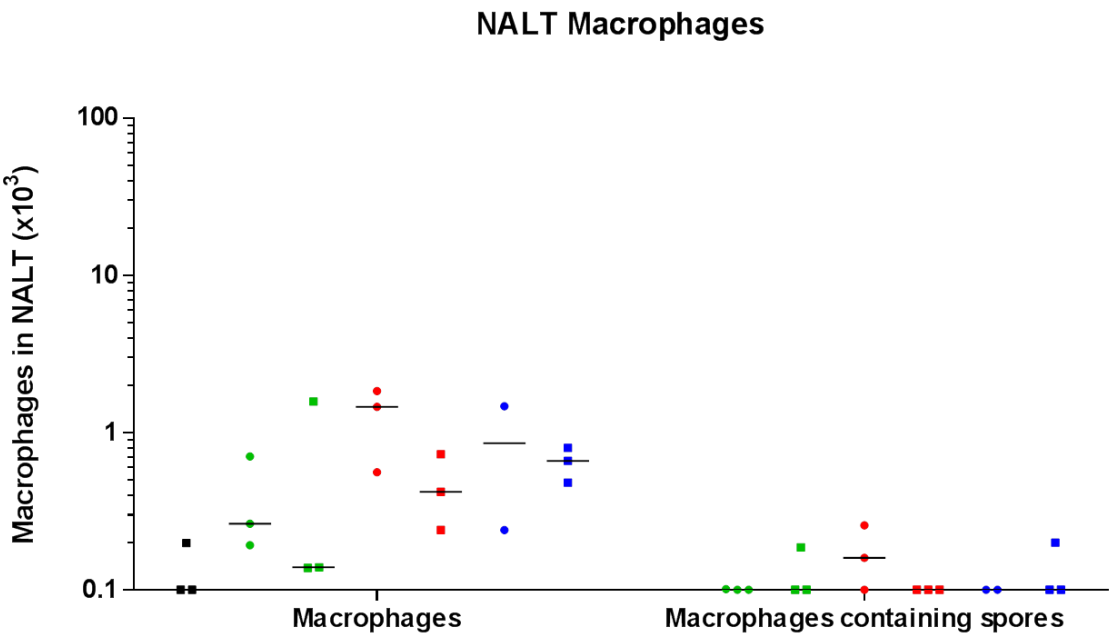

Figure 4-37. Flow cytometric analysis of macrophage populations in the NALT after dosing mice orally, nasally or sublingually with HU58 spores. BALB/c mice (n=5) were dosing with $2x10^9$ HU58 spores nasally, sublingually or orally and the NALT taken at 6h or 24h after dosing. The NALT were homogenised as described in the methods (Section 2.21) and $1x10^6$ cells stained for spores (anti-spore primary with anti-rabbit IgG-FITC secondary) and macrophages(F4/80-PerCP). Black: naïve, green: nasal dosing, red: sublingual dosing, blue: oral dosing at 6h (circles) and 24h (squares). Limit of detection = $0.1x10^3$. Dots indicate individual mice and bars represent the median. Mann-Whitney were used to compare the dosing routes.

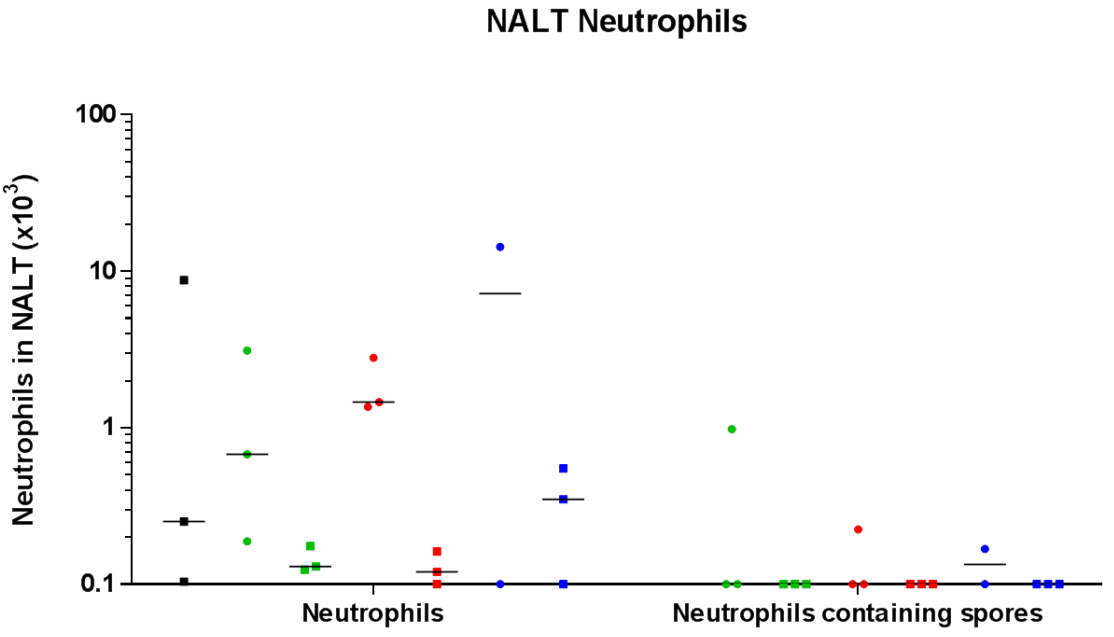

Figure 4-38. Flow cytometric analysis of neutrophil populations in the NALT after dosing mice orally, nasally or sublingually with HU58 spores. BALB/c mice (n=5) were dosing with $2x10^9$ HU58 spores nasally, sublingually or orally and the NALT taken at 6h or 24h after dosing. The NALT were homogenised as described in the methods (Section 2.21) and $1x10^6$ cells stained for spores (anti-spore primary with anti-rabbit IgG-FITC secondary) and neutrophils (Ly6G-APC). Black: naïve, green: nasal dosing, red: sublingual dosing, blue: oral dosing at 6h (circles) and 24h (squares). Limit of detection = $0.1x10^3$. Dots indicate individual mice and bars represent the median. Mann-Whitney were used to compare the dosing routes.

4.2.19. Autoclaved spores infiltrating the lungs

Autoclaved spores are only seen in the M cells following oral dosing at 6h **(Figure 4-39)**, whereas spores were detected in M cells after administration of live spores via the intranasal route. This could mean that in the lungs, M cells are better able to interact with live spores. Autoclaved spores were seen in the DCs and macrophages after nasal and oral administration **(Figure 4-40, Figure 4-41)**. The numbers of spores are highest at 6h so it would appear that the spores are starting to be cleared after 24h. Spores were present only in neutrophils after oral administration of spores to the lungs at 6h **(Figure 4-42)**. It would be expected that more spores would be inside host cells after nasal dosing, because a greater number of spores are delivered to the lungs **(Figure 4-10)** but there appear to be more after oral dosing inside M cells, macrophages and neutrophils.

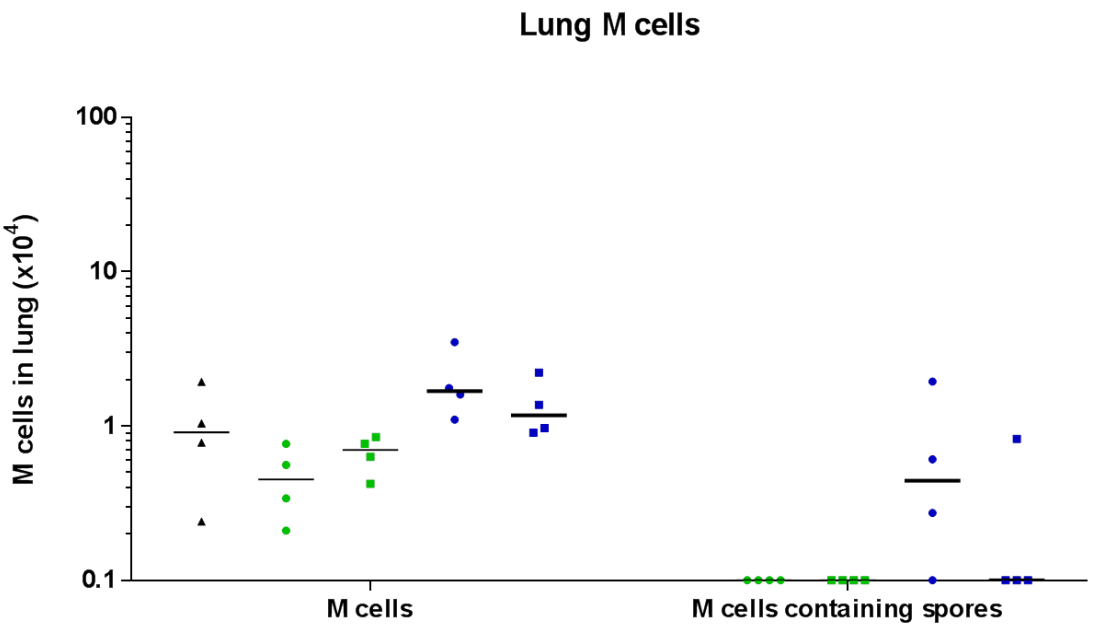

Figure 4-39. Flow cytometric analysis of M cell populations in the lungs after dosing mice orally, nasally or sublingually with autoclaved HU58 spores. BALB/c mice (n=4) were dosing with $2x10^9$ autoclaved HU58 spores nasally, sublingually or orally and the lung taken at 6h or 24h after dosing. The lungs were homogenised as described in the methods (Section 2.21) and $1x10^6$ cells stained for spores (anti-spore primary with anti-rabbit IgG-FITC secondary) and M cells (NKM 16-2-4-PE). Black: naïve, green: nasal dosing, red: sublingual dosing, blue: oral dosing at 6h (circles) and 24h (squares). Limit of detection = $0.1x10^4$. Dots indicate individual mice and lines represent the median. Mann-Whitney were used to compare the dosing routes.

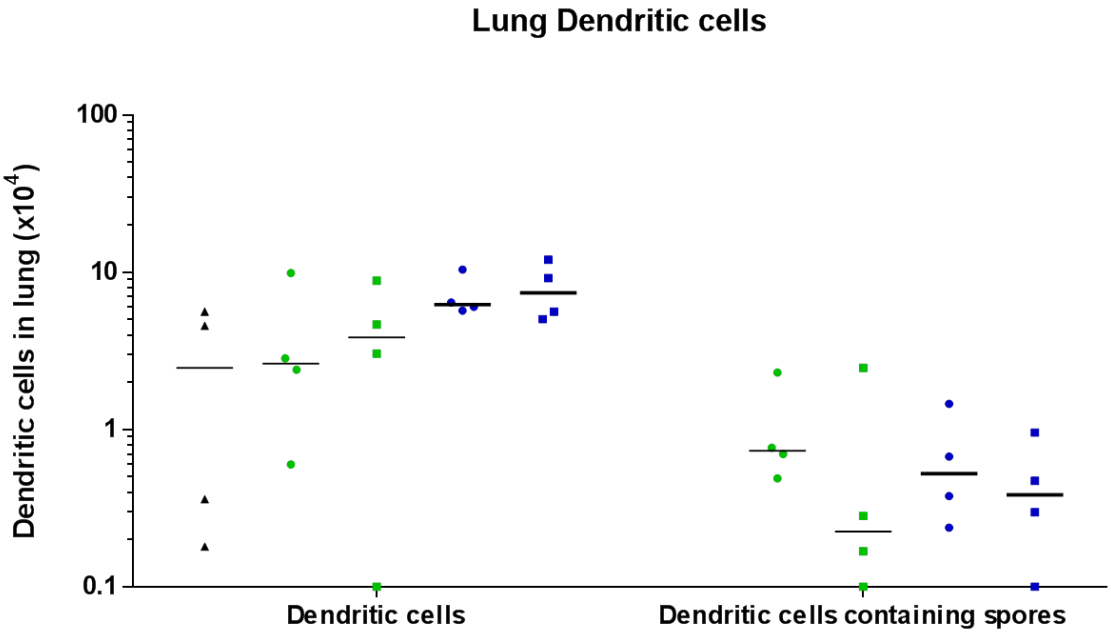

Figure 4-40. Flow cytometric analysis of DC populations in the lungs after dosing mice orally, nasally or sublingually with autoclaved HU58 spores. BALB/c mice (n=4) were dosing with $2x10^9$ autoclaved HU58 spores nasally, sublingually or orally and the lung taken at 6h or 24h after dosing. The lungs were homogenised as described in the methods (Section 2.21) and $1x10^6$ cells stained for spores (anti-spore primary with anti-rabbit IgG-FITC secondary) and DCs (CD11c-APC). Black: naïve, green: nasal dosing, red: sublingual dosing, blue: oral dosing at 6h (circles) and 24h (squares). Limit of detection = $0.1x10^4$. Dots indicate individual mice and lines represent the median. Mann-Whitney were used to compare the dosing routes.

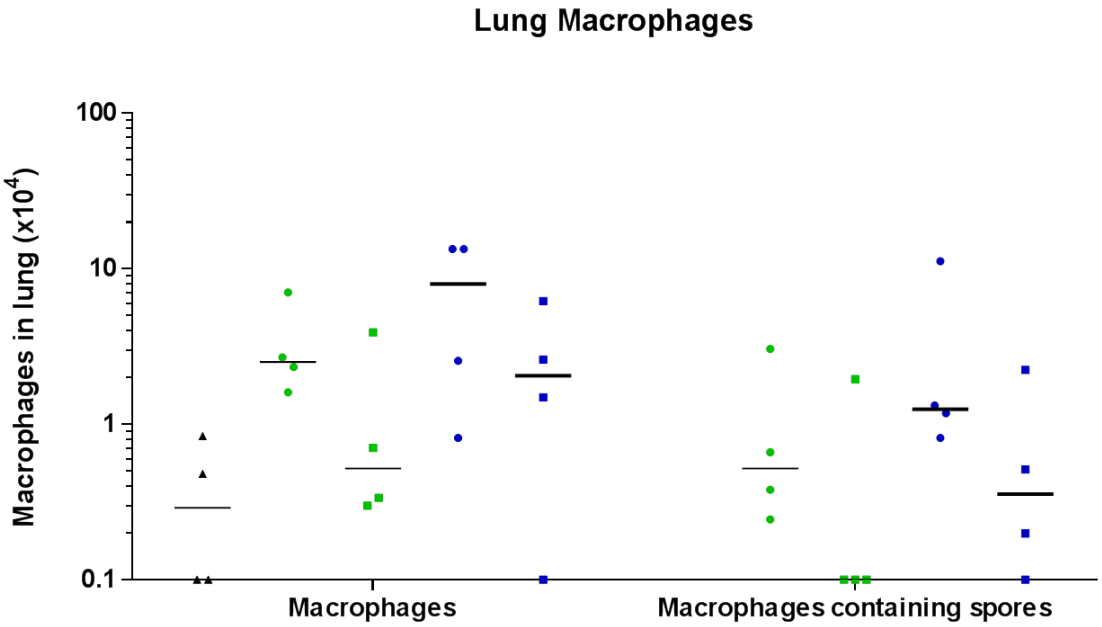

Figure 4-41. Flow cytometric analysis of macrophage populations in the lungs after dosing mice orally, nasally or sublingually with autoclaved HU58 spores. BALB/c mice (n=4) were dosing with $2x10^9$ autoclaved HU58 spores nasally, sublingually or orally and the lung taken at 6h or 24h after dosing. The lungs were homogenised as described in the methods (Section 2.21) and $1x10^6$ cells stained for spores (anti-spore primary with anti-rabbit IgG-FITC secondary) and macrophages (F4/80-PerCP). Black: naïve, green: nasal dosing, red: sublingual dosing, blue: oral dosing at 6h (circles) and 24h (squares). Limit of detection = $0.1x10^4$. Dots indicate individual mice and lines represent the median. Mann-Whitney were used to compare the dosing routes.

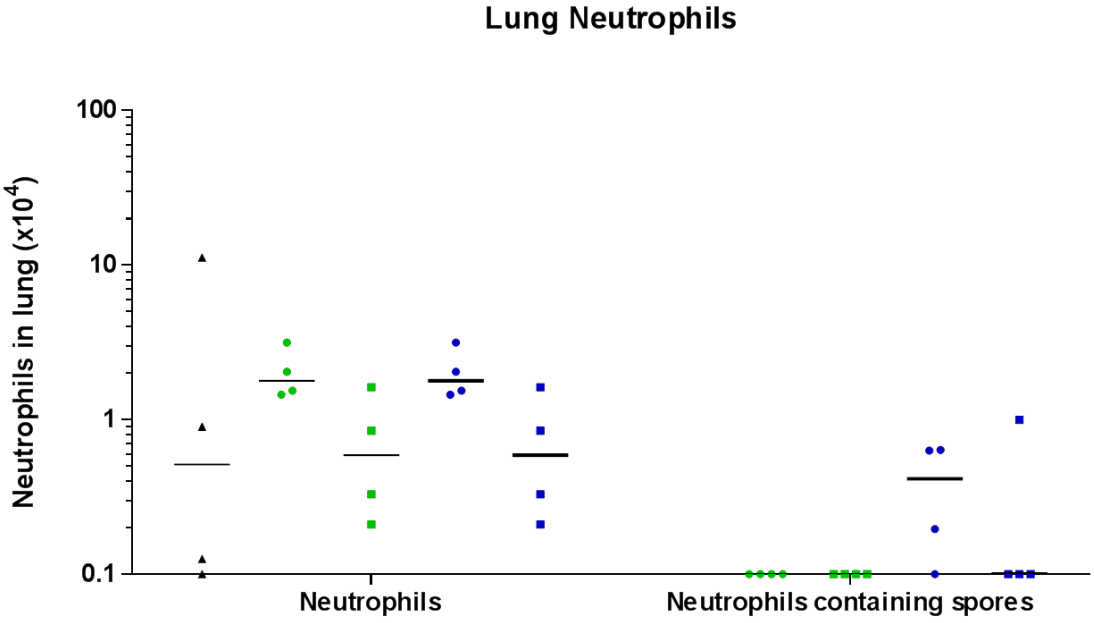

Figure 4-42. Flow cytometric analysis of neutrophil populations in the lungs after dosing mice orally, nasally or sublingually with autoclaved HU58 spores. BALB/c mice (n=4) were dosing with $2x10^9$ autoclaved HU58 spores nasally, sublingually or orally and the lung taken at 6h or 24h after dosing. The lungs were homogenised as described in the methods (Section 2.21) and $1x10^6$ cells stained for spores (anti-spore primary with anti-rabbit IgG-FITC secondary) and neutrophils (Ly6G-APC). Black: naïve, green: nasal dosing, red: sublingual dosing, blue: oral dosing at 6h (circles) and 24h (squares). Limit of detection = $0.1x10^4$. Dots indicate individual mice and lines represent the median. Mann-Whitney were used to compare the dosing routes.

4.2.20. Autoclaved spores infiltrating in the gut

The greatest numbers of spores were seen inside the M cells, dendritic cells, macrophages and neutrophils after oral dosing at 6h **(Figure 4-43 – Figure 4-46)**. This was expected because the spores were being delivered directly to the gut. Following administration of live spores, the numbers inside all of the host cells of the gut measured were lower in comparison to autoclaved spores, and this could be because the spores had germinated and so fewer were detectable as they were vegetative cells and the antibody detects spores only. All four host cell populations were responsible for spore uptake, but the DCs and macrophages were the dominant populations that contained spores, and spores were seen at 6h and 24h. In the gut, it appears that M cells and neutrophils phagocytose autoclaved spores better than in the lungs, but in both cases, macrophages and DCs were the dominant populations.

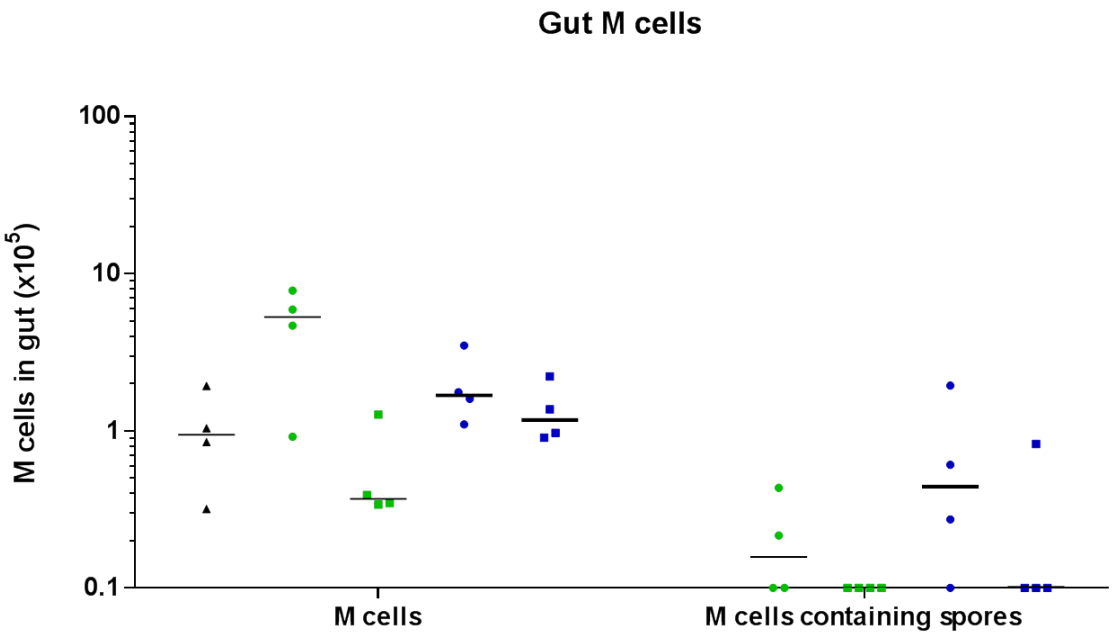

Figure 4-43. Flow cytometric analysis of M cell populations in the gut after dosing mice orally, nasally or sublingually with autoclaved HU58 spores. BALB/c mice (n=4) were dosing with $2x10^9$ autoclaved HU58 spores nasally, sublingually or orally and the gut taken at 6h or 24h after dosing. The gut tissues were homogenised as described in the methods (Section 2.21) and $1x10^6$ cells stained for spores (anti-spore primary with anti-rabbit IgG-FITC secondary) and M cells (NKM 6-2-4-PE). Black: naïve, green: nasal dosing, red: sublingual dosing, blue: oral dosing at 6h (circles) and 24h (squares). Limit of detection = $0.1x10^5$. Dots indicate individual mice and lines represent the median. Mann-Whitney was used to compare the dosing routes.

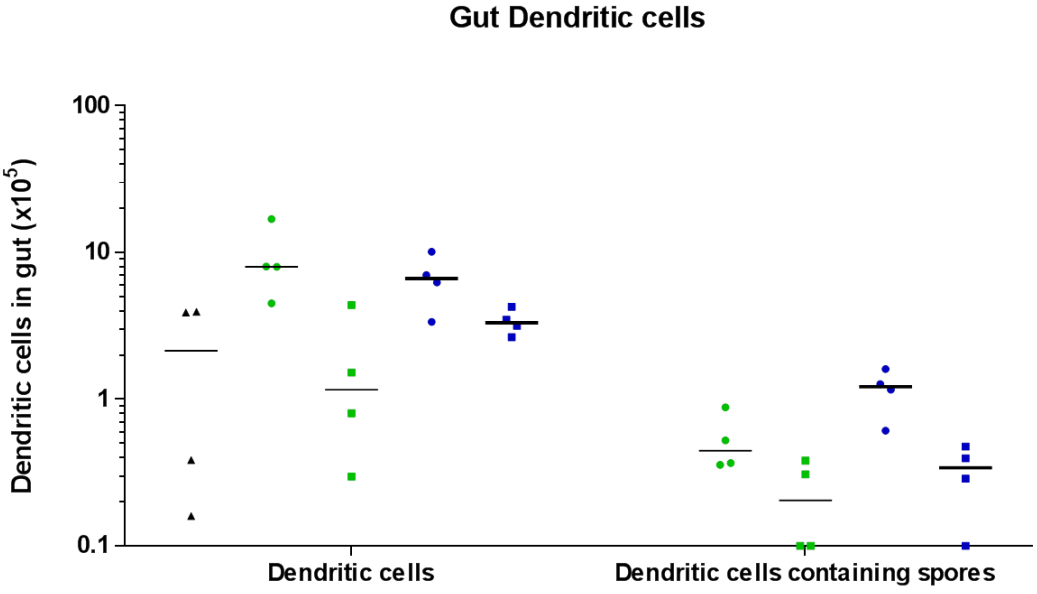

Figure 4-44. Flow cytometric analysis of DC populations in the gut after dosing mice orally, nasally or sublingually with autoclaved HU58 spores. BALB/c mice (n=4) were dosing with $2x10^9$ autoclaved HU58 spores nasally, sublingually or orally and the gut taken at 6h or 24h after dosing. The gut tissues were homogenised as described in the methods (Section 2.21) and $1x10^6$ cells stained for spores (anti-spore primary with anti-rabbit IgG-FITC secondary) and DCs (CD11c-APC). Black: naïve, green: nasal dosing, red: sublingual dosing, blue: oral dosing at 6h (circles) and 24h (squares). Limit of detection = $0.1x10^5$. Dots indicate individual mice and bars represent the median. Mann-Whitney was used to compare the dosing routes.

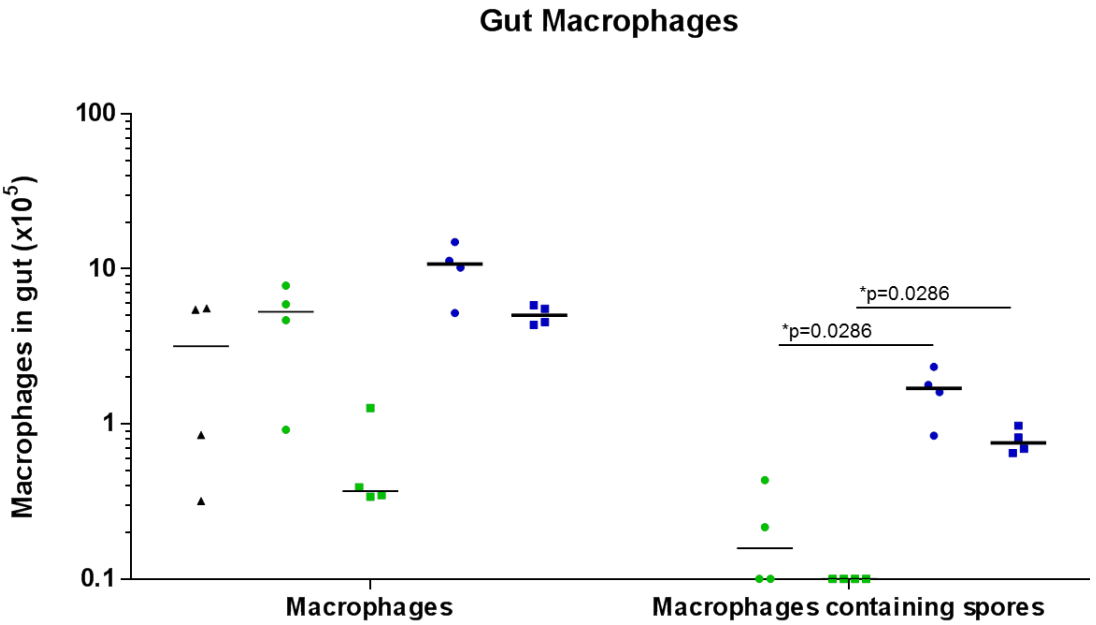

Figure 4-45. Flow cytometric analysis of macrophage populations in the gut after dosing mice orally, nasally or sublingually with autoclaved HU58 spores. BALB/c mice (n=4) were dosing with $2x10^9$ autoclaved HU58 spores nasally, sublingually or orally and the gut taken at 6h or 24h after dosing. The gut tissues were homogenised as described in the methods (Section 2.21) and $1x10^6$ cells stained for spores (anti-spore primary with anti-rabbit IgG-FITC secondary) and macrophages (F4/80-PerCP). Black: naïve, green: nasal dosing, red: sublingual dosing, blue: oral dosing at 6h (circles) and 24h (squares). Limit of detection = $0.1x10^5$. Dots indicate individual mice and lines represent the median. Mann-Whitney was used to compare the dosing routes.

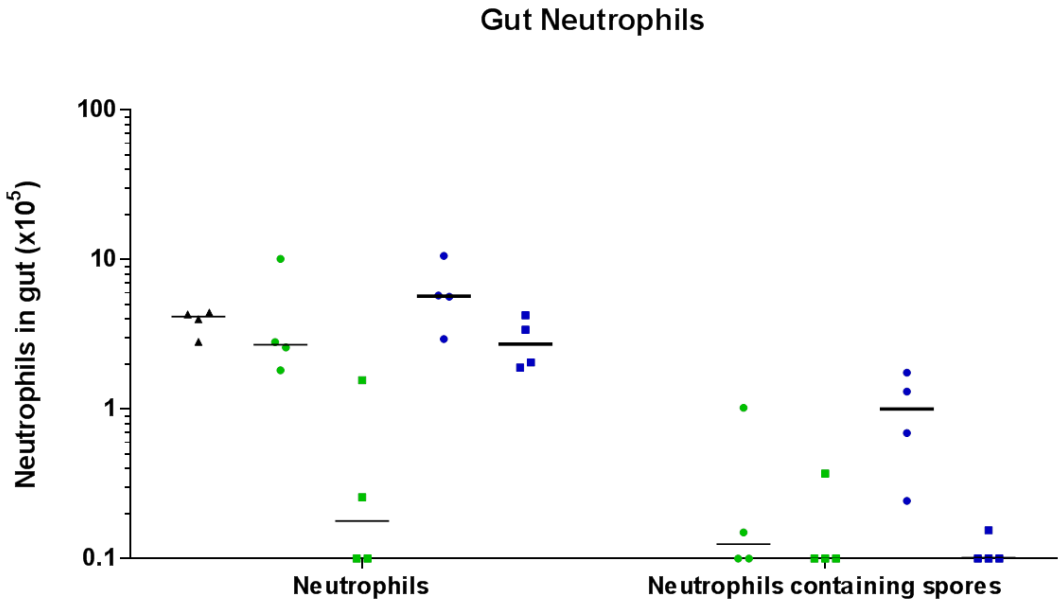

Figure 4-46. Flow cytometric analysis of neutrophil populations in the gut after dosing mice orally, nasally or sublingually with autoclaved HU58 spores. BALB/c mice (n=4) were dosing with $2x10^9$ autoclaved HU58 spores nasally, sublingually or orally and the gut taken at 6h or 24h after dosing. The gut tissues were homogenised as described in the methods (Section 2.21) and $1x10^6$ cells stained for spores (anti-spore primary with anti-rabbit IgG-FITC secondary) and neutrophils (Ly6G-APC). Black: naïve, green: nasal dosing, red: sublingual dosing, blue: oral dosing at 6h (circles) and 24h (squares). Limit of detection = $0.1x10^5$. Dots indicate individual mice and lines represent the median. Mann-Whitney was used to compare the dosing routes.

4.2.21. Autoclaved spores infiltrating the NALT

Spores were identified inside M cells after nasal and oral dosing **(Figure 4-47)** at 6h. After 24h they were cleared after nasal dosing but some were still observed after oral dosing **(Figure 4-47)**. After nasal dosing at 24h, spores were observed inside DCs **(Figure 4-48)**. There were some spores inside DCs 6h after oral dosing, but the numbers were more variable. Spores were also detected inside macrophages after nasal and oral dosing, but this was also variable **(Figure 4-49)**. More spores were seen in neutrophils after nasal dosing compared to oral dosing **(Figure 4-50)**. A greater number of autoclaved spores appeared to enter the NALT in comparison to live spores, and enter all types of cells, whereas the live spores, only when dosed intranasally entered M cells. More repeats would be required to get a clearer picture of distribution of autoclaved spores in the NALT.

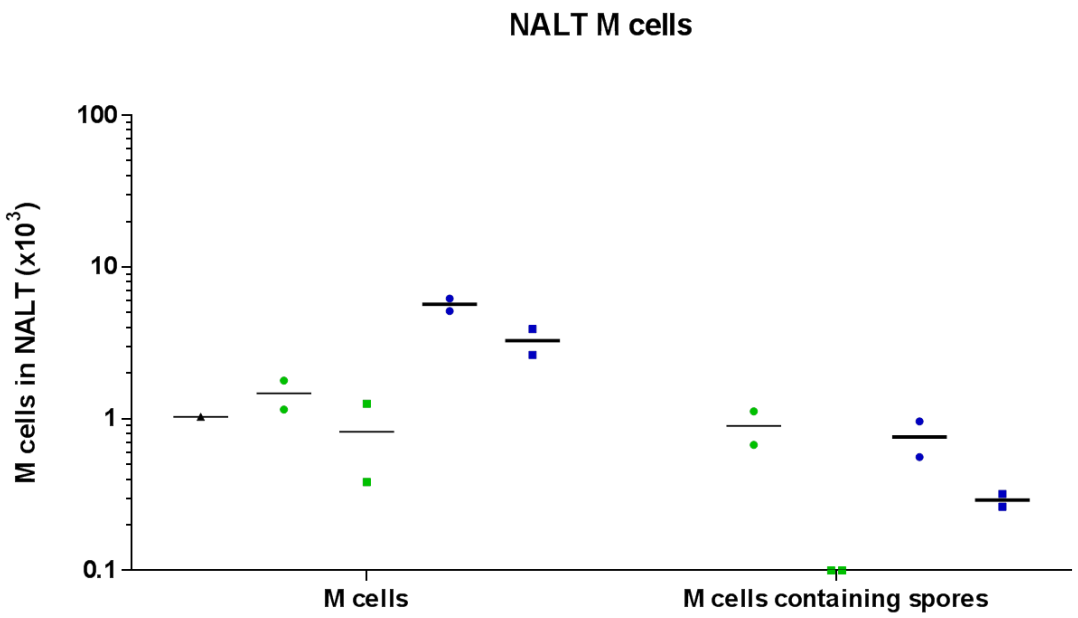

Figure 4-47. Flow cytometric analysis of M cell populations in the NALT after dosing mice orally, nasally or sublingually with autoclaved HU58 spores. BALB/c mice (n=4) were dosing with $2x10^9$ autoclaved HU58 spores nasally, sublingually or orally and the NALT taken at 6h or 24h after dosing. The NALT tissues were homogenised as described in the methods (Section 2.21) and $1x10^6$ cells stained for spores (anti-spore primary with anti-rabbit IgG-FITC secondary) and M cells (NKM 6-2-4-PE). Black: naïve, green: nasal dosing, red: sublingual dosing, blue: oral dosing at 6h (circles) and 24h (squares). Limit of detection = $0.1x10^3$. Dots indicate individual mice and lines represent the median.

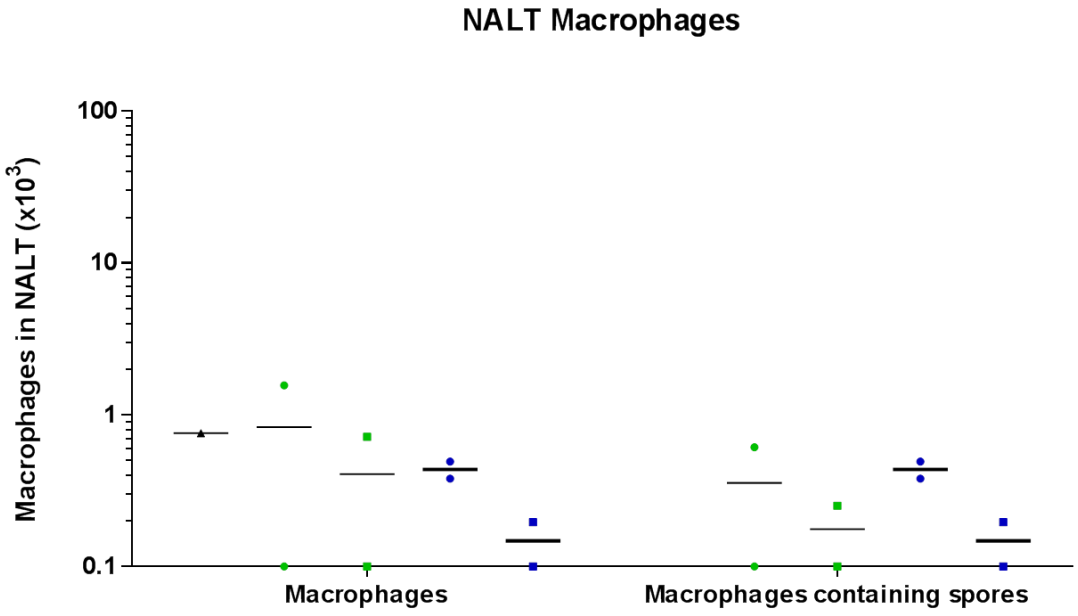

Figure 4-48. Flow cytometric analysis of DC populations in the NALT after dosing mice orally, nasally or sublingually with autoclaved HU58 spores. BALB/c mice (n=4) were dosing with $2x10^9$ autoclaved HU58 spores nasally, sublingually or orally and the NALT taken at 6h or 24h after dosing. The NALT tissues were homogenised as described in the methods (Section 2.21) and $1x10^6$ cells stained for spores (anti-spore primary with anti-rabbit IgG-FITC secondary) and DCs (CD11c-APC).Black: naïve, green: nasal dosing, red: sublingual dosing, blue: oral dosing at 6h (light grey) and 24h (dark grey). Limit of detection = $0.1x10^3$. Dots indicate individual mice and bars represent the median.

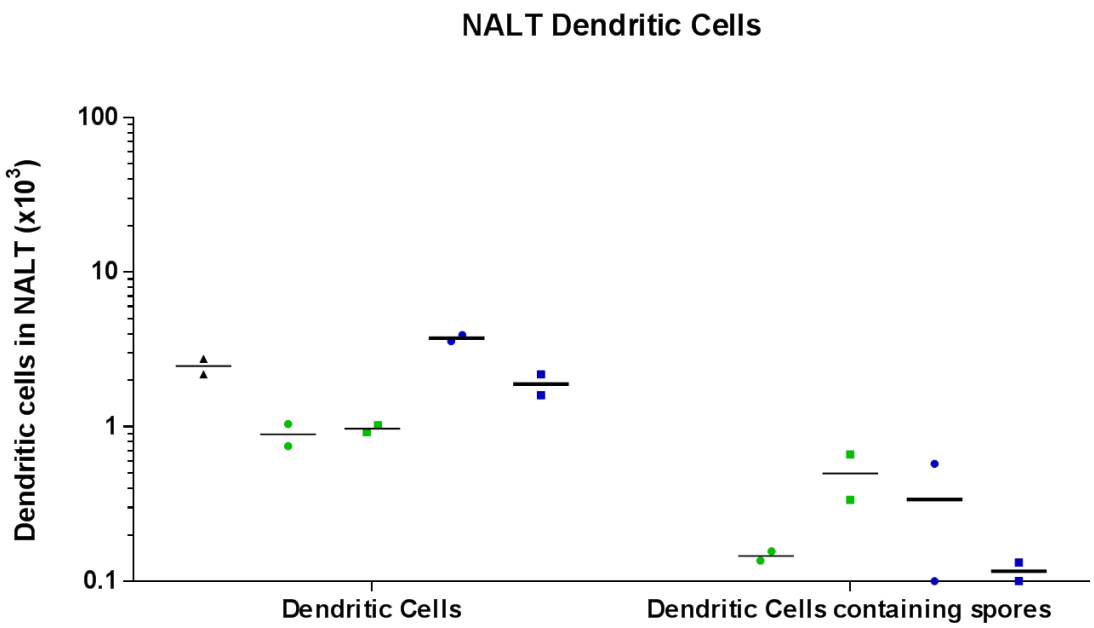

Figure 4-49. Flow cytometric analysis of macrophage populations in the NALT after dosing mice orally, nasally or sublingually with autoclaved HU58 spores. BALB/c mice (n=4) were dosing with $2x10^9$ autoclaved HU58 spores nasally, sublingually or orally and the NALT taken at 6h or 24h after dosing. The NALT tissues were homogenised as described in the methods (Section 2.21) and $1x10^6$ cells stained for spores (anti-spore primary with anti-rabbit IgG-FITC secondary) and macrophages (F4/80-PerCP).Black: naïve, green: nasal dosing, red: sublingual dosing, blue: oral dosing at 6h (circles) and 24h (squares). Limit of detection = $0.1x10^3$. Dots indicate individual mice and bars represent the median.

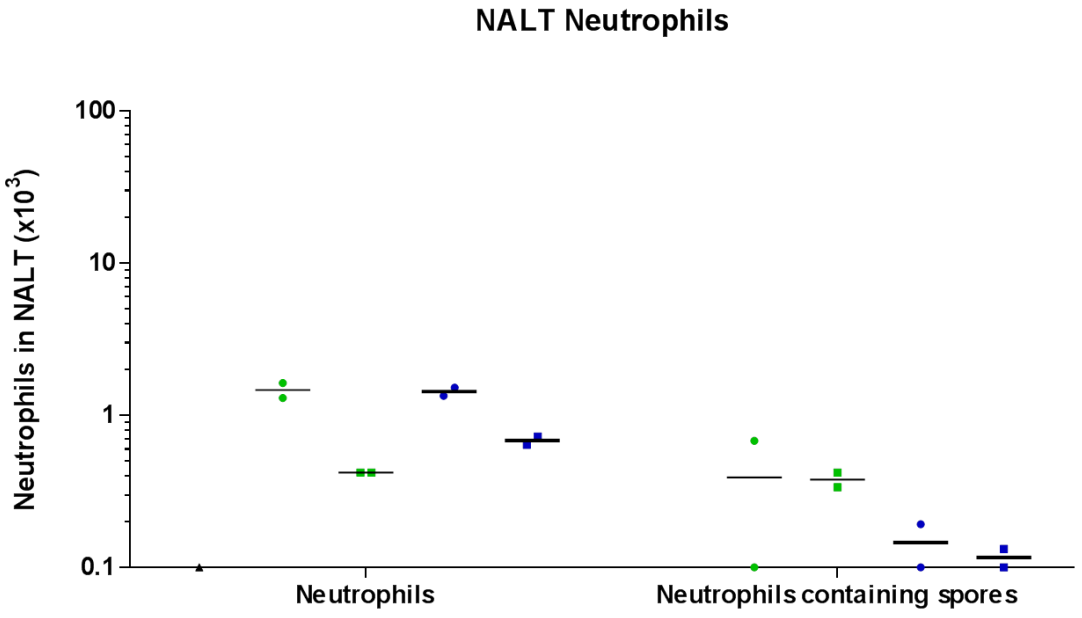

Figure 4-50. Flow cytometric analysis of neutrophil populations in the NALT after dosing mice orally, nasally or sublingually with autoclaved HU58 spores. BALB/c mice (n=4) were dosing with $2x10^9$ autoclaved HU58 spores nasally, sublingually or orally and the NALT taken at 6h or 24h after dosing. The NALT tissues were homogenised as described in the methods (Section 2.21) and $1x10^6$ cells stained for spores (anti-spore primary with anti-rabbit IgG-FITC secondary) and neutrophils (Ly6G-APC).Black: naïve, green: nasal dosing, red: sublingual dosing, blue: oral dosing at 6h (circles) and 24h (squares). Limit of detection = $0.1x10^3$. Dots indicate individual mice and bars represent the median.

4.3. Discussion

Spores must be able to cross epithelial barriers and be presented to leukocytes in order to generate immune responses. In these experiments, it has been demonstrated that spores can cross the epithelial barriers of the lungs, gut and the NALT using flow cytometry, and confirmed in the lungs and gut using immunofluoresence.

4.3.1. Optimisation of method for detecting spores on the flow cytometer

The growth and sporulation of spores was studied using the flow cytometer to assess whether the technique was appropriate to use for detecting spores in tissues. Growth of bacilli could be distinguished from spores and two populations could be detected as the bacteria began to sporulate. The two populations were confirmed by phase-contrast microscopy, and the spores were also confirmed using anti-spore and anti-rabbit IgG-FITC antibody on the flow cytometer. Other spore forming microorganisms have been characterised using FSC and SSC (Tracy *et al*. 2010; Comas-Riu & Vives-Rego 2002) and using fluorescent dyes have been able to detect germinated cells (Tracy *et al*. 2010; Smelt *et al*. 2008). Monitoring spore growth could also be applied to investigate the roles of certain proteins in spore development or germination by using knock-outs of developmental genes and determining any differences in sporulation/germination. The role of BclA proteins in *C. difficile* germination is currently being investigated at RHUL by other lab members using flow cytometry (unpublished).

Strain DS127 that has GFP fused to CotC exhibited fluorescence under the microscope, but when dosed to tissues, the spores could not be detected because they were not brighter than the autofluorescence of the tissue. The

spores were also not sufficiently detectable by flow cytometry so as to be able to truly identify them as DS127 spores. The results are supported by data from Zhou *et al*, who used CotC-TP22.3 expressing spores against *C. sinesis* and found on the flow cytometer than the antigen could be detected, but only 2,900 events out of 10,000 were positive (Zhou *et al*. 2008). When the anti-spore antibody and anti-IgG FITC was used, there was a clear shift in fluorescence and the majority of spores were positive. It was important that the spores could be identifiable for the dosing experiment to be able to investigate the distribution of spores. The spores could be characterised by their FSC-A and SSC-A profile, but there are likely to be other commensal bacteria naturally present in the mice of a similar size and therefore an antibody based system was required.

4.3.2. Sublingual dosing

Very few spores were identified in any tissues after sublingual dosing. From this work it is difficult to determine the fate of the spores, but they could have either i) crossed into the bloodstream or ii) been degraded and soluble proteins crossed into the bloodstream. Amuguni *et al* showed that *B. subtilis* spores carrying TTFC delivered sublingually were able to generate humoral and cellular immune responses so although they were not detectable here, sublingual immunisation with spores has been demonstrated to elicit immune responses (Amuguni *et al*. 2011). Logistically identifying the localisation of spores would be difficult in the mouth but further work to characterise immune responses downstream of sublingual dosing could be carried out to discover how well spores delivered by this route can generate an immune response. Sublingual immunisation is a promising route of mucosal immunisation because it is easy to administer, has been reported to generate strong immune responses in the lungs and genital tract and lower doses can be used (10-50

fold less than oral dosing) (Czerkinsky *et al*. 2011). Sublingual administration of HPV VLPs were able to protect against genital challenged with HPV pseudovirons and they hypothesised that after sublingual vaccination, IgA antibody secreting cells (ASC) have a unique migratory pattern that let them target distant mucosal sites (Cuburu *et al*. 2009).

4.3.3. Distribution of spores in the respiratory tract tissues

The lungs and NALT would be the prime locations targeted by respiratory pathogens such as MTB, therefore this is where a vaccine stimulated immune response would be most useful. Work into the distribution of *B. anthracis* after inhalation has demonstrated that spores are predominately delivered to the lungs and nasopharynx, and that they germinate in the nasopharynx and NALT, but there is very little germination in the lungs (Glomski *et al*. 2007). The data here suggests a similar model for *B. subtilis* as spores were still detected after 24h in the lungs whereas if they had germinated they would have not bound the anti-spore antibody. After influenza infection, it has been presented that the immune cells are increased in the NALT (Asanuma *et al*. 1997) and that when the NALT is injected with antigens, it has been demonstrated to elicit stronger immune responses in comparison to the nasal dosing route (Hou *et al*. 2002). Live spores were found in the NALT after nasal dosing in this experiment, and there were changes in the cell populations within 24h, mainly after nasal dosing so this is promising that spores are able to induce immune responses in the NALT, which could affect the ability of the MALT to respond to pathogens. A wider variety of cells were found to contain spores after administration of autoclaved spores, but a greater quantity were found in the M cells of the NALT after dosing with live spores.

4.3.4. Differences between cell types in different tissues

The cells observed to engulf the most live spores in each tissue varied and may represent the different roles of each tissue. DC populations engulfed the greatest proportion of spores in the lungs, but not in the NALT and this could be due to the NALT physiology as it has been reported that few DCs accumulate under the M cells in the NALT and were not observed to sample the airways and therefore may not be involved in antigen capture here (Kim *et al*. 2011). M cells harboured the most spores in the NALT and other research has demonstrated that M cells in the NALT are key for the uptake of other bacteria such as Group A *Streptococcus* (Park *et al*. 2003). Neutrophils phagocytosed spores in the lungs and gut but not in the NALT, which may be because the NALT is a lymphoid tissue and not a general portal of entry for pathogens. The NALT is comprised mainly of T-cells, B-cells and APCs beneath the FAE containing M cells and therefore it could be less likely that granulocytes will arrive here (Zanvit *et al*. 2010).

DCs in the lungs were dominant in engulfing spores along with neutrophils and may be indicative that in the lungs, DCs are known to extend their dendrites past the epithelial walls to sample the environment (Hasenberg *et al*. 2013). Therefore, it is expected that they would have a major role in antigen sampling of spores. Macrophages in the lungs have been hypothesised to be non-motile and have more of a regulatory role rather than phagocytic, and that bacterial clearance is dependent on neutrophils moving through the lung tissue (Hasenberg *et al*. 2013). M cells have been presented as a portal of entry for MTB in the lungs (Teitelbaum *et al*. 1999) but in this study, low numbers of spores were found in M cells. This could be due to the lung having less epithelial cells than the other tissues and therefore less specialised epithelial M

cells. An alternative hypothesis is that there could be a difference between M cells in the lungs and the receptors they have as it has been reported that M cells in Peyer's patches have a GP-2 (glycoprotein-2) receptor for FimH bacteria that is not found on villus M cells (Kim *et al*. 2011) and therefore there could be other receptors that affect M cell uptake that are tissue specific.

Although DCs are known to sample the gut lumen (Rescigno & Di Sabatino 2009), few spores were found in the gut DCs. This could be because the spores were non-pathogenic and therefore did not activate danger signals to stimulate DCs. Macrophages in the colon have also been reported to be regulatory and produce IL-10 (Hasenberg *et al*. 2013; Barnes & Powrie 2009) which could explain why little phagocytosis by macrophages was observed here. M cells were one of the dominant populations that engulfed spores in the gut and they are well known to sample antigens here and provide entry for some pathogens (Man *et al*. 2004).

4.3.5. M cells

M cells are a target in mucosal vaccine research, and there is a drive to increase the uptake by M cells through various mechanisms, so that the antigens have increased contact with immune cells. For example, by targeting the endocytosis receptor Claudin 4 found on M cells using *C. perfringens* enterotoxin, uptake of haemagglutanin antigen was increased and IgG and IgA in the serum, BAL and faeces were increased compared to antigen alone (Lo *et al*. 2012). It was previously presented that M cells transport *B. subtilis* in the appendix of rabbits (Rhee *et al*. 2004), and in the lung are able to transport MTB in mice (Teitelbaum *et al*. 1999). *B. anthracis* has also been investigated *in vitro* and it was discovered that adherence and translocation was higher in the

M cells in comparison to intestinal cell line Caco-2 cells and therefore suggests further that *Bacillus* species may use M cells to enter tissues (Tonry *et al*. 2013). Here, it was demonstrated that M cells were able to transport live spores in the gut, lung and NALT of the mouse but had a more major role in transport in the NALT and gut. This is important because the gut is exposed to many foreign antigens so confirming that spores are taken up by M cells increases the likelihood of generating immune responses in the gut after both nasal and oral dosing.

4.3.6. Comparison of live and autoclaved spores

A greater quantity of live spores were seen in the gut after intranasal dosing whereas it would have been predicted that oral dosing would deliver most spores to the gut. There are a number of potential reasons for this; i) the spores administered to the gut was in a larger volume of solution, which may have passed rapidly through the gut with little opportunity for spores to dissociate from the liquid into the gut cells. Nasal dosing however, would likely have been more aerosolised and particulate, therefore spores may have passed through the gut more easily and been able to interact with the host cells better, ii) the stomach environment is known to contain germinants (Paidhungat & Setlow 2001) so spores could have germinated and therefore would not have been observed using anti-spore antibody, iii) in previous studies, the oral dose used to immunise mice was $5x10^{10}$ spores (Permpoonpattana *et al*. 2011), which is more than one log higher than that used here, so it could mean that at a higher dose, more spores would be able to cross the epithelium. A lower dose was used here to be able to make a direct comparison between the oral, nasal and sublingual dosing routes, iv) also to be taken into consideration is that transit through the gut of the mouse is thought to be around 3h (Huang, La Ragione, *et*

al. 2008) so the highest amount of uptake may have been missed and looking at other time points in the future could be useful.

A greater number of spores were seen in the gut after oral delivery of autoclaved spores in comparison to live spores. This could be because the live spores germinated and so were not detectable using the anti-spore antibody. This could mean that for practical use as an oral vaccine, autoclaved spores may be better than live spores because more spores were able to enter the tissue, and would be able to present antigens to the immune cells. Another strategy that has been pioneered by iGEM in Munich is to use a technology called 'germinationSTOP', which inactivated germination genes and also had a suicide switch incorporated into the genome. This meant that spores were unable to germinate, but to ensure that only spores were present, if germination occurred the suicide switch would kill the bacterium. The technology in this case was used to display a laccase enzyme on the surface to degrade pollutants (Mascher *et al*. 2012). This strategy would have the advantage of prolonging antigen delivery because the bacteria would stay in the spore form, and would still be able to interact with cell receptors because the surface proteins would not be damaged. Another strategy for improving longevity of antigen presentation using live spores is discussed by Hinc *et al*, where as well as surface display of UreA, the antigen was also incorporated into the genome under germination transcriptional control so the gene would be expressed by the vegetative cell, therefore lengthening the time of antigen exposure (Hinc *et al*. 2010).

Perkins *et al* studied the changes to *B. subtilis* after autoclaving and showed using electron microscopy, that the surface of the spores had a wrinkled

appearance (Perkins *et al*. 2004). They hypothesised that the spores burst during the autoclaving process so the contents were released and therefore the spores afterwards had a smaller volume and the surface was wrinkled. They also showed general differences in protein composition of whole autoclaved spores using Fourier Transform Infrared Reflectance (FT-IR) spectroscopy (Perkins *et al*. 2004). In this study, using light microscopy, a size change could also be detected and the alteration in phase-bright could be due to the lack of internal material. Damage to the coat proteins was also observed in this study because CotB and CotC could not be detected using Western blotting. It has been shown that the surface properties of nanoparticles can affect the mechanism by which they enter cells (Krishnendu Saha 2013) so it could be possible that the surface changes in the spores after autoclaving cause a difference in the way the spores enter cells. Work by Sirec *et al* also may support this theory as they tested the ability of different environmental *Bacillus subtilis* spores to bind antigen and found that they had different hydrophobicity that affected their ability to bind antigen (Sirec *et al*. 2014). Therefore, autoclaved spores would certainly have different surface properties to live spores that could affect their binding capabilities. It was suggested by Huang *et al* that spores that autoclaved spores do not interact with TLR2 or TLR4, but are able to elicit immune responses (Huang, La Ragione, *et al*. 2008). Work by Colenutt *et al* also confirmed that TLR2 expression was much reduced with autoclaved spores in comparison to live spores and germinated cells and suggested that the peptidoglycan present in the spore cortex was released when the spore germinated and could interact with TLR2, whereas autoclaved spores could not release the peptidoglycan (Colenutt & Cutting 2014). In this study, the cells that interacted with the spores when they were autoclaved

differed to live spores, which support the suggestion that there could be differences in interactions between cells and spores depending on their state.

Using immunofluorescence, the distribution of live and autoclaved spores in the lungs was quite different. The live spores were predominately identified around the airways and scattered through the tissue. This data is similar to that reported by Jenkins *et al* with *B. anthracis* spores, that found spores around the alveolar and small airway epithelium (Jenkins & Xu 2013). In contrast, there were many autoclaved spores clustered inside individual round cells. From the flow cytometry analysis, it appears that live spores interact better with neutrophils and M cells in the lungs, but that DCs and macrophages can phagocytose both types of spores. If it is assumed that TLR2 and TLR4 are not involved with interactions with autoclaved spores, there must therefore be other mechanisms by which macrophages and DCs interact with the particles. Handley *et al* demonstrated that DCs do not rely of antigen capture to be able to phagocytose (Handley *et al*. 2005), which may explain why they are able to phagocytose autoclaved spores even though the surface proteins are damaged. Other evidence for this comes from comparing the uptake of latex beads, where the phagocytosis appears to be similar to spores in that they are clustered inside round cells (Byersdorfer & Chaplin 2001). It has been suggested that dendritic cells alternate their shape between dendritic and round, which correlates with their antigen capturing and antigen internalising roles respectively (Handley *et al*. 2005). Macrophages are also round when they are phagocytosing so the cells seen to internalise the autoclaved spores could be DCs and macrophages, which would be consistent with the flow cytometric analysis. It has been shown that macrophages *in vitro* can interact with latex beads and positively and negatively charged beads, which suggests that the

interactions are not due to electrostatic interactions (Seyrantepe *et al*. 2010). This could have been a possibility since *Bacillus* spores have been shown to be hydrophobic (McKenney *et al*. 2013) and proteins can be bound to the surface of spores using electrostatic and hydrophobic interactions (Song *et al*. 2012). There are several other mechanisms by which macrophages can interact with particles as they have many different receptors on the cell surface and uptake mechanisms. Fcγ receptors are involved in recognising opsonised particles (Seyrantepe *et al*. 2010), whereas scavenger receptors (SR) are another type of PRR of which there are several classes that can recognise different types of pathogen and there is also complement activated phagocytosis, where complement proteins deposited on bacteria act as opsonins (DeLoid *et al*. 2009). DeLoid *et al* found that when SRs were blocked, uptake of beads was reduced, but uptake of *S. aureus* was not affected, so the uptake of different particles and pathogens is complex and variable (DeLoid *et al*. 2009). Further investigation into the interactions of live spores compared to autoclaved spores, using *in vitro* methods and blocking different pathways could be investigated. Microparticles are of interest in the adjuvant field and it has been demonstrated that particles of 1-10μM are preferentially taken up by macrophages and dendritic cells so therefore spores would the right size at 1μM for phagocytosis for these cells (Hafner *et al*. 2011).

The mechanisms by which M cells and neutrophils phagocytose particles are different to macrophages and DCs and may explain why their ability to phagocytose autoclaved spores was poor in comparison to live spores. M cells use glycoconjugates to bind to microorganisms and have a variety of types that bind to a wide variety of different microbial peptides (Man *et al*. 2004). Because autoclaved spores will have damaged proteins on the surface, the

glycoconjugates may not bind as efficiently, leading to a reduction in uptake. TLR4 and α5β1 integrin was also found to be expressed more on M cells than other intestinal epithelial cells in the gut and when TLR4 and α5β1 integrin were blocked, uptake of *Haemophilus influenzae* was reduced (Tyrer *et al*. 2006). *H. influenzae* that was mutated to change the LPS structure showed a decrease in uptake, indicating that M cells are dependent on PAMPs for engulfing bacteria (Tyrer *et al*. 2006). Therefore the change in the surface of autoclaved spores may have altered their interactions with M cells. Neutrophils have opsonin dependent and independent mechanisms of uptake, similar to macrophages and dendritic cells and also have PRRs. In a study by Heinzelmann *et al*, the kinetics of uptake of fast growing *S. aureus* with slow growing *K. pneumoniae* was compared and uptake was found to be slower with *K. pneumonia* (Heinzelmann *et al*. 1999). So perhaps in the case of autoclaved *B. subtilis*, since they are inactive, the uptake by neutrophils may be decreased. There is also evidence that neutrophils recognise bacteria by sugar residues (Doolittle *et al*. 1983), therefore autoclaved spores that have damaged surface proteins and sugars, may be less well recognised and phagocytosed.

4.4. Conclusions

In this chapter, the distribution of spores in the lungs, gut and NALT after nasal, oral and sublingual immunisation using HU58 spores was investigated and it was found that nasal dosing distributes spores to all three tissues and that spores can cross epithelial barriers and enter the tissues. Live and autoclaved spores behaved similarly initially, but autoclaved spores were cleared faster from the lungs, and were at higher numbers in the gut, which is probably because they were unable to germinate. Further work could be carried out to directly compare adaptive immune responses stimulated by spores downstream

of nasal, oral and sublingual immunisation, similar to work by Cuburu *et al*, who used Ovalbumin (OVA) with cholera toxin adjuvant and saw that antibody responses were highest after sublingual and nasal dosing in comparison to oral (Cuburu *et al*. 2007).

The types of cells involved with uptake also varied according to the dosing route, and by the tissue involved. After immunisation with live spores, all types of cells were involved in phagocytosis in the lungs, with DCs and neutrophils dominating, whereas in the gut, M cells and neutrophils harboured the most spores and in the NALT, M cells were dominant. After dosing with autoclaved spores, DCs and macrophages have the highest number of spores in the lungs, DCs in the gut and all cells in the NALT, albeit at very low levels.

These results demonstrate that the spores enter the tissue and interact with cells that should lead to the generation of adaptive immune responses and may have implications for choosing which immunisation route to use with spores as a vaccine adjuvant. Whether the differences in the interactions between autoclaved spores with M cells, neutrophils, macrophages and DCs is due to surface changes or their lack of ability to germinate cannot be fully discerned in this project and further work could be done to look at the surface properties of autoclaved spores and their interactions with cells.

Chapter 5: Innate Immune Responses to Spores after Intranasal Dosing

5.1. *Introduction*

The innate immune response is becoming an increasingly important consideration in the development of mucosal vaccines because activation of innate immunity can directly influence the adaptive immune response (Neutra & Kozlowski 2006). Nasal dosing has been demonstrated to be able to elicit systemic immune responses that are comparable to injectable vaccines, as well as stimulating mucosal responses (Czerkinsky *et al*. 2011). This route therefore shows promise as a vaccination route since protection can be induced at the site of potential infection as well as generating circulating antibodies.

BALB/c mice (n=30) were dosed intranasally with $2x10^9$ HU58 spores and n=5 mice were culled on days zero, one, two, three, four and seven. On each day, the numbers of NK cells, macrophages, DCs and neutrophils, as wells as TLR2 and TLR4 expression were monitored in the lungs, gut, spleen and peripheral lymphoid tissues. Splenocytes and NALT tissue were incubated for 48h after removal and the supernatants used to measure cytokine production. Serum was also taken to measured complement activation.

The cell populations examined were the professional phagocytes; neutrophils, macrophages, DCs and NK cells that directly kill infected cells. Macrophages and DCs are particularly important because of their role as APCs, as they bridge the gap between the innate and adaptive immune responses. The primary role of neutrophils and NK cells is to eradicate pathogens (Dempsey *et*

al. 2003). NK cells also produce cytokines including IFNγ that stimulate other immune cells, such as macrophages (Welsh & Waggoner 2013). The information generated from the results from this chapter also implied how long it took for the spores to be cleared and the immune system to return to normal. The spores used in this chapter are inherently non-pathogenic, but if a large and protracted immune response were generated, this might generate inflammation and tissue damage, which would not be advantageous for a vaccine. The variations in cell numbers in the spleen provided information on whether nasal dosing of spores generated systemic immune responses and population changes in the lymphoid tissues provided evidence of activation of the adaptive immune response.

TLRs are expressed on many cell types including DCs, macrophages, monocytes, B-cells, T-cells, Tregs and granulocytes among others (Dembic 2000). TLR2 responds to ligands such as lipopeptides and peptidoglycan that are generally found on Gram-positive bacteria and TLR4 is activated by substances such as LPS, which are typical of Gram-negative bacteria (Christmas 2010). However, this classification is general and the ligands they are activated by are not strict for specific pathogen classes and depend on particular molecular interactions. For example, *C. difficile* has been shown to interact with TLR4 even though it is a Gram-positive organism because the surface layer proteins bind to TLR4 (Ryan *et al*. 2011) and MTB interacts with both TLR2 and TLR4 (Sánchez *et al*. 2010). Work by de Souza *et al* demonstrated that TLR2 knockout mice generated less antibody after dosing with *B. subtilis* spores carrying HIV antigens in comparison to wild-type mice (de Souza *et al*. 2014), therefore changes in TLR2 expression would be expected in response to administration of *B. subtilis* spores. However, there could be

ligands on spores that activate TLR4 as well as TLR2 because TLR2 and TLR4 have both been shown to be activated by *B. subtilis* spores and germinating cells *in vitro* (Huang, La Ragione, *et al*. 2008). In this study the changes in TLR receptor expression on cells using flow cytometry was monitored to see whether stimulation was demonstrable *in vivo*. TLR activation is important because the interaction with PAMPs stimulates intracellular pathways that upregulate genes related to inflammation and activation of other immune cells. It has been demonstrated that TLR4 deficient mice were more susceptible and developed more severe disease to *C. difficile* (Ryan *et al*. 2011). Further to this, pre-stimulation of TLR5 with purified *Salmonella* flagellin was able to provide protection against *C. difficile* infection (Jarchum *et al*. 2011).

Cytokines and chemokines are effectors of the immune response and their production in the innate immune response is in part controlled by the TLR stimulation and downstream signalling to transcriptional activators of genes involved in cytokine production (Dempsey *et al*. 2003). A wide variety of cytokines and chemokines are involved in the innate immune response, and the ones monitored in the study were IL-6, IL-10, IL-12p70, IFNγ, TNFα and MCP-1 **(Table 5-1)**. The inflammatory cytokines; IL-6, IFNγ and TNFα are part of the innate and adaptive immune responses and activate macrophages (Murray & Wynn 2011). Inflammation induces migration of other immune cells to the infected area. IL-12p70 is the active heterodimer of IL-12 (Bette *et al*. 1994) and is produced by macrophages and DCs causing naïve T-cells to differentiate to Th1 cells and stimulate further production of IFNγ and TNFα (Kaiko *et al*. 2008). MCP-1 chemokine recruits monocytes, memory lymphocytes and NK cells to sites of inflammation and is primarily produced by monocytes and macrophages (Deshmane *et al*. 2009). IL-10 is important in anti-inflammatory responses and

Table 5-1. Summary table of a selection of immune cells and some of the cytokines they respond to and produce when activated.

Cell type	Activated by	Produces
Neutrophil	TNF, IFNγ, IL-17	TNF
NK cell	IL-12, MCP-1	IFNγ
M1 Macrophage	TNF, IFNγ, MCP-1	TNF, IL-6, MCP-1
M2 Macrophage	IL-10, MCP-1	IL-10
Dendritic cell	MCP-1, IFNγ, IL-10	IL-12, IL-6, IL-33
Epithelial cell	IL-6	TNF, IL-6
Th1	IL-6, IL-10, IL-12	TNF, IFNγ, IL-2
Th2	IL-4, IL-33	IL-5, IL-10
Tc	IFNγ	TNF, IFNγ
Th17	IL-6	IL-17

enhances B-cell lifespans and is produced by M2 macrophages, Th2 cells and Tregs (Mauri & Bosma 2012). These cytokines were monitored over seven days and provided information about the functionality of the immune cells and the type of immune responses stimulated.

Live spores were used in this experiment since the results from Chapter 4 demonstrated that live spores had a more active role in uptake and interacted with a wider range of host immune cells than autoclaved spores. Also, in other studies, the adaptive immune responses have been ascertained to be higher with live rather than inactive spores (de Souza *et al*. 2014; Colenutt & Cutting 2014). Therefore, using live spores should maximise the chances of detecting any changes in immune responses.

5.1.1. Aims

The primary aim of this chapter was to monitor the immune responses of mice after nasal dosing with spores. This provided information about how the spores acted as an immune-potentiator class of adjuvant, as well as a delivery vehicle when administered mucosally, which could affect the subsequent protective adaptive immune response. The second aim of monitoring the innate immune response was to explore their potential use for prophylaxis against certain infections, primarily respiratory diseases. This hypothesis is based on the work by Song *et al* that demonstrated that mice dosed with PY79 wild-type *B. subtilis* spores were able to provide protection against influenza infection (Song *et al*. 2012). Following this experiment and monitoring the changes in immune cells, a time after dosing was chosen to infect the mice with multi-drug resistant MTB (MDR-TB) to determine whether as a therapy, autoclaved spores were able to reduce infection.

5.2. Results

5.2.1. Changes in cell populations in the lungs

The lungs are, predictably, the main site where spores were delivered following nasal dosing as discussed in Chapter 4, and it is here that we would expect to see the highest level of immunological activity. The NK cell population decreased during the seven day study period **(Figure 5-1)**. The neutrophil population increased from day one to four, and declined at day seven. Neutrophils are vital in the acute phase of infections for bacterial clearance and their increase in numbers suggested that there was production of cytokines and chemokines that were attracting neutrophils to the site of infection. The decrease at day seven suggests that the spores had been mainly cleared from the lungs **(Figure 5-1)**. The DCs increased steadily from day two to seven **(Figure 5-1)**. DCs have an important role in phagocytosis and in presenting antigens to T-cells and it appeared that they were stimulated to proliferate or were attracted from other areas by the presence of spores. M1 macrophages showed a small increase at day four post-vaccination, and M2 macrophages show no change, suggesting that macrophages were not primarily involved with phagocytosis of spores in the lungs **(Figure 5-1)**.

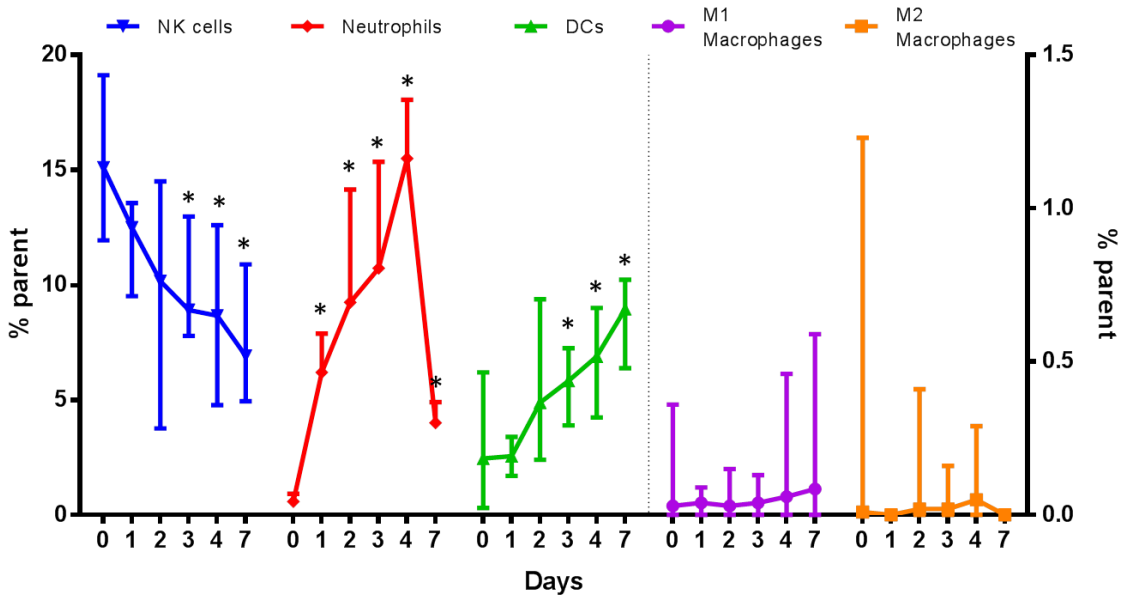

Figure 5-1. Populations of different cell types in the lungs of mice over seven days after intranasal dosing with HU58 spores ($2x10^9$). BALB/c mice (n=6-9) were dosed intranasally with $2x10^9$ HU58 spores and culled on days 0, 1, 2, 3, 4 and 7. The lungs were homogenised as described in the methods (Section 2.21) cells were stained; NK cells (CD49b-PE), neutrophils (Ly6G-APC), DCs (CD11c-APC$^+$, F4/80-PerCP$^-$), M1 (CD11c-APC$^+$, F4/80-PerCP$^+$) and M2 (CD11c-APC$^-$, F4/80-PerCP$^+$) macrophages. Median of the percentage of the population expressing each marker with interquartile range displayed. Left of the black dashed line indicates measured against left axis, right side corresponds to right axis. Mann-Whitney was used to compared each time point to day zero. Asterisks p=<0.05.

5.2.2. Changes in cell populations in the spleen

The spleen is an indicator of the systemic immune response and is important because after immunisation, APCs move to the lymph nodes and spleen as well as secondary lymphoid organs to generate adaptive immune responses. The NK cells increased in general, up to day seven suggesting that they had been activated **(Figure 5-2)** and there was a small increase in neutrophils. NK cells have a role in the lymph nodes whereby they can stimulate DC maturation and affect T-cell differentiation. The DCs increased from day two to four and started decreasing at day seven **(Figure 5-2)**. This suggests that they had been activated and could be stimulating an adaptive response. There was a small increase in M1 macrophages from day two to four so some inflammatory response appears to have been initiated here because M1 macrophages are characteristic of inflammation and produce inflammatory cytokines, and macrophages can also act as APCs to activate T-cells. Macrophages are generally tissue resident so the increase here could be due to differentiation of progenitor cells rather than migration. There was no observable change in the M2 macrophage population **(Figure 5-2)**.

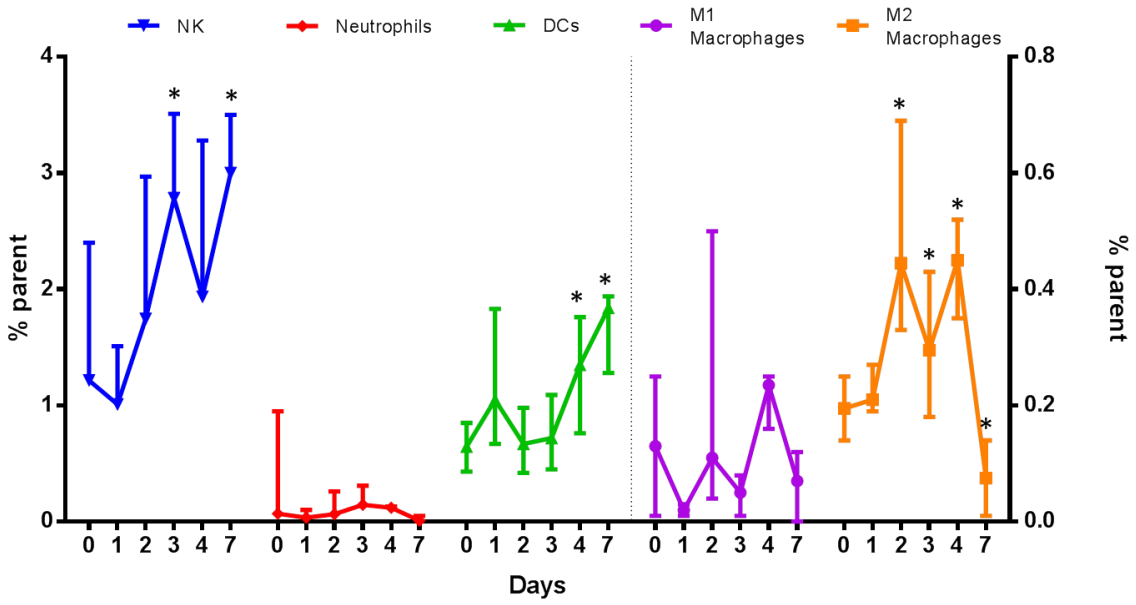

Figure 5-2. Populations of different cell types in the spleen of mice over seven days after intranasal dosing with HU58 spores ($2x10^9$). BALB/c mice (n=6) were dosed intranasally with $2x10^9$ HU58 spores and culled on days 0, 1, 2, 3, 4 and 7. The spleens were homogenised as described in the methods (Section 2.20) cells were stained; NK cells (CD49b-PE), neutrophils (Ly6G-APC), DCs (CD11c-APC$^+$, F4/80-PerCP$^-$), M1 (CD11c-APC$^+$, F4/80-PerCP$^+$) and M2 (CD11c-APC$^-$, F4/80-PerCP$^+$) macrophages. Median of the percentage of the population expressing each marker with interquartile range displayed. Left of the black dashed line indicates measured against left axis, right side corresponds to right axis. Mann-Whitney was used to compared each time point to day zero. Asterisks p=<0.05.

5.2.3. Changes in cell populations in the gut

As discussed in Chapter 4, spores when delivered nasally disperse in the gut. There was a general decrease in NK cells in the gut, suggesting there was no pro-inflammatory response **(Figure 5-3)**. In the neutrophil, DC and macrophage populations, there was an initial decrease, followed by an increase at day three **(Figure 5-3)**. These results confirm those of Chapter 4, that these cells are all involved in the phagocytosis and removal of spores. The increase in APCs suggests that here as well as in the lungs, T-cell activation may take place and homing to the gut could occur. All three populations decrease by day seven so the response is short-lived and it appears that the spores are rapidly cleared from the gut.

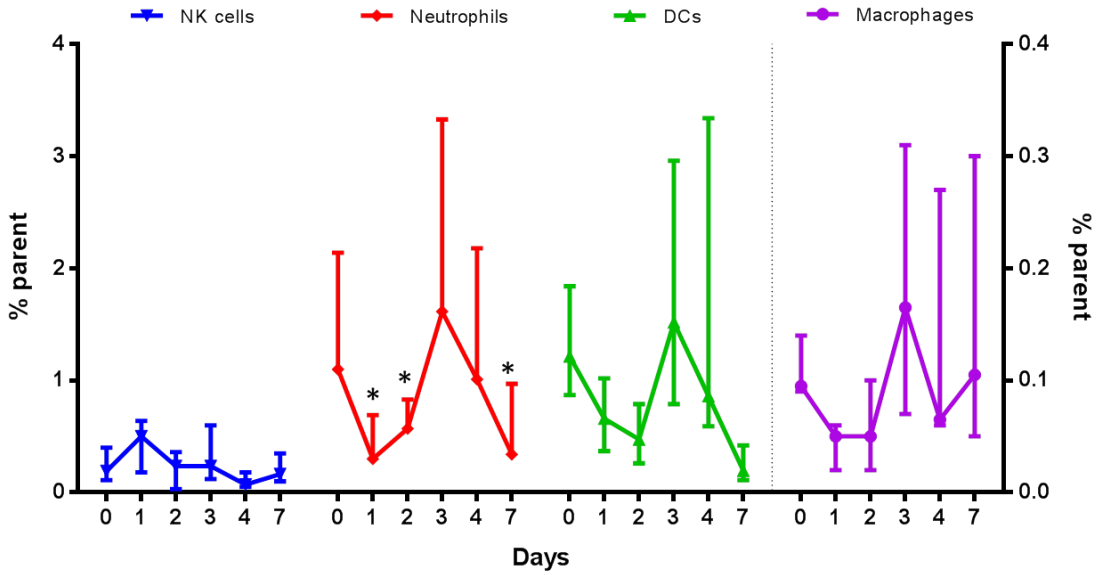

Figure 5-3. Populations of different cell types and in the gut of mice over seven days after intranasal dosing with HU58 spores ($2x10^9$). BALB/c mice (n=6-9) were dosed intranasally with $2x10^9$ HU58 spores and culled on days 0, 1, 2, 3, 4 and 7. The gut was homogenised as described in the methods (Section 2.21) cells were stained; NK cells (CD49b-PE), neutrophils (Ly6G-APC), DCs (CD11c-APC$^+$, F4/80-PerCP$^-$), M1 (CD11c-APC$^+$, F4/80-PerCP$^+$) and M2 (CD11c-APC$^-$, F4/80-PerCP$^+$) macrophages. Median of the percentage of the population expressing each marker with interquartile range displayed. Mann-Whitney was used to compared each time point to day zero. Asterisks p=<0.05.

5.2.4. Cell population changes in the peripheral lymph nodes

After phagocytosis of the pathogens, DCs travel to lymph nodes to prime and activate T-cells and initiate the adaptive immune response. At days four and seven there was an increase in DCs, which could be an indication that the adaptive immune response was stimulated **(Figure 5-4)**. There was a general increase in NK cells over the seven days, and NK cells could promote DC maturation and T-cell differentiation. Therefore, there appears to be some evidence that T-cell and B-cell activation could be occurring here. There is little change in neutrophil and M1 populations **(Figure 5-4)**. Finally, there was a small increase in M2 macrophages at day two to four **(Figure 5-4)**, where they could play a role in reducing inflammation.

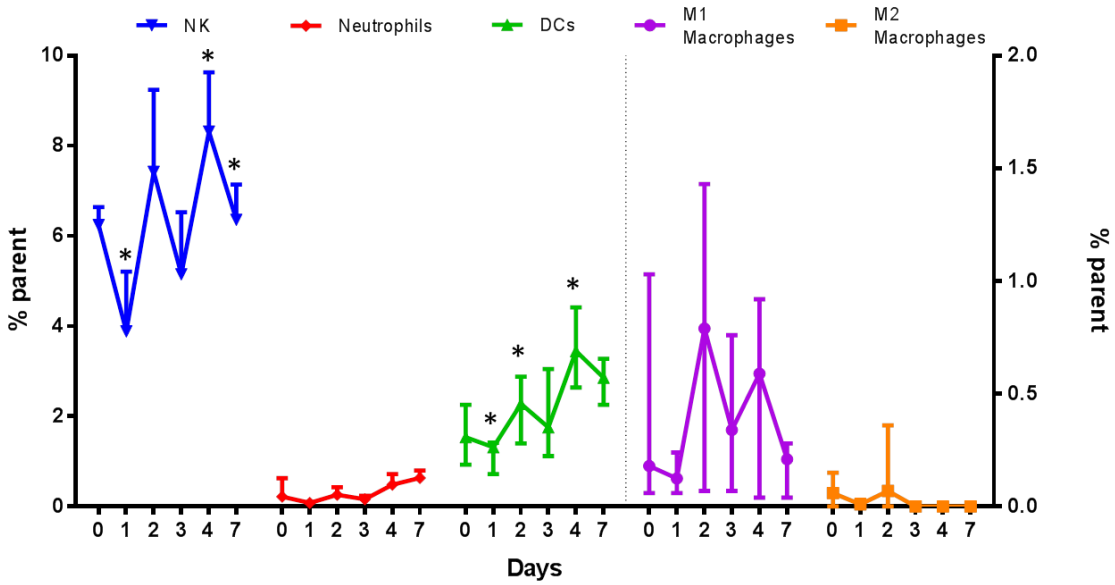

Figure 5-4. Populations of different cell types in the lymph nodes of mice over seven days after intranasal dosing with HU58 spores ($2x10^9$). BALB/c mice (n=6) were dosed intranasally with $2x10^9$ HU58 spores and culled on days 0, 1, 2, 3, 4 and 7. The peripheral lymph nodes were homogenised as described in the methods (Section 2.20) cells were stained; NK cells (CD49b-PE), neutrophils (Ly6G-APC), DCs (CD11c-APC^+, F4/80-$PerCP^-$), M1 (CD11c-APC^+, F4/80-$PerCP^+$) and M2 (CD11c-APC^-, F4/80-$PerCP^+$) macrophages. Median of the percentage of the population expressing each marker with interquartile range displayed. Mann-Whitney was used to compare each time point to day zero. Asterisks p=<0.05.

5.2.5. TLR expression

Expression of TLR2 in the lungs increased from day one, peaked at day three and remained high for the duration of the experiment **(Figure 5-6)**. TLR4 expression was lower than TLR2 for the entire time course **(Figure 5-6)**. In the spleen, both TLRs were at lower levels than in the lungs, but there was a small increase in TLR2 at day one **(Figure 5-6)**. TLR expression was not expected to be high in the spleen because it is not the site of entry of the spores after nasal dosing. In the peripheral lymph nodes, TLR2 and TLR4 levels were both increased at day three, but TLR4 was higher. This may indicate that some bacteria had travelled to the lymph nodes, and may have led to the increase in DCs seen at day four to seven **(Figure 5-5)**. There was a peak in TLR2 expression at day one in the gut, and TLR4 at day three. The levels decreased quickly and were not as high as in the gut in comparison to the lungs, which could suggest that bacteria already present in the gut were causing tolerance, even though there was a transient increase in neutrophil, macrophage and DC populations, these could have been activated by mechanisms other than TLRs.

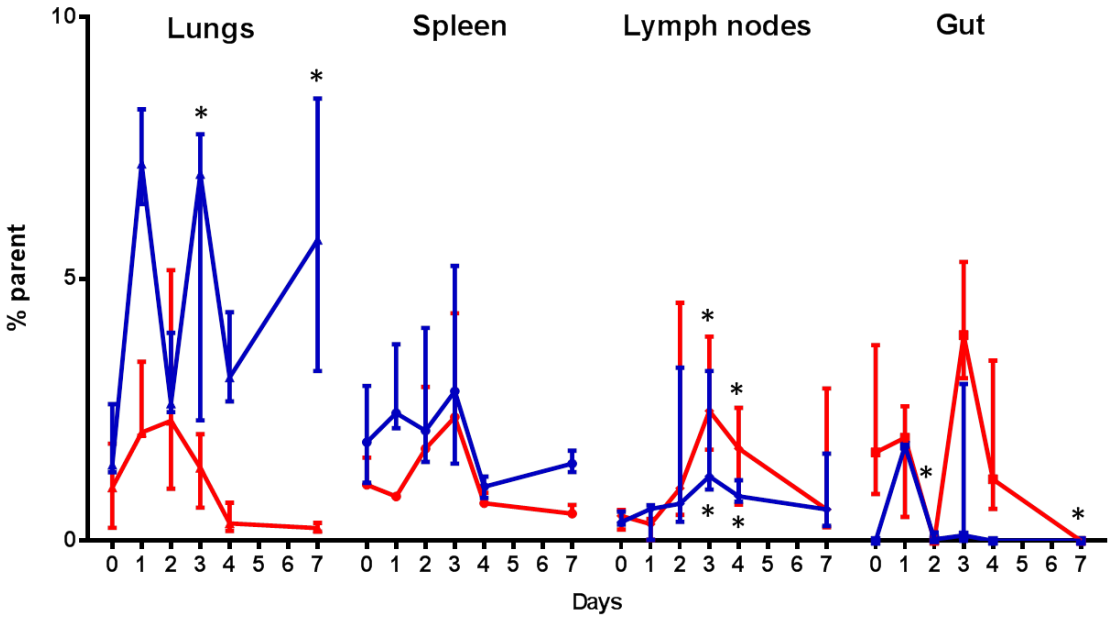

Figure 5-5. Expression of TLR2 and TLR4 in cells from the lung, spleen, peripheral lymph nodes and gut from mice immunised nasally with 2x10^9 HU58 spores. BALB/c mice (n=6) were dosed intranasally with 2x10^9 HU58 spores and culled on days 0, 1, 2, 3, 4 and 7. The lungs, spleen, peripheral lymph nodes and gut were homogenised as described in the methods (Section 2.20 and 2.21) cells were stained; TLR2 (CD282-PE) (blue), TLR4 (CD284-APC) (red). Median of the percentage of the population expressing each marker with interquartile range displayed. Mann-Whitney was used to compare each time point to day zero. Asterisks p=<0.05.

5.2.6. Cytokine production in splenocyte supernatants

Cytokines produced by isolated splenocytes give an indication of the effector functions of the systemic immune response. MCP-1 is a chemoattractant, which recruits immune cells to the organ that is infected/inflamed and is the first indicator of a systemic immune response in the spleen so this cytokine may be partly responsible for the influx of DCs and NK cells to the spleen **(Figure 5-7)**. The proinflammatory cytokines IL-6, TNF and IFNγ increased at day seven. TNF and IFNγ production suggest that the Th1 response had been activated but there was a small increase in IFNγ and TNF before this at day two to three, which could be attributed to NK cells as they increased at this time **(Figure 5-2)**. IL-10 also increased at day seven, which could counteract the proinflammatory cytokines and minimise tissue damage. Although the numbers of DCs increased in the spleen, IL-12p70 did not increase, which would be expected because IL-12p70 is characteristically produced by activated DCs to stimulate differentiation of naïve T-cells to Th1 cells.

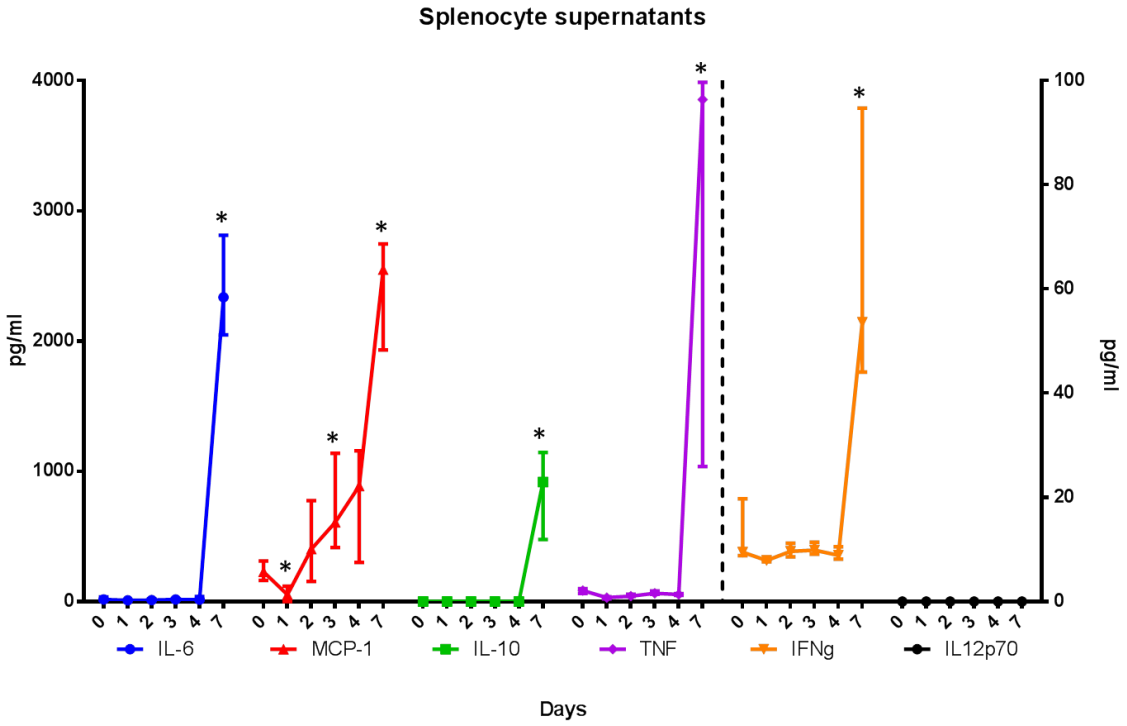

Figure 5-6. Cytokine production from splenocytes isolated from mice immunised with $2x10^9$ HU58 spores. BALB/c mice (n=5) were dosed intranasally with $2x10^9$ HU58 spores and culled on days 0, 1, 2, 3, 4 and 7. Splenocytes were isolated and $5x10^5$ cells were cultured for 48h at 37°C and supernatants collected to measure cytokines using the cytokine bead array on the flow cytometer. Data shown shows the median pg/ml and interquartile range. Left of the black dashed line indicates measured against left axis, right side corresponds to right axis. Mann-Whitney was used to compare each time point to day zero. Asterisks p=<0.05.

5.2.7. Cytokine production in the NALT

Measuring cytokine production in the NALT is way of measuring the immune responses in the nasopharynx, which is where the aim is to generate protective immune responses. IL-6 is a proinflammatory cytokine associated with infection and tissue damage. The levels of this cytokine are high throughout the time course, which suggested that this cytokine was produced due to the tissue damage incurred when removing the NALT **(Figure 5-8)**. MCP-1 increased at day one, but remained above baseline levels until day four and this chemoattractant protein may play a role in attracting immune cells including DCs, macrophages and NK cells to the area. The characteristic Th1 cytokines TNF and IFNγ increased at day one and day four. TNF and IFNγ were both produced by NK cells, macrophages and Th1 cells suggesting a localised proinflammatory reaction. There was also a decrease in these cytokines at day seven, so T-cells may not be activated in the NALT, but could indicate that activated cells have migrated from the NALT.

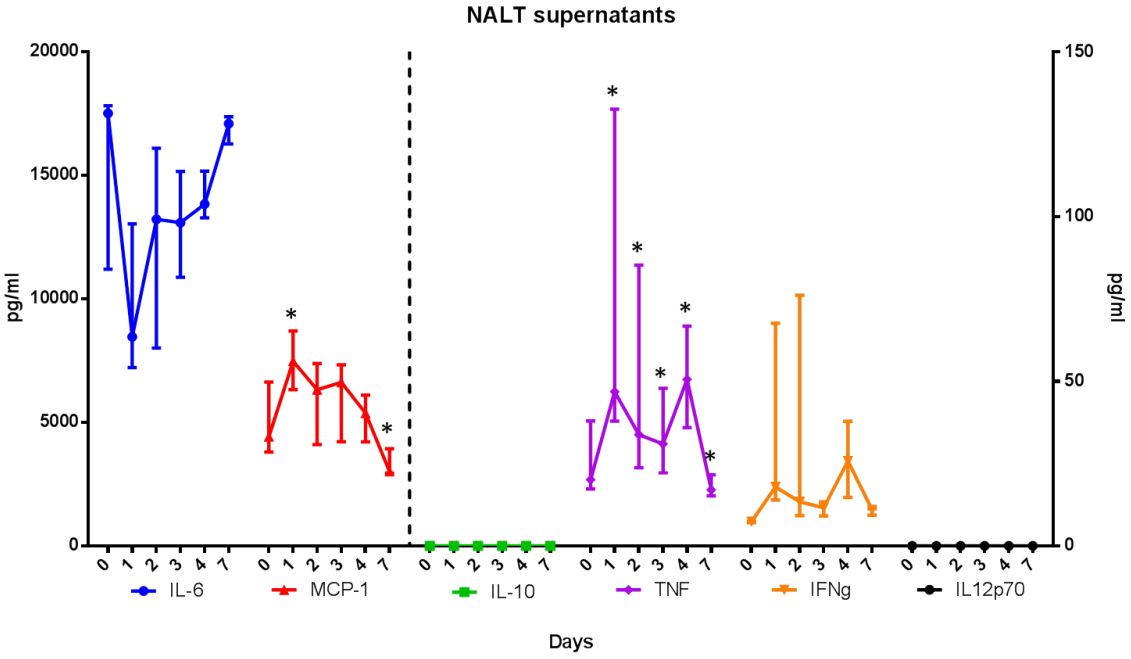

Figure 5-7. Cytokine production from NALT tissue isolated from mice immunised with 2x10^9 HU58 spores. BALB/c mice (n=5) were dosed intranasally with 2x10^9 HU58 spores and culled on days 0, 1, 2, 3, 4 and 7..NALT tissue was cultured for 48h at 37°C and supernatants collected to measure cytokines using the cytokine bead array on the flow cytometer. Data shown shows the median pg/ml and interquartile range. Left of the black dashed line indicates measured against left axis, right side corresponds to right axis. Mann-Whitney was used to compare each time point to day zero. Asterisks p=<0.05.

5.2.8. Complement killing assay

On each day after intranasal dosing with $2x10^9$ HU58 spores, serum was taken from terminal heart bleeds. Serum from two mice from each time point used in a complement killing assay, where sera was incubated with spores and after 90 min was plated out onto agar. Viable count was used to calculate percentage viability from a control sample that had no sera and therefore no complement mediated death. From the viable count results, complement in the sera appeared to be activated at day one and two **(Figure 5-10)**. The assay needs repeating with more samples for serious conclusions to be drawn from the data.

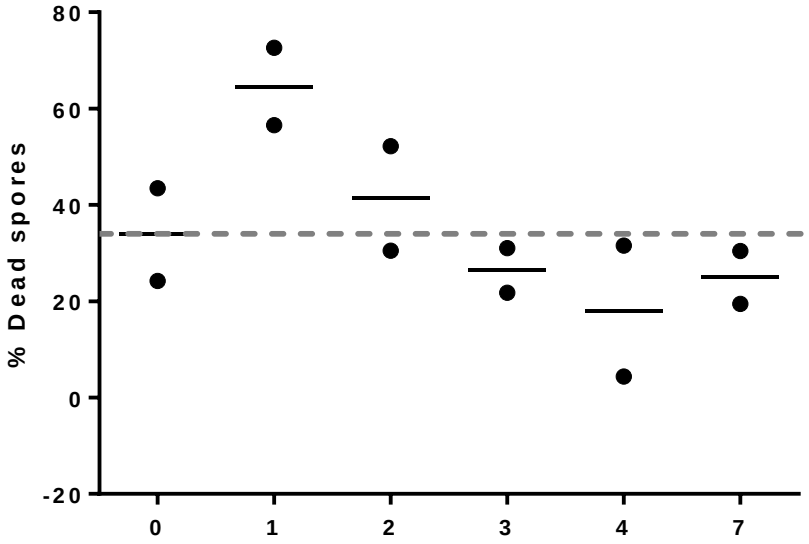

Figure 5-8. Percentage of dead spores when spores were incubated with serum from two mice dosed with HU58 spores ($2x10^9$) intranasally as measured using viable count. BALB/c mice were immunised intranasally with $2x10^9$ HU8 spores and n=5 were culled on days 0, 1, 2, 3, 4 and 7 and serum taken by terminal heart bleeds. $1x10^6$ spores were incubated with 20µl of sera from mice from each time point and incubated at 37°C for 90 min. Spores were then serially diluted and plated out onto DSM agar plates and incubated at 37°C overnight and the viable count calculated. % of dead spores was calculated by number of colonies in sample with sera/number of colonies in sample without sera x 100. Dashed line indicates the baseline level of complement activation in naïve mice (Day 0).

5.2.10. Challenge with MDR-TB

BALB/c mice (n=10) were challenged with MDR-TB three days after nasal administration of autoclaved HU58 spores because an increase in DCs and neutrophils were seen in the lungs in the previous experiment **(Figure 5-1)**. The work was carried out by Gil Reynolds Diogo and Dr Rajko Reljic at SGUL, who also tested the IL-4D2 cytokine, and IL-4D2 with HU58 spores together. After challenge, the mice were given three further doses over the course of seven days, and four weeks after treatment, the mice were culled and the lungs plated out on 7H11 agar plates to examine bacterial burden **(Figure 5-9)**. The results showed that autoclaved HU58 spores alone had little effect on bacterial burden in comparison to PBS **(Figure 5-10)**.

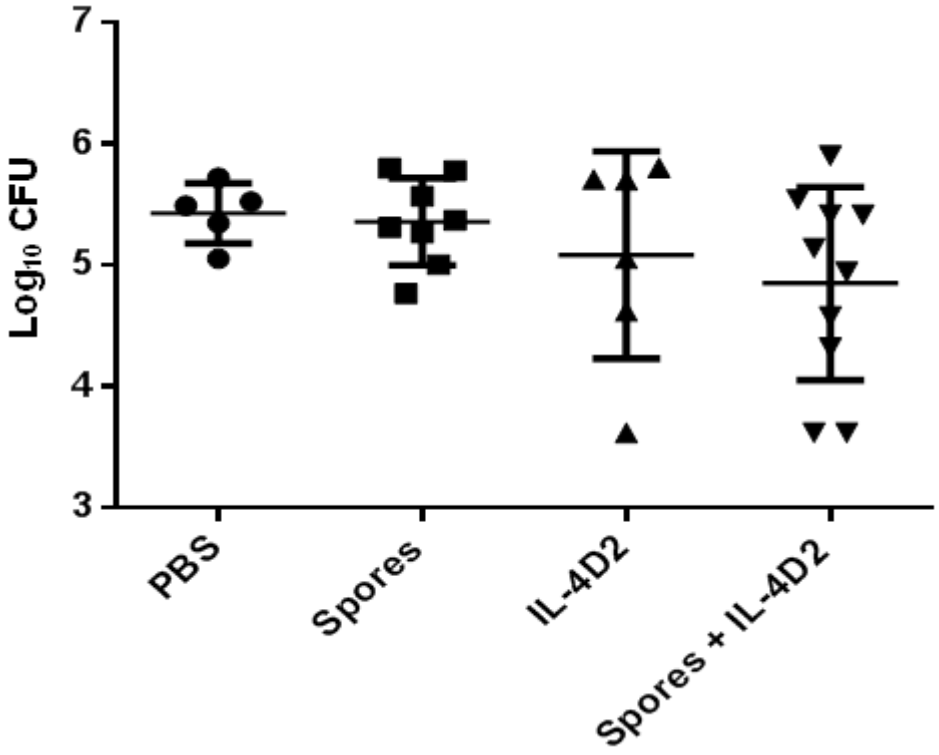

Figure 5-9. CFU of MDR-TB in the lungs of mice treated three days prior to infection and 7 days post-infection with either $2x10^9$ autoclaved HU58 spores, IL-4D2 or both agents. BALB/c mice (n=10/group) were dosed intranasally with either $2x10^9$ autoclaved HU58 spores, IL-4D2 or both agents. Three days later, they were challenged with MDR-TB ($5x10^5$ CFU) and received four further doses of $2x10^9$ autoclaved HU58 spores, IL-4D2 or both agents. Four weeks following infection, the mice were culled and the lungs were homogenised and plated out onto 7H11 agar plates and incubated at 37°C for 8 weeks to examine bacterial burden. ANOVA used to compare groups. Those mice that had no recoverable MTB were removed from analysis because they may not have been successfully challenged with MTB.

5.3. ***Discussion***

Generation of an innate immune response has been shown to be important in vaccine development. Vaccine adjuvants that work as immune-potentiators, such as attenuated pathogens or killed pathogens, that activate the immune response via TLR activation, have been shown to be effective adjuvants. Some vaccines have TLR agonists added to improve their performance. For example, Monophosphoryl Lipid A (MPL), which is a TLR4 agonist has been included in Human Papillomavirus (HPV) vaccines that also contain Alum and has improved vaccine immunogenicity ('Cervarix') (Rappuoli *et al*. 2013).

5.3.1. Responses in mucosal tissues

In this study, TLR2 expression was increased in the lung, as this was the site of delivery of the spores following nasal dosing. The data implies that ligands on *B. subtilis* interact with TLR2 more dominantly than TLR4, which is in contradiction to the *in vitro* work by Huang *et al* that suggested that TLR2 and TLR4 were activated equally (Huang, La Ragione, *et al*. 2008). However, this could be due to the lung environment as there was some expression of TLR4 detected in the lymph nodes and gut. In MTB infection, is has been shown that TLRs are important for protection, as MyD88, TLR2, TLR4 and TLR9 knock-out mice are far more susceptible to MTB infection, which is hypothesised to be due to a deficiency in stimulation of macrophage effector mechanisms (Korbel *et al*. 2008). Therefore, stimulating proliferation of TLR2 expressing cells could be an advantage against pathogens including MTB.

The main populations that altered in the lungs were neutrophils and DCs. DCs phagocytosed live HU58 spores in the lungs and this data agrees with that from Shreton-Rama *et al* that demonstrated phagocytosis of *B. anthracis* spores by DCs (Shetron-Rama *et al*. 2010), therefore there may be a common element

between these *Bacillus* species that stimulates uptake by DCs. In relation to TB, the innate immune response is important for controlling disease and formation of the granuloma. MTB is phagocytosed by macrophages and DCs, DCs produce IL-12, which stimulate NK cells and Th1 cells to produce IFNγ which activates the phagocytic activity of macrophages (Andersen & Woodworth 2014). In this study, demonstrating phagocytosis of *B. subtilis* spores by DCs and proliferation of DCs in the lungs could imply that this is a relevant immune response that could protect against TB infection. DC stimulation and maturation also increases the presentation of antigens to T-cells; therefore spores carrying TB antigens should be able to generate memory cells.

Neutrophils appear to be involved in clearing *B. subtilis* from the lungs and their decrease at day seven probably correlates with the complete clearance of spores. This hypothesis is supported by work from Jenkins *et al*, who compared the persistence of *B. subtilis* and *B. anthracis* after inhalation, to discover whether the persistence of *B. anthracis* for weeks/months was due to the spore in general, or something specific to *B. anthracis*. They found that *B. subtilis* spores did not persist and could not be detected in tissues after two weeks and hypothesised that some component of the exosporium of *B. anthracis* was responsible for its persistence (Jenkins & Xu 2013). Therefore it was expected that *B. subtilis* spores would be cleared as implied here. Neutrophils have been implicated in the killing of *B. anthracis* because it is hypothesised that cutaneous *B. anthracis* infection is less lethal than inhalation or ingestion because more neutrophils are present in the skin than in the lung and gut (Mayer-Scholl *et al*. 2005). In the lungs, neutrophils have been demonstrated to be recruited after *B. anthracis* infection and that IL-17 knock-out mice, were more susceptible to infection because IL-17 recruits neutrophils (Garraud *et al*.

2012). Anthrax toxins however reduce recruitment and neutrophil priming (Wright 1986) so once *B. anthracis* has germinated it can evade killing by neutrophils. Therefore, it is unsurprising that *B. subtilis* spores induce neutrophil recruitment because they are related to *B. anthracis*, but as they are non-pathogenic and do not produce toxins; the neutrophils persist until the spores are removed. An explanation for the decrease seen of NK cells could be that neutrophils are thought to interact with NK cells to inhibit their proliferation but promote their cytotoxic activity and therefore the increase in neutrophils may have inhibited NK cells (Costantini & Cassatella 2011).

In the case of TB, DCs that acquire antigens via phagocytosis of infected neutrophils are considered to be more effective at activating T-cells in comparison to those that phagocytose MTB directly. Neutrophils are known to enhance DC maturation (Alemán *et al*. 2007) and therefore are able to modulate DCs and ultimately antigen presentation. It has been demonstrated that neutrophils increase first in the lungs after MTB infection, followed by migration of DC to the lungs (Blomgran & Ernst 2011).

There was no change in the macrophage populations in the lungs in this experiment **(Figure 5-1)**, which was not expected and conflicts with information on *B. anthracis* where *B. anthracis* spores survive and germinate in macrophages (Guidi-Rontani 2002) as well as *in vitro* data demonstrating *B. subtilis* germination inside macrophages (Duc *et al*. 2004). There are four possible reasons for this; i) that lung macrophages are not the primary phagocyte in the lung that engulf *B. subtilis* spores and infers a difference between *B. subtilis* and *B. anthracis*, especially as *B. subtilis* is thought to be a gut resident rather than lung (Huynh A Hong *et al*. 2009) whereas *B. anthracis* can cause infection here ii) the number of macrophages was low in the lungs

and because macrophages are predominately tissue resident and an influx from the bloodstream is less likely, iii) Kirby *et al* suggested that macrophages undergo apoptosis after phagocytosis so the numbers may not significantly change until later on (Kirby *et al*. 2006) or, iv) Kirby *et al* also suggested that pulmonary DCs and alveolar macrophages were compartmentalised differently (Kirby *et al*. 2006) and therefore BAL washes could have provided more information about macrophage activity. Macrophages are important in the chronic phase of infection and clearing debris (Silva 2009) so they may be increased after seven days and so monitoring the responses for longer could be useful to garner more information about the macrophage involvement. Measurements of macrophage activity (cytokines, reactive oxygen species (ROS) (Mosser & Zhang 2008)) may also be relevant to measure in future experiments because the numbers of macrophages may not alter but their activation status could.

In Chapter 4, spores were revealed to be able to cross the gut epithelium when dosed nasally. The neutrophils, macrophages and DCs, all show a transient increase at day three after dosing. In Chapter 4, all of these cell types were shown to phagocytose spores, consequently it correlates that there is an effect on the levels of these cells over time; although the increase was three days after dosing **(Figure 5-3)**. There were also increases in the TLR2 and TLR4 expression in the gut, but they were both low level and short-lived in comparison to the lungs **(Figure 5-6)**. The transient increase in cell populations and low TLR expression could represent that the gut is more likely to be tolerant of antigens in comparison to the lungs because of the high number of commensal bacteria present (Barnes & Powrie 2009). The alternative explanation is that the activated cells migrated to local lymph nodes. In practice,

oral dosing would be used to target the gut, and would use a higher dose than used in this experiment, and therefore may overcome any issues of tolerance. This was demonstrated by Permpoonpattana *et al* who used $5x10^{10}$ spores delivered orally and observed protection against *C. difficile* infection (Permpoonpattana *et al*. 2011).

5.3.2. Responses in lymphoid tissues

The importance of looking at the immune responses in the lymphoid tissues of the peripheral lymph nodes (thymus, axillary and inguinal), NALT and spleen is because this is where T-cell and B-cell maturation occurs. DCs in the lymph nodes present the antigen to naïve T-cells so that they differentiate and proliferate and become Th cells, which can then leave the lymph nodes and travel to other tissues. T-cells can also differentiate into T follicular helper cells (Tfh) that interact with B-cells to stimulate antibody production.

Cytokine production in the NALT tissue was used to monitor lymphoid activity in the mucosal immune system. The secretion of MCP-1 may be from macrophages and monocytes in the tissue and attracted other immune cells to the tissue. The increase in the pro-inflammatory cytokines IFNγ and TNF at day one and four **(Figure 8)** could be attributed to NK cells, neutrophils or macrophages because due to the timing of production they are unlikely to be produced by Th1 cells. Observation of immune responses in the NALT was found to be as previous work has shown that inducing immune responses in the NALT can lead to protection against infection, for example against influenza (Matsuo *et al*. 2000). Therefore, to use spores as a mucosal vaccine, it is important to induce responses in the NALT that can activate mucosal immunity. Previous research by Glomski *et al* demonstrated the NALT as a site of entry of *B. anthracis* when aerosolised (Glomski *et al*. 2007) so there could be some

common component between these *Bacillus* species that interact with the NALT M cells.

The spleen is a lymphoid tissue that is able to filter blood and remove bacteria from circulation and contains large numbers of lymphocytes (Mebius & Kraal 2005). Overall, there was an increase in NK cells, DCs and a small increase in neutrophils and M1 macrophages, indicating that a systemic immune response had been mounted **(Figure 5-2)**. NK cells have been demonstrated to be able to interact with DCs by the production of IFNγ (Bajénoff *et al*. 2006), which can stimulate DC maturation and also influence T-cell differentiation. Therefore, the increase in NK cells **(Figure 5-2)** in the spleen could be due to an influx from the bloodstream, attracted by the increase in MCP-1 **(Figure 5-7)** where they can then interact with DCs. MCP-1, which could be produced by monocytes and be responsible for the increase in DCs as well as NK cells. The presence of pro-inflammatory cytokines IL-6, IFNγ and TNF all increased at day seven after dosing with spores, suggests differentiation of naïve T-cells to Th1 cells. However, the anti-inflammatory cytokine IL-10 also increased at day seven, which could have been produced to counteract the pro-inflammatory cytokines and so prevent inflammation and potential damage by Th2 or Tregs. MCP-1 also has an effect on the polarisation of naïve T-cells to Th2 cells and secretion of IL-4 (Deshmane *et al*. 2009) and therefore may support evidence that an adaptive immune response has been stimulated and indicate that a Th2 response had been mounted. In a study by Qu *et al*, *B. subtilis* spores carrying *C. sinensis* antigens were dosed orally to mice, and IL-6, IFNγ, IL-10 and TNF levels were also measured and found to be elevated in splenocyte supernatants and so, regardless of mucosal immunisation route these could be the set of cytokines that are stimulated by spores (Qu *et al*. 2014). There was a lack of IL-

12p70 produced, which is typically produced by DCs to stimulate naïve T-cells to differentiate to Th1 cells. Because there was an increase in DCs, it would be expected that there would be an increase in IL-12p70 as it is produced by DCs, and data from de Souza *et al* demonstrated production of IL-12 from bone marrow derived DCs *in vitro* after incubation with *B. subtilis* spores (de Souza *et al*. 2014). One reason why there was a lack of IL-12p70 production could be because DCs require co-stimulation with IFNγ from T-cells to produce IL-12, so that DCs activate T-cells, which in turn signal to DCs to produce IL-12 (Lenz *et al*. 2001). Therefore, if the time course of the experiment were increased and T-cells were activated, as we hypothesise by the increase in IFNγ and TNF at day seven, an increase in IL-12p70 may follow. A second hypothesis could be a problem with the assay (e.g. not adding the IL-12p70 beads), but the IL-12p70 standard curve was present so this is unlikely. A third reason is that MCP-1 has been demonstrated to inhibit IL-12 (Deshmane *et al*. 2009) and there is production of MCP-1 in the spleen. The final hypothesis is that there are different types of effector DCs that can produce a wide variety of cytokines. Some DCs produce IL-6 that can stimulate Th17 cells, which are antimicrobial and produce cytokines that can attract neutrophils (Perona-Wright *et al*. 2009). Other DCs are able to produce IL-33, which activates differentiation to Th2 cells (Rank *et al*. 2009). The increase in IL-6 observed in the splenocyte supernatants therefore could be attributed to DCs inducing anti-bacterial mechanisms to clear spores by activating Th17 cells. Support for this theory comes from Qu *et al*, who demonstrated that IL-17 was produced in response to oral immunisation with spores carrying antigens for *C. sinensis* (Qu *et al*. 2014). From this set of cytokine data from the spleen, the type of Th response cannot

be definitively proven and further work to characterise the T-cell phenotypes should be carried out.

There was an increase in TLR2 and TLR4 expression in the lymph nodes at day three following intranasal dosing with spores, which was interesting because it was prior to an increase in DCs suggesting that spores migrated to the peripheral lymph nodes and were able to activate DCs, which could later influence T-cell development. The increase in DCs could also be DCs that have travelled from the lungs and gut. Changes in the populations of DCs and NK cells in the lymph nodes was evidence that the spores were having an impact here, and the NK cells could be influencing the DCs, as similarly described in the spleen, which would then lead to initiation of the adaptive immune response.

To further investigate the link between the innate and adaptive immune responses, the events in the lymphoid tissue could be examined further. Immunohistochemistry of the lymph nodes could provide information about the germinal centre reaction and show interactions between the spores and DCs, T-cells and B-cells in different regions in the lymph nodes, as described by Moon *et al* who examined delivery of nanoparticles carrying malaria antigens (Moon *et al*. 2012). The data as it stands could be interpreted to support that naïve T-cells could be differentiated to; Th1, Th2 or Th17 cells, and so more work could be done to elucidate the types of T-cells that were stimulated using immunophenotyping and measuring more cytokines.

5.3.3. Responses in the blood

Complement is an important innate mechanism for removing pathogens from circulation by either opsonisation or lysis. In this study, bacterial killing after addition of sera from immunised mice was used as an indicator of complement

activation. The highest numbers of bacteria were killed using sera from mice one day after dosing with spores and that serum from after day two or three, the effect had reduced. This data confirmed the cytokine and cell population data from the spleen that a systemic immune response had been activated following intranasal dosing. There is evidence that *B. anthracis* binds C3 complement protein and that phagocytosis is dependent on complement binding (Gu *et al*. 2012). The complement killing assay infers that complement is able to bind and kill *B. subtilis* spores and may also aid phagocytosis.

5.3.4. Spores as an immunotherapeutic

After nasal dosing with autoclaved HU58 spores, mice were challenged with MDR-TB and given further HU58 doses but succumbed to infection **(Figure 5-11)**. Higher levels of the IL-4 antagonist, IL-4D2 have been seen in individuals that are infected but are controlling the TB disease in comparison to those with active TB, and is associated with promotion of Th1 responses and suppression of Th2 responses (Demissie *et al*. 2004). It is hypothesised that MTB stimulates IL-4 production which increases the M2 phenotype of macrophages that enhances uptake of MTB by increasing expression of the mannose binding receptor and also decreases the oxidative burst inside macrophages to enhance MTB survival (Buccheri *et al*. 2007). Therefore, by increasing the levels of IL-4D2, the disease control could be improved which is why Dr Rajko Reljic and Gil Reynolds Diogo were interested in testing IL-D42 as a therapeutic against MTB infection. Dr Rajko Reljic has also previously investigated blocking IL-4 activity using anti-IL-4 antibodies and demonstrated a reduction in bacterial burden (Buccheri *et al*. 2007). There appeared to be no difference in bacterial burden between different treatment groups. As demonstrated in Chapter 4, the interactions with host cells differ between live and autoclaved spores and

therefore the innate immune responses may also be different. Colenutt *et al* compared live and autoclaved spores as a therapeutic against *C. difficile* when delivered orally and found that live spores provided greater protection (Colenutt & Cutting 2014). Therefore autoclaved spores may be less useful therapeutic agents and live spores may perform better against MTB, and this should be investigated in future work. To improve the spores as a treatment for TB, perhaps substances could be added to the preparations that stimulate macrophage activity, for example IFNγ, as macrophages are essential for MTB killing. Immunotherapy for TB is important because of the increasing numbers of people who are succumbing to MDR-TB (85,085 cases globally in 2012, in comparison to 11,988 in 2005 (WHO 2013)), even in patients that have not received drug treatment (Kumar 2012). Therefore, a therapy avoiding drugs would avoid the development of drug resistance altogether. There are two main post-exposure therapies in development for TB; RUTI which contains semi-purified MTB fragments, and another that contains inactivated *M. vaccae* (Stop TB Partnership Working Vaccines New T B 2009). RUTI has been tested after a short course of antibiotics and has shown to induce Th1/Th2/Th3 responses, increase the number of CD8+ cells and enhance control of TB infection (Cardona 2006). Reducing the antibiotic therapy from nine months to one month has huge advantages for improving patient treatment compliance and reducing the development of MDR-TB.

It has been shown that virus-like nanoparticles stimulated neutrophil migration to the lungs and an increase in TNFα and IL-6 in the spleen and were able to protect against influenza and *S. pneumoniae* challenge (Mathieu *et al*. 2013). TNFα and IL-6 cytokines and neutrophil migration to the lungs were observed in this study with administration of HU58 spores so perhaps spores could be used

for other respiratory pathogens where neutrophil and DC infiltration to the lungs could be protective, and so spores could be tested as a therapy/prevention against *S. pneumoniae* and *B. anthracis* infections.

5.4. ***Conclusions***

In this chapter, *B. subtilis* spores dosed nasally were able to induce innate immune responses in both the mucosal and systemic immune compartments **(Figure 5-13)**. This initiation of the innate immune response confirms that *B. subtilis* is an immune-potentiator, which has now been demonstrated when used mucosally and therefore this should increase the ability of the spores to generate adaptive immune responses. In the future, it would be interesting to test the level of protection that this innate immune response could deliver against different diseases. A more thorough analysis of the innate immune response consequences on the adaptive immune response could be conducted to examine generation of memory cells. Other experiments could study the bronchoalveloar lavage (BAL) to see immune cells including DCs, in the airways as demonstrated in other studies (Kalsdorf *et al*. 2009; Kirby *et al*. 2006) and more complex flow cytometry could be used to determine cell subsets. For example, CD11c is highly expressed on DCs, but is also weakly expressed on other cells including granulocytes and NK cells and so using other markers would be more specific (B D Pharmingen 2014). DC maturation markers such as MHC II, CD40 and CD86 could also be included.

Chapter 6: General Discussion

6.1. B. subtilis spores as a vaccine against tuberculosis

B. subtilis spores have previously been demonstrated to adsorb antigen on the spore surface (Song *et al*. 2012) and in this work, this was developed further by testing their capacity to carry more than one antigen. This attribute has implications for the design of multivalent spore-based vaccines by improving immunogenicity and versatility of this platform technology. Recombinant spores were also examined and a method for spore inactivation was tested; a method that is currently being further optimised in the Cutting laboratory for a *C. difficile* vaccine to be taken to a human clinical trial (CDVAX 2014). Spores carrying the TB antigens MPT64 and Ag85B-Acr were shown to elicit some Th1 immune responses when delivered nasally to mice, and demonstrated a reduction in bacterial burden when challenged with MTB in the lungs and spleen compared to PBS, which was equivalent to BCG. The limitations of this study are that only two animals were used for the immunogenicity studies, and that no MTB was recoverable from some animals, so although the results suggest that spores were able to elicit Th1 responses and showed a reduction in bacterial burden, strong conclusions cannot be drawn.

The main model for initial testing of the immunogenicity of novel TB vaccines is to use the mouse model, and therefore this study sits alongside other studies that have explored nanoparticle and DNA TB vaccines (Stylianou *et al*. 2013, J. Vipond *et al.* 2006). Due to the lead candidate TB vaccine, MVA85A showing no significant benefit in recent clinical trials (Tameris *et al*. 2013), this highlights that research into novel TB vaccines is still required. Spores show potential as a

TB vaccine adjuvant because they are heat stable, easily transportable, safe and relatively cheap to manufacture. TB is a disease that is most prevalent in developing countries therefore a cost effective vaccine with no cold chain is essential.

6.2. Distribution of spores in the lung, gut and NALT after nasal, sublingual and oral dosing

Nasal, sublingual and oral are the main routes under investigation for administration of mucosal vaccines and they were compared in this thesis to understand how the route affected the distribution of spores. The method for identifying spores inside tissues and cells using the flow cytometer was optimised and could provide a useful tool in the future for exploring spore interactions with host cells and antigen delivery. Characterising spore development using the flow cytometer has also proved informative and is being used by other lab members to characterise germination of *C. difficile* and comparing the physiological states of *B. subtilis*.

Nasal and oral dosing distributed the spores to the lung, gut and NALT, but the nasal route delivered the highest proportion of spores, most probably because the spores were aerosolised. It proved difficult to identify where spores were dispersed after sublingual dosing, and this will require further investigation by examining other tissues. The distribution of spores is important because it proves that spores can cross epithelial barriers, and implies that spores will be able to generate immune responses, especially as it is known that the strongest immune responses are generated at the site of administration (Holmgren & Czerkinsky 2005). The NALT is a prime inductive site for the MALT and it is

important that spores can infiltrate the NALT where they can promote immune responses against respiratory pathogens.

The alternative method for examining dissemination of bacteria to different tissues is to use viable count from homogenised tissue and this could be used to validate the results of the spores distribution is tissues, but could not be used to examine autoclaved spores. Hoa *et al* used viable count to observe dissemination of *B. subtilis* after oral dosing and detected spores in the lungs, spleen, mesenteric lymph nodes as well as the gut (Hoa *et al*. 2001). Viable counting is a traditional method for quantifying bacteria, but there are problems associated with reliability and contamination from other bacteria, especially as tissues are not sterile and therefore flow cytometry is a more sensitive method because the bacteria of interest are specifically stained using antibodies. The other method that is becoming more popular for investigating dissemination of pathogens is whole body imaging, where the infectious agent is tagged with luciferase which can be detected through the tissue, and the development of the infection can be observed. The major advantage of this method is that it is non-invasive and the whole time course of infection can be observed. However, individual bacteria cannot be detected so infection has to be established to be visible and for non-pathogenic bacteria such as *B. subtilis* it is probably unsuitable because these bacteria are expected to be cleared and not establish themselves in the host. An interesting study could be to use *in vivo* imaging of an infection after vaccination or treatment with spores to see whether the disease development was different to unvaccinated animals.

6.3. Cell interactions with spores in different tissues after nasal, sublingual and oral dosing

Neutrophils, dendritic cells, macrophages, along with epithelial M cells were investigated for their ability to phagocytose spores after nasal, oral and sublingual administration in the lungs, gut and NALT. This provided information on i) how the spores were cleared from the system, ii) the cells that were likely to induce immune responses and iii) the differences in the partiality of particular phagocytes depending on location. The lungs showed that neutrophils and DCs preferentially phagocytosed spores, whereas in the gut, M cells and neutrophils were dominant and the highest numbers of spores were observed in the M cells localised in the NALT. This information supports data from Rhee *et al* that revealed uptake of spores by M cells in the appendix of rabbits (Rhee *et al*. 2004), but here the data demonstrated that M cells in the NALT also played a significant role in the uptake of spores. *In vitro*, data has shown that macrophages phagocytose spores, but in this research, they appeared to play a minor role in uptake, and DCs and neutrophils were more dominant, which agrees with data demonstrating that spores enhance DC maturation (de Souza *et al*. 2014) and the close relative of *B. subtilis*, *B. anthracis*, has also been shown to be phagocytosed by DCs (Shetron-Rama *et al*. 2010). These results were interesting because it revealed that certain cells favour phagocytosis of spores in different tissues, which could have downstream effects on the immune response. For example, in the gut, if a pathogen specifically targets M cells, such as *Shigella*, spores could be used as a therapeutic because the M cells and underlying immune cells would be primed and rendered able to clear the pathogen. Spores may be more readily adaptable for some diseases than

others, but due to their antigen carrying properties, they could be modified genetically or non-genetically to carry activators of other cell types.

There are published studies that examine cellular interactions with bacteria *in vitro*, for example Trouillet *et al* examined the adhesion and invasion of *S. aureus* using flow cytometry intracellular staining (Trouillet *et al*. 2011). *In vitro* assays have the advantage of being more controllable and can offer useful information about individual interactions but cannot always be translated *in vivo* or provide details about relative contributions by certain populations. *In vivo* studies that have examined particle distribution using flow cytometry include those that demonstrated migration of DCs carrying OVA or latex beads from the lungs to the lymph nodes (Vermaelen 2000, Byersdorfer & Chaplin 2001). Work by Reljic *et al* identified DCs and macrophages in the lungs that had internalised BCG expressing GFP (Reljic *et al*. 2005) and a study by Geddes *et al* demonstrated *Salmonella* expressing red fluorescence could be observed inside CD4+, CD8+, B-cells, macrophages, monocytes, neutrophils and DCs in the spleen after injection (Geddes *et al*. 2007). Using intracellular staining of *B. subtilis* in more than one tissue is a novel application of this technology and has provided information about phagocytosis in three different tissues and two different physiological states of the spores.

6.4. Cell interactions with live and autoclaved spores

Spores, whether inactivated by autoclaving or by formaldehyde treatment could be a form used as a vaccine adjuvant since i) spores with antigen on the spore surface will lose the antigenic determinant when they germinate and, ii) if the spores are genetically modified they require inactivation for safety reasons. However, the differences in the interactions of live and inactivated spores with host cells could affect their immunogenicity. In this study, the initial distribution

of spores was similar after nasal and oral dosing, but the cells they interacted with were different. The denatured proteins on the autoclaved spores, as demonstrated by Western blotting, appear to prohibit spore interaction with neutrophils and M cells but they were still phagocytosed by antigen presenting cells; macrophages and DCs. Data from Huang *et al* indicated that autoclaved spores could not activate TLRs *in vitro* (Huang, La Ragione, *et al*. 2008), which probably partially accounts for the lack of interaction with neutrophils and M cells, whereas DCs and macrophages, can phagocytose independently of antigen presence. Autoclaved spores were able to generate immune responses as shown in Chapter 3 but in the literature, inactivated spores were found to be less immunogenic than live spores (de Souza *et al*. 2014). Further to this, Colenutt *et al* found inactive spores to be less protective than live spores against *C. difficile* infection (Colenutt & Cutting 2014). Autoclaved spores could therefore be used as a vaccine adjuvant in the future as they are still processed by APCs and could present their antigens and stimulate adaptive immune responses, but live spores appear to be more immunogenic and interact with a wider array of immune cells. Future work could examine the interactions between cells and formaldehyde treated spores, and to also compare the downstream adaptive immune responses between live and inactivated spores after mucosal immunisation. If live spores are more immunogenic, other strategies could be utilised to prevent germination (e.g. using 'germinationSTOP' technology (Mascher *et al*. 2012)) whilst maintaining the surface proteins for cell interactions.

6.5. ***Innate immune responses after nasal dosing with spores***

The innate immune responses to spores after nasal dosing were investigated because there has been shown to be a link between activation of the innate

immune response affecting the adaptive immune response, which could have important implications for designing spore-based vaccines. There are also consequences for using the spores as a therapy for respiratory diseases as protection against influenza has been demonstrated a few days after dosing with nanoparticles (Mathieu *et al*. 2013) and with wild-type inactive *B. subtilis* spores (Song *et al*. 2012).

Following nasal dosing of HU58 spores to mice, it was demonstrated that immune responses in the mucosal tissues (lungs, gut), lymphoid tissues (peripheral lymph nodes, NALT) and systemic compartments (spleen, serum complement activation) could be stimulated. DCs were found to be stimulated in all tissues measured, which is positive because DCs bridge the gap between the innate and adaptive immune systems. Neutrophils numbers increased in the lungs, which confirmed the results from Chapter 4 that discovered spores internalised by neutrophils. This finding could have consequences for enhancing antigen presentation because apoptotic neutrophils are phagocytosed by DCs and the antigens presented by DCs, as well as spore clearance to prevent pathogenic immune responses. NK cells increased in the secondary lymphoid tissues, and have a role in enhancing DC antigen presentation and T-cell differentiation. Therefore, the data implies that DCs are indeed stimulated to present antigens carried by spores to the lymphoid tissues to activate T-cells. Further work could be carried out to investigate the pattern of events in the lymphoid tissue, and correlate the involvement of DCs with numbers of T and B-cells and investigate how the adaptive immune responses could be enhanced.

The innate immune responses to spores has been previously been examined *in vivo* by de Souza *et al*, but the major difference is that they investigated the

immune responses after injection rather than by mucosal dosing, and did not track the distribution of spores as described here (de Souza *et al*. 2014). The data from de Souza *et al* demonstrated that spores enhanced maturation of DCs (de Souza *et al*. 2014), which corresponds to the data generated in this work because mature DCs migrate to lymphoid tissue to deliver antigens Hill *et al*. 1990.

After nasal dosing of autoclaved spores, mice were challenged with MDR-TB, and the mice still succumbed to infection indicating that the innate immune response initiated was either not strong enough or the relevant cells required to combat TB were not activated. However, it must be noted that autoclaved spores were examined in Chapter 4 and indicated that neutrophils were not activated, and numbers of DCs phagocytosing spores were lower so this should be repeated with live spores to see whether the outcome could be improved. Spores could be further investigated as a therapy against other respiratory pathogens, where neutrophils and DCs are known to be important. The implications of these results are that live spores delivered nasally were able to stimulate mucosal and systemic immune responses and thus are immune-potentiators, and therefore as an adjuvant could enhance vaccines against respiratory pathogens.

6.6. Final Remarks

In conclusion, it has been demonstrated that spores can act as an immune-potentiator when used as a mucosal vaccine and that their distribution and phagocytosis by certain cells depends on i) their dosing route, ii) the tissue and iii) whether the spores were live or autoclaved. Most previous work testing *B. subtilis* as a vaccine adjuvant delivered mucosally has focused on protection and adaptive immune responses; therefore this work adds to the field by

suggesting initial mechanisms and cell interactions that have implications for the downstream adaptive immune response. The spores have the potential to be a successful vaccine adjuvant and immunotherapeutic because of their safety profile and their ability to stimulate immune responses. The addition of different antigens or other components could be utilised to further enhance the immunogenicity or targeting towards specific tissues or pathogens.

Chapter 7: Posters, Presentations and Publications

7.1. Posters

- 'An investigation into using *Bacillus subtilis* spores as a vaccine adjuvant for Tuberculosis', British Society for Immunology Infection and Immunity and Vaccine Group meeting, Porton Down. June 2013.
- '*Bacillus subtilis* as a vaccine adjuvant', British Society for Immunology Congress, Liverpool. December 2013.

7.2. Presentations

- '*Bacillus subtilis* spores as a vaccine adjuvant for TB'. British Society for Immunology, Infection and Immunity group meeting, London. April 2013.
- '*Bacillus subtilis* as a mucosal vaccine adjuvant', European Spores Conference, Egham. April 2014.

7.3. Publications

- Reljic, R., **Sibley, L**., Huang, J.-M., Pepponi, I., Hoppe, A., Hong, H. A., & Cutting, S. M. (2013). Mucosal Vaccination against TB Using Inert Bioparticles. Infection and Immunity 81 (11): 4071
- **Sibley, L.**, Reljic, R., Huang, J-M., Radford, D., Huynh, H., Cranenburgh, R., Cutting, S. (2014) Recombinant *Bacillus subtilis* Spores Expressing MPT64 Evaluated as a Vaccine Against Tuberculosis in the Murine Model. FEMS Microbiology Letters.1-10.

Chapter 8 : References

Aagaard, C., Hoang, T., Dietrich, J., Cardona, P.-J., Izzo, A., Dolganov, G., … Andersen, P. (2011). A multistage tuberculosis vaccine that confers efficient protection before and after exposure. Nature Medicine, 17(2), 189–94.

Abebe, F. (2012). Is interferon-gamma the right marker for bacille Calmette-Guérin-induced immune protection? The missing link in our understanding of tuberculosis immunology. Clinical and Experimental Immunology, 169(3), 213–9.

Abebe, F., & Bjune, G. (2009). The protective role of antibody responses during Mycobacterium tuberculosis infection. Clinical and Experimental Immunology, 157(2), 235–43.

Abebe, F., Mustafa, T., Nerland, A. H., & Bjune, G. A. (2006). Cytokine profile during latent and slowly progressive primary tuberculosis: a possible role for interleukin-15 in mediating clinical disease. Clinical and Experimental Immunology, 143(1), 180–92.

Aderem, A. (2003). Phagocytosis and the inflammatory response. The Journal of Infectious Diseases, 187 Suppl (Supplement_2), S340–5.

Aderem, A., & Underhill, D. M. (1999). Mechanisms of phagocytosis in macrophages. Annual Review of Immunology, 17, 593–623.

AFRC, R. F. (1989). Probiotics in man and animals. Journal of Applied Microbiology, 66(5), 365–378.

Alemán, M., de la Barrera, S., Schierloh, P., Yokobori, N., Baldini, M., Musella, R., … Sasiain, M. (2007). Spontaneous or Mycobacterium tuberculosis-induced apoptotic neutrophils exert opposite effects on the dendritic cell-mediated immune response. European Journal of Immunology, 37(6), 1524–37.

Amuguni, H., & Tzipori, S. (2012). Bacillus subtilis: a temperature resistant and needle free delivery system of immunogens. Human Vaccines & Immunotherapeutics, 8(7), 979–86.

Amuguni, H., Lee, S., Kerstein, K., Brown, D., Belitsky, B., Herrmann, J., … Tzipori, S. (2012). Sublingual immunization with an engineered Bacillus subtilis strain expressing tetanus toxin fragment C induces systemic and mucosal immune responses in piglets. Microbes and Infection / Institut Pasteur, 14(5), 447–56.

Amuguni, J. H., Lee, S., Kerstein, K. O., Brown, D. W., Belitsky, B. R., Herrmann, J. E., … Tzipori, S. (2011). Sublingually administered Bacillus subtilis cells expressing tetanus toxin C fragment induce protective systemic and mucosal antibodies against tetanus toxin in mice. Vaccine, 29(29-30), 4778–84.

Andersen, P., & Woodworth, J. S. (2014). Tuberculosis vaccines - rethinking the current paradigm. Trends in Immunology, 35(8), 387–395.

Andrew G. C. Barnes, Vuk Cerovic, P. S. H. and L. S. K., & Peter. (2007). Bacillus subtilis spores: A novel microparticle adjuvant which can instruct a balanced Th1 and Th2 immune response to specific antigen. European Journal of Immunology.

Angert, E. R. (2005). Alternatives to binary fission in bacteria. Nature Reviews. Microbiology, 3(3), 214–24.

Asanuma, H., Thompson, A. H., Iwasaki, T., Sato, Y., Inaba, Y., Aizawa, C., … Tamura, S. (1997). Isolation and characterization of mouse nasal-associated lymphoid tissue. Journal of Immunological Methods, 202(2), 123–31.

Attarwala, H. (2010). TGN1412: From Discovery to Disaster. Journal of Young Pharmacists : JYP, 2(3), 332–6.

B D Pharmingen, 2014. Technical Data Sheet APC Hamster Anti-Mouse CD11c. , pp.3–4.

Bacon, J., & Marsh, P. D. (2007). Transcriptional responses of Mycobacterium tuberculosis exposed to adverse conditions in vitro. Current Molecular Medicine, 7(3), 277–86.

Bajénoff, M, Breart, B, Huang, A Y C, Qi, H, Cazareth, J, Braud, V M, Germain, R N, Glaichenhaus, N., 2006. Natural killer cell behavior in lymph nodes revealed by static and real-time imaging. The Journal of experimental medicine, 203(3), pp.619–31.

Barnes, M. J., & Powrie, F. (2009). Regulatory T cells reinforce intestinal homeostasis. Immunity, 31(3), 401–11.

BD Biosciences. (2014). BD Biosciences Reagents - Bead-Based Immunoassays - Tools.

Behr, M. a, & Small, P. M. (1999). A historical and molecular phylogeny of BCG strains. Vaccine, 17(7-8), 915–22.

Bette, M, Jin, S C, Germann, T, Schäfer, M K, Weihe, E, Rüde, E, Fleischer, B., 1994. Differential expression of mRNA encoding interleukin-12 p35 and p40 subunits in situ. European journal of immunology, 24(10), pp.2435–40.

Beveridge, N. E. R., Price, D. A., Casazza, J. P., Pathan, A. A., Sander, C. R., Asher, T. E., … McShane, H. (2007). Immunisation with BCG and recombinant MVA85A induces long-lasting, polyfunctional Mycobacterium tuberculosis-specific CD4+ memory T lymphocyte populations. European Journal of Immunology, 37(11), 3089–100.

Black, G. F., Weir, R. E., Floyd, S., Bliss, L., Warndorff, D. K., Crampin, A. C., … Dockrell, H. M. (2002). BCG-induced increase in interferon-gamma response to mycobacterial antigens and efficacy of BCG vaccination in Malawi and the UK: two randomised controlled studies. Lancet, 359(9315), 1393–401.

Blomgran, R. & Ernst, J.D., 2011. Lung neutrophils facilitate activation of naive antigen-specific CD4+ T cells during Mycobacterium tuberculosis infection. Journal of immunology (Baltimore, Md. : 1950), 186(12), pp.7110–9.

Blomgran, R. *et al*., 2012. Mycobacterium tuberculosis inhibits neutrophil apoptosis, leading to delayed activation of naive CD4 T cells. Cell host & microbe, 11(1), pp.81–90.

Boom, W. H. (1999). Gammadelta T cells and Mycobacterium tuberculosis. Microbes and Infection / Institut Pasteur, 1(3), 187–95.

Buccheri, S, Reljic, R, Caccamo, N, Ivanyi, J, Singh, M, Salerno, A, Dieli, F., 2007. IL-4 depletion enhances host resistance and passive IgA protection against tuberculosis infection in BALB/c mice. European journal of immunology, 37(3), pp.729–37.

Byersdorfer, C. a, & Chaplin, D. D. (2001). Visualization of early APC/T cell interactions in the mouse lung following intranasal challenge. Journal of Immunology (Baltimore, Md. : 1950), 167(12), 6756–64.

Cardona, P.-J., 2006. RUTI: a new chance to shorten the treatment of latent tuberculosis infection. Tuberculosis (Edinburgh, Scotland), 86(3-4), pp.273–89.

CDVAX. (2014). CDVAX. http://cdvax.org/

Ceragioli, M., Cangiano, G., Esin, S., Ghelardi, E., Ricca, E., & Senesi, S. (2009). Phagocytosis, germination and killing of Bacillus subtilis spores presenting heterologous antigens in human macrophages. Microbiology (Reading, England), 155(Pt 2), 338–46.

Chang, M. H., Cirillo, S. L. G., & Cirillo, J. D. (2011). Using luciferase to image bacterial infections in mice. Journal of Visualized Experiments : JoVE, (48).

Checkley, A. M., & McShane, H. (2011). Tuberculosis vaccines: progress and challenges. Trends in Pharmacological Sciences, 32(10), 601–6.

Chen, C. Y., Huang, D., Wang, R. C., Shen, L., Zeng, G., Yao, S., … Chen, Z. W. (2009). A critical role for CD8 T cells in a nonhuman primate model of tuberculosis. PLoS Pathogens, 5(4), e1000392.

Chen, M., Divangahi, M., Gan, H., Shin, D. S. J., Hong, S., Lee, D. M., … Remold, H. G. (2008). Lipid mediators in innate immunity against tuberculosis: opposing roles of PGE2 and LXA4 in the induction of macrophage death. The Journal of Experimental Medicine, 205(12), 2791–801.

Chinen, T, Komai, K, Muto, G, Morita, R, Inoue, N, Yoshida, H, Sekiya, T, Yoshida, R, Nakamura, K, Takayanagi, R, Yoshimura, A., 2011. Prostaglandin E2 and SOCS1 have a role in intestinal immune tolerance. Nature communications, 2, p.190.

Cho, W.-S., Cho, M., Jeong, J., Choi, M., Cho, H.-Y., Han, B. S., … Jeong, J. (2009). Acute toxicity and pharmacokinetics of 13 nm-sized PEG-coated gold nanoparticles. Toxicology and Applied Pharmacology, 236(1), 16–24.

Christmas, P., 2010. Toll-Like Receptors: Sensors that Detect Infection. Nature Education, 3(9), p.85.

Ciabattini, A., Parigi, R., Isticato, R., Oggioni, M. R., & Pozzi, G. (2004). Oral priming of mice by recombinant spores of Bacillus subtilis. Vaccine, 22(31-32), 4139–43.

Ciabattini, A., Parigi, R., Isticato, R., Oggioni, M. R., & Pozzi, G. (2004). Oral priming of mice by recombinant spores of Bacillus subtilis. Vaccine, 22(31-32), 4139–43.

Colenutt, C. & Cutting, S.M., 2014. Use of Bacillus subtilis PXN21 spores for suppression of Clostridium difficile infection symptoms in a murine model. FEMS microbiology letters.

Comas-Riu, J., & Vives-Rego, J. (2002). Cytometric monitoring of growth, sporogenesis and spore cell sorting in Paenibacillus polymyxa (formerly Bacillus polymyxa). Journal of Applied Microbiology, 92(3), 475–481.

Cooper, A. M. (2009). T cells in mycobacterial infection and disease. Current Opinion in Immunology, 21(4), 378–84.

Cooper, A. M., Dalton, D. K., Stewart, T. A., Griffin, J. P., Russell, D. G., & Orme, I. M. (1993). Disseminated tuberculosis in interferon gamma gene-disrupted mice. The Journal of Experimental Medicine, 178(6), 2243–7.

Costantini, C. & Cassatella, M.A., 2011. The defensive alliance between neutrophils and NK cells as a novel arm of innate immunity. Journal of leukocyte biology, 89(2), pp.221–33.

Cronin, U. P., & Wilkinson, M. G. (2010). The potential of flow cytometry in the study of Bacillus cereus. Journal of Applied Microbiology, 108(1), 1–16.

Cuburu, N., Kweon, M. N., Song, J. H., Hervouet, C., Luci, C., Sun, J. Bin, … Czerkinsky, C. (2007). Sublingual immunization induces broad-based systemic and mucosal immune responses in mice. Vaccine, 25(51), 8598–8610.

Cuburu, N., Kweon, M.-N., Hervouet, C., Cha, H.-R., Pang, Y.-Y. S., Holmgren, J., … Czerkinsky, C. (2009). Sublingual immunization with nonreplicating antigens induces antibody-forming cells and cytotoxic T cells in the female genital tract mucosa and protects against genital papillomavirus infection. Journal of Immunology (Baltimore, Md. : 1950), 183(12), 7851–7859.

Culley, F. J. (2009). Natural killer cells in infection and inflammation of the lung. Immunology, 128(2), 151–63.

Cutting, S. M., Hong, H. A., Baccigalupi, L., & Ricca, E. (2009). Oral vaccine delivery by recombinant spore probiotics. International Reviews of Immunology, 28(6), 487–505.

Czerkinsky, C., Cuburu, N., Kweon, M.-N., Anjuere, F., & Holmgren, J. (2011). Sublingual vaccination. Human Vaccines, 7(1), 110–4.

De Souza, R. D., Batista, M. T., Luiz, W. B., Cavalcante, R. C. M., Amorim, J. H., Bizerra, R. S. P., … de Souza Ferreira, L. C. (2014). Bacillus subtilis Spores as Vaccine Adjuvants: Further Insights into the Mechanisms of Action. PloS One, 9(1), e87454.

DeLoid, G. M., Sulahian, T. H., Imrich, A., & Kobzik, L. (2009). Heterogeneity in macrophage phagocytosis of Staphylococcus aureus strains: high-throughput scanning cytometry-based analysis. PloS One, 4(7), e6209.

Dembic, Z., 2000. The Function of Toll-Like Receptors. Madame Curie Bioscience Database.

Demissie, A, Abebe, M, Aseffa, A, Rook, G, Fletcher, H, Zumla, A, Weldingh, K, Brock, I, Andersen, P, Doherty, T M, 2004. Healthy individuals that control a latent infection with Mycobacterium tuberculosis express high levels of Th1 cytokines and the IL-4 antagonist IL-4delta2. Journal of immunology (Baltimore, Md. : 1950), 172(11), pp.6938–43.

Dempsey, P.W., Vaidya, S.A. & Cheng, G., 2003. The art of war: Innate and adaptive immune responses. Cellular and molecular life sciences : CMLS, 60(12), pp.2604–21.

Deshmane, S L, Kremlev, S, Amini, S, Sawaya, Bl E., 2009. Monocyte chemoattractant protein-1 (MCP-1): an overview. Journal of interferon & cytokine research : the official journal of the International Society for Interferon and Cytokine Research, 29(6), pp.313–26.

Doolittle, R. L., Packman, C. H., & Lichtman, M. A. (1983). Amino-sugars enhance recognition and phagocytosis of particles by human neutrophils. Blood, 62(3), 697–701.

Driks, A. (1999). Bacillus subtilis Spore Coat. Microbiol. Mol. Biol. Rev., 63(1), 1–20.

Duc, L. H., Hong, H. a, Uyen, N. Q., & Cutting, S. M. (2004). Intracellular fate and immunogenicity of B. subtilis spores. Vaccine, 22(15-16), 1873–85.

Duc, L. H., Hong, H. A., & Cutting, S. M. (2003). Germination of the spore in the gastrointestinal tract provides a novel route for heterologous antigen delivery. Vaccine, 4215–4224.

Duc, L. H., Hong, H. A., Atkins, H. S., Flick-Smith, H. C., Durrani, Z., Rijpkema, S., … Cutting, S. M. (2007). Immunization against anthrax using Bacillus subtilis spores expressing the anthrax protective antigen. Vaccine, 25(2), 346–355.

Duc, L. H., Hong, H. A., Fairweather, N., Ricca, E., & Cutting, S. M. (2003). Bacterial Spores as Vaccine Vehicles. Infection and Immunity, 71(5), 2810–2818.

Duc, L H, Hong, H, Uyen, N Q, Cutting, S M., 2004. Intracellular fate and immunogenicity of B. subtilis spores. Vaccine, 22(15-16), pp.1873–85.

Ehrt, S., & Schnappinger, D. (2009). Mycobacterial survival strategies in the phagosome: defence against host stresses. Cellular Microbiology, 11(8), 1170–8.

Esparza-Gonzalez, S. C., Troy, A. R., & Izzo, A. A. (2014). Comparative analysis of Bacillus subtilis spores and monophosphoryl lipid A as adjuvants of protein-based mycobacterium tuberculosis-based vaccines: partial requirement for interleukin-17a for induction of protective immunity. Clinical and Vaccine Immunology : CVI, 21(4), 501–8.

Feng, C. G., & Britton, W. J. (2000). CD4+ and CD8+ T cells mediate adoptive immunity to aerosol infection of Mycobacterium bovis bacillus Calmette-Guérin. The Journal of Infectious Diseases, 181(5), 1846–9.

Ferguson, J. S., Weis, J. J., Martin, J. L., & Schlesinger, L. S. (2004). Complement protein C3 binding to Mycobacterium tuberculosis is initiated by the classical pathway in human bronchoalveolar lavage fluid. Infection and Immunity, 72(5), 2564–73.

Fletcher, H. A., Tanner, R., Wallis, R. S., Meyer, J., Manjaly, Z.-R., Harris, S., … McShane, H. (2013). Inhibition of mycobacterial growth in vitro following primary but not secondary vaccination with Mycobacterium bovis BCG. Clinical and Vaccine Immunology : CVI, 20(11), 1683–9.

Fujisaka, S., Usui, I., Bukhari, A., Ikutani, M., Oya, T., Kanatani, Y., … Tobe, K. (2009). Regulatory mechanisms for adipose tissue M1 and M2 macrophages in diet-induced obese mice. Diabetes, 58(11), 2574–82.

Garcia-Betancur, J. C., Yepes, A., Schneider, J., & Lopez, D. (2012). Single-cell analysis of Bacillus subtilis biofilms using fluorescence microscopy and flow cytometry. Journal of Visualized Experiments : JoVE, (60).

Garraud, K, Cleret, A, Mathieu, J, Fiole, D, Gauthier, Y, Quesnel-Hellmann, A, Tournier, J-N, 2012. Differential role of the interleukin-17 axis and neutrophils in resolution of inhalational anthrax. Infection and immunity, 80(1), pp.131–42.

Geddes, K., Cruz, F., & Heffron, F. (2007). Analysis of cells targeted by Salmonella type III secretion in vivo. PLoS Pathogens, 3(12), e196.

Gideon, H. P., & Flynn, J. L. (2011). Latent tuberculosis: what the host “sees”? Immunologic Research, 50(2-3), 202–12.

Glomski, I. J., Piris-Gimenez, A., Huerre, M., Mock, M., & Goossens, P. L. (2007). Primary involvement of pharynx and peyer’s patch in inhalational and intestinal anthrax. PLoS Pathogens, 3(6), e76.

Gu, C., Jenkins, S. A., Xue, Q., & Xu, Y. (2012). Activation of the classical complement pathway by Bacillus anthracis is the primary mechanism for spore phagocytosis and involves the spore surface protein BclA. Journal of Immunology (Baltimore, Md. : 1950), 188(9), 4421–31.

Guidi-Rontani, C., 2002. The alveolar macrophage: the Trojan horse of Bacillus anthracis. Trends in Microbiology, 10(9), pp.405–409.

Guidi-Rontani, C., Weber-Levy, M., Labruyère, E., & Mock, M. (1999). Germination of Bacillus anthracis spores within alveolar macrophages. Molecular Microbiology, 31(1), 9–17.

Guirado, E., Amat, I., Gil, O., Díaz, J., Arcos, V., Caceres, N., … Cardona, P.-J. (2006). Passive serum therapy with polyclonal antibodies against Mycobacterium tuberculosis protects against post-chemotherapy relapse of tuberculosis infection in SCID mice. Microbes and Infection / Institut Pasteur, 8(5), 1252–9.

Hafner, A. M., Corthésy, B., Textor, M., & Merkle, H. P. (2011). Tuning the immune response of dendritic cells to surface-assembled poly(I:C) on microspheres through synergistic interactions between phagocytic and TLR3 signaling. Biomaterials, 32(10), 2651–61.

Hampshire, T., Soneji, S., Bacon, J., James, B. W., Hinds, J., Laing, K., … Butcher, P. D. (2004). Stationary phase gene expression of Mycobacterium tuberculosis following a progressive nutrient depletion: a model for persistent organisms? Tuberculosis (Edinburgh, Scotland), 84(3-4), 228–38.

Handley, M. E., Pollara, G., Chain, B. M., & Katz, D. R. (2005). The use of targeted microbeads for quantitative analysis of the phagocytic properties of human monocyte-derived dendritic cells. Journal of Immunological Methods, 297(1-2), 27–38.

Harty, J. T., Tvinnereim, A. R., & White, D. W. (2000). CD8+ T cell effector mechanisms in resistance to infection. Annual Review of Immunology, 18, 275–308.

Hasenberg, M., Stegemann-Koniszewski, S., & Gunzer, M. (2013). Cellular immune reactions in the lung. Immunological Reviews, 251(1), 189–214.

Hawkridge, T., & Mahomed, H. (2011). Prospects for a new, safer and more effective TB vaccine. Paediatric Respiratory Reviews, 12(1), 46–51.

Heinzelmann, M., Gardner, S. A., Mercer-Jones, M., Roll, A. J., & Polk, H. C. (1999). Quantification of Phagocytosis in Human Neutrophils by Flow Cytometry. Microbiology and Immunology, 43(6), 505–512.

Hinc, K, Stasiłojć, M, Piątek, I, Peszyńska-Sularz, G, Isticato, R, Ricca, E, Obuchowski, M, Iwanicki, A, 2014. Mucosal Adjuvant Activity of IL-2 Presenting Spores of Bacillus subtilis in a Murine Model of Helicobacter pylori Vaccination. PloS one, 9(4), p.e95187.

Hinc, K., Isticato, R., Dembek, M., Karczewska, J., Iwanicki, A., Peszyńska-Sularz, G., … Ricca, E. (2010). Expression and display of UreA of Helicobacter acinonychis on the surface of Bacillus subtilis spores. Microbial Cell Factories, 9(1), 2.

Hinc, K., Stasiłojć, M., Piątek, I., Peszyńska-Sularz, G., Isticato, R., Ricca, E., … Iwanicki, A. (2014). Mucosal Adjuvant Activity of IL-2 Presenting Spores of Bacillus subtilis in a Murine Model of Helicobacter pylori Vaccination. PloS One, 9(4), e95187.

Hoa, T. T., Duc, L. H., Isticato, R., Baccigalupi, L., Ricca, E., Van, P. H., & Cutting, S. M. (2001). Fate and dissemination of Bacillus subtilis spores in a murine model. Applied and Environmental Microbiology, 67(9), 3819–23.

Holm, C., Mathiasen, T., & Jespersen, L. (2004). A flow cytometric technique for quantification and differentiation of bacteria in bulk tank milk. Journal of Applied Microbiology, 97(5), 935–41.

Holmgren, J., & Czerkinsky, C. (2005). Mucosal immunity and vaccines. Nature Medicine, 11(4 Suppl), S45–53.

Hong, H. A., Duc, L. H., & Cutting, S. M. (2005). The use of bacterial spore formers as probiotics. FEMS Microbiology Reviews, 29(4), 813–835.

Hong, H. A., Khaneja, R., Tam, N. M. K., Cazzato, A., Tan, S., Urdaci, M., … Cutting, S. M. (2009). Bacillus subtilis isolated from the human gastrointestinal tract. Research in Microbiology, 160(2), 134–43.

Hong, H. A., To, E., Fakhry, S., Baccigalupi, L., Ricca, E., & Cutting, S. M. (2009). Defining the natural habitat of Bacillus spore-formers. Research in Microbiology, 160(6), 375–379.

Hou, Y., Hu, W.-G., Hirano, T., & Gu, X.-X. (2002). A new intra-NALT route elicits mucosal and systemic immunity against Moraxella catarrhalis in a mouse challenge model. Vaccine, 20(17-18), 2375–2381.

Hu, C., Mayadas-Norton, T., Tanaka, K., Chan, J., & Salgame, P. (2000). Mycobacterium tuberculosis Infection in Complement Receptor 3-Deficient Mice. The Journal of Immunology, 165(5), 2596–2602.

Huang, J.-M., Hong, H. A., Tong, H. Van, Hoang, T. H., Brisson, A., & Cutting, S. M. (2010). Mucosal delivery of antigens using adsorption to bacterial spores. Vaccine, 28(4), 1021–1030.

Huang, J.-M., La Ragione, R. M., Nunez, A., & Cutting, S. M. (2008). Immunostimulatory activity of Bacillus spores. FEMS Immunology and Medical Microbiology, 53(2), 195–203.

Huang, J.-M., Ragione, R. M. La, Cooley, W. A., Todryk, S., & Cutting, S. M. (2008). Cytoplasmic delivery of antigens, by Bacillus subtilis enhances Th1 responses. Vaccine, 26(48), 6043–6052.

Huang, J.-M., Sali, M., Leckenby, M. W., Radford, D. S., Huynh, H. a, Delogu, G., … Cutting, S. M. (2010). Oral delivery of a DNA vaccine against tuberculosis using operator-repressor titration in a Salmonella enterica vector. Vaccine, 28(47), 7523–8.

Ibanga, H. B., Brookes, R. H., Hill, P. C., Owiafe, P. K., Fletcher, H. A., Lienhardt, C., … McShane, H. (2006). Early clinical trials with a new tuberculosis vaccine, MVA85A, in tuberculosis-endemic countries: issues in study design. The Lancet Infectious Diseases, 6(8), 522–528.

Imamura, D., Kuwana, R., Takamatsu, H., & Watabe, K. (2011). Proteins involved in formation of the outermost layer of Bacillus subtilis spores. Journal of Bacteriology, 193(16), 4075–80.

Isticato, R., Cangiano, G., Tran, H. T., Ciabattini, A., Medaglini, D., Oggioni, M. R., … Ricca, E. (2001). Surface display of recombinant proteins on Bacillus subtilis spores. Journal of Bacteriology, 183(21), 6294–301

Isticato, R., Scotto Di Mase, D., Mauriello, E., De Felice, M., & Ricca, E. (2007). Amino terminal fusion of heterologous proteins to CotC increases display efficiencies in the Bacillus subtilis spore system. BioTechniques, 42(2), 151–156.

Isticato, R., Sirec, T., Giglio, R., Baccigalupi, L., Rusciano, G., Pesce, G., … Ricca, E. (2013). Flexibility of the programme of spore coat formation in Bacillus subtilis: bypass of CotE requirement by over-production of CotH. PloS One, 8(9), e74949.

Isticato, R., Sirec, T., Treppiccione, L., Maurano, F., De Felice, M., Rossi, M., & Ricca, E. (2013). Non-recombinant display of the B subunit of the heat labile toxin of Escherichia coli on wild type and mutant spores of Bacillus subtilis. Microbial Cell Factories, 12, 98.

Iwasaki, A., & Kelsall, B. L. (1999). Freshly Isolated Peyer's Patch, but Not Spleen, Dendritic Cells Produce Interleukin 10 and Induce the Differentiation of T Helper Type 2 Cells. Journal of Experimental Medicine, 190(2), 229–240.

Jarchum, I, Liu, M, Lipuma, L, Pamer, E Gl., 2011. Toll-like receptor 5 stimulation protects mice from acute Clostridium difficile colitis. Infection and immunity, 79(4), pp.1498–503.

Jenkins, S. A., & Xu, Y. (2013). Characterization of Bacillus anthracis persistence in vivo. PloS One, 8(6), e66177.

Joosten, S. A., Fletcher, H. A., & Ottenhoff, T. H. M. (2013). A helicopter perspective on TB biomarkers: pathway and process based analysis of gene expression data provides new insight into TB pathogenesis. PloS One, 8(9), e73230.

Junqueira-kipnis, A. P., Kipnis, A., Jamieson, A., Gonzalez, M., Diefenbach, A., Raulet, D. H., … Orme, I. M. (2003). NK Cells Respond to Pulmonary Infection with Mycobacterium tuberculosis , but Play a Minimal Role in Protection 1. The Journal of Immunology 171, pp.6039-6045

Kaiko, G E, Horvat, J C, Beagley, K W, Hansbro, P M., 2008. Immunological decision-making: how does the immune system decide to mount a helper T-cell response? Immunology, 123(3), pp.326–38.

Kalsdorf, B., Scriba, T. J., Wood, K., Day, C. L., Dheda, K., Dawson, R., … Wilkinson, R. J. (2009). HIV-1 infection impairs the bronchoalveolar T-cell response to mycobacteria. American Journal of Respiratory and Critical Care Medicine, 180(12), 1262–70.

Kamath, A. T., Feng, C. G., Macdonald, M., Briscoe, H., & Britton, W. J. (1999). Differential protective efficacy of DNA vaccines expressing secreted proteins of Mycobacterium tuberculosis. Infection and Immunity, 67(4), 1702–7.

Kaufmann, S. H. E., & Gengenbacher, M. (2012). Recombinant live vaccine candidates against tuberculosis. Current Opinion in Biotechnology, 23(6), 900–7.

Kaveh, D. a, Bachy, V. S., Hewinson, R. G., & Hogarth, P. J. (2011). Systemic BCG immunization induces persistent lung mucosal multifunctional CD4 T(EM) cells which expand following virulent mycobacterial challenge. PloS One, 6(6), e21566.

Keane, J. (2004). Tumor necrosis factor blockers and reactivation of latent tuberculosis. Clinical Infectious Diseases : An Official Publication of the Infectious Diseases Society of America, 39(3), 300–2.

Khader, S. A., & Cooper, A. M. (2008). IL-23 and IL-17 in tuberculosis. Cytokine, 41(2), 79–83.

Khera, A., Singh, R., Shakila, H., Rao, V., Dhar, N., Narayanan, P. R., … Tyagi, A. K. (2005). Elicitation of efficient, protective immune responses by using DNA vaccines against tuberculosis. Vaccine, 23(48-49), 5655–65.

Kidd, P. (2003). Th1/Th2 balance: the hypothesis, its limitations, and implications for health and disease. Alternative Medicine Review : A Journal of Clinical Therapeutic, 8(3), 223–46.

Kim, D.-Y., Sato, A., Fukuyama, S., Sagara, H., Nagatake, T., Kong, I. G., … Kiyono, H. (2011). The airway antigen sampling system: respiratory M cells as an alternative gateway for inhaled antigens. Journal of Immunology (Baltimore, Md. : 1950), 186(7), 4253–62.

Kim, J.-H., Lee, C.-S., & Kim, B.-G. (2005). Spore-displayed streptavidin: a live diagnostic tool in biotechnology. Biochemical and Biophysical Research Communications, 331(1), 210–4.

Kim, J.-H., Roh, C., Lee, C.-W., Kyung, D., Choi, S.-K., Jung, H.-C., … Kim, B.-G. (2007). Bacterial surface display of GFP(uv) on bacillus subtilis spores. Journal of Microbiology and Biotechnology, 17(4), 677–80.

Kirby, A.C., Raynes, J.G. & Kaye, P.M., 2006. CD11b regulates recruitment of alveolar macrophages but not pulmonary dendritic cells after pneumococcal challenge. The Journal of infectious diseases, 193(2), pp.205–13.

Korbel, D. S., Schneider, B. E., & Schaible, U. E. (2008). Innate immunity in tuberculosis: myths and truth. Microbes and Infection, 10(9), 995–1004.

Kozlowski, P A; Williams S B; Lynch R M; Flanigan T P; Patterson R B; Cu-Uvin S; R Neutra M R (2002). Differential induction of mucosal and systemic antibody responses in women after nasal, rectal, or vaginal immunization: influence of the menstrual cycle. The Journal of Immunology 169, pp.566-574.

Saha K, Kim S T, Yan B , Miranda O R, Alfonso F S, Shlosman S and Rotello V M. (2013). Surface Functionality of Nanoparticles DeterminesCellular Uptake Mechanisms in Mammalian Cells. Uptake Mechanisms, 9(2), 300–305.

Kumar, P., 2012. Preventing Transmission of Drug-Resistant TB. National Academies Press (US).

Küppers, R., 2003. B cells under influence: transformation of B cells by Epstein-Barr virus. Nature reviews. Immunology2, 3, pp.801–812.

Lenz, P, Day, P M, Pang, Y Y, Frye, S A, Jensen, P N, Lowy, D R, Schiller, J T., 2001. Papillomavirus-like particles induce acute activation of dendritic cells. Journal of immunology (Baltimore, Md. : 1950), 166(9), pp.5346–5355.

Lepone, L., Rappocciolo, G., Knowlton, E., Jais, M., Piazza, P., Jenkins, F. J., & Rinaldo, C. R. (2010). Monofunctional and polyfunctional CD8+ T cell responses to human herpesvirus 8 lytic and latency proteins. Clinical and Vaccine Immunology : CVI, 17(10), 1507–16.

Li, P., Lu, M., Nguyen, M. T. A., Bae, E. J., Chapman, J., Feng, D., … Olefsky, J. M. (2010). Functional heterogeneity of CD11c-positive adipose tissue macrophages in diet-induced obese mice. The Journal of Biological Chemistry, 285(20), 15333–45.

Lin, P. L., Myers, A., Smith, L., Bigbee, C., Bigbee, M., Fuhrman, C., … Flynn, J. L. (2010). Tumor necrosis factor neutralization results in disseminated disease in acute and latent Mycobacterium tuberculosis infection with normal granuloma structure in a cynomolgus macaque model. Arthritis and Rheumatism, 62(2), 340–50.

Lin, P. L., Rodgers, M., Smith, L., Bigbee, M., Myers, A., Bigbee, C., … Flynn, J. L. (2009). Quantitative comparison of active and latent tuberculosis in the cynomolgus macaque model. Infection and Immunity, 77(10), 4631–42.

Lindenstrøm, T., Agger, E. M., Korsholm, K. S., Darrah, P. A., Aagaard, C., Seder, R. A., … Andersen, P. (2009). Tuberculosis subunit vaccination provides long-term protective immunity characterized by multifunctional CD4 memory T cells. Journal of Immunology (Baltimore, Md. : 1950), 182(12), 8047–55.

Lo, D. D., Ling, J., & Eckelhoefer, A. H. (2012). M cell targeting by a Claudin 4 targeting peptide can enhance mucosal IgA responses. BMC Biotechnology, 12, 7.

Loring, W. W., Melvin, I., Vandiviere, H. M., & Willis, H. S. (1955). The death and resurrection of the tubercle bacillus. Transactions of the American Clinical and Climatological Association, 67, 132–8.

Luker, K. E., & Luker, G. D. (2010). Bioluminescence imaging of reporter mice for studies of infection and inflammation. Antiviral Research, 86(1), 93–100.

Magge, A., Setlow, B., Cowan, A. E., & Setlow, P. (2009). Analysis of dye binding by and membrane potential in spores of Bacillus species. Journal of Applied Microbiology, 106(3), 814–24.

Malek, T. R., & Castro, I. (2010). Interleukin-2 receptor signaling: at the interface between tolerance and immunity. Immunity, 33(2), 153–65.

Man, A. L., Prieto-Garcia, M. E., & Nicoletti, C. (2004). Improving M cell mediated transport across mucosal barriers: do certain bacteria hold the keys? Immunology, 113(1), 15–22.

Marrack, P., McKee, A. S., & Munks, M. W. (2009). Towards an understanding of the adjuvant action of aluminium. Nature Reviews. Immunology, 9(4), 287–93.

Marsay, L., Matsumiya, M., Tanner, R., Poyntz, H., Griffiths, K. L., Stylianou, E., … McShane, H. (2013). Mycobacterial growth inhibition in murine splenocytes as a surrogate for protection against Mycobacterium tuberculosis (M. tb). Tuberculosis (Edinburgh, Scotland), 93(5), 551–7.

Martin, J. (2003). Characterization of formaldehyde-inactivated poliovirus preparations made from live-attenuated strains. Journal of General Virology, 84(7), 1781–1788.

Mascher, T., Tina, W., & Fritz, G. (2012). Team:LMU-Munich/Germination Stop - 2012.igem.org. http://2012.igem.org/Team:LMU-Munich/Germination_Stop

Mathieu, C., Rioux, G., Dumas, M.-C., & Leclerc, D. (2013). Induction of innate immunity in lungs with virus-like nanoparticles leads to protection against influenza and Streptococcus pneumoniae challenge. Nanomedicine : Nanotechnology, Biology, and Medicine, 9(7), 839–48. doi:10.1016/j.nano.2013.02.009

Matsuo, K, Yoshikawa, T, Asanuma, H, Iwasaki, T, Hagiwara, Y, Chen, Z, Kadowaki, S, Tsujimoto, H, Kurata, T, Tamura, S., 2000. Induction of innate immunity by nasal influenza vaccine administered in combination with an adjuvant (cholera toxin). Vaccine, 18(24), pp.2713–2722.

Mauri, C. & Bosma, A., 2012. Immune regulatory function of B cells. Annual review of immunology, 30, pp.221–41.

Mauriello, E. M. F., Duc, L. H., Isticato, R., Cangiano, G., Hong, H. A., Felice, M. De, … Cutting, S. M. (2004). Display of heterologous antigens on the Bacillus subtilis spore coat using CotC as a fusion partner. Vaccine, 1177–1187.

Mayer-Scholl, A, Hurwitz, R, Brinkmann, V, Schmid, M, Jungblut, P, Weinrauch, Y, Zychlinsky, A, 2005. Human neutrophils kill Bacillus anthracis. J. Young, ed. PLoS pathogens, 1(3), p.e23.

McKenney, P. T., Driks, A., & Eichenberger, P. (2013). The Bacillus subtilis endospore: assembly and functions of the multilayered coat. Nature Reviews. Microbiology, 11(1), 33–44

McShane, H., Jacobs, W. R., Fine, P. E., Reed, S. G., McMurray, D. N., Behr, M., … Orme, I. M. (2012). BCG: Myths, realities, and the need for alternative vaccine strategies. Tuberculosis, 92(3), 283–288.

Mebius, R.E. & Kraal, G., 2005. Structure and function of the spleen. Nature reviews. Immunology, 5(8), pp.606–16.

Moghimi, S. M., Hunter, A. C., & Andresen, T. L. (2012). Factors controlling nanoparticle pharmacokinetics: an integrated analysis and perspective. Annual Review of Pharmacology and Toxicology, 52, 481–503.

Moon, J J, Suh, H, Li, A V, Ockenhouse, C F, Yadava, A, Irvine, D, J 2012. Enhancing humoral responses to a malaria antigen with nanoparticle vaccines that expand Tfh cells and promote germinal center induction. Proceedings of the National Academy of Sciences of the United States of America, 109(4), pp.1080–5.

Mosser, D.M. & Zhang, X., 2008. Activation of murine macrophages. Current protocols in immunology / edited by John E. Coligan ... [*et al*.], Chapter 14, p.Unit 14.2.

Murray, P.J. & Wynn, T.A., 2011. Protective and pathogenic functions of macrophage subsets. Nature reviews. Immunology, 11(11), pp.723–37.

Nasser Eddine, A., Baumann, S., & Kaufmann, S. H. E. (2006). New tuberculosis vaccines approaching clinical trial – An overview. Drug Discovery Today: Therapeutic Strategies, 3(2), 113–119.

Negri, A., Potocki, W., Iwanicki, A., Obuchowski, M., & Hinc, K. (2013). Expression and display of Clostridium difficile protein FliD on the surface of Bacillus subtilis spores. Journal of Medical Microbiology, 62(Pt 9), 1379–85.

Neutra, M. R., & Kozlowski, P. A. (2006). Mucosal vaccines: the promise and the challenge. Nature Reviews. Immunology, 6(2), 148–58.

Nguyen, A. T. Van, Pham, C. K., Pham, H. T. T., Pham, H. L., Nguyen, A. H., Dang, L. T., … Phan, T.-N. (2014). Bacillus subtilis Spores Expressing the VP28 Antigen: A Potential Oral Treatment to Protect Litopenaeus vannamei Against White Spot Syndrome. FEMS Microbiology Letters.

NHS. (2014). Angina - Treatment - NHS Choices. NHS. Department of Health. http://www.nhs.uk/Conditions/Angina/Pages/Treatment.aspx

NHS. (2014). Clinical trials and medical research - Phases of trials - NHS Choices. Department of Health. http://www.nhs.uk/Conditions/Clinical-trials/Pages/Phasesoftrials.aspx

Nicholson, W. L. (2002). Roles of Bacillus endospores in the environment. Cellular and Molecular Life Sciences (CMLS), 59(3), 410–416.

Nicholson, W., & Setlow, P. (1990). Molecular biological methods for Bacillus. (C. Harwood & S. Cutting, Eds.). Chichester, UK: John Wiley & Sons Ltd.

Ning, D., Leng, X., Li, Q., & Xu, W. (2011). Surface-displayed VP28 on Bacillus subtilis spores induce protection against white spot syndrome virus in crayfish by oral administration. Journal of Applied Microbiology, 111(6), 1327–36.

Odutola, A. A., Owolabi, O. A., Owiafe, P. K., McShane, H., & Ota, M. O. C. (2012). A new TB vaccine, MVA85A, induces durable antigen-specific responses 14 months after vaccination in African infants. Vaccine, 30(38), 5591–5594.

Oggioni, M. R., Ciabattini, A., Cuppone, A. M., & Pozzi, G. (2003). Bacillus spores for vaccine delivery. Vaccine, S96–S101.

Orme, I. M. (1999). Beyond BCG: the potential for a more effective TB vaccine. Molecular Medicine Today, 5(11), 487–492.

Paidhungat, M., & Setlow, P. (2001). Localization of a germinant receptor protein (GerBA) to the inner membrane of Bacillus subtilis spores. Journal of Bacteriology, 183(13), 3982–90.

Park, H.-S., Francis, K. P., Yu, J., & Cleary, P. P. (2003). Membranous Cells in Nasal-Associated Lymphoid Tissue: A Portal of Entry for the Respiratory Mucosal Pathogen Group A Streptococcus. The Journal of Immunology, 171(5), 2532–2537.

Pellegrini, V., Fineschi, N., Matteucci, G., Marsili, I., Nencioni, L., Puddu, M., … Zuckerman, a J. (1993). Preparation and immunogenicity of an inactivated hepatitis A vaccine. Vaccine, 11(3), 383–7

Pepponi, I., Stylianou, E., van Dolleweerd, C., Diogo, G. R., Paul, M. J., Drake, P. M. W., … Reljic, R. (2013). Immune-complex mimics as a molecular platform for adjuvant-free vaccine delivery. PloS One, 8(4), e60855.

Perkins, D. L., Lovell, C. R., Bronk, B. V, Setlow, B., Setlow, P., & Myrick, M. L. (2004). Effects of autoclaving on bacterial endospores studied by Fourier transform infrared microspectroscopy. Applied Spectroscopy, 58(6), 749–53.

Permpoonpattana, P., Hong, H. A., Phetcharaburanin, J., Huang, J.-M., Cook, J., Fairweather, N. F., & Cutting, S. M. (2011). Immunization with Bacillus spores expressing toxin A peptide repeats protects against infection with Clostridium difficile strains producing toxins A and B. Infection and Immunity, 79(6), 2295–302.

Perona-Wright, G. *et al*., 2009. A pivotal role for CD40-mediated IL-6 production by dendritic cells during IL-17 induction in vivo. Journal of immunology (Baltimore, Md. : 1950), 182(5), pp.2808–15.

Pharmacopeia, E. (2014). European Pharmacopoeia Version 8.0. 2014. http://online.edqm.eu/EN/entry.htm

Qu, H., Xu, Y., Sun, H., Lin, J., Yu, J., Tang, Z., … Yu, X. (2014). Systemic and local mucosal immune responses induced by orally delivered Bacillus subtilis spore expressing leucine aminopeptidase 2 of Clonorchis sinensis. Parasitology Research.

Rank, M A, Kobayashi, T, Kozaki, H, Bartemes, K R, Squillace, D L, Kita, H, 2009. IL-33-activated dendritic cells induce an atypical TH2-type response. The Journal of allergy and clinical immunology, 123(5), pp.1047–54.

Rappuoli, R. *et al*., 2013. Vaccine adjuvant formulations: A pharmaceutical perspective. Seminars in Immunology, 25(2), pp.130–145.

Rath, B., Linder, T., Cornblath, D., Hudson, M., Fernandopulle, R., Hartmann, K., … Wong, V. (2007). All that palsies is not Bell's -the need to define Bell's palsy as an adverse event following immunization. Vaccine, 26(1), 1–14.

Reljic, R, Sibley, L, Huang, J-M, Pepponi, I, Hoppe, A, Hong, H, Cutting, S M, 2013. Mucosal Vaccination against TB Using Inert Bioparticles. Infection and immunity, 81(11), pp.4071–80.

Reljic, R., Di Sano, C., Crawford, C., Dieli, F., Challacombe, S., & Ivanyi, J. (2005). Time course of mycobacterial infection of dendritic cells in the lungs of intranasally infected mice. Tuberculosis (Edinburgh, Scotland), 85(1-2), 81–8.

Rescigno, M., & Di Sabatino, A. (2009). Dendritic cells in intestinal homeostasis and disease. The Journal of Clinical Investigation, 119(9), 2441–50.

Rhee, K.-J., Sethupathi, P., Driks, A., Lanning, D. K., & Knight, K. L. (2004). Role of Commensal Bacteria in Development of Gut-Associated Lymphoid Tissues and Preimmune Antibody Repertoire. J. Immunol., 172(2), 1118–1124.

Ryan, A, Lynch, M, Smith, S M, Amu, S, Nel, H J, McCoy, C E, Dowling, J K, Draper, E, O'Reilly, V, McCarthy, C, O'Brien, J, Ní Eidhin, D, O'Connell, M J, Keogh, B, Morton, C O, Rogers, T R, Fallon, P G, O'Neill, L A, Kelleher, D, Loscher, C E., 2011. A role for TLR4 in Clostridium difficile infection and the recognition of surface layer proteins. D. S. Schneider, ed. PLoS pathogens, 7(6), p.e1002076.

Salk, D., & Salk, J. (1984). Vaccinology of poliomyelitis. Vaccine, 2(1), 59–74.

Sánchez, D, Rojas, M, Hernández, I, Radzioch, D, García, L F, Barrera, L F., 2010. Role of TLR2- and TLR4-mediated signaling in Mycobacterium tuberculosis-induced macrophage death. Cellular immunology, 260(2), pp.128–36.

Santosuosso, M., McCormick, S., Zhang, X., Zganiacz, A., & Xing, Z. (2006). Intranasal boosting with an adenovirus-vectored vaccine markedly enhances protection by parenteral Mycobacterium bovis BCG immunization against pulmonary tuberculosis. Infection and Immunity, 74(8), 4634–43.

Savina, A., & Amigorena, S. (2007). Phagocytosis and antigen presentation in dendritic cells. Immunological Reviews, 219, 143–56.

Schechter, M., Zajdenverg, R., Falco, G., Barnes, G. L., Faulhaber, J. C., Coberly, J. S., … Chaisson, R. E. (2006). Weekly rifapentine/isoniazid or daily rifampin/pyrazinamide for latent tuberculosis in household contacts. American Journal of Respiratory and Critical Care Medicine, 173(8), 922–6.

Selwyn, P. A., Hartel, D., Lewis, V. A., Schoenbaum, E. E., Vermund, S. H., Klein, R. S., … Friedland, G. H. (1989). A prospective study of the risk of tuberculosis among intravenous drug users with human immunodeficiency virus infection. The New England Journal of Medicine, 320(9), 545–50.

Seyrantepe, V., Iannello, A., Liang, F., Kanshin, E., Jayanth, P., Samarani, S., … Pshezhetsky, A. V. (2010). Regulation of phagocytosis in macrophages by neuraminidase 1. The Journal of Biological Chemistry, 285(1), 206–15.

Sharpe, S. A., McShane, H., Dennis, M. J., Basaraba, R. J., Gleeson, F., Hall, G., … Marsh, P. D. (2010). Establishment of an aerosol challenge model of tuberculosis in rhesus macaques and an evaluation of endpoints for vaccine testing. Clinical and Vaccine Immunology : CVI, 17(8), 1170–82.

Shetron-Rama, L. M., Herring-Palmer, A. C., Huffnagle, G. B., & Hanna, P. (2010). Transport of Bacillus anthracis from the lungs to the draining lymph nodes is a rapid process facilitated by CD11c+ cells. Microbial Pathogenesis, 49(1), 38–46.

Shim, B.-S., Choi, Y., Cheon, I. S., & Song, M. K. (2013). Sublingual delivery of vaccines for the induction of mucosal immunity. Immune Network, 13(3), 81–5.

Sibley, L. S., White, A. D., Marriott, A., Dennis, M. J., Williams, A., Marsh, P. D., & Sharpe, S. A. (2012). ELISPOT Refinement Using Spot Morphology for Assessing Host Responses to Tuberculosis. Cells, 1(1), 5–14.

Siggins, M.K. *et al*., 2014. Differential timing of antibody-mediated phagocytosis and cell-free killing of invasive African Salmonella allows immune evasion. European journal of immunology, 44(4), pp.1093–8.

Silva, M.T., 2009. When two is better than one: macrophages and neutrophils work in concert in innate immunity as complementary and cooperative partners of a myeloid phagocyte system. Journal of Leukocyte Biology, 87(1), pp.93–106.

Sirec, T., Cangiano, G., Baccigalupi, L., Ricca, E., & Isticato, R. (2014). The spore surface of intestinal isolates of Bacillus subtilis. FEMS Microbiology Letters.

Smelt, J. P. P. M., Bos, a P., Kort, R., & Brul, S. (2008). Modelling the effect of sub(lethal) heat treatment of Bacillus subtilis spores on germination rate and outgrowth to exponentially growing vegetative cells. International Journal of Food Microbiology, 128(1), 34–40.

Sojka, D. K., Huang, Y.-H., & Fowell, D. J. (2008). Mechanisms of regulatory T-cell suppression - a diverse arsenal for a moving target. Immunology, 124(1), 13–22.

Song, M., Hong, H. A., Huang, J.-M., Colenutt, C., Khang, D. D., Nguyen, T. V. A., … Cutting, S. M. (2012). Killed Bacillus subtilis spores as a mucosal adjuvant for an H5N1 vaccine. Vaccine, 30(22), 3266–3277

Stop TB Partnership | About Us. (n.d.). Stop TB Partnership. http://www.stoptb.org/about/

Stop TB Partnership Working Vaccines New T B, 2009. TUBERCULOSIS VACCINE CANDIDATES – 2009. , pp.2006–2015.

Stylianou, E., Diogo, G. R., Pepponi, I., van Dolleweerd, C., Arias, M. A., Locht, C., … Reljic, R. (2013). Mucosal delivery of antigen-coated nanoparticles to lungs confers protective immunity against tuberculosis infection in mice. European Journal of Immunology.

Tameris, M. D., Hatherill, M., Landry, B. S., Scriba, T. J., Snowden, M. A., Lockhart, S., … McShane, H. (2013). Safety and efficacy of MVA85A, a new tuberculosis vaccine, in infants previously vaccinated with BCG: a randomised, placebo-controlled phase 2b trial. Lancet, 381(9871), 1021–8.

Tan, B. H., Meinken, C., Bastian, M., Bruns, H., Legaspi, A., Ochoa, M. T., … Stenger, S. (2006). Macrophages Acquire Neutrophil Granules for Antimicrobial Activity against Intracellular Pathogens. The Journal of Immunology, 177(3), 1864–1871.

Teitelbaum, R., Schubert, W., Gunther, L., Kress, Y., Macaluso, F., Pollard, J. W., … Bloom, B. R. (1999). The M cell as a portal of entry to the lung for the bacterial pathogen Mycobacterium tuberculosis. Immunity, 10(6), 641–50.

Todar, K. (2012). Todar's Online Textbook of Bacteriology. Todar's Online Textbook of Bacteriology. http://textbookofbacteriology.net/adaptive_2.html

Tonry, J. H., Popov, S. G., Narayanan, A., Kashanchi, F., Hakami, R. M., Carpenter, C., … Chung, M.-C. (2013). In vivo murine and in vitro M-like cell models of gastrointestinal anthrax. Microbes and Infection / Institut Pasteur, 15(1), 37–44.

Tracy, B. P., Gaida, S. M., & Papoutsakis, E. T. (2010). Flow cytometry for bacteria: enabling metabolic engineering, synthetic biology and the elucidation of complex phenotypes. Current Opinion in Biotechnology, 21(1), 85–99.

Trouillet, S., Rasigade, J.-P., Lhoste, Y., Ferry, T., Vandenesch, F., Etienne, J., & Laurent, F. (2011). A novel flow cytometry-based assay for the quantification of Staphylococcus aureus adhesion to and invasion of eukaryotic cells. Journal of Microbiological Methods, 86(2), 145–149.

Trunz, B. B., Fine, P., & Dye, C. (2006). Effect of BCG vaccination on childhood tuberculous meningitis and miliary tuberculosis worldwide: a meta-analysis and assessment of cost-effectiveness. Lancet, 367(9517), 1173–80.

Turnbull, P. C. B. (1991). Anthrax vaccines: Past, present and future. Vaccine. pp. 533-539

Tyrer, P., Foxwell, A. R., Cripps, A. W., Apicella, M. A., & Kyd, J. M. (2006). Microbial pattern recognition receptors mediate M-cell uptake of a gram-negative bacterium. Infection and Immunity, 74(1), 625–31.

Uyen, N. Q., Hong, H. A., & Cutting, S. M. (2007). Enhanced immunisation and expression strategies using bacterial spores as heat-stable vaccine delivery vehicles. Vaccine, 25(2), 356–365.

Van Kampen, K. R., Shi, Z., Gao, P., Zhang, J., Foster, K. W., Chen, D.-T., … Tang, D. C. (2005). Safety and immunogenicity of adenovirus-vectored nasal and epicutaneous influenza vaccines in humans. Vaccine, 23(8), 1029–36.

Vermaelen, K. Y. (2000). Specific Migratory Dendritic Cells Rapidly Transport Antigen from the Airways to the Thoracic Lymph Nodes. Journal of Experimental Medicine, 193(1), 51–60.

Virta, M., Lineri, S., Kankaanpää, P., Karp, M., Peltonen, K., Nuutila, J., & Lilius, E. M. (1998). Determination of complement-mediated killing of bacteria by viability staining and bioluminescence. Applied and Environmental Microbiology, 64(2), 515–9.

Vordermeier, H. M., Venkataprasad, N., Harris, D. P., & Ivanyi, J. (1996). Increase of tuberculous infection in the organs of B cell-deficient mice. Clinical and Experimental Immunology, 106(2), 312–6.

Wareham, A. S., Tree, J. A., Marsh, P. D., Butcher, P. D., Dennis, M., & Sharpe, S. A. (2014). Evidence for a role for interleukin-17, Th17 cells and iron homeostasis in protective immunity against tuberculosis in cynomolgus macaques. PloS One, 9(2), e88149.

Welsh, R.M. & Waggoner, S.N., 2013. NK cells controlling virus-specific T cells: Rheostats for acute vs. persistent infections. Virology, 435(1), pp.37–45.].

White, A. D., Sibley, L., Dennis, M. J., Gooch, K., Betts, G., Edwards, N., … Sharpe, S. A. (2013). Evaluation of the Safety and Immunogenicity of a Candidate Tuberculosis Vaccine, MVA85A, Delivered by Aerosol to the Lungs of Macaques. Clinical and Vaccine Immunology : CVI, 20(5), 663–72.

WHO, 2014. Tuberculosis: Multi-drug resistant TB - Data by WHO region. WHO. http://apps.who.int/gho/data/view.main.MDRTBWHOREG?lang=en

WHO. (2014). Tuberculosis: Co-epidemics of TB and HIV - Data by WHO region. Global Health Observatory. http://apps.who.int/gho/data/view.main.TBHIVWHOREG?lang=en

WHO. (2014a). Tuberculosis: Co-epidemics of TB and HIV - Data by WHO region. Global Health Observatory. http://apps.who.int/gho/data/view.main.TBHIVWHOREG?lang=en

WHO. (2014b). WHO | Tuberculosis. WHO. World Health Organization. http://www.who.int/mediacentre/factsheets/fs104/en/

Williams, A., Hall, Y., & Orme, I. M. (2009). Evaluation of new vaccines for tuberculosis in the guinea pig model. Tuberculosis (Edinburgh, Scotland), 89(6), 389–97.

Wright, G.G., 1986. Anthrax toxin blocks priming of neutrophils by lipopolysaccharide and by muramyl dipeptide. Journal of Experimental Medicine, 164(5), pp.1700–1709.

Yu, L. H., & Cutting, S. M. (2009). The effect of anti-spore antibody responses on the use of spores for vaccine delivery. Vaccine, 27(34), 4576–4584.

Zanvit, P., Tichopád, A., Havlíčková, M., Novotná, O., Jirkovská, M., Kološtová, K., … Prokešová, L. (2010). Adjuvant effect of Bacillus firmus on the expression of cytokines and toll-like receptors in mouse nasopharynx-associated lymphoid

tissue (NALT) after intranasal immunization with inactivated influenza virus type A. Immunology Letters, 134(1), 26–34.

Zeigler, D. R., Prágai, Z., Rodriguez, S., Chevreux, B., Muffler, A., Albert, T., … Perkins, J. B. (2008). The origins of 168, W23, and other Bacillus subtilis legacy strains. Journal of Bacteriology, 190(21), 6983–95.

Zhou, Z., Xia, H., Hu, X., Huang, Y., Li, Y., Li, L., … Yu, X. (2008). Oral administration of a Bacillus subtilis spore-based vaccine expressing Clonorchis sinensis tegumental protein 22.3 kDa confers protection against Clonorchis sinensis. Vaccine, 26(15), 1817–25.

Zinn, K. R., Chaudhuri, T. R., Szafran, A. A., O'Quinn, D., Weaver, C., Dugger, K., … Frank, S. J. (2008). Noninvasive Bioluminescence Imaging in Small Animals. ILAR Journal, 49(1), 103–115.

Zwerling, A., Behr, M. a, Verma, A., Brewer, T. F., Menzies, D., & Pai, M. (2011). The BCG World Atlas: a database of global BCG vaccination policies and practices. PLoS Medicine, 8(3), e1001012.

Chapter 9 : Appendix

Recipes:

10x Tris-buffered saline (TBS)	
Tris	24.2g
NaCl	84g

pH7.6, 1L dH_2O

Acrylamide	
Acrylamide	30g
Bis-Acrylamide	0.8g

100ml dH_2O

5x Sample buffer	
Glycerol	1ml
SDS	1g
Tris-Hcl 0.5M pH6.8	6.5ml
2-mercaptoethanol	2.5ml
0.5% bromophenol	1ml

Up to 10ml with dH_2O

Spore coat extraction buffer	
Tris-HCl 0.5M	0.1ml
10% SDS	0.1ml
dH_2O	0.75ml
1M DTT	0.5ml

10x Running Buffer	
Tris	30g
Glycine	142g
SDS	5g

1L dH_2O

Stacking gel buffer	
Tris-HCl 0.5M ph6.8	

Resolving gel buffer	
Tris-HCl 1.5M pH8.8	

10x Transfer buffer	
Tris	30.3g
Glycine	144g

1L dH_2O

1x Transfer buffer	
10x Transfer buffer	100ml
Methanol	200ml
dH_2O	700ml

Stain	
R250 Coomassie blue	1g
Methanol	400ml
Glacial acetic acid	100ml
dH_2O	500ml

Destain	
Methanol	100ml
Glacial acetic acid	100ml
dH_2O	800ml

12% Resolving gel	
dH_20	1.75ml
Resolving gel buffer	1.25ml
Acrylamide	2ml
10% AMPS	25µl
20% SDS	25µl
TEMED	2.5µl

Stacking gel	
dH_2O	1.2ml
Stacking gel buffer	0.5ml
Acrylamide	0.3ml
10% AMPS	10µl
20% SDS	10µl
TEMED	4µl

TMB stock	
TMB	6mg/ml

Dissolve in ethanol

TMB	
dH_2O	9ml
Sodium acetate pH5.5	1ml
H_2O_2	2µl
TMB stock	167µl

A1 binding buffer (AKTA)	
Sodium phosphate	20mM
NaCl	0.5M
Imidazole	10mM

pH 7.4. dH_2O

A3 buffer (AKTA)	
$NiSO_4$	100mM

dH_20

B elution buffer (AKTA)	
Sodium phosphate	20mM
NaCl	0.5M
Imidazole	0.5M

pH 7.4. dH_2O

Difco Sporulation Media (DSM)	
Oxoid Nutrient Broth	8g
KCl	1g
$MgSO_4.7H_20$	0.25g
NaOH 1N	0.7ml

dH_20 1L

DSM Supplements (add after autoclaving)	
$Ca(NO_3)$ 1M	1ml/1L
$MnCl_2$ 10mM	1ml/1L
$FeSO_4$ 1mM	1ml/1L

LB (Luria Bertani) media	
Oxoid Tryptone	10g
Yeast extract	5g
NaCl	10g
NaOH 1N	0.7ml

10% Neutral Buffered Formalin (NBF)	
37% formaldehyde	10%
dH_20	90%
NaH_2PO_4	4g/L
Na_2HPO_4	6.5g/L

10x Phosphate buffered saline (PBS)	
Na_2HPO_4 0.1M	800ml
NaH_2PO_4 0.1M	200ml
pH7.4	
NaCl	85g

Chapter 4 flow cytometry example gating plots

Lungs

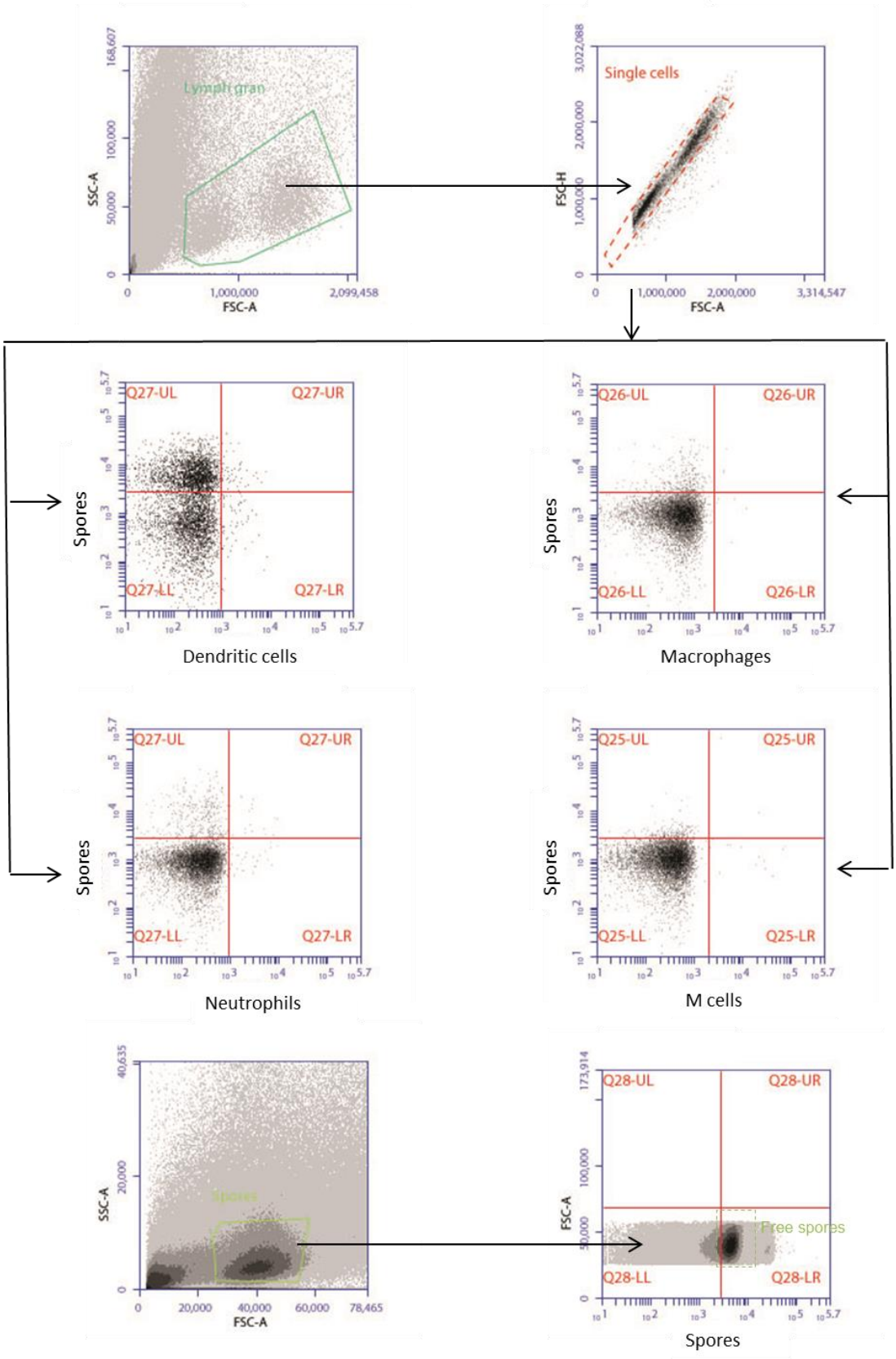

Gut

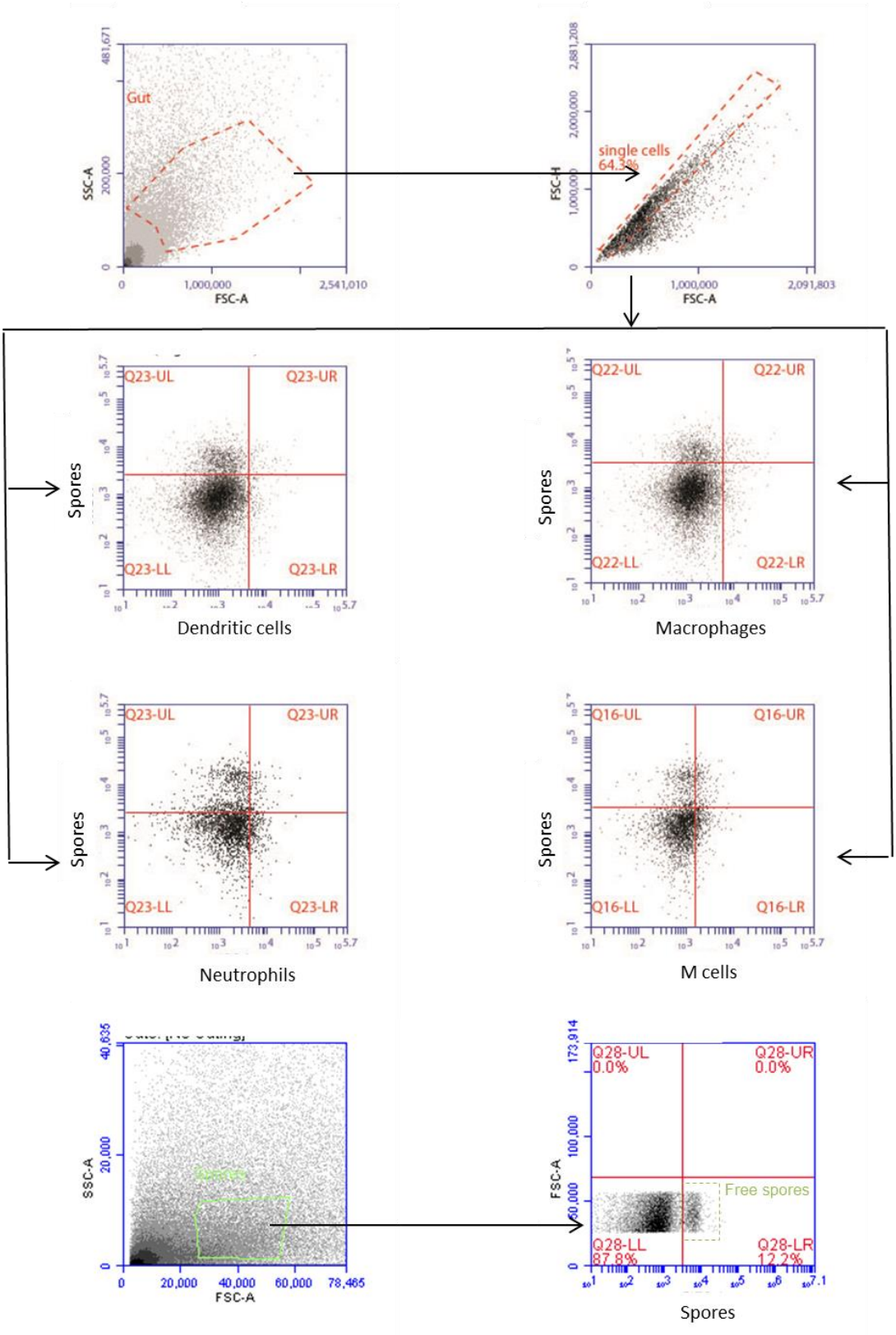
Gut
SSC-A
FSC-A
single cells
64.3%
FSC-H
FSC-A
Q23-UL
Q23-UR
Q23-LL
Q23-LR
Spores
Dendritic cells
Q22-UL
Q22-UR
Q22-LL
Q22-LR
Spores
Macrophages
Q23-UL
Q23-UR
Q23-LL
Q23-LR
Spores
Neutrophils
Q16-UL
Q16-UR
Q16-LL
Q16-LR
Spores
M cells
Spores
SSC-A
FSC-A
Q28-UL
0.0%
Q28-UR
0.0%
Free spores
Q28-LL
87.8%
Q28-LR
12.2%
FSC-A
Spores

NALT

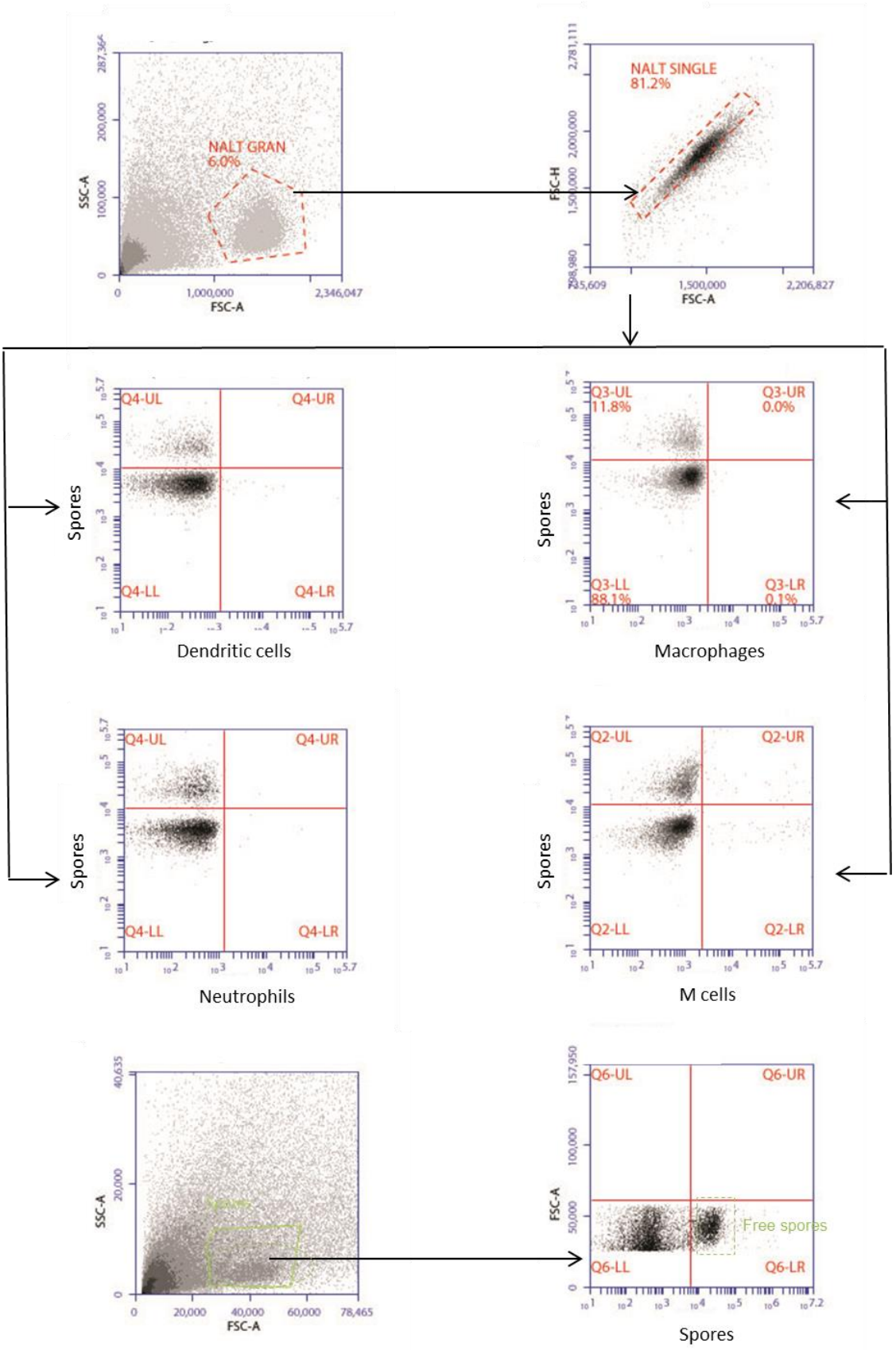
NALT GRAN
6.0%
SSC-A
FSC-A
NALT SINGLE
81.2%
FSC-H
FSC-A
Q4-UL
Q4-UR
Q4-LL
Q4-LR
Spores
Dendritic cells
Q3-UL
11.8%
Q3-UR
0.0%
Q3-LL
88.1%
Q3-LR
0.1%
Spores
Macrophages
Q4-UL
Q4-UR
Q4-LL
Q4-LR
Spores
Neutrophils
Q2-UL
Q2-UR
Q2-LL
Q2-LR
Spores
M cells
SSC-A
FSC-A
Free spores
Q6-UL
Q6-UR
Q6-LL
Q6-LR
FSC-A
Spores

Chapter 5 Flow cytometry example gating plots

Lungs

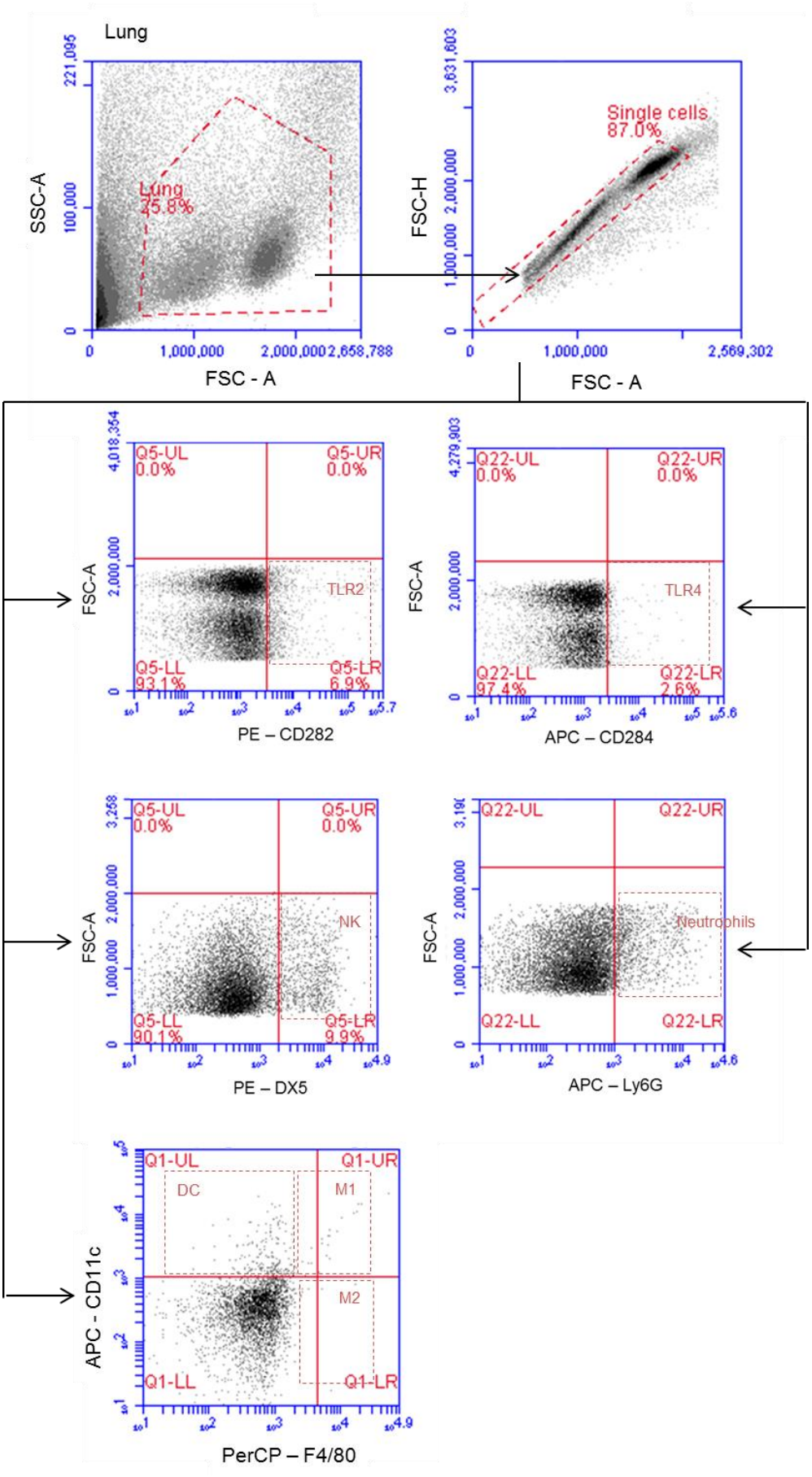

Lymph nodes

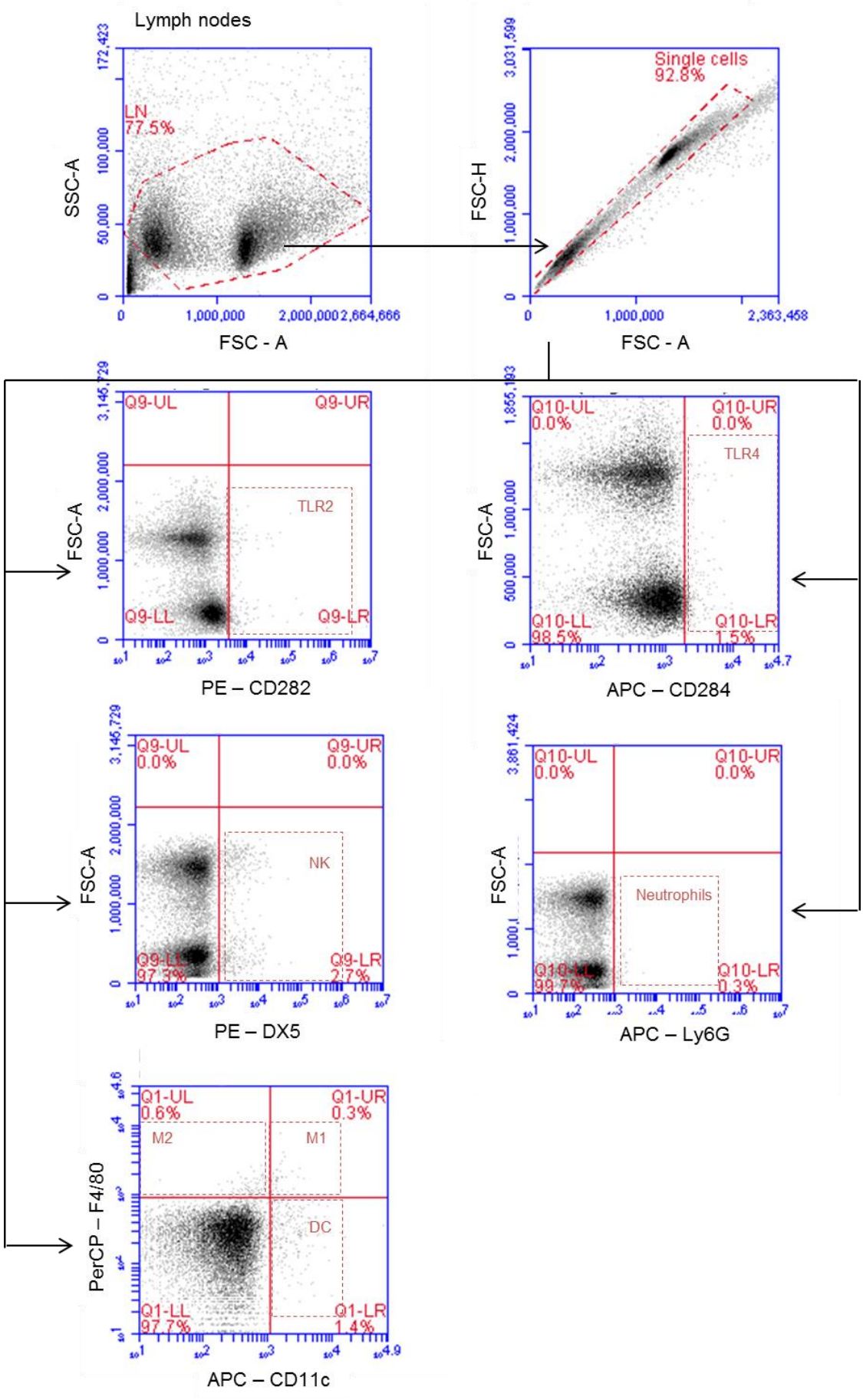
Lymph nodes
LN
77.5%
SSC-A
FSC - A
Single cells
92.8%
FSC-H
FSC - A
Q9-UL
Q9-UR
TLR2
Q9-LL
Q9-LR
FSC-A
PE – CD282
Q10-UL
0.0%
Q10-UR
0.0%
TLR4
Q10-LL
98.5%
Q10-LR
1.5%
FSC-A
APC – CD284
Q9-UL
0.0%
Q9-UR
0.0%
NK
Q9-LL
97.3%
Q9-LR
2.7%
FSC-A
PE – DX5
Q10-UL
0.0%
Q10-UR
0.0%
Neutrophils
Q10-LL
99.7%
Q10-LR
0.3%
FSC-A
APC – Ly6G
Q1-UL
0.6%
Q1-UR
0.3%
M2
M1
DC
Q1-LL
97.7%
Q1-LR
1.4%
PerCP – F4/80
APC – CD11c

Spleen

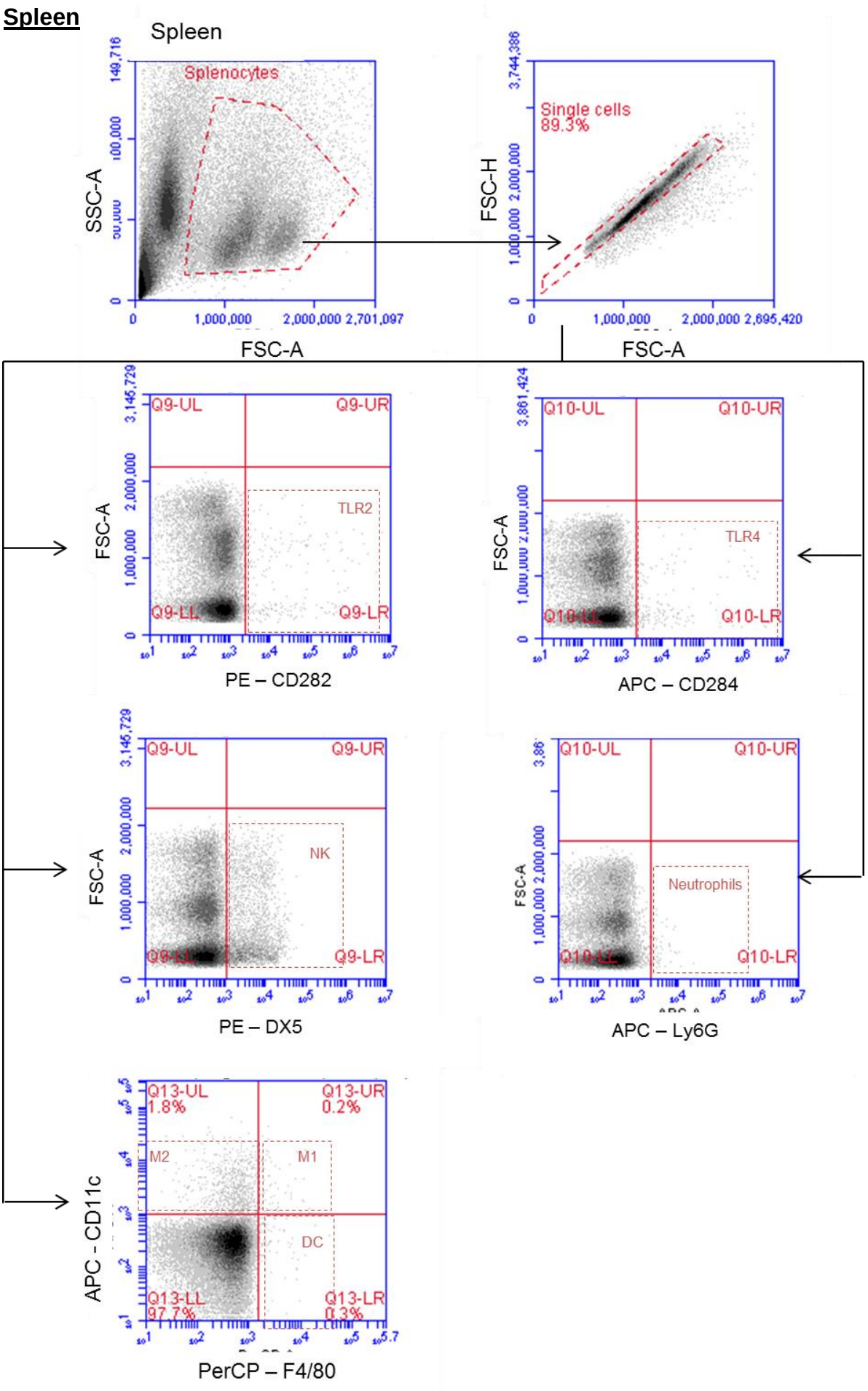
Spleen
Splenocytes
SSC-A
FSC-A
Single cells
89.3%
FSC-H
FSC-A
Q9-UL
Q9-UR
TLR2
Q9-LL
Q9-LR
FSC-A
PE – CD282
Q10-UL
Q10-UR
TLR4
Q10-LL
Q10-LR
FSC-A
APC – CD284
Q9-UL
Q9-UR
NK
Q9-LL
Q9-LR
FSC-A
PE – DX5
Q10-UL
Q10-UR
Neutrophils
Q10-LL
Q10-LR
FSC-A
APC – Ly6G
Q13-UL
1.8%
Q13-UR
0.2%
M2
M1
DC
Q13-LL
97.7%
Q13-LR
0.3%
APC - CD11c
PerCP – F4/80

Gut

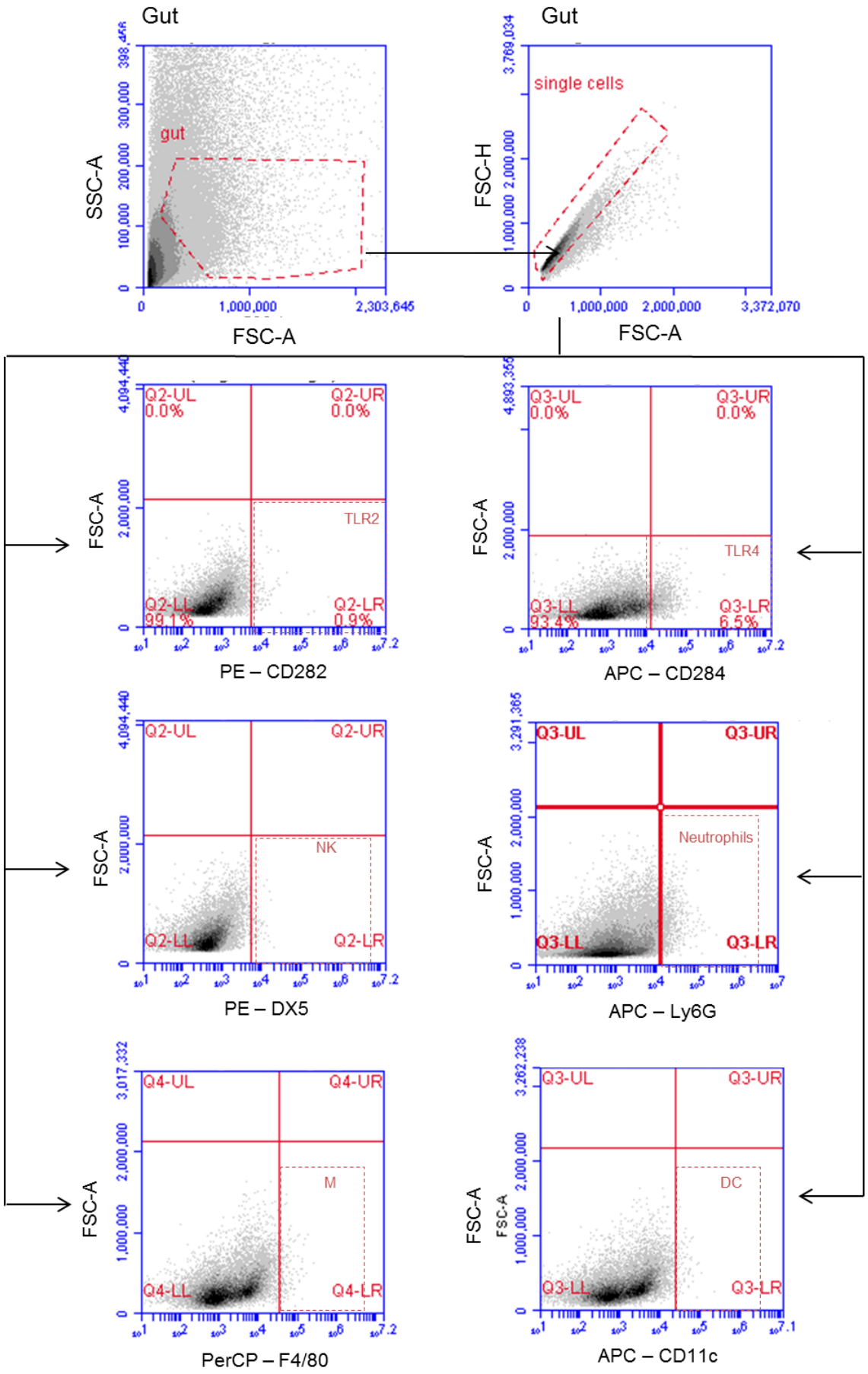
Gut
gut
SSC-A
FSC-A
Gut
single cells
FSC-H
FSC-A
Q2-UL 0.0%
Q2-UR 0.0%
TLR2
Q2-LL 99.1%
Q2-LR 0.9%
FSC-A
PE – CD282
Q3-UL 0.0%
Q3-UR 0.0%
TLR4
Q3-LL 93.4%
Q3-LR 6.5%
FSC-A
APC – CD284
Q2-UL
Q2-UR
NK
Q2-LL
Q2-LR
FSC-A
PE – DX5
Q3-UL
Q3-UR
Neutrophils
Q3-LL
Q3-LR
FSC-A
APC – Ly6G
Q4-UL
Q4-UR
M
Q4-LL
Q4-LR
FSC-A
PerCP – F4/80
Q3-UL
Q3-UR
DC
Q3-LL
Q3-LR
FSC-A
APC – CD11c